BWR TRANSIENT ANALYSIS MODEL

WPPSS-FTS-129, Rev. 01

September 1990

Principal Engineers

Y. Y. YUNG
S. H. BIAN
D. E. BUSH

Contributing Engineer

B. M. Moore

Approved: R O Vosburgh Date: 8/31/90
R. O. Vosburgh
Manager, Safety & Reliability Analysis

D L Larkin Date: 9/4/90
D. L. Larkin
Manager, Engineering Analysis & Nuclear Fuel

DISCLAIMER

This report was prepared by the Washington Public Power Supply System ("Supply System") for submittal to the Nuclear Regulatory Commission, NRC. The information contained herein is accurate to the best of the Supply System's knowledge. The use of information contained in this document by anyone other than the Supply System, or the NRC is not authorized and with respect to any unauthorized use, neither the Supply System nor its officers, directors, agents, or employees assume any obligation, responsibility, or liability or makes any warranty or representation concerning the contents of this document or its accuracy or completeness.

ACKNOWLEDGEMENTS

The Supply System acknowledges the consulting reviews and recommendations provided by Energy Incorporated and Yankee Atomic Electric Company during the course of development of this model. The Supply System also acknowledges the efforts of Mr. J. C. Chandler, Consultant, and Mr. J. T. Cronin, Yankee Atomic Electric Company for their reviews and comments on this report. The technical discussions with Philadelphia Electric Company and Pennsylvania Power & Light Company regarding the Peach Bottom benchmarks is greatly appreciated.

ABSTRACT

System-wide models, based on the WNP-2 plant-specific design and utilizing the RETRAN-02 computer code, are described. Both best-estimate and conservative models are included. The models are applicable to a wide range of transients and will initially be used for, but not limited to, analysis of the limiting pressurization transients considered for reload core licensing. The best-estimate model is qualified by comparisons to a range of power ascension test transients and to the Peach Bottom Unit 2 Turbine Trip Tests. A representative application of the model for licensing basis calculations of the limiting pressurization transients (based on WNP-2 end of cycle 4 conditions) is also presented.

The benchmark comparisons show good agreement between calculated and measured data, thereby demonstrating the Supply System's capability to perform transient analyses for licensing applications.

TABLE OF CONTENTS

TABLE OF CONTENTS (Continued)

TABLE OF CONTENTS (Continued)

LIST OF FIGURES

LIST OF FIGURES (Continued)

LIST OF FIGURES (Continued)

LIST OF FIGURES (Continued)

LIST OF FIGURES (Continued)

LIST OF TABLES

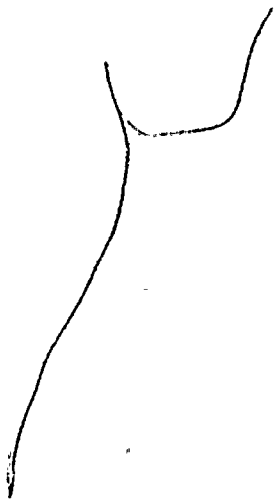

1.0 INTRODUCTION

This report describes and presents qualification results of a transient analysis model for WNP-2. WNP-2 is a boiling water reactor using a BWR/5 Nuclear Steam Supply System (NSSS) provided by General Electric (GE) and operated by the Washington Public Power Supply System (The Supply System). The transient analysis model, developed by the Supply System, uses the RETRAN-02 MOD04 ("RETRAN-02" or "RETRAN") computer code[1]. As demonstrated in this topical report, the transient analysis model shows good agreement to operational transients using plant data and with proper input assumptions gives limiting or conservative results applicable to core reload or licensing analyses.

RETRAN-02 is a versatile time dependent computer code developed by the Electric Power Research Institute (EPRI) to model complex thermal-hydraulic systems. It is capable of providing realistic responses to system upset conditions. A user inputs a system model consisting of control volumes, heat slabs, and a flow path network; for nuclear reactor systems a kinetics model utilizing either point or one-dimensional kinetics is available.

The RETRAN-02 computer code was developed by utility sponsorship through EPRI. The computer code qualification studies were based on code predictions of various separate effects tests, system effects experiments, and power reactor startup tests which can be

found in the RETRAN-02 documentation. The NRC Staff's Safety Evaluation Report (SER) for RETRAN-02 has been issued. The NRC found "... RETRAN-02 is an acceptable computer program for use in licensing applications for calculating the transients described in Chapter 15 ... and other transients and events as appropriate and necessary for nuclear power plant operation.". The RETRAN-02 limitations discussed in the SER and applicable to reload licensing analysis will be addressed in the Supply System Applications Topical Report (to be submitted later).

The Supply System has developed the input for the model presented in this report, representing the WNP-2 plant, from as-built drawings and vendor specifications. The nodalization network was developed over many years by trial and error, comparison to similar plant models, and finally through comparison of model predictions to actual WNP-2 data. This report provides qualification of the WNP-2 RETRAN model and of the Supply System's ability to analyze WNP-2 transient behavior through the application of RETRAN-02 to the analysis of

1. WNP-2 Power Ascension Tests;
2. Peach Bottom 2 Cycle 2 Turbine Trip Tests; and
3. WNP-2 Licensing Basis Analysis.

The Supply System's reload transient analysis methods are based on the EPRI code package as depicted in Figure 1.1. The steady

state core physics codes and models used to provide input to the transient analysis models are described and qualified elsewhere[2]. The SIMTRAN-E MOD3A ("SIMTRAN-E") code[3] collapses the three-dimensional neutronics data generated by the steady state core physics codes to the one-dimensional neutronics input required by RETRAN-02 and calculates the moderator density and fuel temperature dependencies. The one-dimensional kinetics parameter dependencies generated by SIMTRAN-E are modified as described in Section 2.6 to account for differences between the RETRAN-02 one-dimensional and SIMULATE-E three-dimensional moderator density calculations. RETRAN-02 is used to model the NSSS and the VIPRE-01 MOD02 ("VIPRE-01") code[4] is used to model a single fuel assembly for thermal margin evaluations. Thermal margin evaluation for WNP-2 is described and qualified in a separate Applications Topical Report (to be submitted later).

The base WNP-2 RETRAN-02 model is described in Chapter 2. It is designed to serve as a best-estimate, time dependent (transient), systems analysis tool. Intended uses of the best-estimate model include simulator qualification, evaluating operational transients, and evaluating proposed system design changes. In Chapter 3, the WNP-2 RETRAN-02 model is qualified by comparison of best-estimate data predictions with plant data collected during startup testing. To analyze limiting transients for core reload design in support of technical specification action, a Licensing Basis Model is developed by modifying the best estimate

model with conservative assumptions. The Licensing Basis Model is described in Chapter 4, which also contains example calculations with the conservative model. The Applications Topical Report that will be published later will provide additional detail on a) the process and interface between the EPRI codes for licensing analyses, b) the Licensing Basis Model input sensitivity and uncertainity analyses, and c) the hot channel thermal margin methodology. Chapter 5 contains the Summary and Conclusions and Chapter 6 the References.

FIGURE 1.1

Supply System Reload Transient Analysis Methods
Computer Code Flow Chart

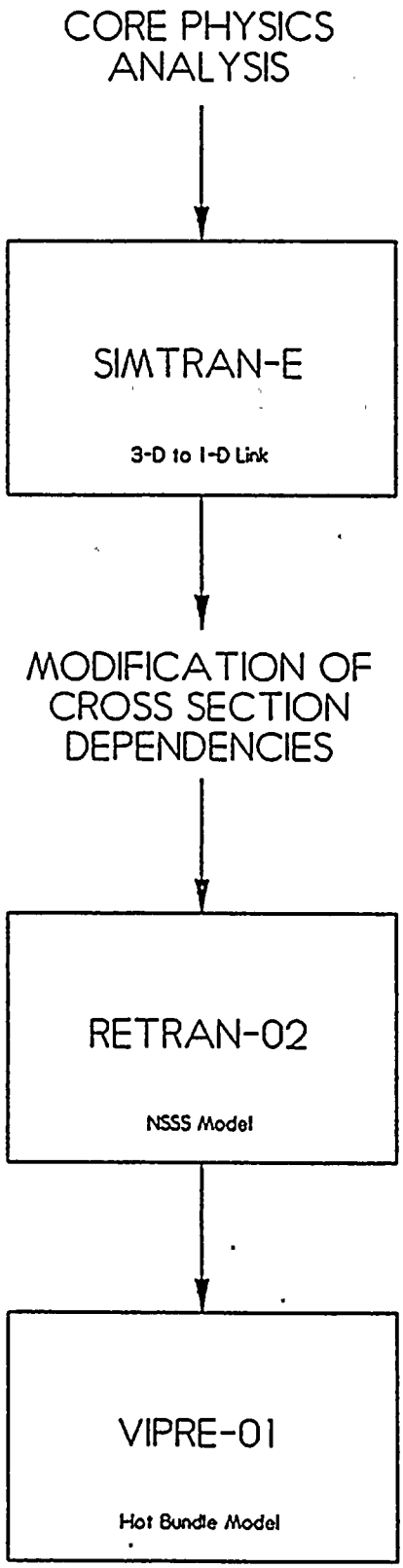

2.0 MODEL DESCRIPTION

This chapter describes the WNP-2 RETRAN-02 Best Estimate Model developed to analyze a wide range of transients. The Supply System has been involved with the RETRAN development effort since 1979 and the WNP-2 model has evolved over time with our code development involvement. In addition, the Supply System has had two separate and independent reviews performed on the WNP-2 model, by Energy Incorporated (now a Division of NUS Corp) and by Yankee Atomic. These reviews have provided valuable insights into the model and options used and are documented as part of the model development file.

The best estimate model description is given in the following sections. Figures 2.1 through 2.4 depict the nodalization scheme utilized for the WNP-2 model, whereas Section 2.1 provides additional detail on the Model Geometry, Section 2.2 discusses models of special components such as the jet pumps and the safety relief valves, and the trip logic and control systems models are described in Sections 2.3 and 2.4, respectively. The steady-state initialization is discussed in Section 2.5. The WNP-2 model uses twelve active core nodes as is shown in Figure 2.2 and the interface/input between the RETRAN WNP-2 model and the reactor physics input to the kinetics model is given in Section 2.6.

FIGURE 2.1

WNP-2 RETRAN MODEL (Vessel)

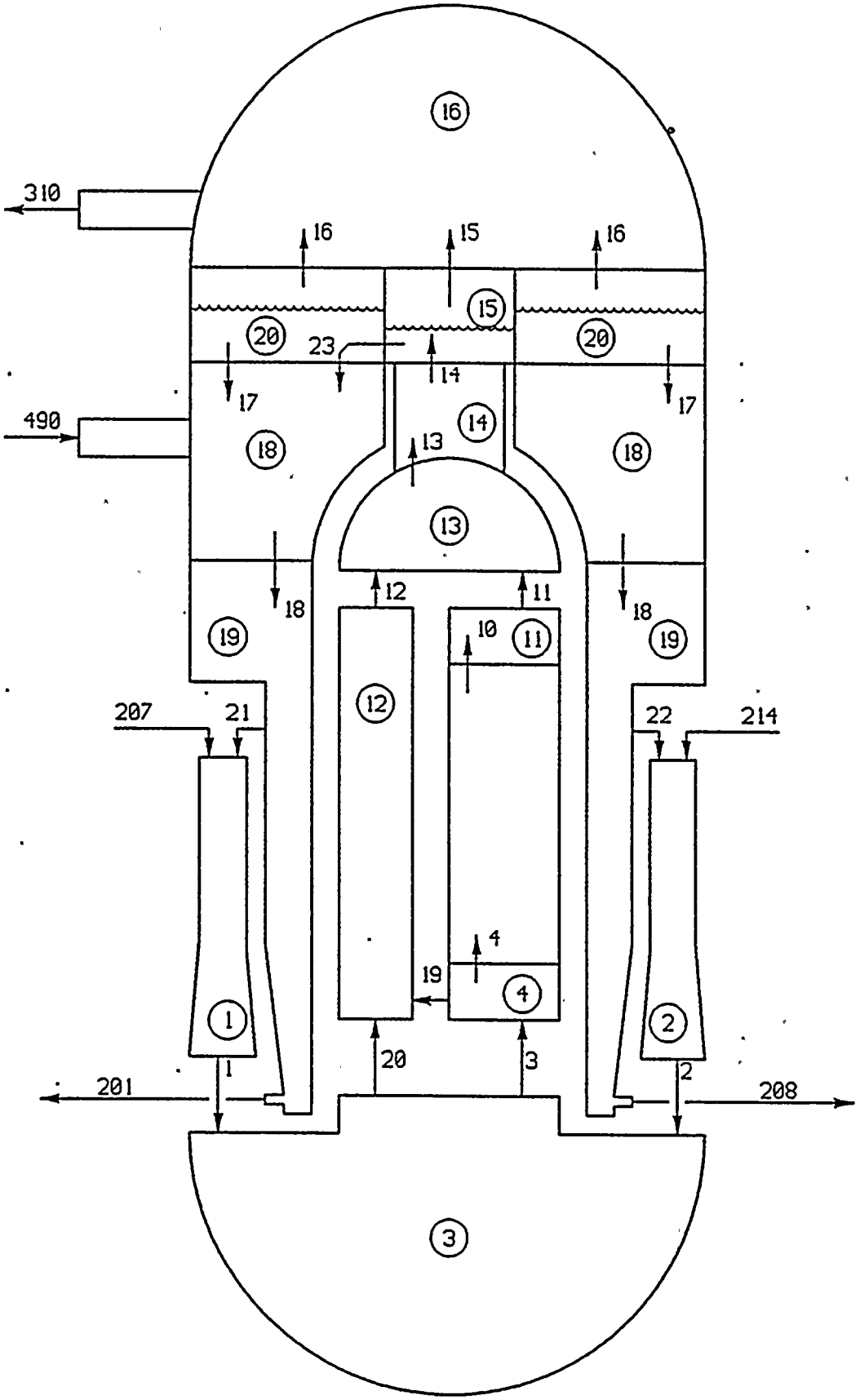

FIGURE 2.2

WNP-2 RETRAN MODEL (Active Core Region)

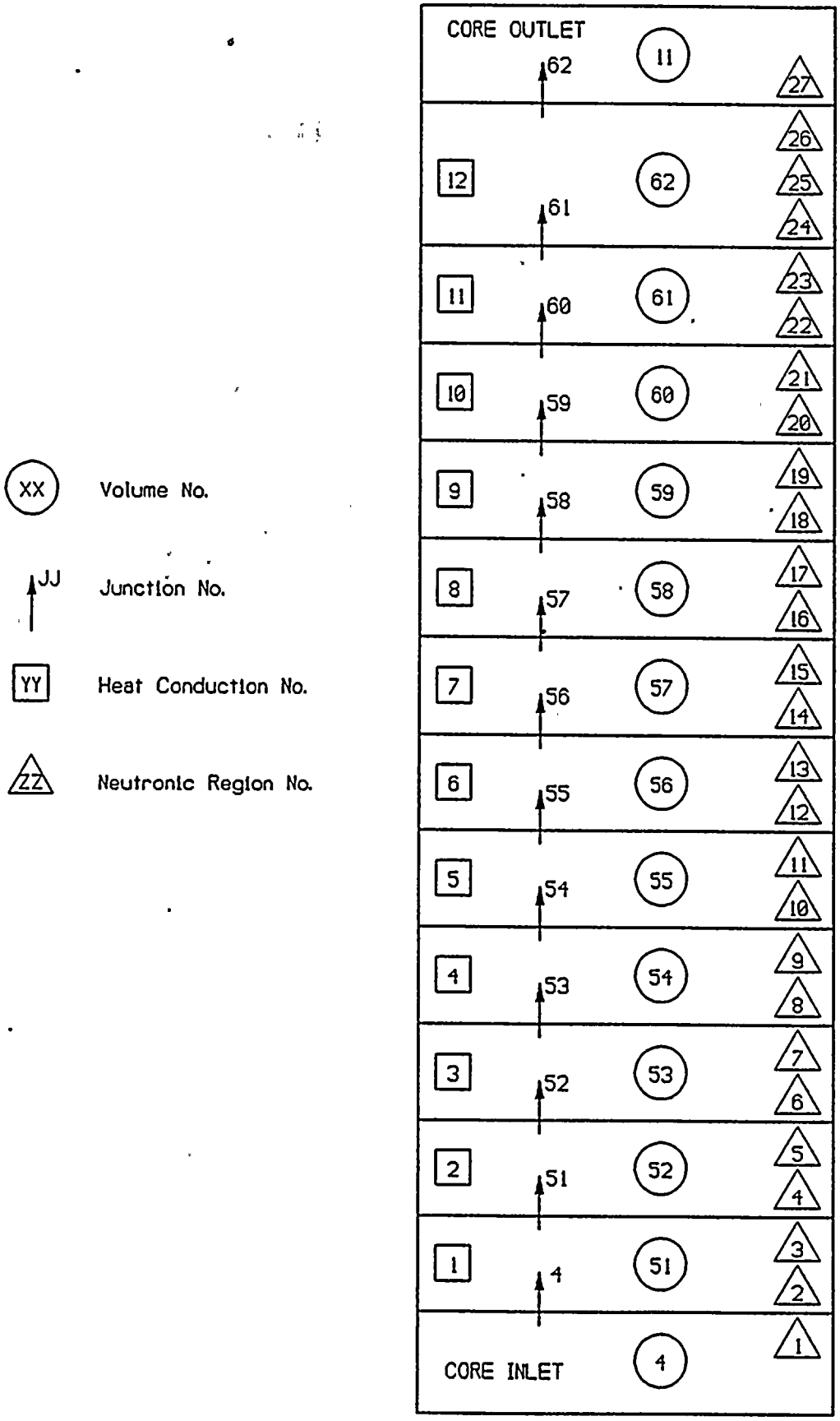

FIGURE 2.3

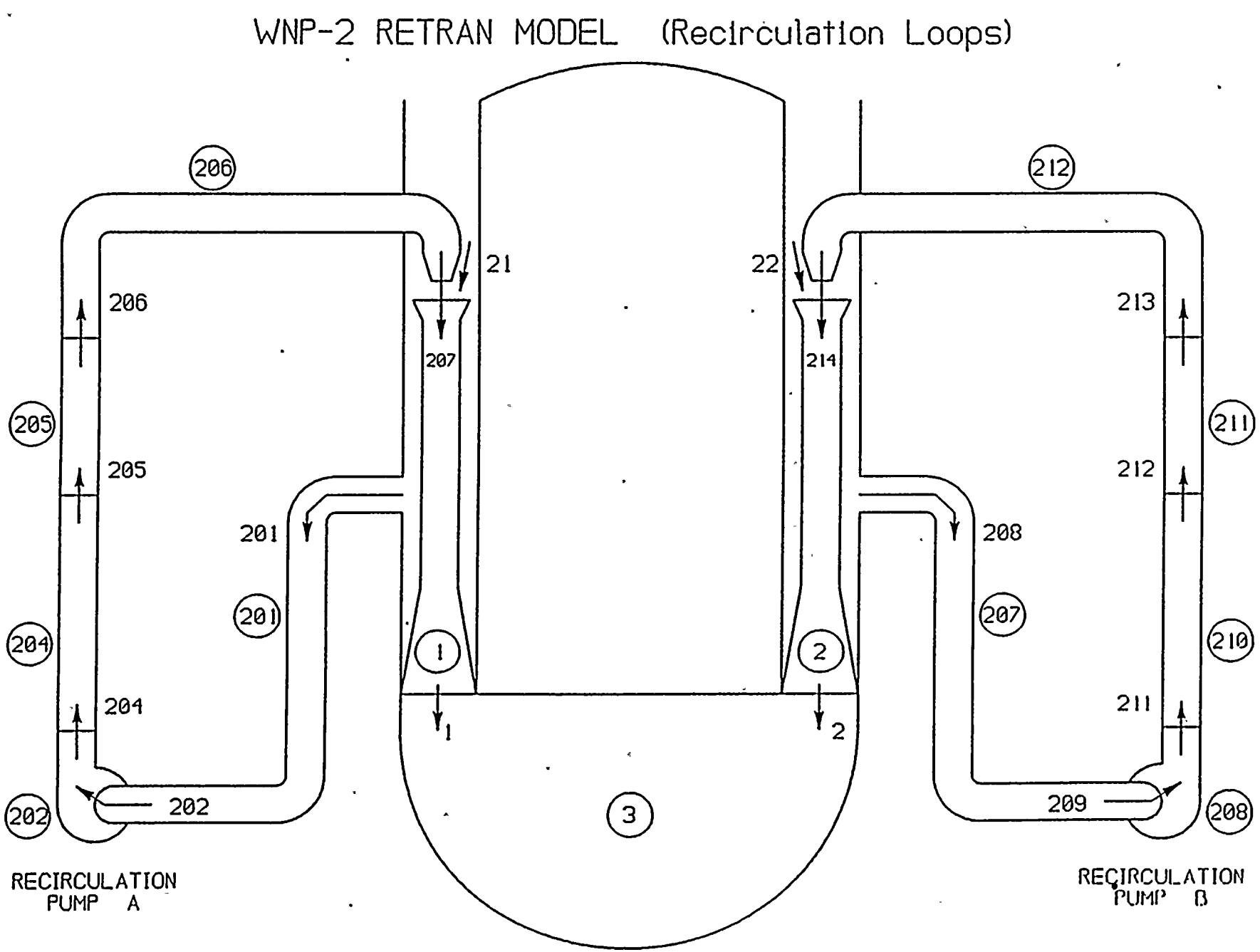
WNP-2 RETRAN MODEL (Recirculation Loops)
206
212
21
22
206
213
207
214
205
211
205
212
201
208
201
207
204
210
1
2
204
211
1
2
202
202
209
208
3
RECIRCULATION PUMP A
RECIRCULATION PUMP B

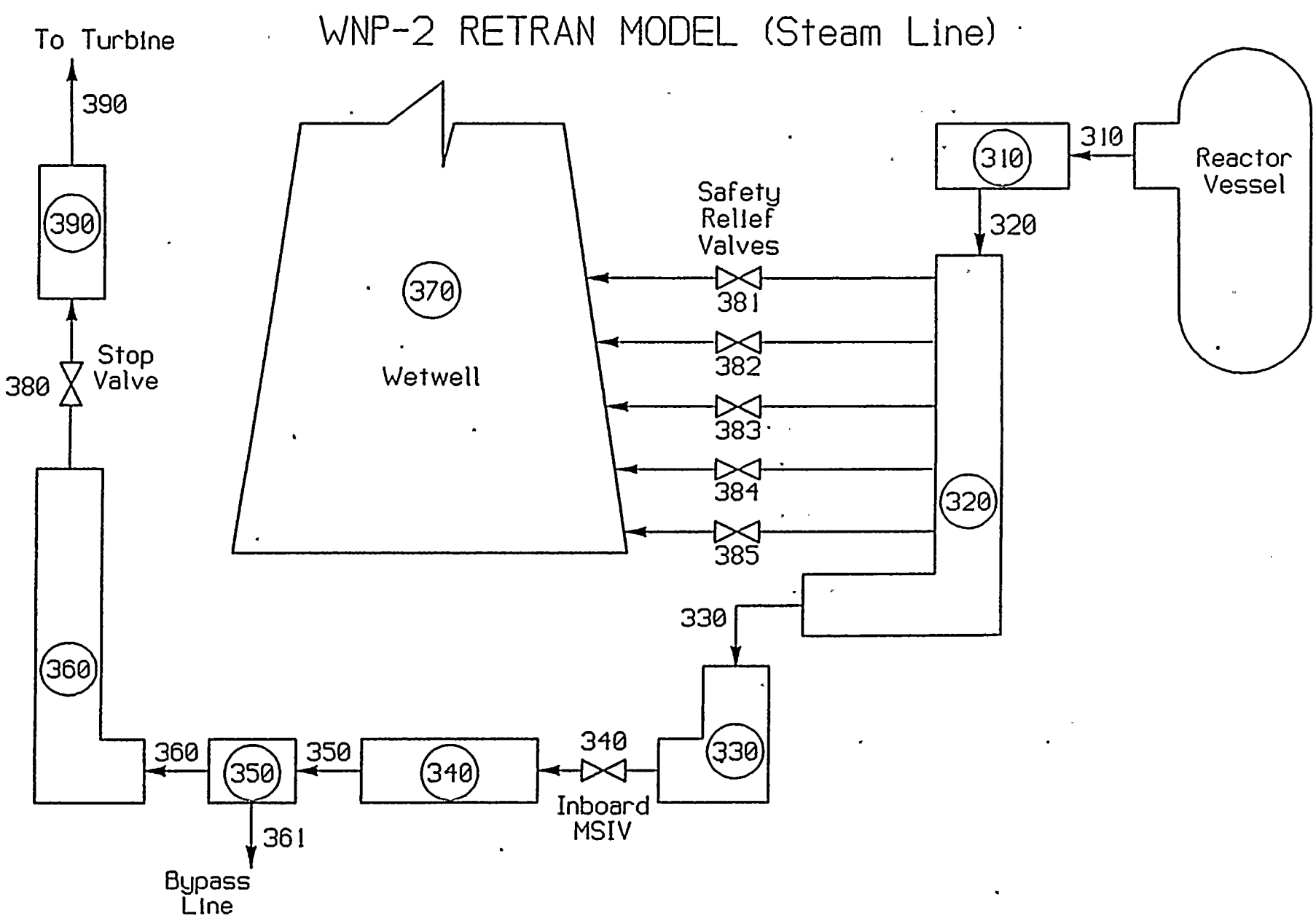
WNP-2 RETRAN MODEL (Steam Line)
To Turbine
390
390
Stop Valve
380
360
370
Wetwell
Safety Relief Valves
381
382
383
384
385
310
310
Reactor Vessel
320
320
330
330
340
340
Inboard MSIV
350
350
360
361
Bypass Line

2.1 Model Geometry

The physical geometry and volume of the WNP-2 nuclear steam supply system is modeled as series of control volumes and junctions. The following sections discuss this physical arrangement and how it is modeled in the WNP-2 RETRAN model.

2.1.1 Control volumes, Junctions, and Heat Conductors

The control volume nodes are defined as distinct regions within the primary system, such as the steam dome or downcomer, as shown in Figures 2.1 through 2.4. The physical dimensions of the volumes, junction areas, lengths, etc. were obtained from WNP-2 plant specific as-built drawings. The nodalization scheme used has been developed over several years and is based on code limitations, solution stability, economical run-times, and, most importantly, agreement to experimental or test data.

In Figures 2.1 through 2.4, the nodal volumes are denoted by numbers in small circles. The pertinent data associated with each of these volumes is given in Table 2.1.1. The mass/energy transfer between volumes is through junctions, depicted in Figures 2.1 through 2.4 as numbered arrows. The junction input data is given in Table 2.1.2. In Figure 2.2, the heat conduction in the active core region is shown as small squares numbered 1

through 12 for each active core volume. The pertinent data for each heat conductor is given in Table 2.1.3.

Additional discussion of the salient nodalization by region is given in Subsections 2.1.2 through 2.1.5 below. Features of WNP-2 that are represented by special control volumes, e.g., safety/relief valves, are discussed in Section 2.2.

2.1.2 Vessel Internals (Refer to Figure 2.1)

Volumes 18, 19, and 20 constitute the middle, lower, and upper downcomer regions, respectively, of the reactor vessel. The middle downcomer region, Vol. 18, is the volume in which the feedwater and the saturated liquid and steam carryunder from the steam separators are mixed. The upper downcomer region, Vol. 20, models the liquid/steam interface region and utilizes the RETRAN "non-equilibrium" option. This option is used in this volume to accurately account for the superheating of steam during pressurization transients (the pressurization/de-pressurization effects are governed by this interface region).

As shown in Figure 2.1, the steam dome, Vol. 16, and the fluid region below the core support plate (lower plenum), Vol. 3, are single large volumes. The jet pump volumes, Vol. 1 and 2, are discussed further in Section 2.2.4.

The upper plenum region above the upper guide plate, Vol. 13, and the standpipes, Vol. 14, are both modeled as single volumes. A single volume, Vol. 15, is used to model the internal region of the 225 steam separators. From the steam separator internal region, the major steam flow is to the steam dome, Vol. 16, whereas the steam carryunder flows to and mixes in the middle downcomer, Vol. 18, as mentioned above.

2.1.3 Core Region (Refer to Figure 2.2)

The WNP-2 core region is considered to be the twelve control volumes used to model the active region of the core (Vols. 51 through 62), the single volumes for the unheated core inlet and outlet regions (Vols. 4 and 11), and the core bypass single volume region. (The core bypass volume is shown on Figure 2.1 as Vol. 12).

There are two means of energy deposition modeled in the core region. In the active core volumes, twelve heat conductors are used to represent the reactor fuel. The geometric data for the heat conductors is presented in Table 2.1.3. In addition, a direct moderator heating model is included to account for direct energy deposition into the active core volumes due to gamma and neutron heating. For the core bypass volume, a constant fraction of the core thermal power is directly deposited via a RETRAN non-conducting heat exchanger model.

As shown in Figure 2.2, the one-dimensional kinetics calculations are supported by twenty-seven neutronic regions, i.e., twenty-five in the active core volumes and one per reflector volume. Thermal-hydraulic feedback of each active core and reflector volume is provided to the associated neutronic regions. This feedback of the calculated water density of each active core and reflector volume and the attendant corrections are discussed further in Section 2.6 of this report.

The fuel temperature feedback for each region is provided by the heat conductor models in each active core volume. The average fuel rod is represented by three cylindrical regions - fuel, gap, and cladding. The cladding is modeled with four nodes, the gap one node, and the fuel region is modeled with six nodes. The material conductivity and heat capacity for the UO2 fuel and the Zircaloy cladding are taken from MATPRO[5] and WREM[6] data. For purposes of the model benchmarking, the gap conductance of the average core region is assumed to be a constant value[7].

2.1.4 Recirculation Loops (Refer to Figure 2.3)

The two recirculation loops are modeled separately. In each recirculation loop, five control volumes are used to represent the recirculation pump and loop piping. In each loop, a single volume is used to model ten jet pumps driven by the recirculation

loop. A special two-stream momentum mixing option is used by RETRAN to describe the interaction of the recirculation loop drive flow with the suction flow from the downcomer. Additional detail of the jet pump and the recirculation pump modeling is provided in Section 2.2.

2.1.5 Steam and Feedwater Lines (Refer to Figure 2.4)

The four main steam lines are lumped into one composite line, which is divided into seven control volumes (see Figure 2.4). From the reactor vessel there are three volumes modeling the steam lines to the Main Steam Isolation Valves (MSIVs), Vols. 310, 320, and 330. The middle of these volumes (Vol. 320) is connected to the junctions representing the safety/relief valves. Due to their redundancy, the MSIVs are modeled as a single valve. The steam lines from the MSIVs to the turbine stop valves are also modeled in three volumes, Vols. 340, 350, and 360. The middle of these volumes, Vol. 350, provides a line model for the turbine bypass, whereas the third volume, Vol. 360 provides the pressure feedback signal to the Pressure Control System. The steam line volume between the turbine stop valve and the turbine control valves is modeled as Vol. 390.

The flows from steam line to the turbine (through Jct. 390) and, subsequently, to the condenser (through Jct. 361) are modeled as

negative fill junctions with flow rates controlled by the Pressure Control System (see Section 2.4.2).

The feedwater lines are modeled as a positive fill junction with flow rate controlled by the Feedwater Control System. For simulation of very fast transients, the feedwater is constant and explicit modeling of the lines and pumps is not necessary.

TABLE 2.1.1

VOLUME GEOMETRIC DATA

VOLUME NUMBER	VOLUME (FT3)	HEIGHT (FT)	FLOW LENGTH (FT)	FLOW AREA (FT2)	HYDRAULIC DIAMETER (FT)	ELEV. (FT)	DESCRIPTION
1	136.942	16.517	16.517	19.897	1.592	9.917	JET PUMP
2	136.942	16.517	16.517	19.897	1.592	9.917	JET PUMP
3	2240.000	17.281	21.450	114.280	0.781	0.000	LOWER PLENUM
4	66.640	0.745	0.745	89.474	0.045	17.281	CORE INLET
11	111.280	1.198	1.198	83.955	0.045	30.526	CORE EXIT
12	950.708	14.443	14.443	65.825	0.182	17.281	CORE BYPASS
13	943.000	3.816	3.816	247.120	17.738	31.724	UPPER PLENUM
14	400.000	8.918	8.918	44.853	0.505	35.540	STANDPIPE
15	442.834	6.167	7.092	71.807	0.641	44.458	SEPARATOR
16	6285.300	18.544	21.100	270.000	20.768	50.615	DOME
18	2196.700	10.221	8.531	257.496	2.256	34.302	MID DOWNCOMER
19	2498.700	24.177	9.960	103.350	2.162	10.125	LOWER DOWNCOMER
20	1901.700	7.812	7.812	149.621	0.732	42.823	UPPER DOWNCOMER
51	83.955	1.000	1.000	83.955	0.045	18.026	CORE #1
52	83.955	1.000	1.000	83.955	0.045	19.026	CORE #2
53	83.955	1.000	1.000	83.955	0.045	20.026	CORE #3
54	83.955	1.000	1.000	83.955	0.045	21.026	CORE #4
55	83.955	1.000	1.000	83.955	0.045	22.026	CORE #5
56	83.955	1.000	1.000	83.955	0.045	23.026	CORE #6
57	83.955	1.000	1.000	83.955	0.045	24.026	CORE #7
58	83.955	1.000	1.000	83.955	0.045	25.026	CORE #8
59	83.955	1.000	1.000	83.955	0.045	26.026	CORE #9
60	83.955	1.000	1.000	83.955	0.045	27.026	CORE #10
61	83.955	1.000	1.000	83.955	0.045	28.026	CORE #11
62	125.933	1.500	1.500	83.955	0.045	29.026	CORE #12
201	148.000	34.682	58.360	2.536	1.797	-19.409	RRC #1 SUCTION
202	30.500	3.375	12.027	2.536	1.797	-16.510	RRC #1 PUMP
204	115.000	21.979	45.347	2.536	1.797	-15.492	RRC #1 HEADER INLET
205	43.500	1.193	9.727	2.236	1.193	6.487	RRC #1 HEADER
206	91.710	20.116	25.980	3.530	0.948	7.680	RRC #1 RISER
207	148.000	34.682	58.360	2.536	1.797	-19.409	RRC #2 SUCTION
208	30.500	3.375	12.027	2.536	1.797	-16.510	RRC #2 PUMP
210	115.000	21.979	45.347	2.536	1.797	-15.492	RRC #2 HEADER INLET
211	43.500	1.193	9.727	2.236	1.193	6.487	RRC #2 HEADER
212	91.710	20.116	25.980	3.530	0.948	7.680	RRC #2 RISER
310	446.430	33.509	37.490	11.908	1.947	21.464	STEAM OUTLET
320	275.370	2.200	23.125	11.908	1.947	21.206	STEAM LINE
330	555.400	39.090	46.641	11.908	1.947	-15.930	STEAM LINE
340	504.280	7.146	42.348	11.908	1.947	-21.792	STEAM LINE
350	2747.160	6.861	170.589	16.104	2.264	-28.650	STEAM LINE
360	1654.540	25.882	102.741	16.104	2.264	-40.903	STEAM LINE
370	2.56E+5	42.610	42.610	4520.000	75.862	21.460	CONTAINMENT
390	86.750	2.350	10.001	8.674	2.350	-16.196	STEAM LINE

TABLE 2.1.2

JUNCTION GEOMETRIC DATA

JCT. NO.	CONNECTS VOLUME FROM	TO	FLOW AREA (FT2)	ELEV. (FT)	INERTIA (1/FT)	LOSS COEF.	HYDRAULIC DIAMETER (FT)	DESCRIPTION
1	1	3	19.8970	9.9170	0.5089	1.8300	1.5920	JET PUMP #1 DISCH
2	2	3	19.8970	9.9170	0.5089	1.8300	1.5920	JET PUMP #2 DISCH
3	3	4	22.6680	17.2813	0.0980	-1.0000	0.1960	CORE INLET
4	4	51	54.1390	18.0261	0.0101	3.2690	0.0270	CORE #1 INLET
10	62	11	63.0464	30.5261	0.0161	0.4117	0.0319	CORE #12 EXIT
11	11	13	83.9550	31.7240	0.0149	0.7300	0.0446	CORE OUTLET
12	12	13	55.9920	31.7240	0.1174	0.6800	0.3022	BYPASS OUTLET
13	13	14	45.1400	35.5400	0.1071	0.4100	0.5054	STANDPIPE INLET
14	14	15	33.7960	44.4580	0.4390	-1.0000	0.1569	SEPARATOR INLET
15	15	16	30.6800	50.6250	0.0885	-1.0000	0.4167	SEPARATOR OUTLET
16	20	16	239.3200	50.6250	0.0652	23.5000	0.0518	LOWER DOME INLET
17	20	18	149.6210	42.8330	0.0427	0.1800	0.7320	MID DOWNCOMER INLET
18	18	19	85.1340	34.3020	0.0648	0.2700	2.7500	LOWER DOWNCOMER INLET
19	4	12	1.5000	17.2813	0.1139	-1.0000	0.0028	CORE BYPASS INLET #2
20	3	12	0.8420	17.2813	0.2036	6.9851	0.0019	CORE BYPASS INLET #1
21	19	1	1.7730	26.4340	4.7330	0.0542	0.2100	JET PUMP #1 SUCTION
22	19	2	1.7730	26.4340	4.7330	0.0542	0.2100	JET PUMP #2 SUCTION
23	15	18	51.8250	44.5030	0.0659	4.0100	0.0895	SEP. TO MID DOWNCOMER
51	51	52	83.9550	19.0261	0.0119	0.0000	0.0446	CORE #1 EXIT
52	52	53	83.9550	20.0261	0.0119	1.2400	0.0446	CORE #2 EXIT
53	53	54	83.9550	21.0261	0.0119	1.2400	0.0446	CORE #3 EXIT
54	54	55	83.9550	22.0261	0.0119	0.0000	0.0446	CORE #4 EXIT
55	55	56	83.9550	23.0261	0.0119	1.2400	0.0446	CORE #5 EXIT
56	56	57	83.9550	24.0261	0.0119	0.0000	0.0446	CORE #6 EXIT
57	57	58	83.9550	25.0261	0.0119	1.2400	0.0446	CORE #7 EXIT
58	58	59	83.9550	26.0261	0.0119	1.2400	0.0446	CORE #8 EXIT
59	59	60	83.9550	27.0261	0.0119	0.0000	0.0446	CORE #9 EXIT
60	60	61	83.9550	28.0261	0.0119	1.2400	0.0446	CORE #10 EXIT
61	61	62	83.9550	29.0261	0.0149	1.2400	0.0446	CORE #11 EXIT
201	19	201	2.5360	14.3750	11.5544	0.2450	1.7969	RRC LOOP #1
202	201	202	2.5360	-16.5100	13.8775	0.6300	1.7969	RRC LOOP #1
204	202	204	1.7924	-15.4920	11.3119	-1.0000	1.7969	RRC LOOP #1
205	204	205	2.5360	6.4870	11.1157	0.5460	1.7969	RRC LOOP #1
206	205	206	3.5300	7.6800	5.8550	1.2860	0.9480	RRC LOOP #1
207	206	1	0.4609	26.4340	3.8530	0.2122	0.1083	RRC LOOP #1
208	19	207	2.5360	14.3750	11.5544	0.2450	1.7969	RRC LOOP #2
209	207	208	2.5360	-16.5100	13.8775	0.6300	1.7969	RRC LOOP #2
211	208	210	1.7924	-15.4920	11.3119	-1.0000	1.7969	RRC LOOP #2
212	210	211	2.5360	6.4870	11.1157	0.5460	1.7969	RRC LOOP #2
213	211	212	3.5300	7.6800	5.8550	1.2860	0.9480	RRC LOOP #2
214	212	2	0.4609	26.4340	3.8530	0.2122	0.1083	RRC LOOP #2
310	16	310	11.9080	54.0000	1.6132	0.2721	1.9470	STEAM LINE
320	310	320	11.9080	22.4300	2.5451	0.3391	1.9470	STEAM LINE

TABLE 2.1.2 (CONT.)

JUNCTION GEOMETRIC DATA

JCT. NO.	CONNECTS VOLUME FROM	TO	FLOW AREA (FT2)	ELEV. (FT)	INERTIA (1/FT)	LOSS COEF.	HYDRAULIC DIAMETER (FT)	DESCRIPTION
330	320	330	3.6370	22.1800	2.9294	0.1852	1.0760	STEAM LINE
340	330	340	4.1250	-15.1300	3.7365	0.1541	1.1460	STEAM LINE
350	340	350	16.1040	-21.7920	7.0746	0.4203	1.9470	STEAM LINE
360	350	360	16.1040	-27.5200	8.4864	1.1780	2.2640	STEAM LINE
380	360	390	14.1860	-15.0210	3.7664	2.5762	2.1250	STEAM LINE
381	320	370	0.2238	21.4600	0.9757	0.2630	0.3775	SRV INLET
382	320	370	0.4477	21.4600	0.9757	0.2630	0.3775	SRV INLET
383	320	370	0.4477	21.4600	0.9757	0.2630	0.3775	SRV INLET
384	320	370	0.4477	21.4600	0.9757	0.2630	0.3775	SRV INLET
385	320	370	0.4477	21.4600	0.9757	0.2630	0.3775	SRV INLET
602	0	13	1.0000	31.7240	0.0077	0.0000	1.1284	HPCS
601	0	16	1.0000	69.1580	0.0391	0.0000	1.1284	RCIC LINE
490	0	18	5.0000	41.1000	0.0166	0.0000	0.1333	FEEDWATER LINE
390	0	390	1.0000	-16.1960	0.5765	-1.0000	1.1280	TURBINE NEG FILL
361	0	350	1.0000	-28.6500	5.2965	-1.0000	1.3440	STEAM BYP NEG FILL

TABLE 2.1.3

HEAT CONDUCTOR GEOMETRIC DATA

HEAT COND. NO.	VOLUME ON: LEFT (INSIDE)	RIGHT (OUTSIDE)	GEOMETRY TYPE	NO.	CONDUCTOR VOLUME (FT3)	SURFACE AREA LEFT (FT2)	RIGHT (FT2)	DESCRIPTION
1	0	51	CYL.	1	60.27	0.	5990.	FUEL RODS CORE 1
2	0	52	CYL	1	60.27	0.	5990.	FUEL RODS CORE 2
3	0	53	CYL.	1	60.27	0.	5990.	FUEL RODS CORE 3
4	0	54	CYL.	1	60.27	0.	5990.	FUEL RODS CORE 4
5	0	55	CYL.	1	60.27	0.	5990.	FUEL RODS CORE 5
6	0	56	CYL	1	60.27	0.	5990.	FUEL RODS CORE 6
7	0	57	CYL.	1	60.27	0.	5990.	FUEL RODS CORE 7
8	0	58	CYL.	1	60.27	0.	5990.	FUEL RODS CORE 8
9	0	59	CYL.	1	60.27	0.	5990.	FUEL RODS CORE 9
10	0	60	CYL	1	60.27	0.	5990.	FUEL RODS CORE 10
11	0	61	CYL.	1	60.27	0.	5990.	FUEL RODS CORE 11
12	0	62	CYL.	1	60.27	0.	5990.	FUEL RODS CORE 12

2.2 Component Models

The transient behavior of a BWR is affected by system components such as jet pumps, recirculation pumps and steam separators. The following sections describe the major component models of the WNP-2 RETRAN model.

2.2.1 Jet Pumps

There are ten jet pumps in each of the two recirculation loops. The ten jet pumps per loop are modeled as a single jet pump. This jet pump is modeled as a single control volume in the WNP-2 RETRAN model. Jet pump performance is represented by a M-N characteristic curve (N as a function of M, M = The ratio of the suction flow to the driving flow, N = The ratio of the specific energy increase of the suction flow to the specific energy decrease of the driving flow). To determine RETRAN input parameters that produce the expected M-N characteristic curve for the WNP-2 jet pump, a RETRAN sub-model of the recirculation loop and jet pumps was set up. Pressure distribution data from the vendor[10] was used to determine the suction and drive nozzle loss coefficients. The momentum mixing formulation was applied to the suction and nozzle junctions. All other junction and volume geometry data were calculated using design drawings. The M-N curve generated with this model is compared to vendor's data in

Figure 2.2.1. The comparison shows that this modeling technique provides an acceptable representation for the WNP-2 jet pumps.

2.2.2 Recirculation Pumps

The centrifugal pump model in RETRAN is used to represent the WNP-2 recirculation pumps. The pump unique characteristics (i.e., moment of inertia, rated values for pump flow, head and torque) and the pump homologous curves supplied to the RETRAN pump model are based on pump manufacturer's data[9]. Since the recirculation flow control is achieved by varying the position of the flow control valve, not by varying the pump speed, the recirculation pump motor is modeled with a constant speed.

2.2.3 Steam Separators

The steam separators couple the reactor core and the steam dome. The emphasis in modeling the separators is on achieving the appropriate coupling between these regions.

The 225 steam separators are modeled as a single control volume. The Bubble Rise model in RETRAN is used to simulate the separator performance. Referring to Figure 2.1, the interior of the separators is represented by Volume 15. The entering two-phase fluid flow is represented by Junction 14. Separation takes place

within Volume 15. The exiting steam and liquid flows are represented by Junction 15 and Junction 23 respectively.

The most important separator input parameters relative to the coupling between the reactor core and steam dome are the separator inlet inertia and the pressure drop across the separators. The separator inertia is determined from vendor's data[8]. It is calculated as a function of the separator inlet quality at the transient initial condition. The separator inlet and exit loss coefficients are determined by RETRAN using the steady state initialization option. The pressure drop distribution at the rated operating condition is in agreement with vendor's calculation[7].

2.2.4 Safety/Relief Valves

WNP-2 has 18 relief valves arranged in groups of 2 to 4 valves at a common setpoint. Each of the groups of valves at a common setpoint is represented by a junction connecting the steam line to a sink volume in the RETRAN model. The area of the junctions is taken as the flow area of the valve times the number of valves being modeled. When the valve is opened with the steam line pressurized, the junction flow becomes choked and the Moody critical flow option is chosen in RETRAN to calculate the choked flow rate. Contraction coefficients of the relief valve junctions

are adjusted to match the specified flow at the reference pressure.

The opening and closing of the relief valves is modeled using RETRAN trips. When the pressure in the steam line volume containing the relief valves reaches the specified setpoint , the valve is opened linearly after a time delay. The valve stays fully open until the pressure drops to the reclosing setpoint. It is then completely closed in a stepwise manner.

2.2.5 Core Hydraulic

The core region is modeled using the compressible, single-stream flow with momentum flux form of flow equation. The two-phase friction multiplier is computed with the Baroczy correlation. The form loss coefficients are set to match values calculated with a steady-state thermal-hydraulic model. This model was developed with the FIBWR code[11] and has been benchmarked against plant data. Initial values of core bypass flow and core support plate pressure drop are also determined by steady-state thermal-hydraulic calculation and input to RETRAN. The algebraic slip model allowing the liquid and vapor phases to flow with unequal velocities is used to simulate the two-phase flow phenomena. The profile fit subcooled void model is included for neutronic feedback calculation.

FIGURE 2.2.1

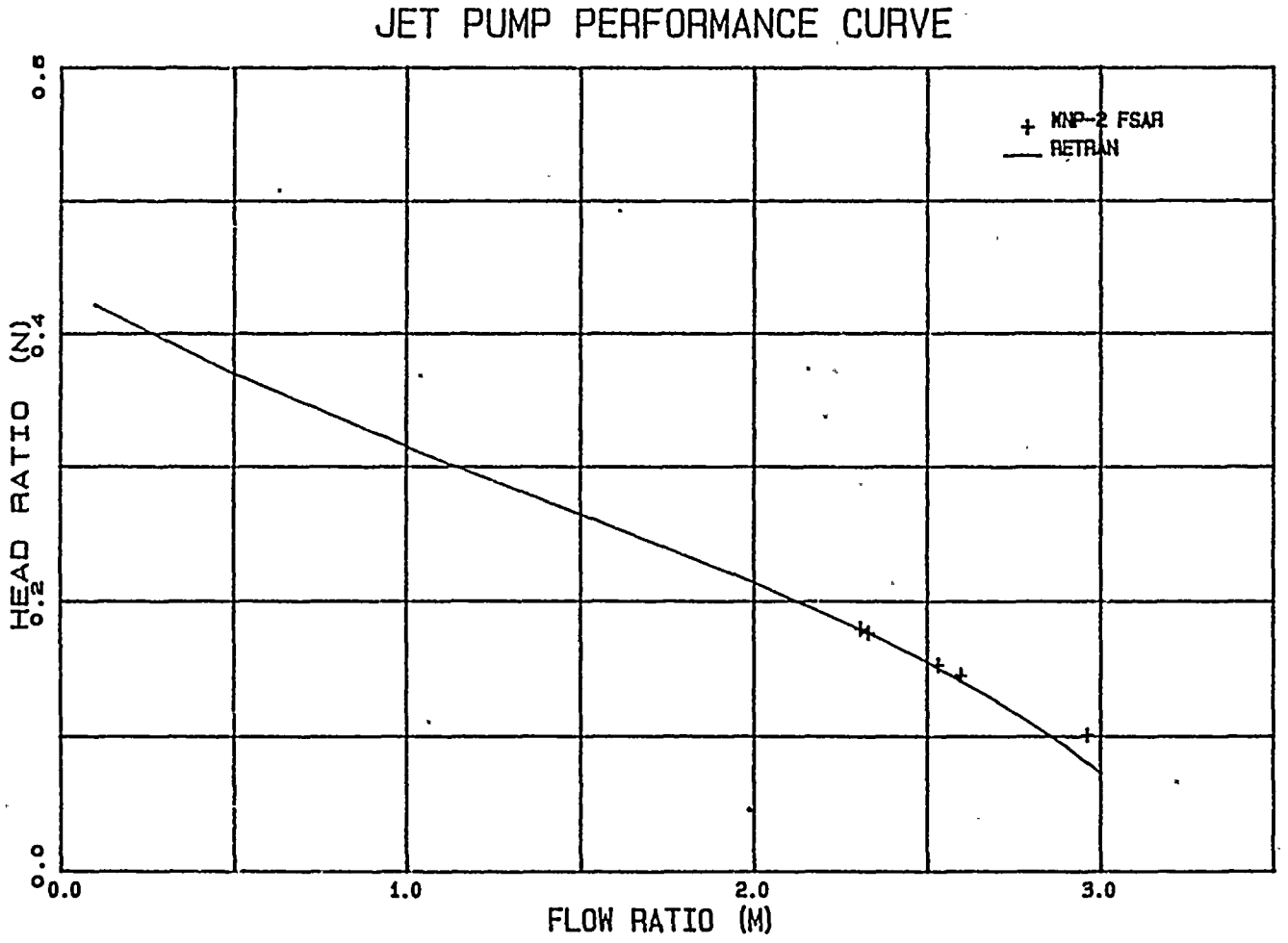
JET PUMP PERFORMANCE CURVE
+ KNP-2 FSAR
RETRAN
HEAD RATIO (N)
0.0
0.2
0.4
0.6
0.0
1.0
2.0
3.0
FLOW RATIO (M)

2.3 Trip Logic

The trip capability in RETRAN allows parameters (e.g., elapsed time, normalized reactor power, pressure, control block output, etc.) to be tested against a high or low threshold (trip setpoint). The test can then be used to activate or deactivate a system. This trip logic is used in the WNP-2 RETRAN model to simulate the actuation of the Reactor Protection System (RPS) and to initiate various valves and pump actions. Table 2.3.1 provides a description of the trip logic used in the WNP-2 RETRAN model. This trip logic can be expanded to incorporate additional trips if they are needed.

TABLE 2.3.1

DESCRIPTION OF TRIP LOGIC

TRIP ID	ACTION TAKEN	CAUSES OF TRIP ACTIVATION
01	End calculation	Simulate transient time > setpoint
02	Turbine Trip (initiate stop valve closure)	Control block -8 (water level) > setpoint (L8)
03	Initiate MSIV closure	Control block -8 (water level) < setpoint (L2) Volume 360 (turbine inlet) pressure < setpoint
05	Initiate Scram	Normalized power > setpoint Volume 16 (steam dome) pressure > setpoint Control block -8 (water level) < setpoint (L3) Trip #02 activated Trip #03 activated
06	Open S/R valve group 1	Volume 320 (steam line) pressure > setpoint
-06	reclose S/R valve group 1	Volume 320 (steam line) Pressure < setpoint
	Trips +07 through +10 are used for other four S/R valve groups	
11	Trip recirculation pumps	Simulated transient time > setpoint Trip #02 activated Volume 16 (steam dome) pressure > setpoint Control block -8 (water level) < setpoint (L2)
12	Trip FW turbine	Control block -8 (water level) > setpoint (L8)
13	RCIC initiation	Control block -8 (water level) < setpoint (L2)
-13	Trip RCIC	Control block -8 (water level) > setpoint (L8)
14	Initiate HPCS	Control block -8 (water level) < setpoint (L2)
-14	Trip HPCS	Control block -8 (water level) > setpoint (L8)

2.4 Control System Models

RETRAN control blocks (e.g., integrator, multiplier, function generator, etc.) provide for the simulation of a variety of reactor control systems. These control blocks can also be used to prepare combinations of parameters for editing and to perform other special functions as may be necessary. All of the RETRAN minor edit variables are available for use as control block inputs. Table 2.4.1 lists the control inputs used in the WNP-2 RETRAN model. The WNP-2 specific control system models are described below.

2.4.1 Feedwater Control System

The Feedwater Control System comprises a level control system and a feedwater flow delivery system. The level control system allows for either one-element or three-element control. In one-element control, the controller output is only a function of the difference in setpoint and sensed level. In the three-element control which is normally used, an additional steam-feed mismatch is added to the level error. All controller settings and gains are based on actual plant settings and the vendor's Control System Design Report[12]. The feedwater delivery system is represented by the simulation of the pump flow actuator based on vendor provided plant specific information.

Figure 2.4.1 illustrates the WNP-2 Feedwater Control System model. Upon reactor scram, the Feedwater Control System switches to one-element control and the water level setpoint is lowered 18 inches.

2.4.2 Pressure Control System

The Pressure Control System is composed of a reactor pressure regulation system, a turbine control valve system, and a steam bypass valve system. The signals from the pressure regulation system to turbine control valve and steam bypass system can be regulated either by the difference in turbine inlet pressure and its setpoint or by the load-speed error signal. The primary settings which affect the pressure regulation system output are the regulation gain and lag-lead time constants. They are based on vendor provided data[12,13]. The turbine-generator is not modeled and the turbine speed is specified as a function of time.

Figure 2.4.2 illustrates the WNP-2 Pressure Control System model. Upon a turbine trip, the turbine control valve demand signal is grounded, thus the turbine bypass valve demand is set equal to the pressure regulator demand. This will cause the bypass valves to open immediately, rather than waiting through the pressure regulator lag time constant.

2.4.3 Recirculation Flow Control System

WNP-2 is operated with the recirculation flow control system set in manual control mode. No control element is required and the flow control valve position is modeled with a function generator.

2.4.4 Direct Bypass Heating

The nonconducting heat exchanger model is used to account for direct bypass heating. The heat removal rate for this heat exchanger is determined by a control system. It is assumed to be a constant fraction of the transient core power as shown in Figure 2.4.3.

TABLE 2.4.1

CONTROL INPUT DEFINITION

ID NO.	VARIABLE SYMBOL	DESCRIPTION
01	WP**	Steam (Jct. 330) flow (% NBR)
02	WP**	FW (Jct. 490) flow (% NBR)
03	LIQV	Middle downcomer (Vol. 18) liquid volume (ft**3)
04	LIQV	Lower downcomer (Vol. 19) liquid volume (ft**3)
05	LIQV	Upper downcomer (Vol. 20) liquid volume (ft**3)
06	CONS	Fraction of total core power deposited directly in core bypass region
07	CONS	Constant of 1.0
08	POWR	active core (less core bypass) power (MW)
09	PRES	Turbine inlet (Vol. 390) pressure (psia)
10	TRIP	Scram (trip ID=5) activation indicator
11	CONS	Constant of 0.0
12	WP**	Steam (Jct. 16) flow (% NBR)
13	PRES	Turbine stop valve inlet (Vol. 360) pressure (psia)
18	TIMX	Simulation time (sec)
19	PRES	Turbine bypass inlet (Vol. 350) pressure (psia)
21	WQCR	Heat transferred from clad to coolant for core section 1 (Btu/lbm)
		ID No. 22 through 32 are used for heat to coolant for other core sections
50	CONS	Constant of 1.0
51	TRIP	Turbine trip (ID=2) activation indicator
52	CONS	Turbine speed reference (100%)
53	CONS	Load bias (10%)

FIGURE 2.4.1

Feedwater Control System

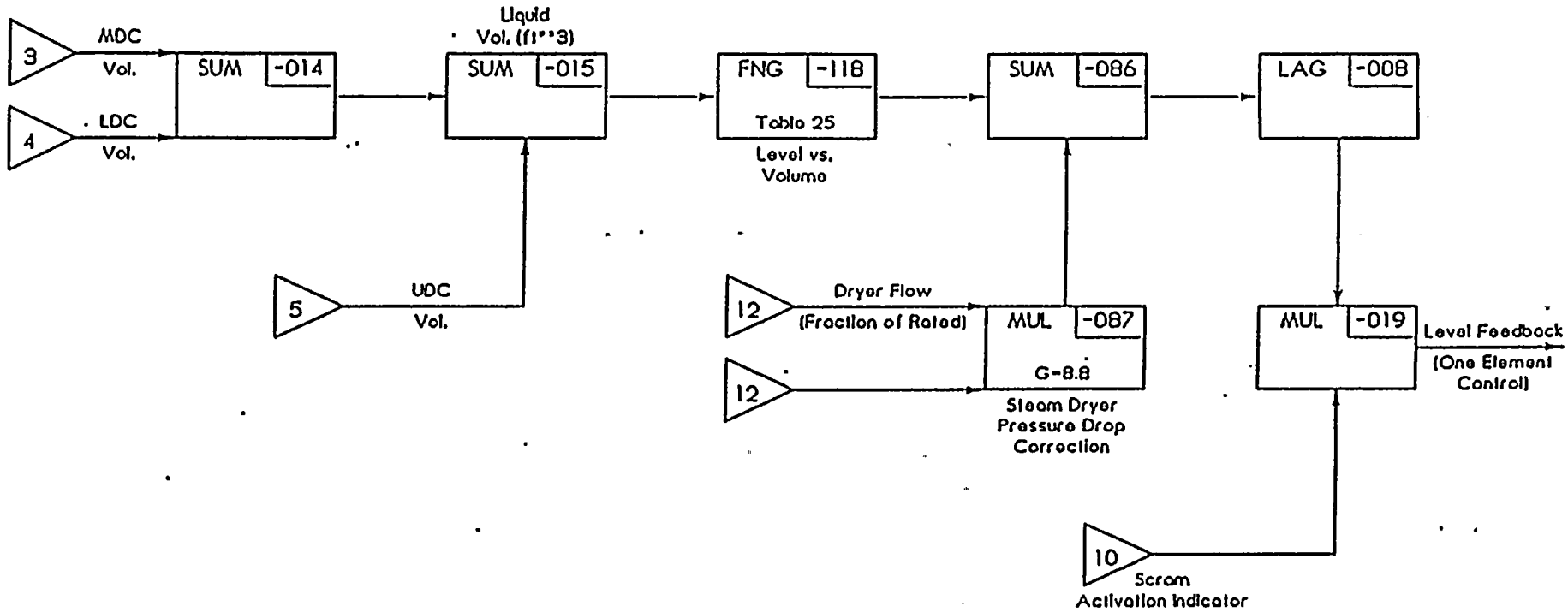

FIGURE 2.4.1 (CONT.)

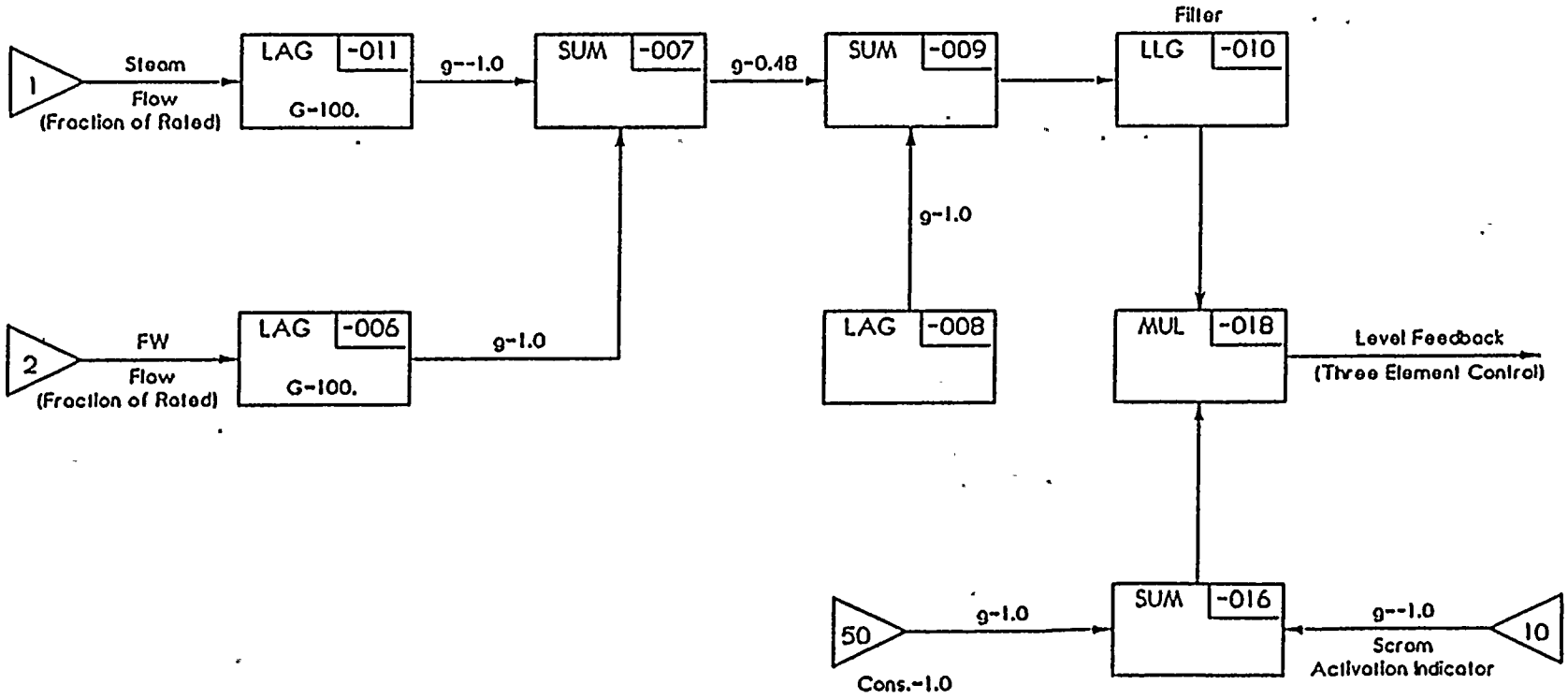

FIGURE 2.4.1 (CONT.)

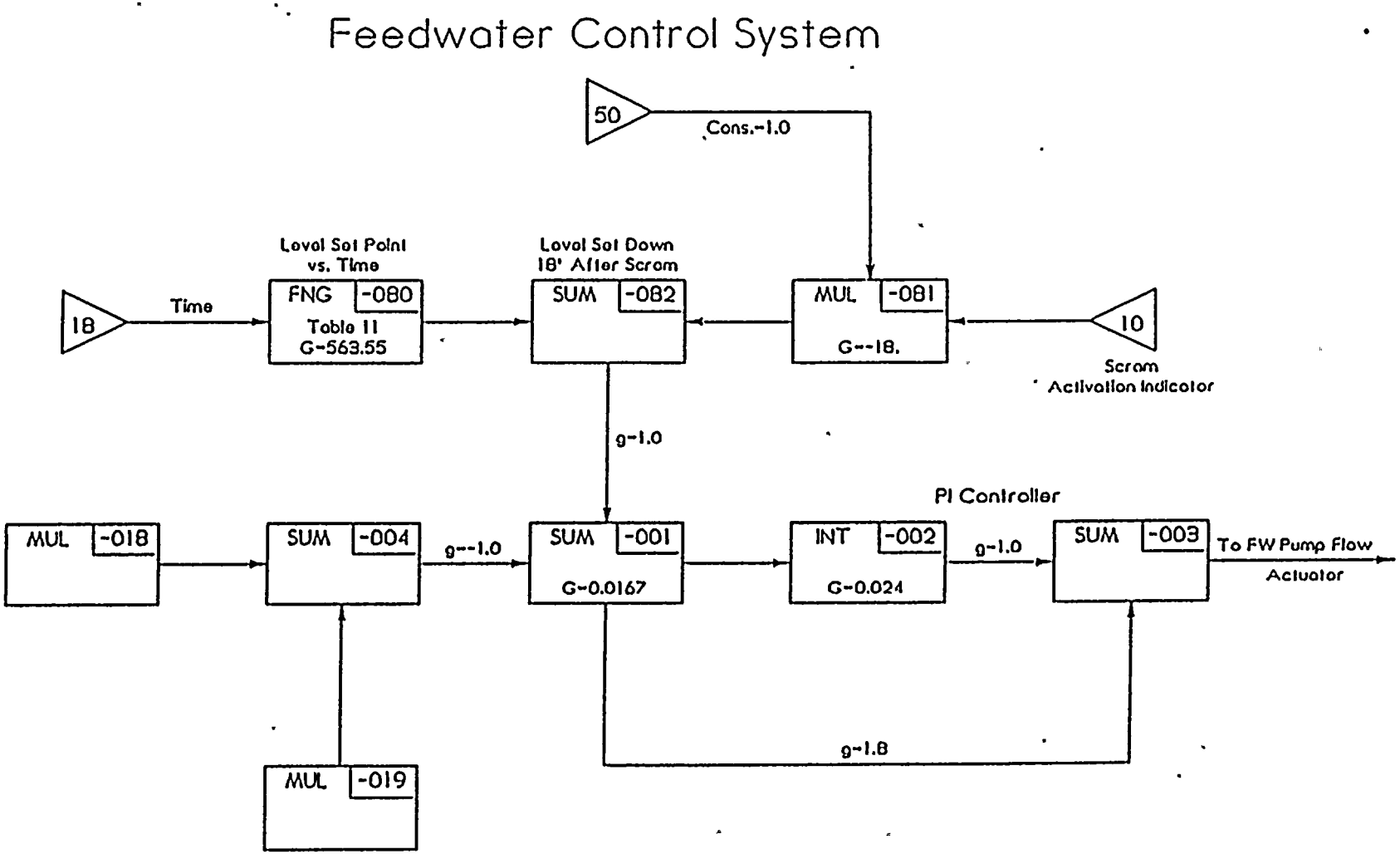

FIGURE 2.4.1 (CONT.)

Feedwater Control System
FW Pump Flow Actuator

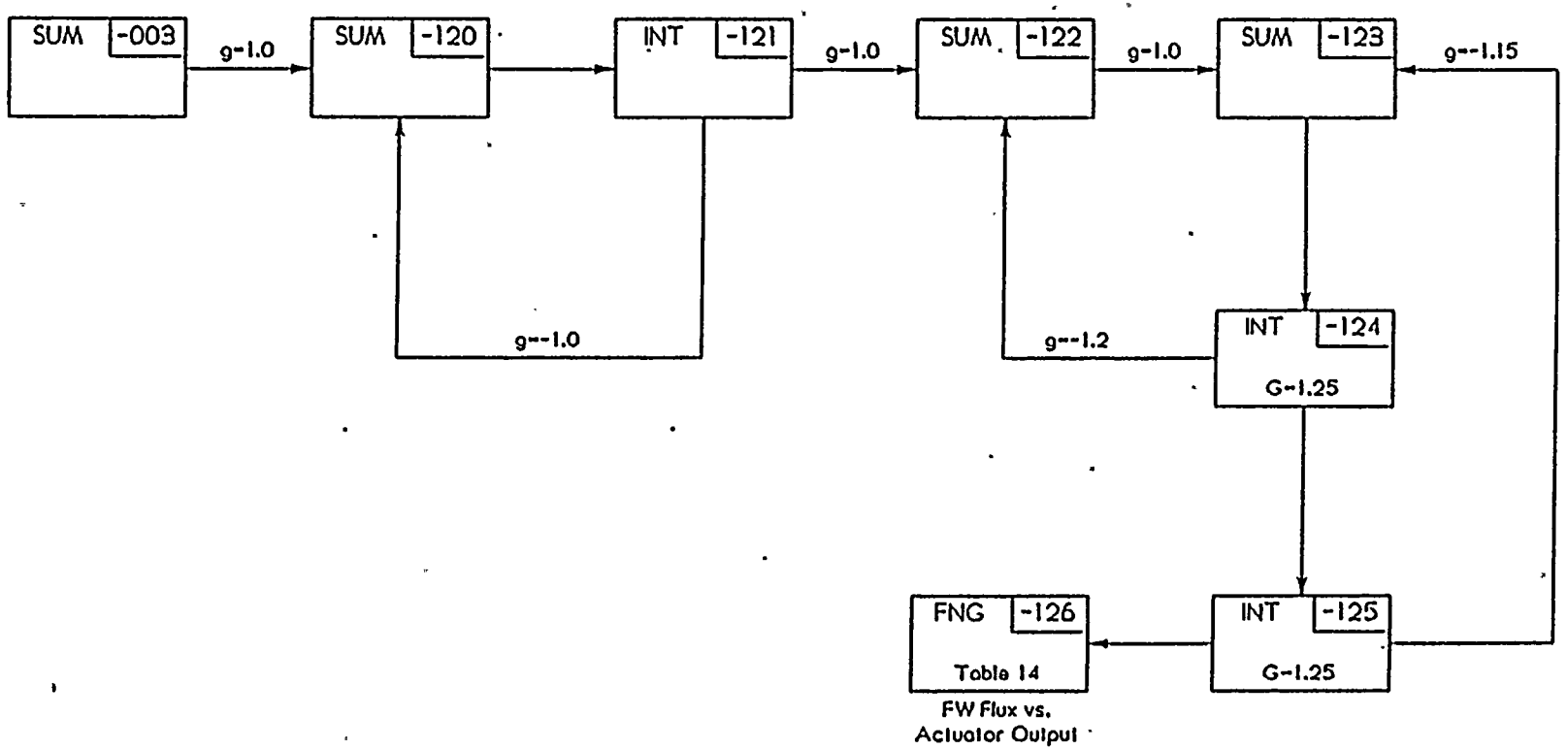

FIGURE 2.4.2

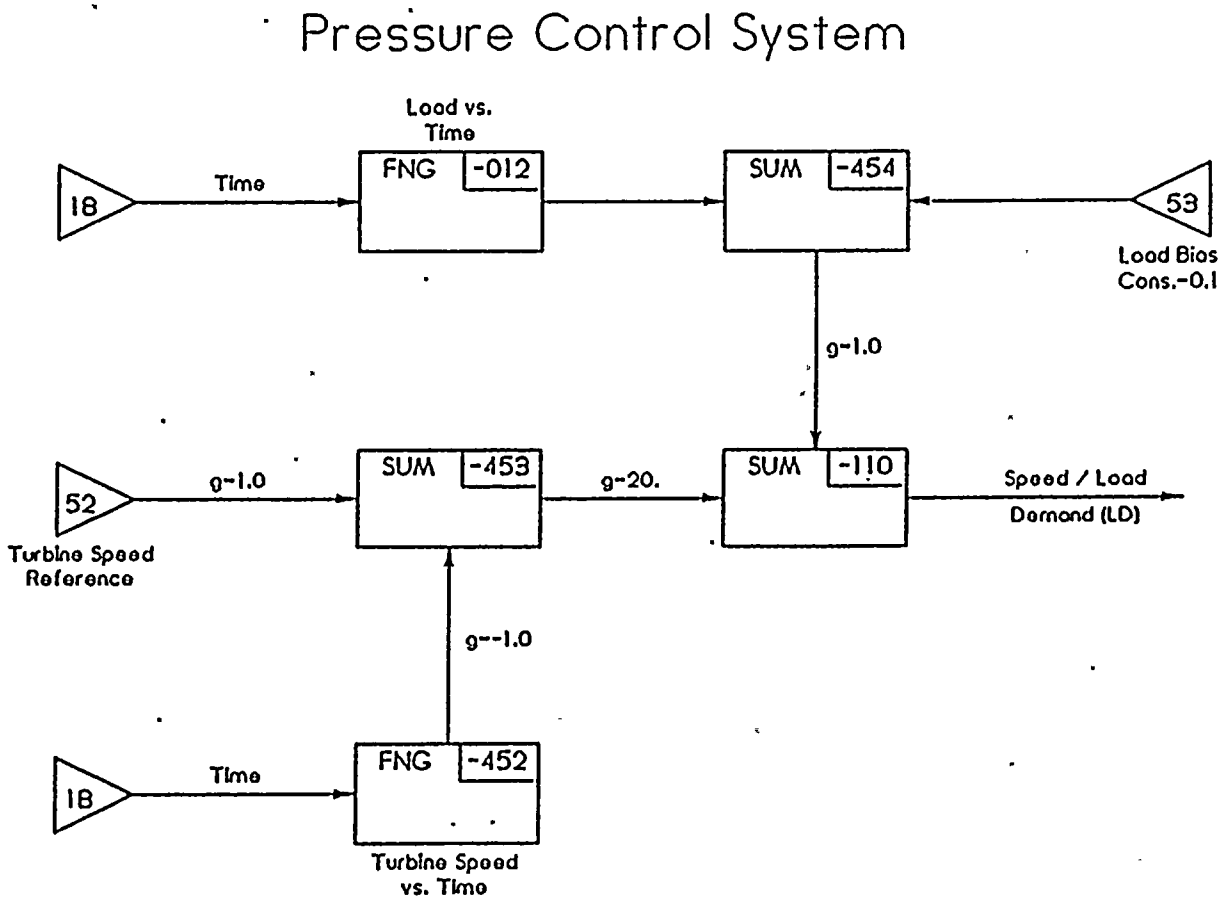
Pressure Control System
Load vs. Time
FNG -012
18
Time
SUM -454
53
Load Bias Cons.-0.1
g-1.0
SUM -453
g-20.
SUM -110
Speed / Load Demand (LD)
52
g-1.0
Turbine Speed Reference
g--1.0
FNG -452
18
Time
Turbine Speed vs. Time

FIGURE 2.4.2 (CONT.)

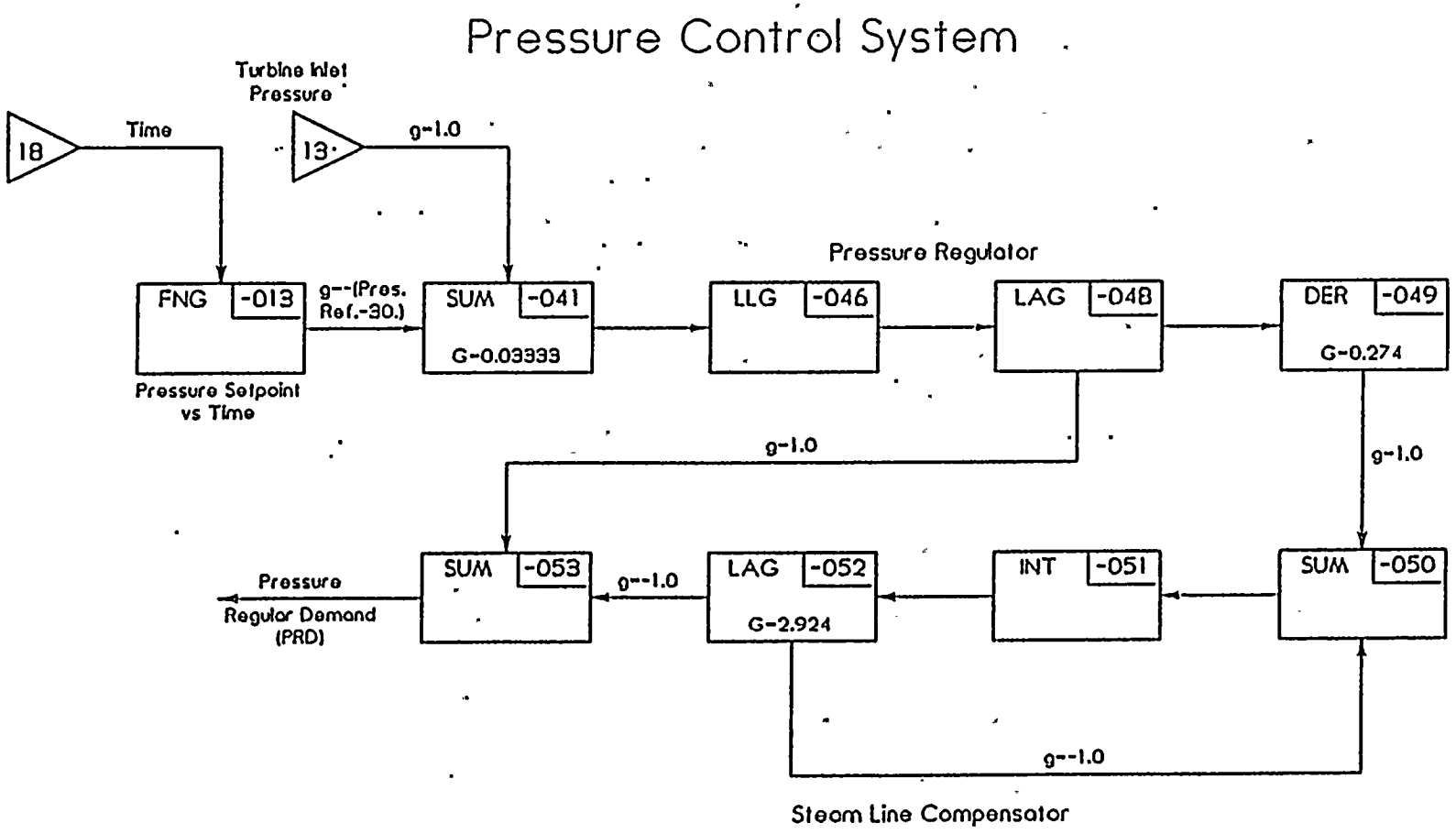

FIGURE 2.4.2 (CONT.)

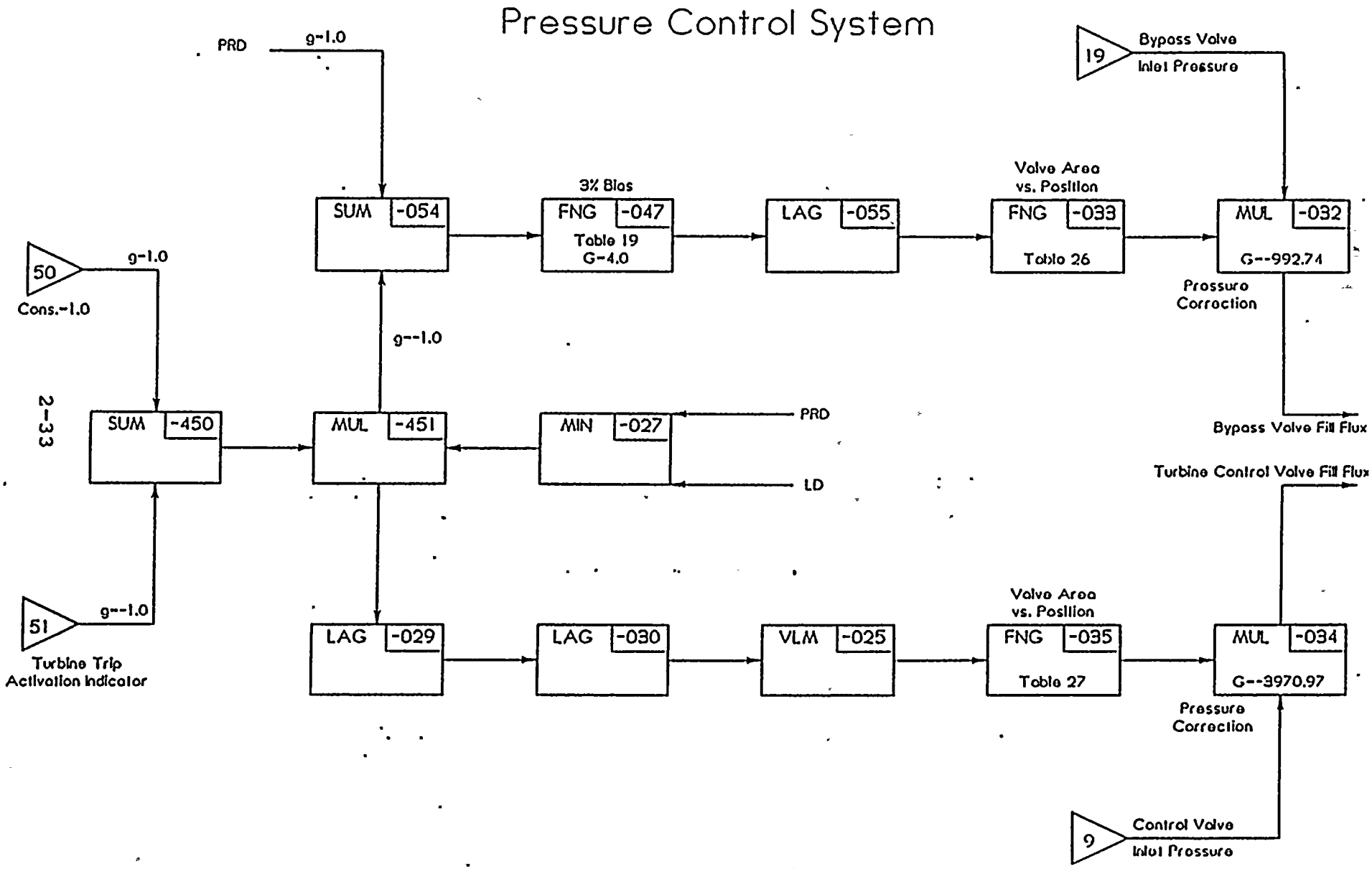

FIGURE 2.4.3

Direct Bypass Heating

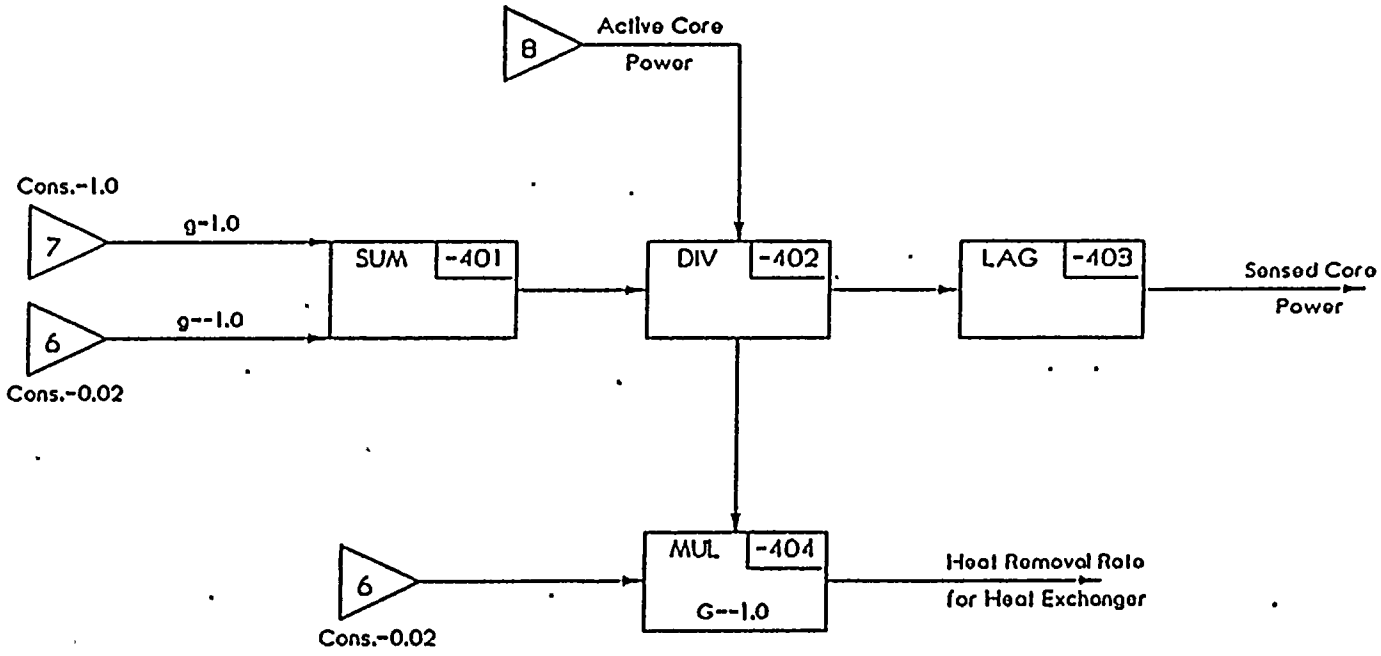

2.5 Steady-state Initialization

The RETRAN steady-state initialization option is used to initialize the model. The parameters specified for the initialization of WNP-2 model are dome pressure, core inlet enthalpy, core flows (flow through core active region and flow from lower plenum to core inlet region), recirculation flow, jet pump suction flow, feedwater and steam flows.

In addition to the inputs for the thermal-hydraulic initialization, the values of the various controller setpoints and the initial output of control elements are specified. A null transient run is performed to confirm the consistency of the thermal-hydraulic and control system initialization and to verify that the steady-state is well established.

2.6 RETRAN Kinetics

The RETRAN-02 MOD04 code has both point kinetics and one-dimensional kinetics capabilities. Selection of point or one-dimensional kinetics for a given transient depends on the accuracy requirements of the simulation. Point kinetics is used in a simulation when the axial power shape is relatively constant during the period of interest. Pressurization transients are typically analyzed with one-dimensional kinetics because the reactivity effects of void collapse and control rod movement play

an important role in determining the overall results of the calculation. The one-dimensional kinetics model provides a more accurate calculation of these effects (particularly control rod reactivity) than the point kinetics model.

The RETRAN model described herein uses nuclear cross-section information prepared by the core analysis methodology described in Reference 2. Files containing kinetics data for the various fuel types present in the reactor core are produced by CASMO-2[14], and three-dimensional nodal characteristics of the core are determined by SIMULATE-E[15]. SIMTRAN-E[3] collapses corewide cross-sections from three-dimensional form to one-dimensional or point kinetics form as required by RETRAN. Since SIMULATE-E and RETRAN calculate moderator density differently, the SIMTRAN-E cross-sections are adjusted manually to account for the difference. This process is described more fully in Section 2.6.1 below.

2.6.1 General Description of the Generation of One-dimensional Data

The first step in the process uses the EPRI codes SIMULATE-E and SIMTRAN-E. SIMULATE-E predicts core power and burnup distributions during detailed depletion analyses of the reactor core. Qualification of the Supply System's SIMULATE-E methodology is provided elsewhere[2].

SIMTRAN-E was developed under EPRI sponsorship for linking SIMULATE-E and RETRAN. SIMTRAN-E reads restart files written by SIMULATE-E, extracts the appropriate information for determining the kinetics parameters, and generates the direct RETRAN input for transient analysis.

In this first step, SIMTRAN-E produces a one-dimensional kinetics data file in the form of polynomials which describe the effects of relative changes in water density and fuel temperature on calculated two-group cross sections, diffusion coefficients, inverse neutron velocities, radial bucklings, and delayed neutron fractions. This data file could be used directly by RETRAN. However, without the adjustments described below, this approach would lead to very conservative RETRAN predictions for severe pressurization events. For benchmark analysis of pressurization events, this conservatism would create artificially large uncertainty factors.

The kinetics conservatism is due to differences between the SIMULATE-E model of core average thermal hydraulics and the RETRAN model of average channel thermal hydraulics. As a result of these difference, SIMULATE-E and RETRAN predict different changes in average moderator density for the same change in core pressure. Since SIMTRAN-E receives data only from SIMULATE-E, it cannot adjust for the differences. Therefore, a manual adjustment is made to the SIMTRAN-E output in the second step in

the kinetics process. This step produces a revised data file consisting of a set of adjusted polynomials that can be used directly by RETRAN in the best estimate mode.

Except as noted in the text, all of the transient benchmark and example analyses described in this report used the adjusted kinetics parameters as produced by the second step of the kinetics process. For transients which do not involve a substantial change in moderator density, the adjustment is unnecessary because the induced conservatism is small.

Verification of the Supply System's methodology utilizing a pre-released version of SIMTRAN-E is discussed in Section 2.6.4, below.

2.6.2. Calculation of the Initial Kinetics Input Data

To begin the first step in the generation of the one-dimensional data, a nominal SIMULATE-E case is run at a core configuration consistent with the initial conditions for the given transient. This nominal SIMULATE-E case uses power and void feedback to determine the three-dimensional core power and flux distributions and the critical eigenvalue. The nominal SIMULATE-E case uses cross-sections which have not been adjusted to match k-infinities of the lattice physics code (i.e. unadjusted Σ_{a1}), but it is run from a SIMULATE-E restart file generated with cross-sections

which were adjusted to match k-infinities of the lattice physics code (i.e. adjusted Σ_{a1}).

For transients in which it is necessary to model the effects of control rod insertion resulting from a scram, an additional SIMULATE-E case is required. This case is based on the nominal case and is run with power feedback disabled. The only difference between this case and the nominal case is the control rod position array, which has all rods fully inserted.

As noted above, SIMTRAN-E reads the restart files generated by the SIMULATE-E cases. It then collapses the three-dimensional SIMULATE-E data to one-dimensional data for RETRAN and determines the dependence of the kinetics parameters on relative water density, square root of fuel temperature, and control state.

SIMTRAN-E generates all kinetics parameters except $k\Sigma_{f1}$ and $k\Sigma_{f2}$ by radial collapse with adjoint flux weighting. $k\Sigma_{f1}$ and $k\Sigma_{f2}$ are radially collapsed with volume weighting. The dependence of the kinetics parameters on water density and fuel temperature is determined by making perturbations in these quantities. All relative water density and square root of average fuel temperature perturbations are done in three dimensions and are then radially collapsed. The one-dimensional nominal and perturbed kinetics variables are then analyzed to produce polynomials that are functions of the relative change in water

density and the change in the square root of the average fuel temperature at each axial node. This procedure is performed for both the nominal case and for the controlled case.

2.6.3. Adjustment of Kinetics Data

To begin the second step in the generation of the one-dimensional data, the SIMTRAN-E output from the first step is used and parallel SIMULATE-E and RETRAN cases are run to quantify the difference in axial moderator density distributions between the two models for identical variations in core pressure.

The coefficients in the kinetics parameter polynomials that are associated with the changes in relative moderator density are then modified so the change in each kinetics variable in RETRAN for a given pressure change is the same as that pressure change would give in the one-dimensional SIMTRAN-E model. Thus reactivity changes at each axial node generated by a pressure change are preserved between SIMTRAN-E and RETRAN. The constant term in each kinetics parameter polynomial determines the initial steady state eigenvalue in the RETRAN unperturbed state. The constant terms are not modified when new polynomial fits are developed; consequently, the SIMULATE-E eigenvalue is preserved in the RETRAN unperturbed state.

The cross section libraries used in the core physics analysis are based on ENDF/B-III. ENDF/B-III includes delayed neutron fractions which are artificially low. Preliminary ENDF/B-V data shows an increase in delayed neutron fraction ranging upwards from 5.4% in all fissile isotopes. To bring the delayed neutron fraction closer to those specified in ENDF/B-V, a +5% manual adjustment is applied to all delayed neutron fractions before final data is put into the RETRAN input file.

2.6.4. Verification of the Supply System's Methodology

The Supply System's version of SIMTRAN-E is not a formally released EPRI code. Results obtained by this version were reviewed by EI International and were found to be acceptable[16]. Further verification was obtained by the Supply System for the steady state results by comparing the axial power distributions produced by SIMTRAN-E for the initial states of the three Peach Bottom turbine trip tests. Figures 2.6.1, 2.6.2 and 2.6.3 show the axial power shapes predicted by RETRAN compared to those predicted by SIMULATE-E and by the process computer for the initial state of each of these turbine trips. In each case, the RETRAN model is based on the one-dimensional kinetics input produced by SIMTRAN-E and modified as described above.

The ultimate validation of the SIMTRAN-E calculation is the accuracy with which RETRAN predicts system behavior in benchmark

transient analyses. The transient mode is validated by the predictions of the Peach Bottom turbine trip tests, which also match the data closely. These results are shown in Section 3.2.

FIGURE 2.6.1
Initial Axial Power Distribution
Peach Bottom Unit 2 TT1

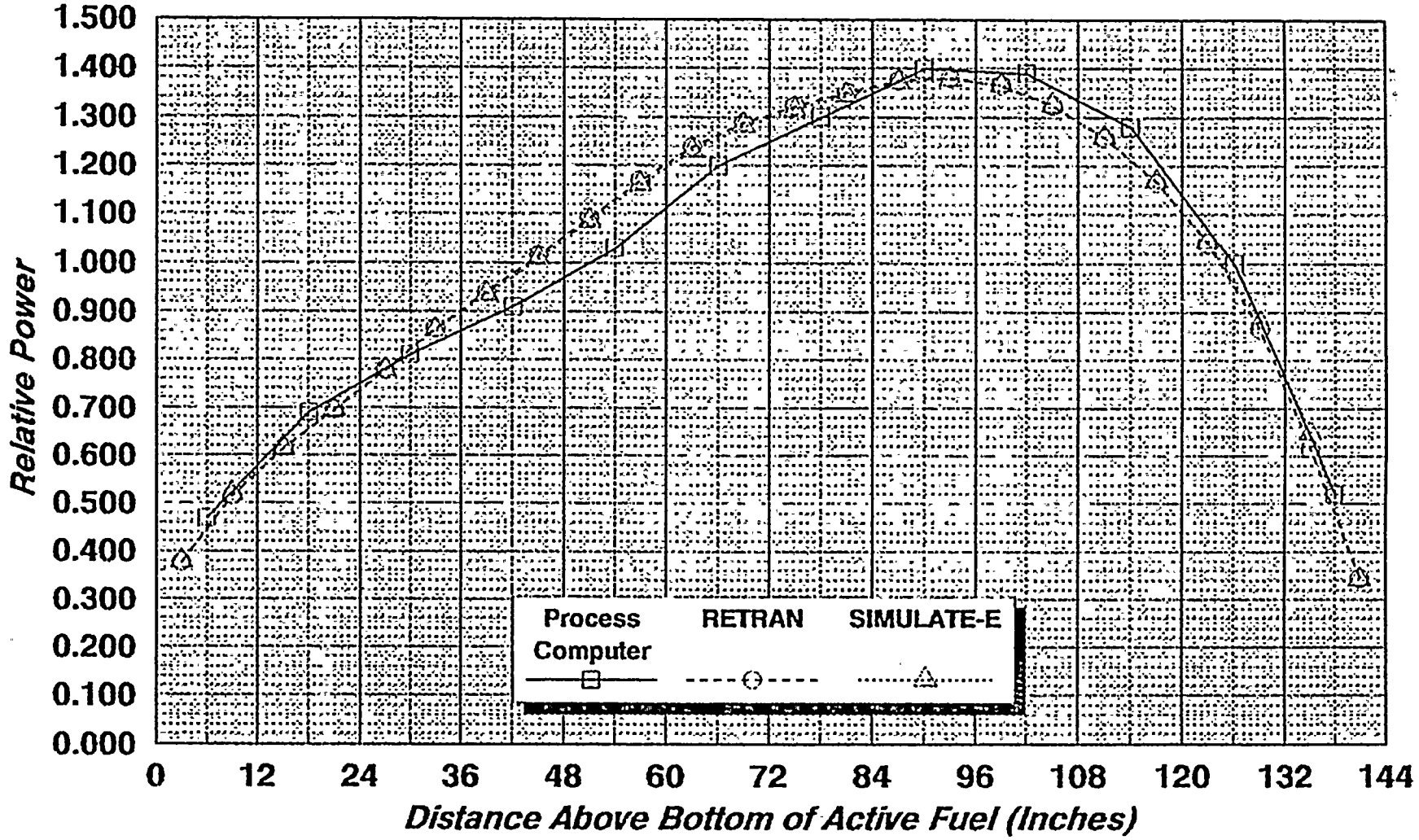

FIGURE 2.6.2
Initial Axial Power Distribution
Peach Bottom Unit 2 TT2

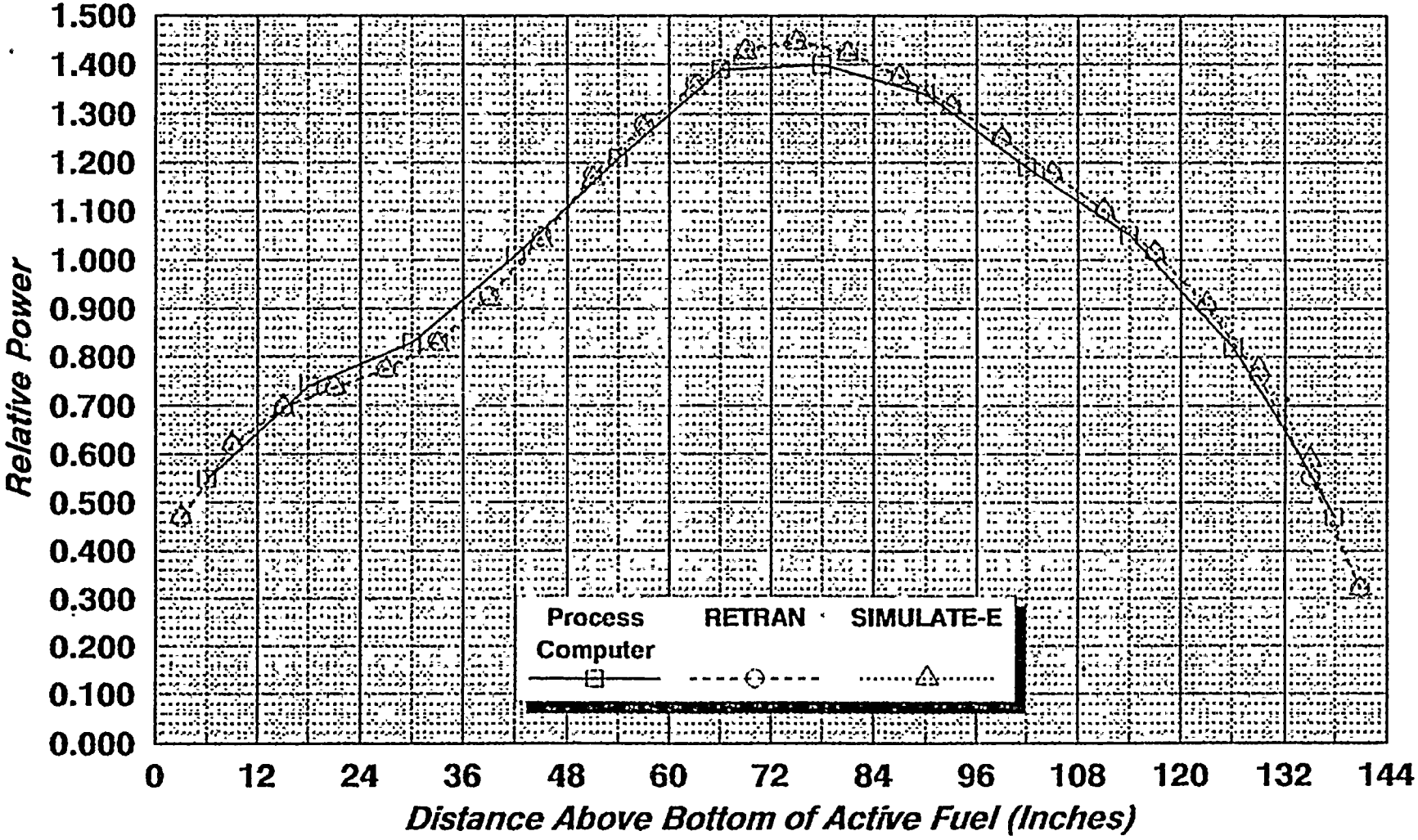

FIGURE 2.6.3
Initial Axial Power Distribution
Peach Bottom Unit 2 TT3

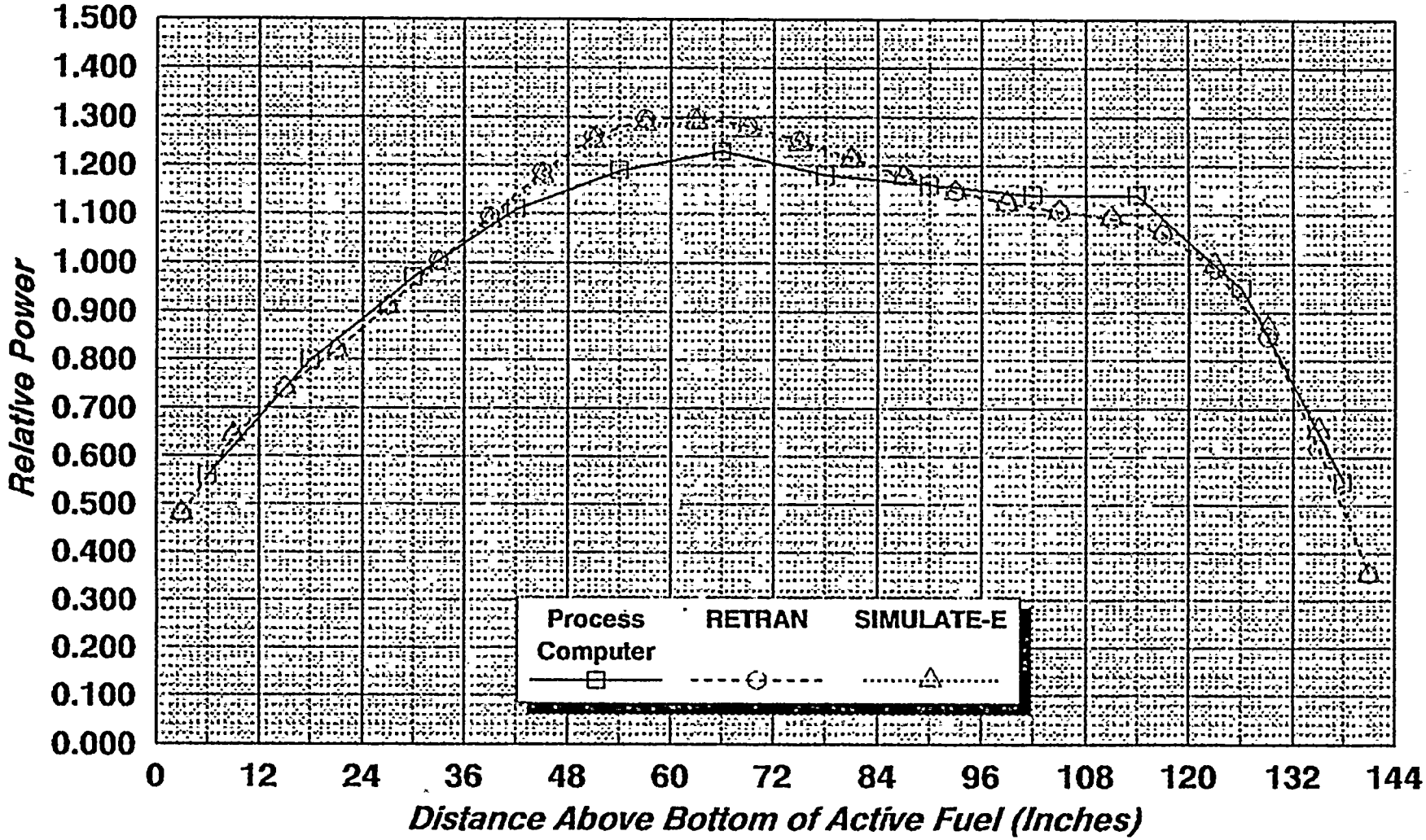

3.0 QUALIFICATION

The objective of this chapter is to compare the Supply System's RETRAN simulation with WNP-2 power ascension tests (PAT) and Peach Bottom turbine trip tests. The Supply System performed these benchmark analyses to qualify the WNP-2 RETRAN model and to demonstrate user qualifications. The benchmarks comprise four WNP-2 PAT tests and three Peach Bottom turbine trip tests.

These benchmark analyses, which were performed in the best-estimate mode, qualify the WNP-2 RETRAN model for the licensing basis analysis presented in the next chapter.

3.1 WNP-2 Power Ascension Tests

During the period of October -December 1984, a series of power ascension tests (PAT) at near full power were performed at WNP-2[17]. The data from these tests is available for verifying the WNP-2 RETRAN model. All of the transients analyzed in this chapter were recorded during the initial WNP-2 PAT testing.

The best-estimate model described in Chapter 2 was used in the PAT analyses and the best-estimate analyses, discussed below, verify the modeling. For future reload analysis, the licensing basis model will be used to assure conservatism in the output. The licensing basis model is discussed in Chapter 4.

The power ascension tests chosen for benchmark are as follows:

1. Water level setpoint change - This transient is used mainly to benchmark the feedwater control system, water level prediction and general stability of the RETRAN model.

2. Pressure regulator setpoint changes - This transient is used to benchmark the pressure regulator control system, RETRAN stability and system model accuracy.

3. One recirculation pump trip - This transient is to benchmark the pump coastdown characteristics and system response to an asymmetric recirculation flow variation.

4. Generator load rejection with bypass - This transient is used to benchmark the steam line modeling and system pressurization behavior.

Since the PAT transients are milder than the limiting transients in licensing basis analysis, the first three transients were analyzed using the point-kinetics core modeling. The one-dimensional kinetics model was also run for the recirculation pump trip case to demonstrate the validity of the point kinetics model for these relatively mild events.

The load rejection with bypass transient was analyzed using the

one-dimensional kinetics model. This treatment is consistent with the example licensing basis transient analysis (load rejection without bypass) in the next chapter.

3.1.1 Water level Setpoint Change (Test PAT 23A)

The purpose of Test PAT 23A was to demonstrate the stability of the level control system. Test PAT 23A was initiated at 95.1% power and 96.8% flow. The test procedure consisted of a six-inch step increase in vessel water level setpoint, a delay to allow the system to reach a new equilibrium condition, and a six-inch step decrease in vessel water level setpoint.

3.1.1.1 RETRAN Model for Test PAT 23A

Since the test condition is near the rated condition, the standard RETRAN base model at rated condition as presented in Chapter 2 is used to start the transient simulation. To model the step change of the level setpoint, a general function table used in the level setpoint control block (Control Block 80) is modified.

3.1.1.2 Results and Discussions

The water level setpoint step change test was analyzed mainly to qualify the feedwater control system and vessel water level models. It also confirms the adequacy of the RETRAN thermal-hydraulic and neutronic coupling.

The vessel water level in this test is maintained at a specified setpoint through the variation of the feedwater flow which is

controlled by the feedwater control system. The feedwater controller uses vessel water level and the mismatch between steam flow and feedwater flow to determine the feedwater pump speed, which controls feedwater flow. The controller responds to an increase in vessel water level setpoint by increasing feedwater flow. This increased feedwater flow causes water level in downcomer to increase and the water temperature in core inlet to decrease. The reduced core inlet temperature leads to a reduced core void, resulting in a core power increase. The feedwater controller, after detecting water level increase, will reduce feedwater flow, which leads to a reduction in power. This combination of feedwater control logic and core response will lead to a new steady state for both core power and feedwater flow close to their initial values and the water level will be stabilized at the new setpoint.

Figure 3.1.1 shows the measured and calculated feedwater flow response. Similarly, Figure 3.1.2 shows the measured and calculated water level. These plots show that the RETRAN model predicts events and timing consistent with the data.

Figure 3.1.2 indicates that RETRAN calculates a water level that approaches a value that is six inches higher than the initial water level at about 20 seconds after the setpoint change. The measured data indicates a higher asymptotic value of 7.8 inches in water level change, which may indicate an inconsistency between the level step change used in the analysis and actual test.

Other parameters (steam flow, dome pressure and core power) are not plotted because they did not show any significant changes (less than 3% variation from steady state values) throughout the test.

Figure 3.1.1

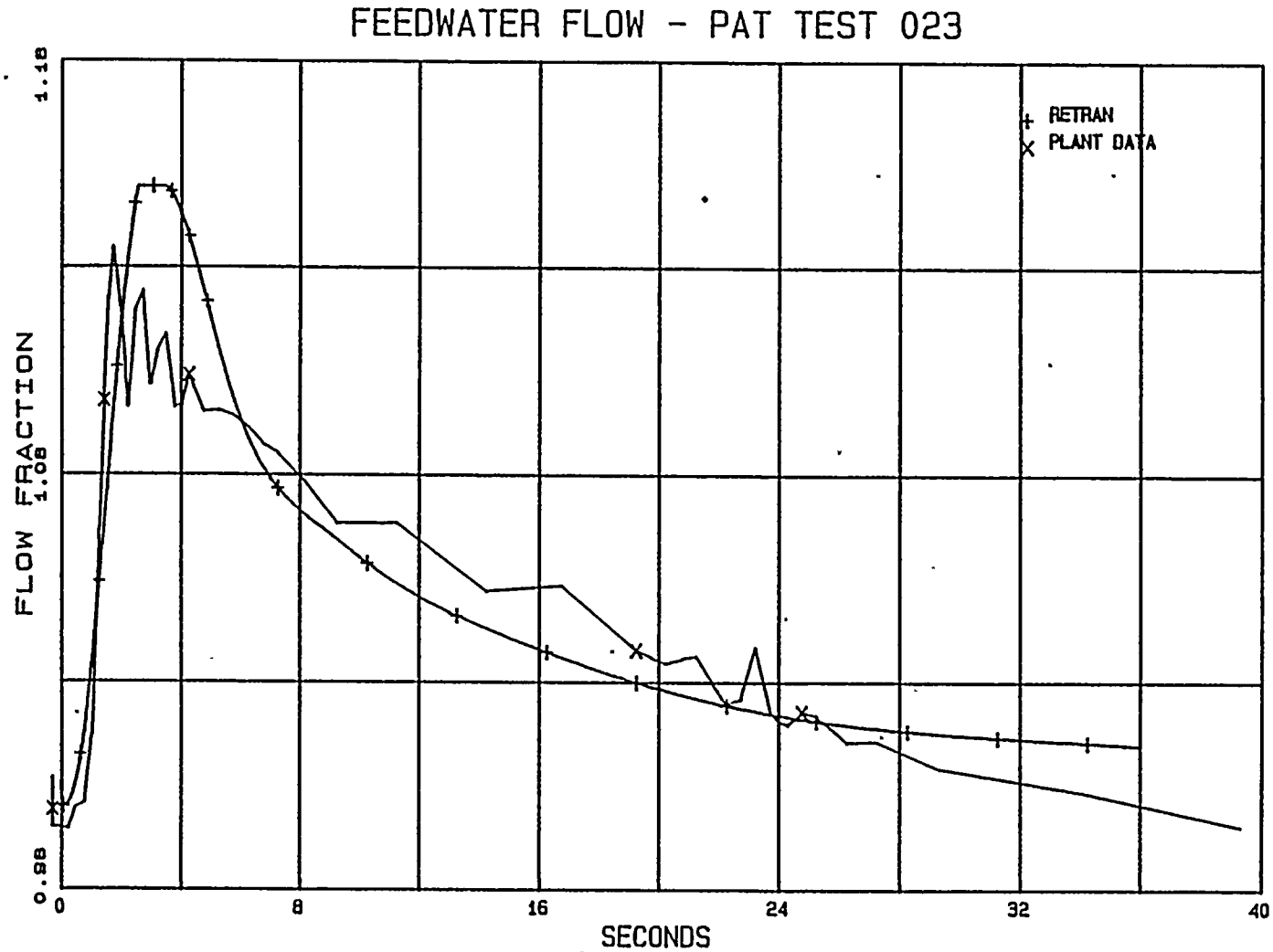
FEEDWATER FLOW - PAT TEST 023
RETRAN
PLANT DATA
FLOW FRACTION
1.18
1.08
0.98
0
8
16
24
32
40
SECONDS

Figure 3.1.2

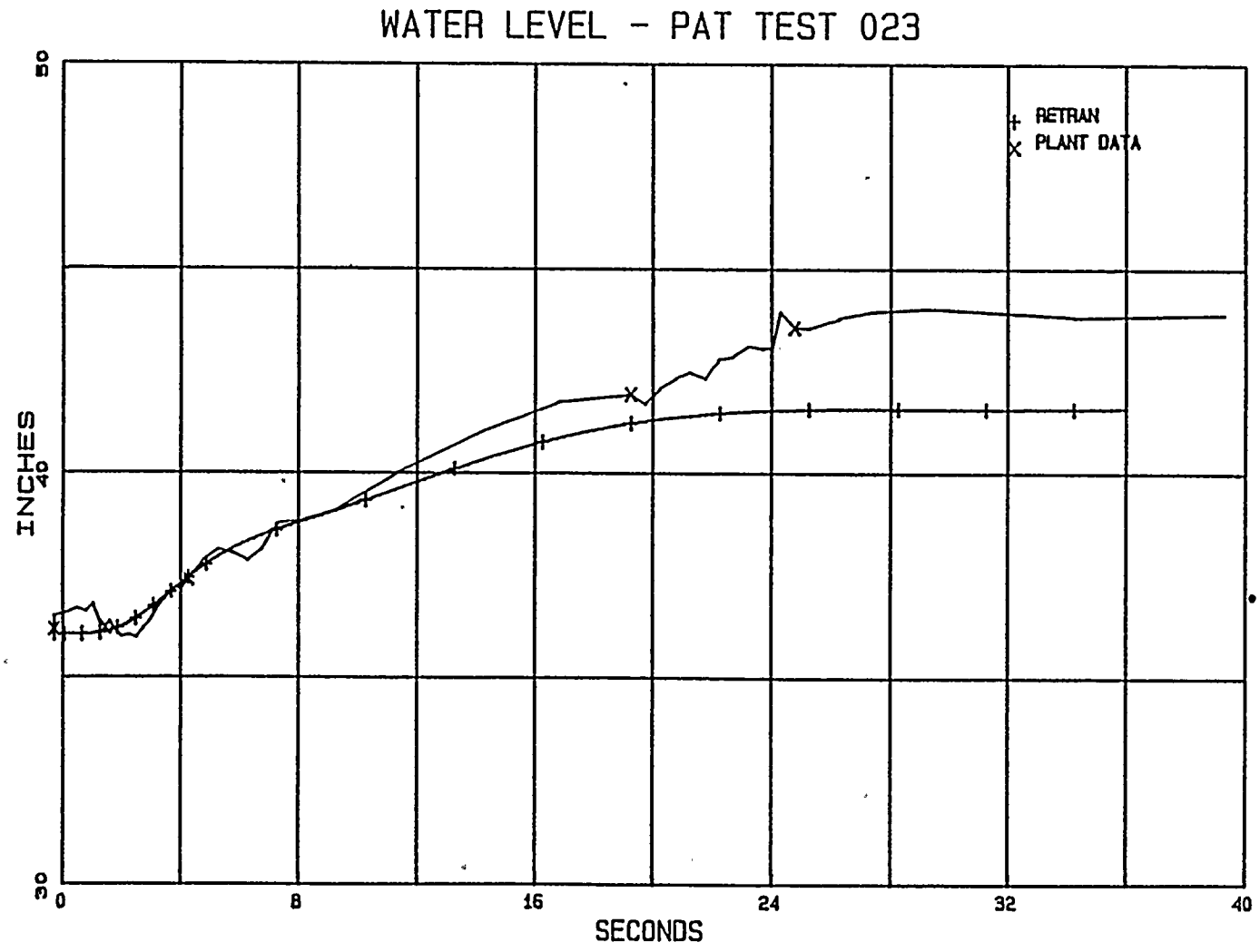
WATER LEVEL - PAT TEST 023
RETRAN
PLANT DATA
INCHES
50
40
30
0
8
16
24
32
40
SECONDS

3.1.2 Pressure Regulator Setpoint Change (Test PAT 22)

Test PAT 22 was performed to demonstrate the stability of the pressure control system. Test PAT 22 was initiated at 97.5% power and 95.9% flow. The test procedure consisted of a 10-psi step decrease in pressure regulator setpoint, a delay to allow the system to reach a new equilibrium condition, and a 10-psi step increase in pressure regulator setpoint to the original value.

3.1.2.1 RETRAN Model for Test PAT 22

Test PAT 22 was analyzed with the standard RETRAN base model (cf. Chapter 2). The initial dome pressure in the RETRAN base model is 1020 psia, which differs slightly from the 990-psia test pressure. The transient is very mild and the response to the step change in pressure setpoint was not expected to be sensitive to the small difference in initial pressure.

To model the test, a general function table used for the pressure setpoint control block (Control Block 13) is changed to reflect the step change of the pressure setpoint.

3.1.2.2 Results and Discussions

In this test, the pressure regulator and the Digital Electro-Hydraulic Control System (DEH) will respond to a decrease in

pressure regulator setpoint by opening the turbine control valves to allow more steam flow which reduces system pressure. The resulting decreased system pressure increases core voiding and thus reduces core power. As pressure decreases, the pressure regulator and DEH control system starts to close the turbine control valve. The pressure will eventually be stablized at the new setpoint.

Figure 3.1.3 shows the measured and calculated transient pressure response. The pressure settles out at about 10 psi below the initial pressure, indicating good alignment of the pressure system control model.

Figure 3.1.4 presents the measured and calculated power behavior. The system stabilizes back to the initial power rapidly, and the RETRAN model predicts this behavior consistently with the data.

Figure 3.1.5 shows the measured and calculated steam flow. Figure 3.1.6 presents the measured and calculated feedwater flow. The calculation matches the plant data closely in both of these areas.

The simulation/data comparisons indicate that the pressure regulation control system in the WNP-2 RETRAN model performs as intended.

Figure 3.1.3

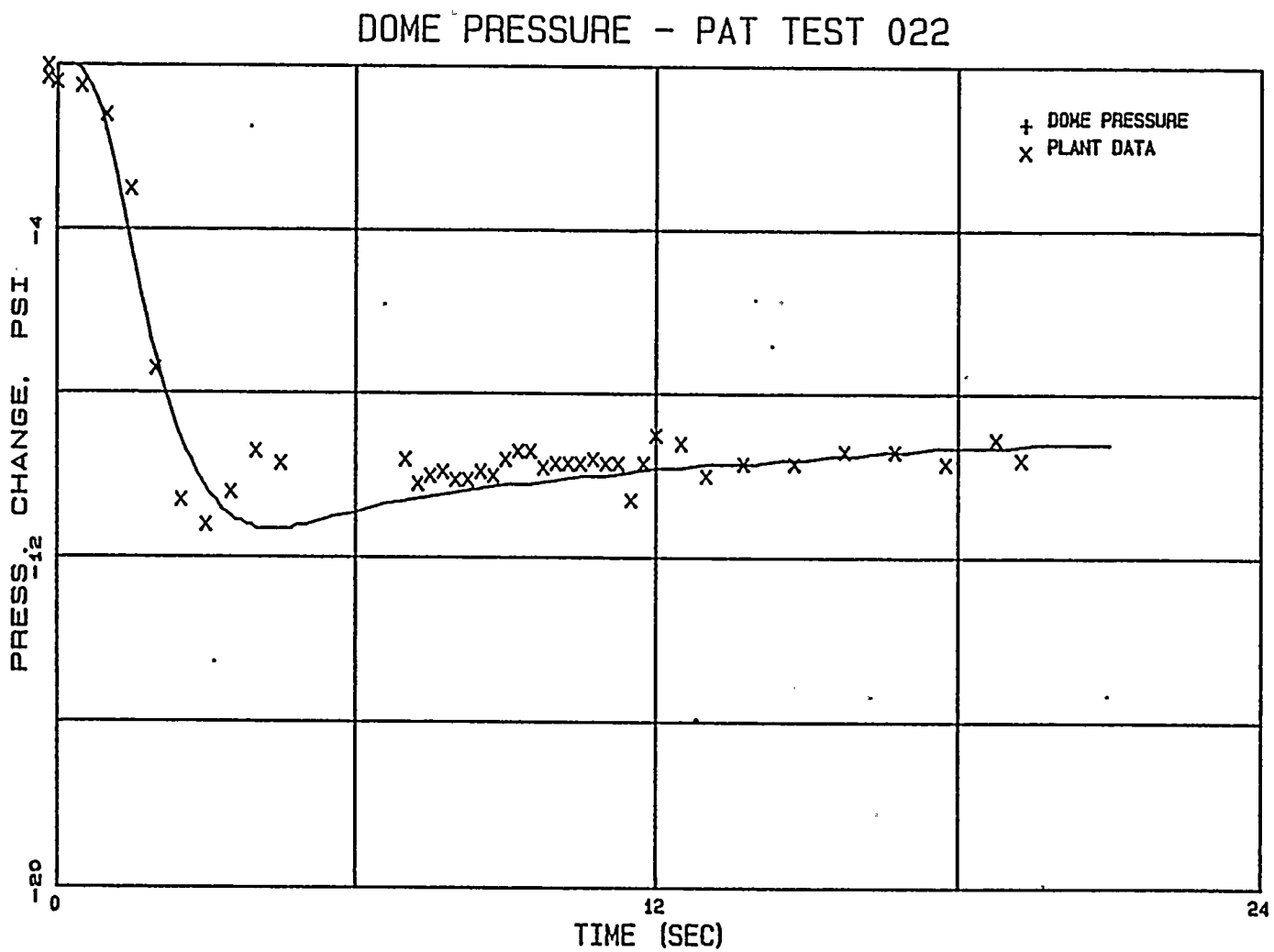
DOME PRESSURE - PAT TEST 022
DOME PRESSURE
PLANT DATA
PRESS. CHANGE, PSI
-4
-12
-20
0
12
24
TIME (SEC)

Figure 3.1.4

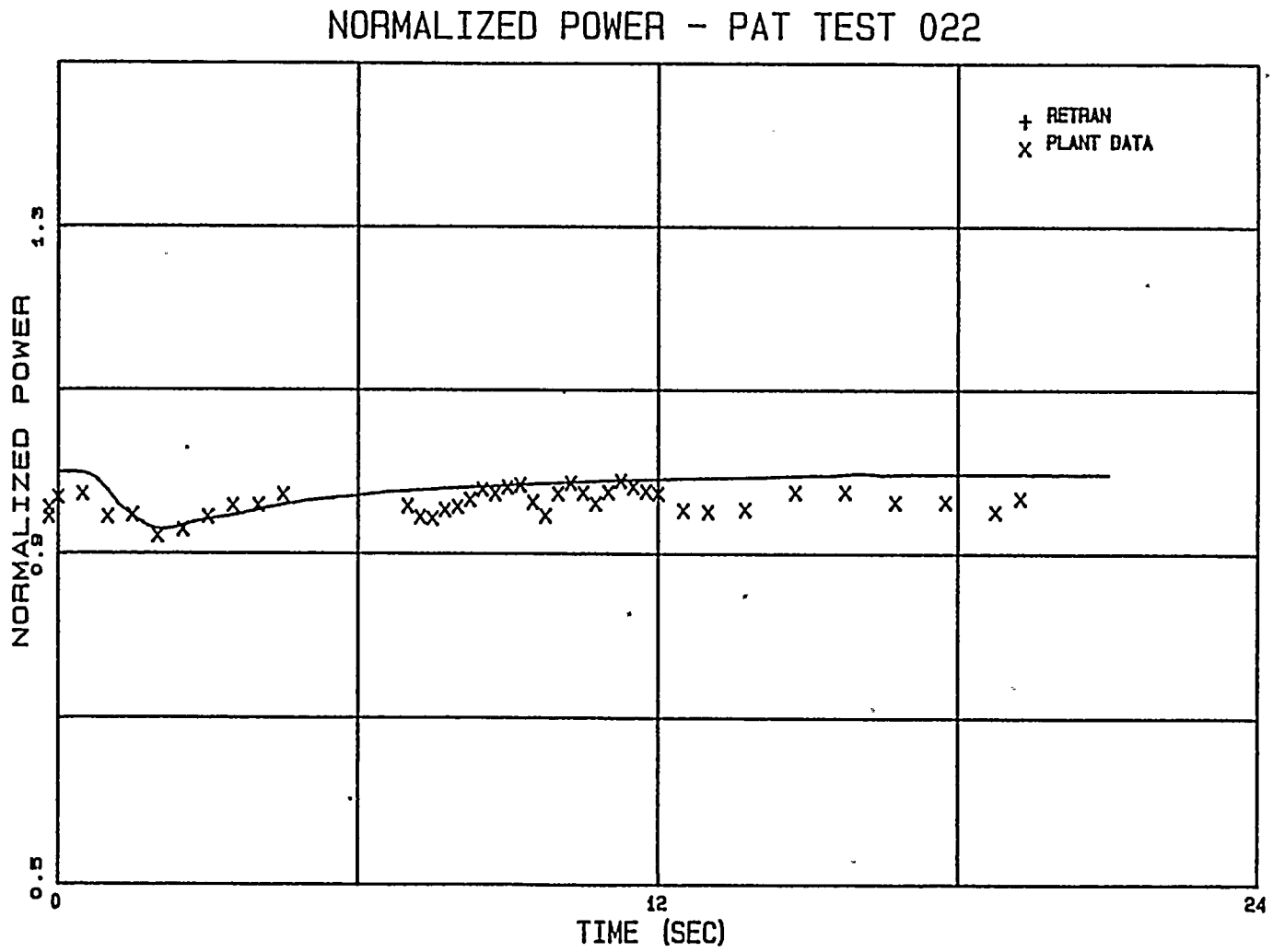
NORMALIZED POWER - PAT TEST 022
+ RETRAN
X PLANT DATA
NORMALIZED POWER
1.3
0.9
0.5
0
12
24
TIME (SEC)

Figure 3.1.5

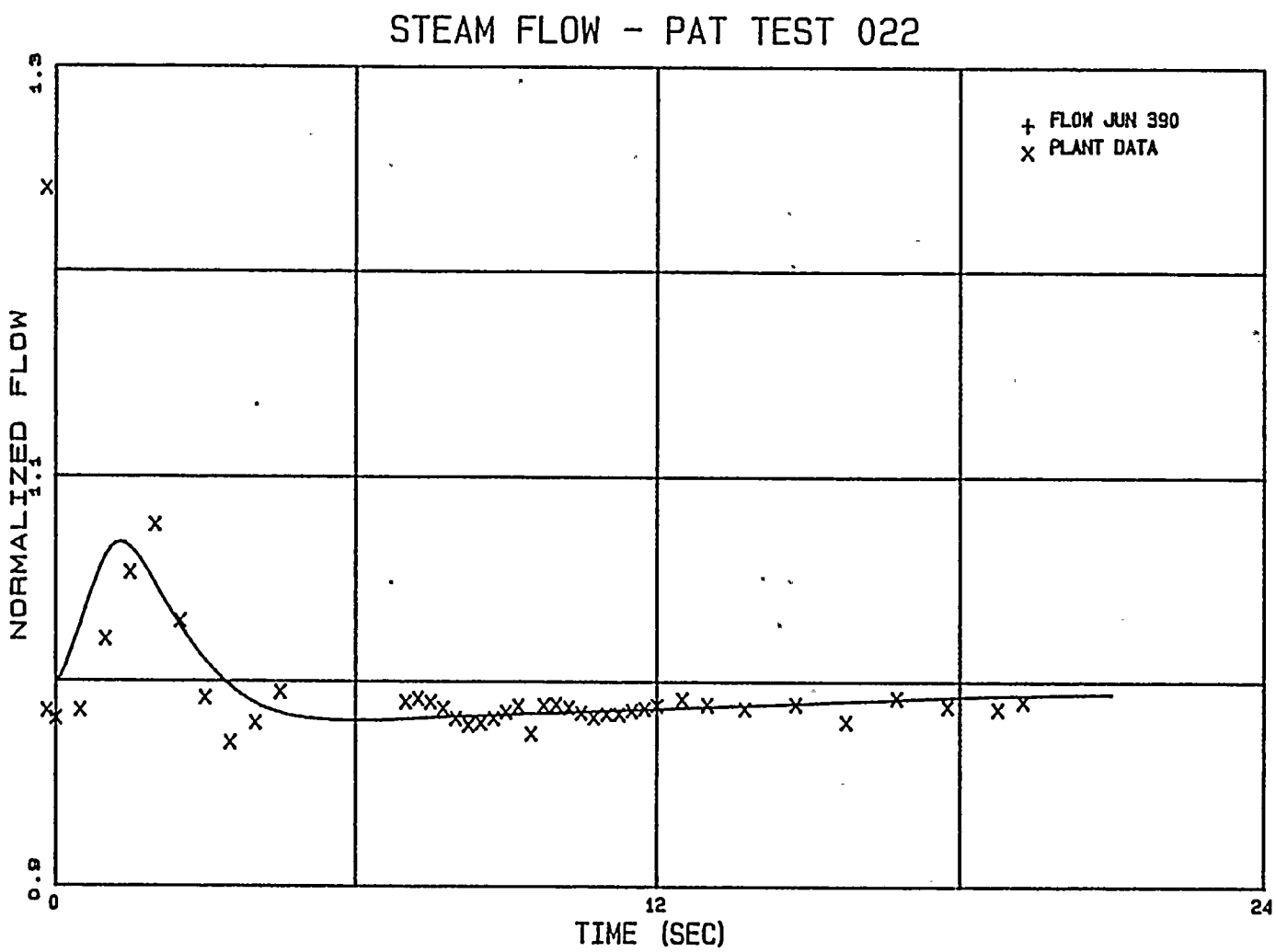
STEAM FLOW - PAT TEST 022
FLOW JUN 390
PLANT DATA
NORMALIZED FLOW
1.3
1.1
0.9
0
12
24
TIME (SEC)

Figure 3.1.6

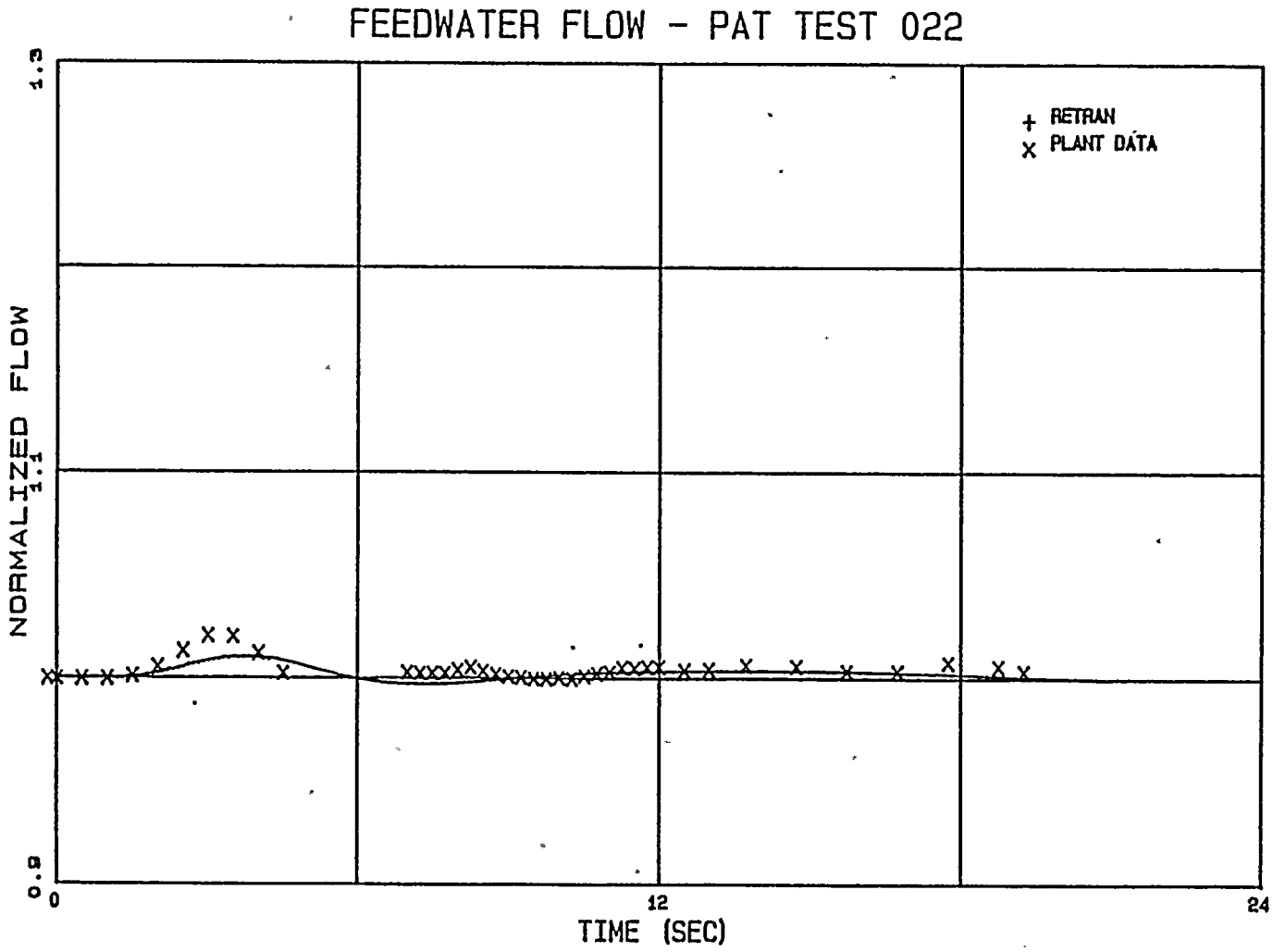
FEEDWATER FLOW - PAT TEST 022
+ RETRAN
X PLANT DATA
NORMALIZED FLOW
1.3
1.1
0.9
0
12
24
TIME (SEC)

3.1.3 One Recirculation Pump Trip (Test PAT 30A)

Test PAT 30A was performed to verify the performance of the recirculation system. The test also demonstrated that the water level could be controlled without resulting in turbine trip and/or scram. Test PAT 30A was initiated at 96.2% power and 100% flow. The test was initiated by tripping one recirculation pump.

3.1.3.1 RETRAN Model for Test PAT 30A

Test PAT 30A was analyzed with the standard RETRAN base model at rated power and flow. The transient was initiated by introducing a recirculation pump trip in Recirculation Loop A at time zero.

A Test PAT 30A case with one-dimensional kinetics was run to evaluate the effect of void feedback on the core power calculation at lower core flow conditions such as in this test and the results compared to the point-kinetics model. Unadjusted cross sections for Beginning of Cycle 1 conditions were used in the one-dimensional core analysis. (See Section 2.6 for a description of cross section adjustments.) Use of the unadjusted cross sections is acceptable because the one-pump trip transient is very mild. The data comparison in the next section supports this assumption.

3.1.3.2 Results and Discussions

The benchmark verifies the coastdown characteristics of the tripped recirculation pump and the system model response to asymmetric recirculation flow disturbances. Neutronics, core hydraulics, pressure regulator control system, and feedwater models were validated in the analysis. Figure 3.1.7 shows measured and calculated recirculation drive flow for the tripped loop (Loop A) for the point kinetics case. Figure 3.1.8 shows measured and calculated recirculation drive flow for the unaffected loop (Loop B). The calculated flow tracks measured data in both comparisons. The Loop B flow increases slightly as the transient is initiated and stabilizes at a higher value. The unaffected loop sees a lower flow resistance after one pump is tripped. Figures 3.1.9 and 3.1.10 show the same comparisons for the case using one-dimensional kinetics. These comparisons are very similar to the cases with point-kinetics model, supporting the use of the point kinetics model in the other PAT test benchmarks.

Figure 3.1.11 shows the normalized jet pump flow for Loop A. Figure 3.1.12 shows the jet pump flow for Loop B. Again the RETRAN results track the data. Figures 3.1.13 and 3.1.14 are the same comparisons for the case using one-dimensional kinetics. A comparison of the one-dimensional case with the point-kinetics model showed no difference in the calculated jet pump flows.

Figure 3.1.15 shows that the RETRAN core hydraulic and neutronic models calculate transient core power consistently with the data. Initial core power decrease is caused by the increased core void after the single pump trip. As the core power decreases, the core void will eventually decrease (after a fuel heat transfer time constant). The core power begins to increase and level off at a new equilibrium. Figure 3.1.16 is the corresponding plot for the one-dimensional RETRAN model. The one-dimensional model gives a slightly better match with the plant data than the point kinetics model later in the transient because the one-dimensional model tracks the void feedback in the core more accurately than the point kinetics model. The fluctuations observed at about 4 seconds and 16 seconds in the one-dimensional case are also the results of detailed axial void feedback.

Figures 3.1.17 and 3.1.18 show the core heat flux behavior calculated by the point-kinetics model and the one-dimensional model respectively. Both track the plant data with the one-dimensional model yielding slightly better results.

Figure 3.1.7

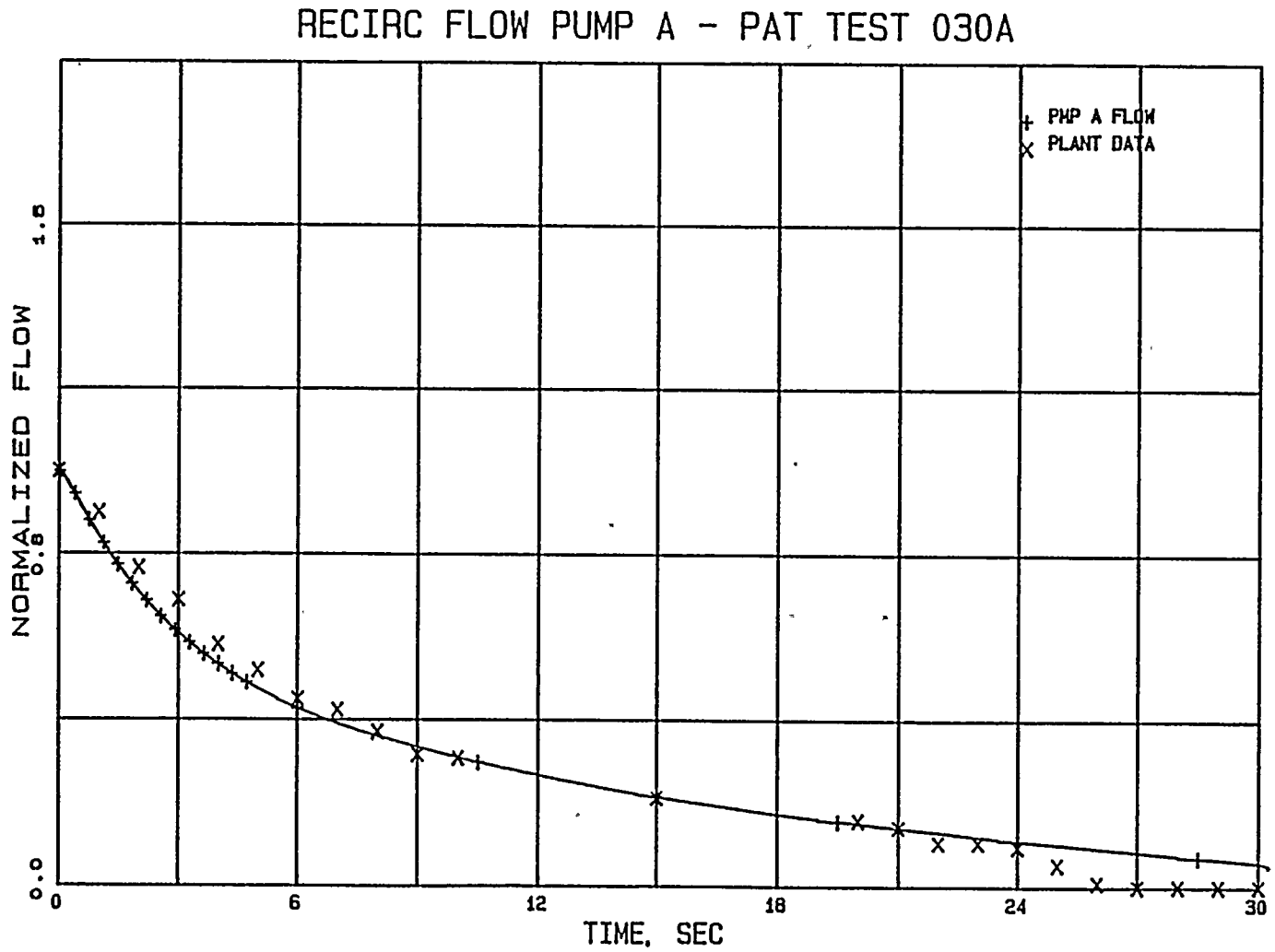
RECIRC FLOW PUMP A - PAT TEST 030A
PHP A FLOW
PLANT DATA
NORMALIZED FLOW
1.6
0.8
0.0
0
6
12
18
24
30
TIME, SEC

Figure 3.1.8

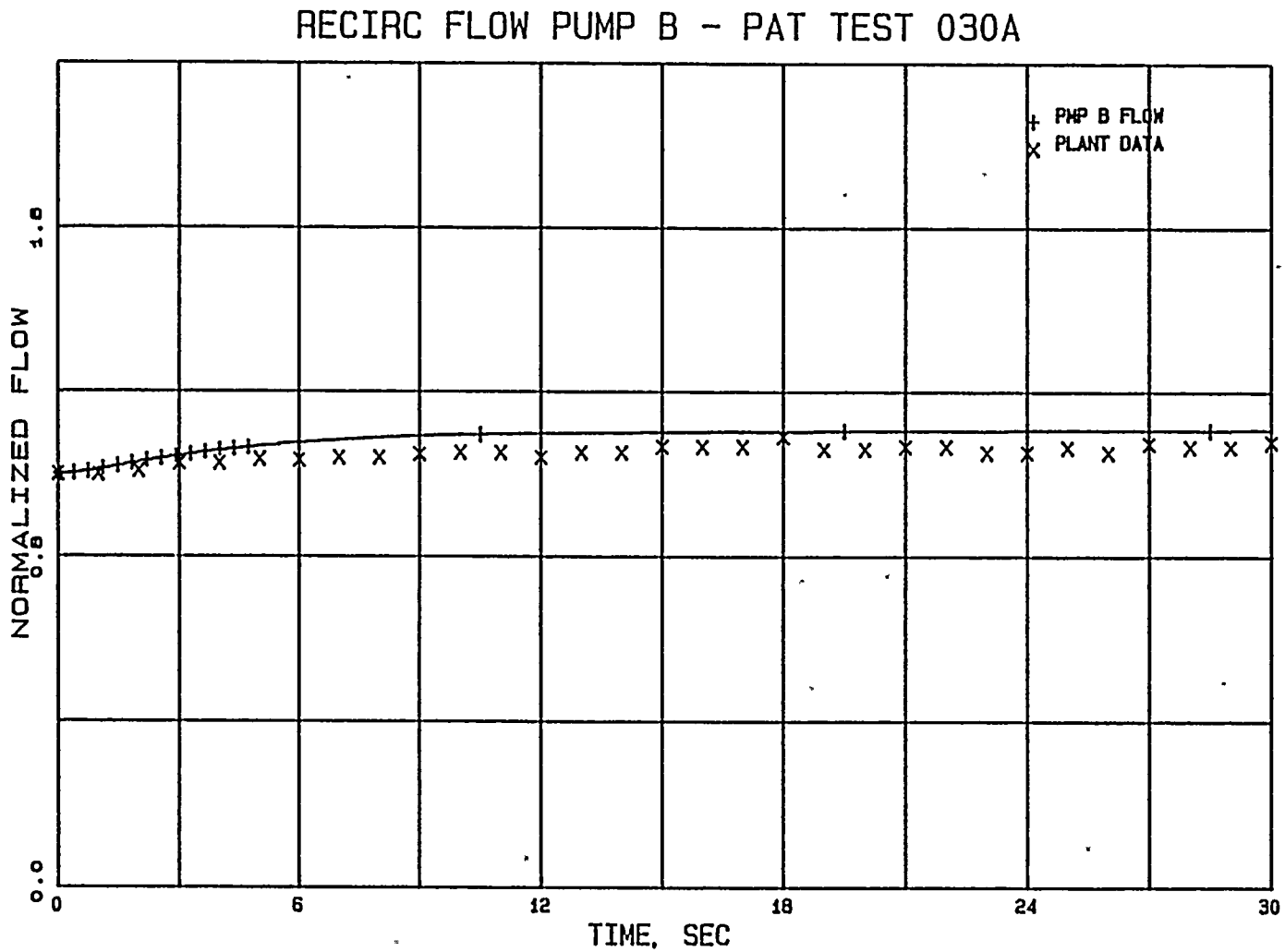
RECIRC FLOW PUMP B - PAT TEST 030A
PMP B FLOW
PLANT DATA
NORMALIZED FLOW
1.6
0.8
0.0
0
6
12
18
24
30
TIME, SEC

Figure 3.1.9

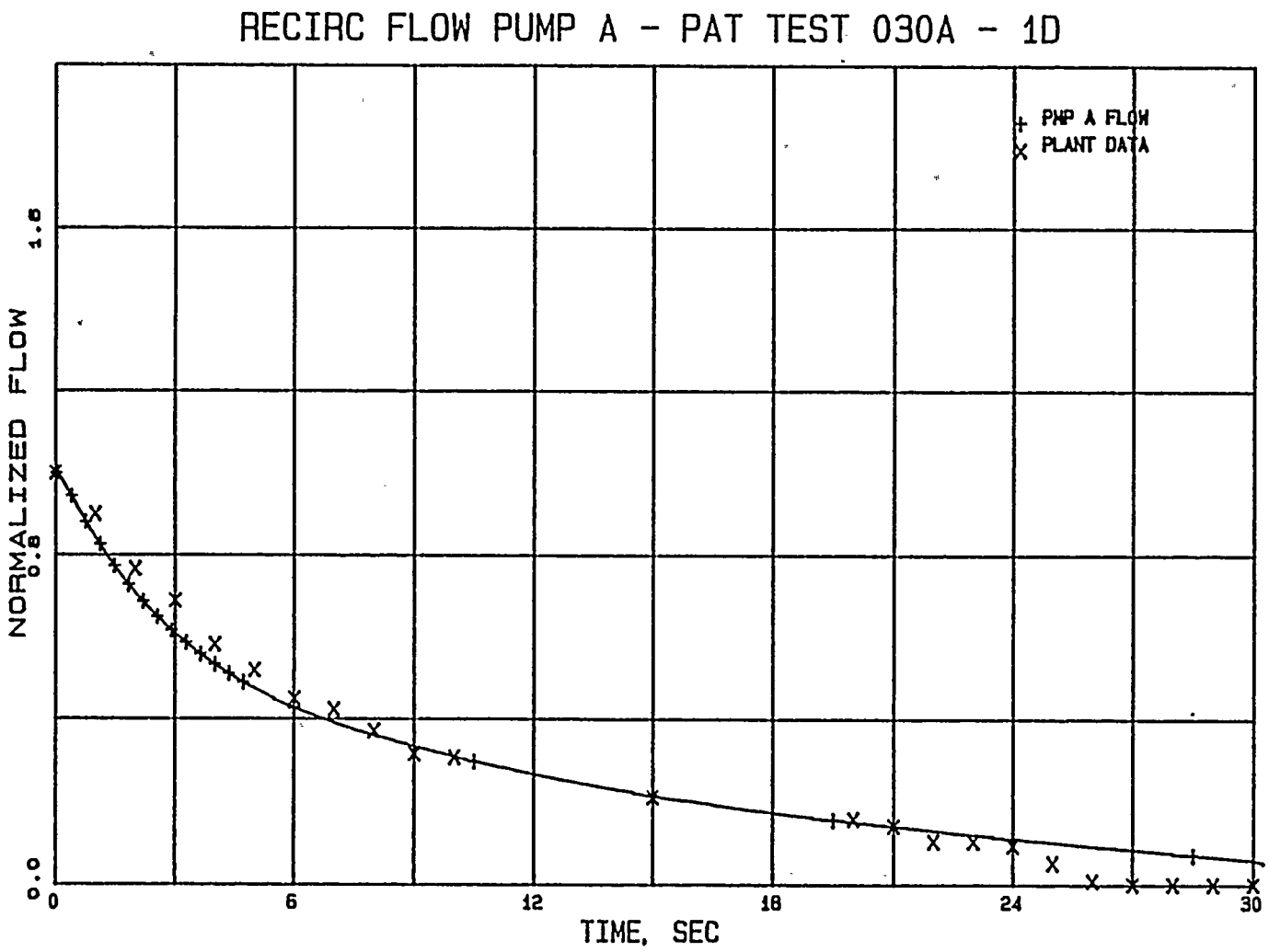
RECIRC FLOW PUMP A - PAT TEST 030A - 1D
PMP A FLOW
PLANT DATA
NORMALIZED FLOW
1.6
0.8
0.0
0
6
12
18
24
30
TIME, SEC

Figure 3.1.10

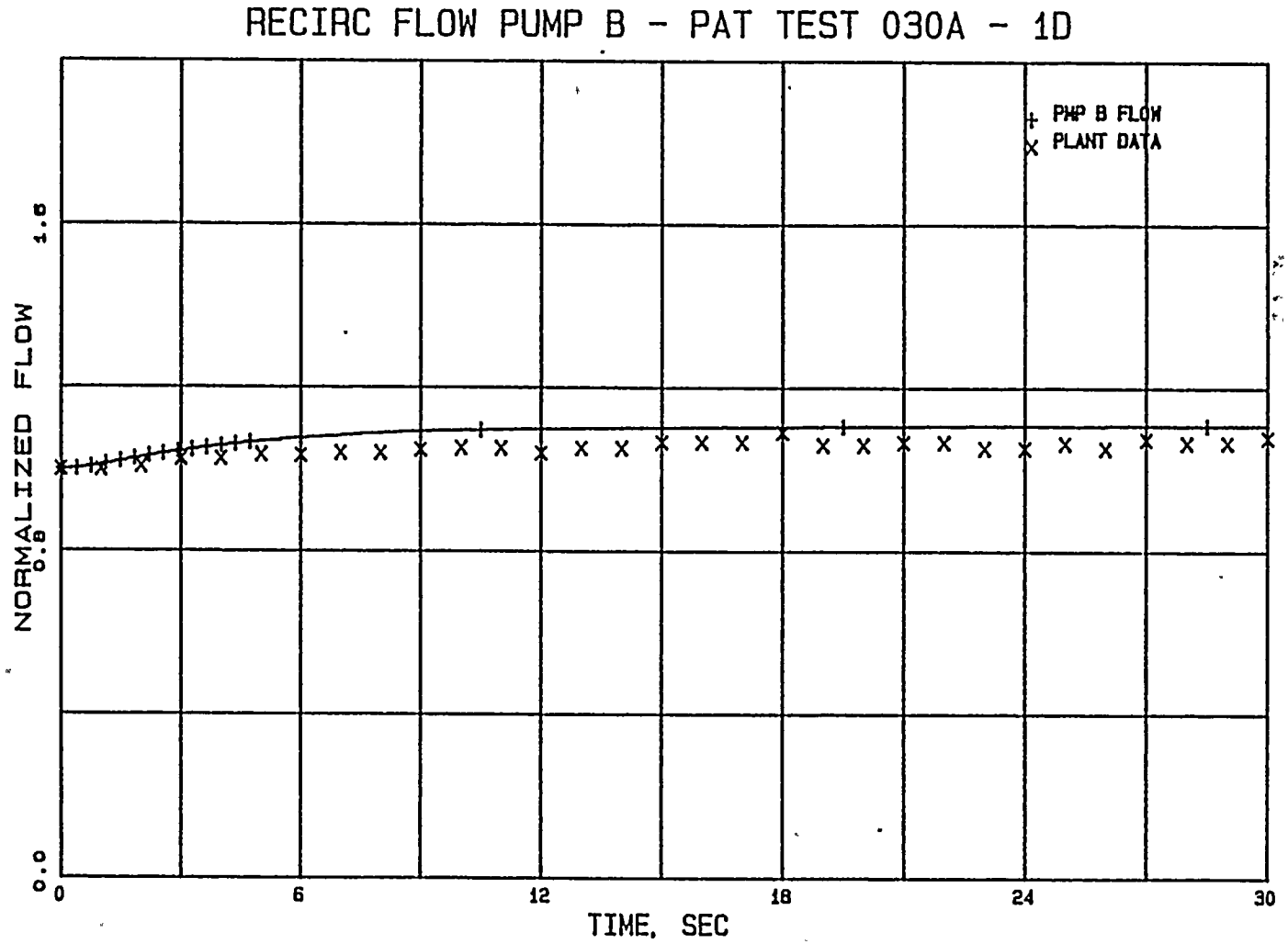
RECIRC FLOW PUMP B - PAT TEST 030A - 1D
PHP B FLOW
PLANT DATA
NORMALIZED FLOW
1.6
0.8
0.0
0
6
12
18
24
30
TIME, SEC

Figure 3.1.11

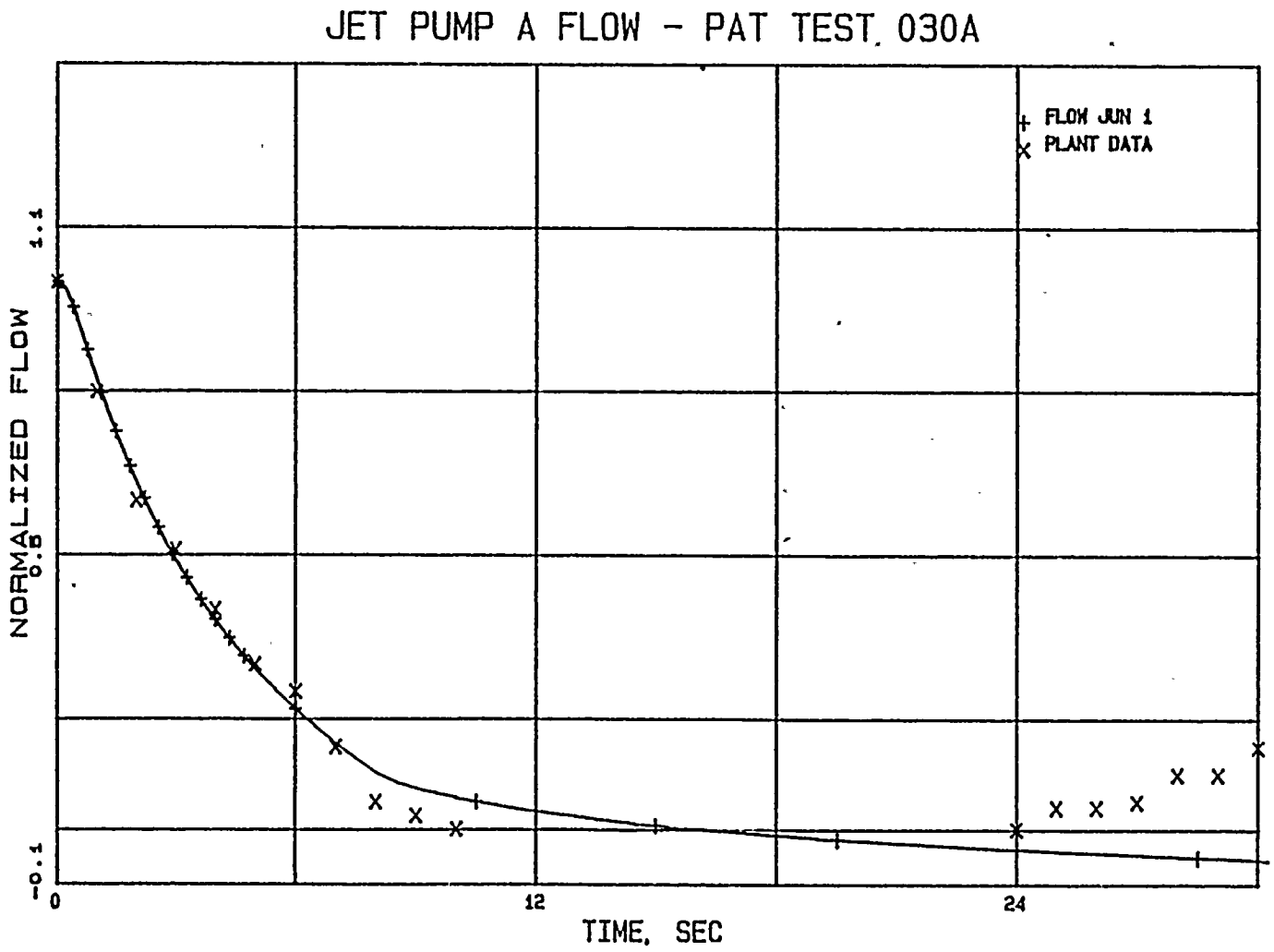
JET PUMP A FLOW - PAT TEST 030A
FLOW JUN 1
PLANT DATA
NORMALIZED FLOW
1.1
0.8
-0.1
0
12
24
TIME, SEC

Figure 3.1.12

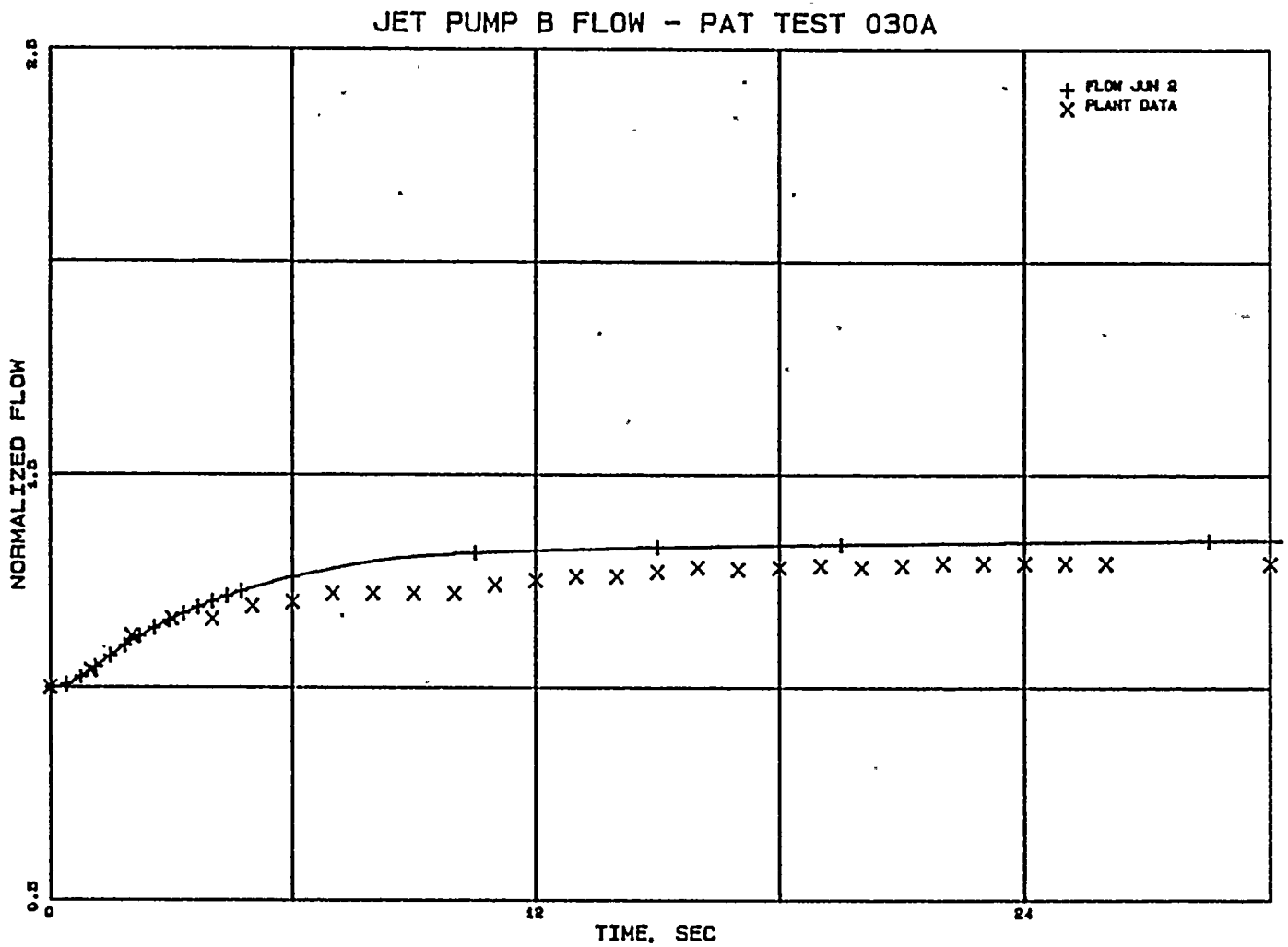
JET PUMP B FLOW - PAT TEST 030A
FLOW JUN 2
PLANT DATA
NORMALIZED FLOW
2.5
1.5
0.5
0
12
24
TIME, SEC

Figure 3.1.13

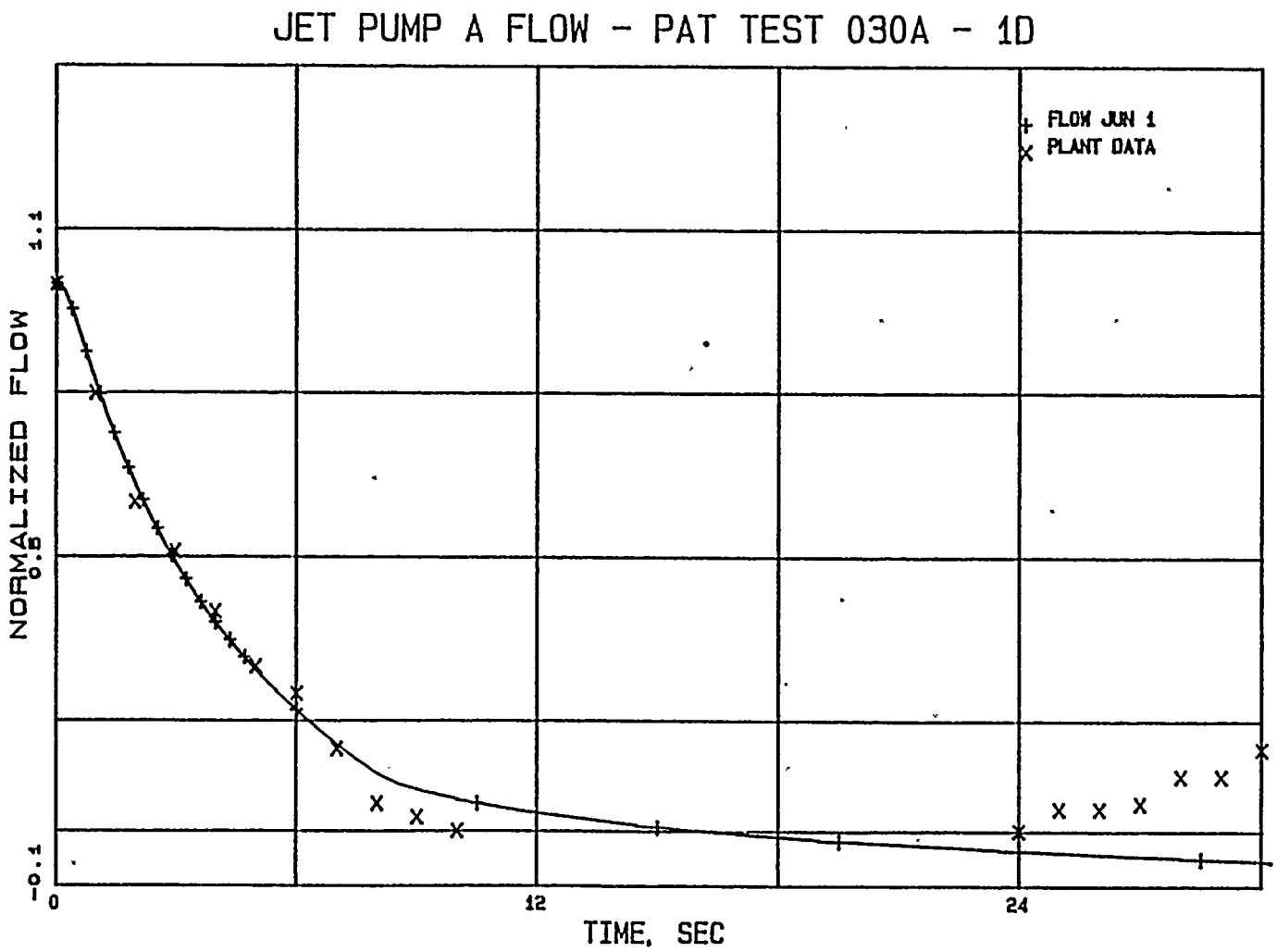
JET PUMP A FLOW - PAT TEST 030A - 1D
FLOW JUN 1
PLANT DATA
NORMALIZED FLOW
1.1
0.5
-0.1
0
12
24
TIME, SEC

Figure 3.1.14

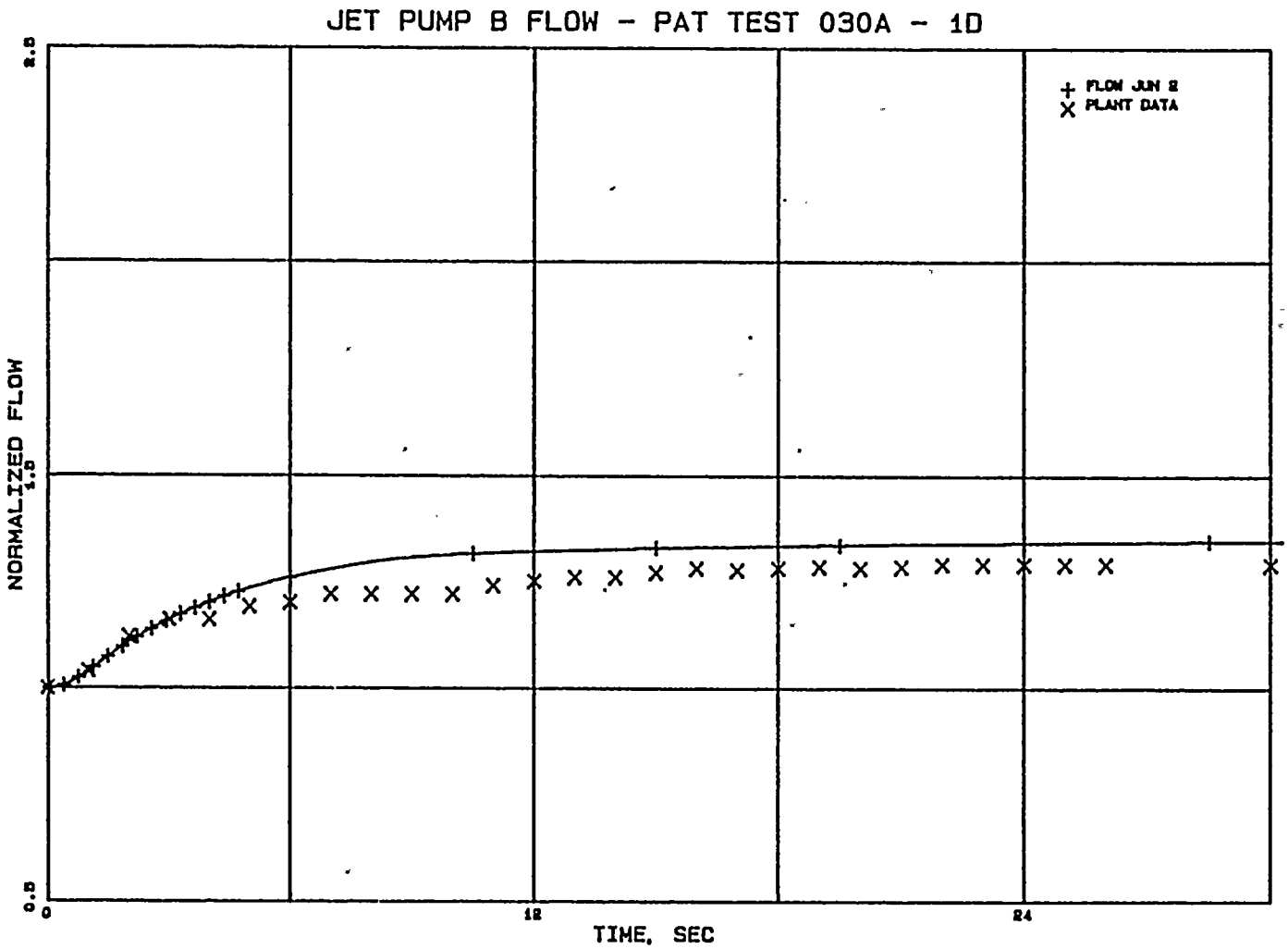
JET PUMP B FLOW - PAT TEST 030A - 1D
FLOW JUN 2
PLANT DATA
NORMALIZED FLOW
2.0
1.5
0.5
0
12
24
TIME, SEC

Figure 3.1.15

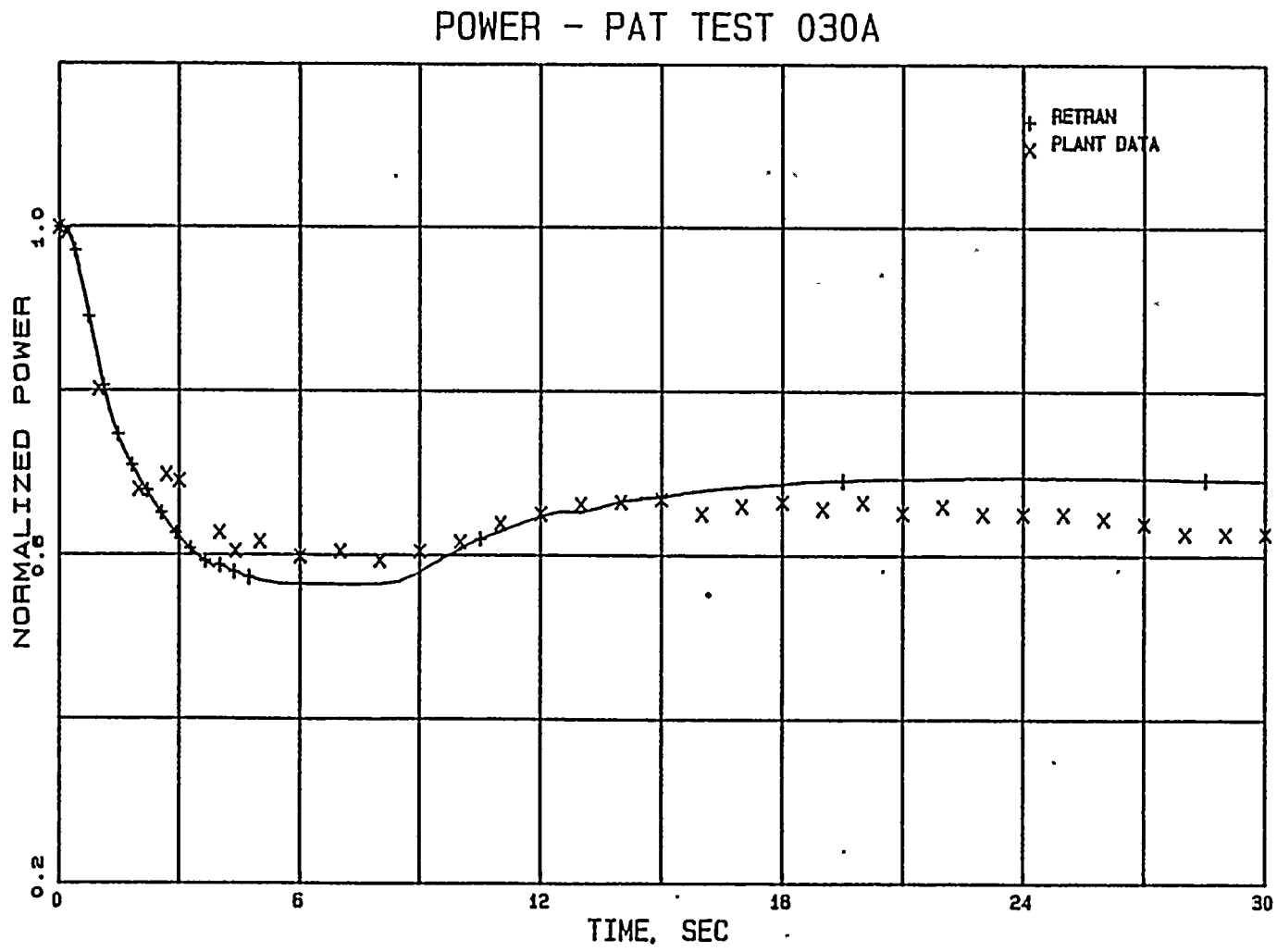
POWER - PAT TEST 030A
RETRAN
PLANT DATA
NORMALIZED POWER
1.0
0.6
0.2
0
6
12
18
24
30
TIME, SEC

Figure 3.1.16

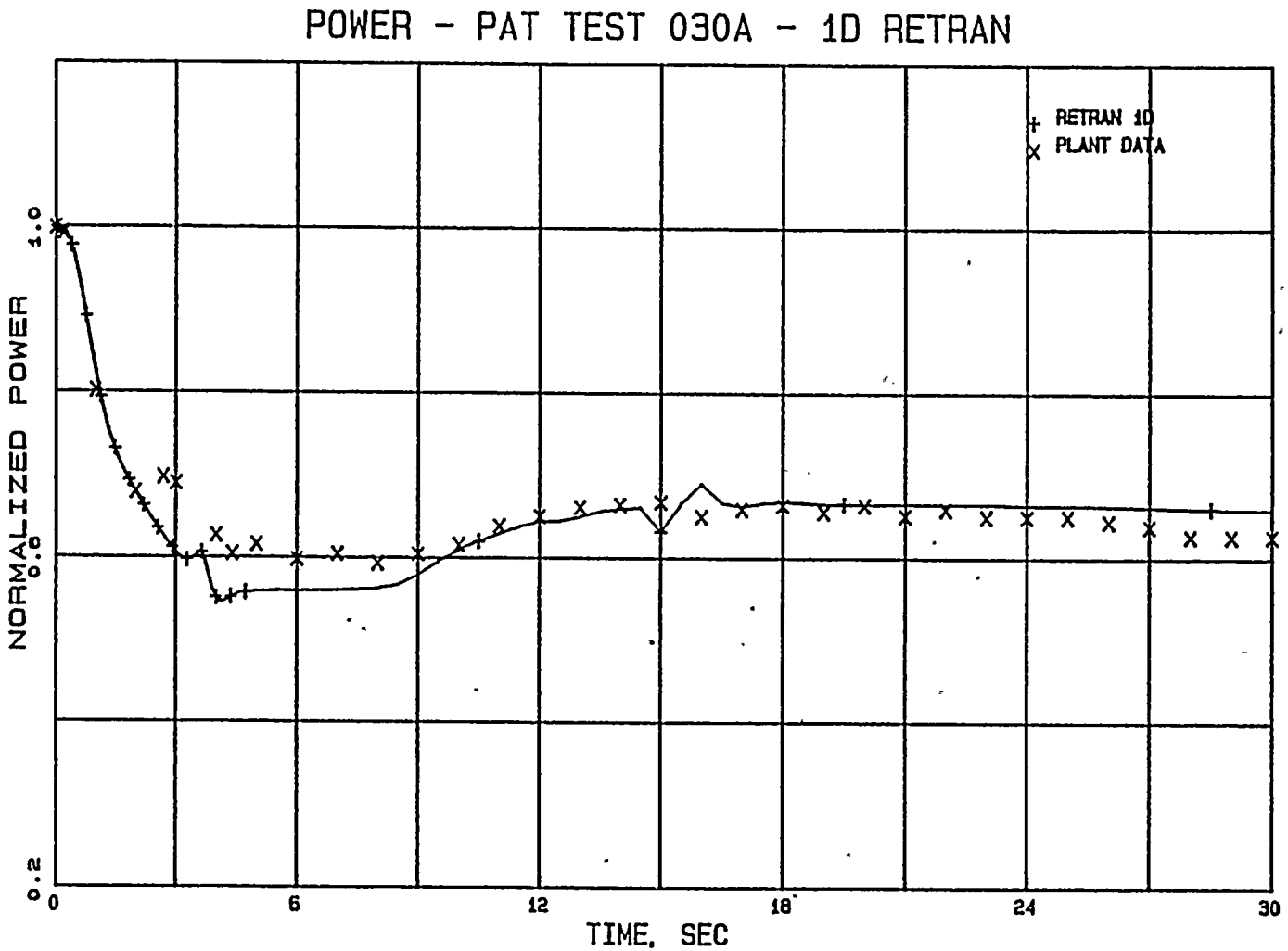
POWER - PAT TEST 030A - 1D RETRAN
RETRAN 1D
PLANT DATA
NORMALIZED POWER
1.0
0.6
0.2
0
6
12
18
24
30
TIME, SEC

Figure 3.1.17

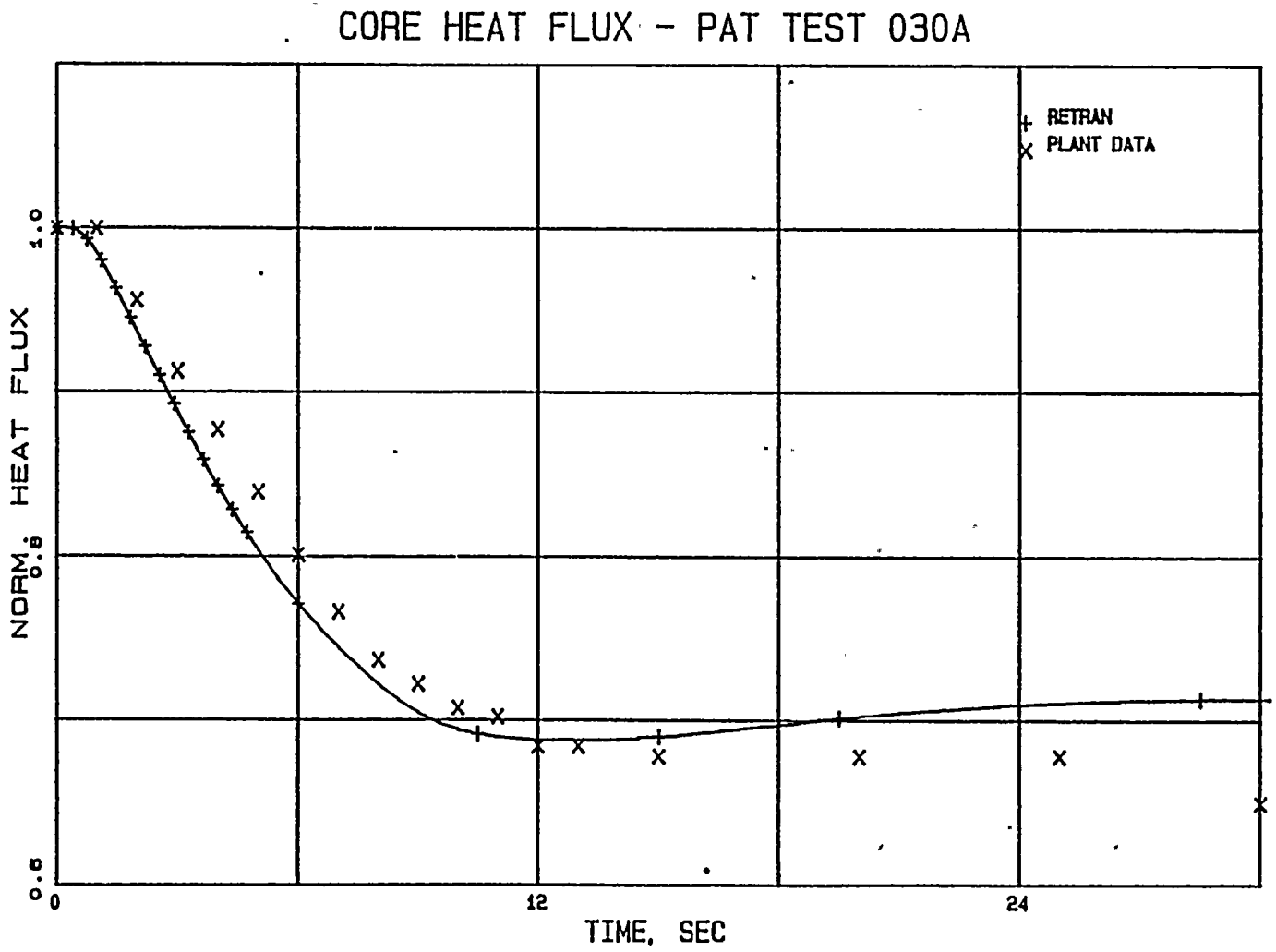
CORE HEAT FLUX - PAT TEST 030A
RETRAN
PLANT DATA
NORM. HEAT FLUX
1.0
0.8
0.6
0
12
24
TIME, SEC

Figure 3.1.18

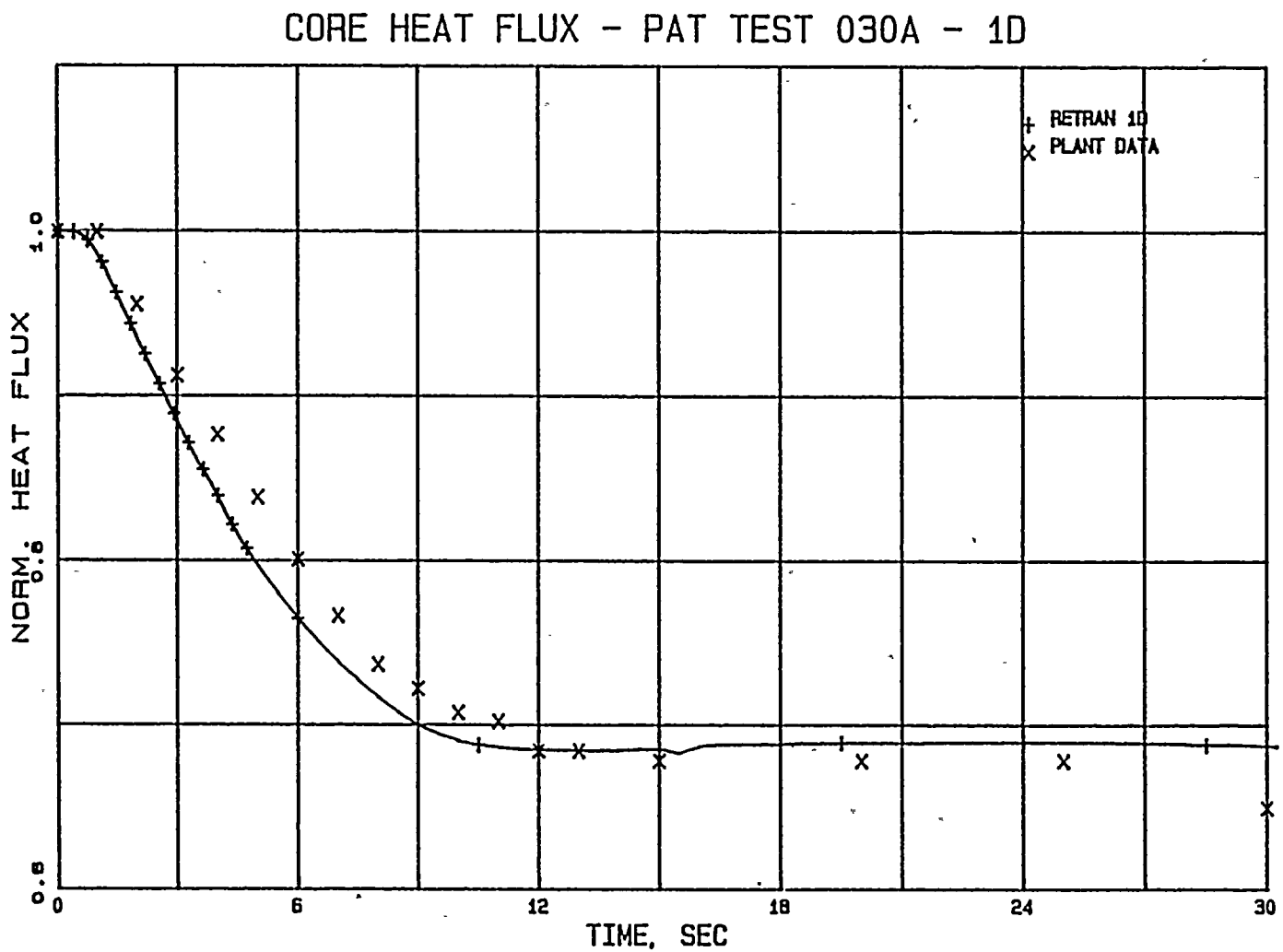
CORE HEAT FLUX - PAT TEST 030A - 1D
RETRAN 1D
PLANT DATA
NORM. HEAT FLUX
1.0
0.8
0.6
0
6
12
18
24
30
TIME, SEC

3.1.4 Generator Load Rejection With Bypass (Test PAT 27)

Test PAT 27 was initiated at 97.5% power and 95.4% flow. The transient was started by the activation of the main generator trip pushbutton.

The rapid closure of the turbine control valves pressurizes the steam lines and the core. As the void collapses, positive void reactivity is induced. Scram is initiated by the turbine control valve fast closure pressure switch. The early scram results in negative overall reactivity throughout the test. The net effect is a power decrease shortly after the initiation of the transient. The turbine control valve closure also initiates the recirculation pump trip (RPT).

The turbine control valve closure and subsequent steamline pressurization activate the opening of the turbine bypass valves to relieve vessel pressure. Since the capacity of the bypass is less than the test power level, dome pressure continues to increase. Eventually the SRVs open to limit the pressure rise. For this event Group 1 SRVs opened.

3.1.4.1 RETRAN Model for Test PAT 27

The main generator trip is set at 0.0 seconds. The turbine control valve performance was taken from the test data. In the WNP-2

RETRAN model a single valve (Junction 380) at the end of steam line simulates both turbine control and stop valves. When the control valve fast closure is activated, its corresponding delay time and closure time are input so that Junction 380 simulates a control valve. Observed control rod performance data was used as the RETRAN scram time.

The maximum bypass flow for the base deck is set at the design value of 25% of rated steam flow. Plant data supports a value of 37% maximum bypass flow, which was used for this simulation.

The one-dimensional kinetics model was used in this simulation. As mentioned in Section 3.1.3, for a mild transient as in this case, uncorrected one-dimensional cross sections are sufficient.

3.1.4.2 Results and Discussions

Figure 3.1.19 shows the calculated and measured variation in the Average Power Range Monitor (APRM) signal during Test PAT 27. The APRM signal is proportional to the neutron flux. The output from RETRAN is adjusted so that the decay power is subtracted from the total power before it is compared to the measured data.

Test PAT 27 is the only benchmarked power ascension test which resulted in a reactor scram. Figure 3.1.19 shows that the RETRAN prediction tracks the initiation and progress of the scram closely,

indicating acceptable scram modeling.

The WNP-2 RETRAN model contains two separate recirculation loops. Figure 3.1.20 and 3.1.21 show that RETRAN follows the rates of decrease for both loops. The lower flow predicted for Loop B is due to uncertainty of delay time for RPT initiation and a RETRAN deficiency which results in calculating slightly asymmetrical loop flows in a symmetric system with symmetric transient conditions. However, the differences in flows are small. They are not expected to affect the overall accuracy of the simulation. Figure 3.1.22 compares the calculated and measured core flow. The results verify the capability to calculate recirculation loop and core flows after a Recirculation Pump Trip (RPT).

Figure 3.1.23 shows measured and calculated dome pressure during the test. Turbine control and stop valve closure causes a rapid system pressurization. RETRAN predicts the pressure transient accurately, particularly during the early stages of the transient (0-4 seconds) when the fuel thermal behavior is important for the thermal limit predictions. The measured pressure spike at 0.3 seconds appeared only in the wide range Division 2 signal; wide range Division 1 and narrow range signals do not show this deviation. The apparent pressure spike may have been an instrument aberration. The plant data shows that one relief valve opened while a second one opened and closed repeatedly. The WNP-2 RETRAN model treats the first two SRVs with lowest pressure setpoint as a

single equivalent valve. Both SRVs opened in the RETRAN simulation and the RETRAN pressure results are lower after about 5 seconds.

Figure 3.1.24 shows the steam flow variation. The oscillation in the flow rate from 0 to 3 seconds is caused by pressurization waves after the turbine control and stop valves are closed.

Figure 3.1.19

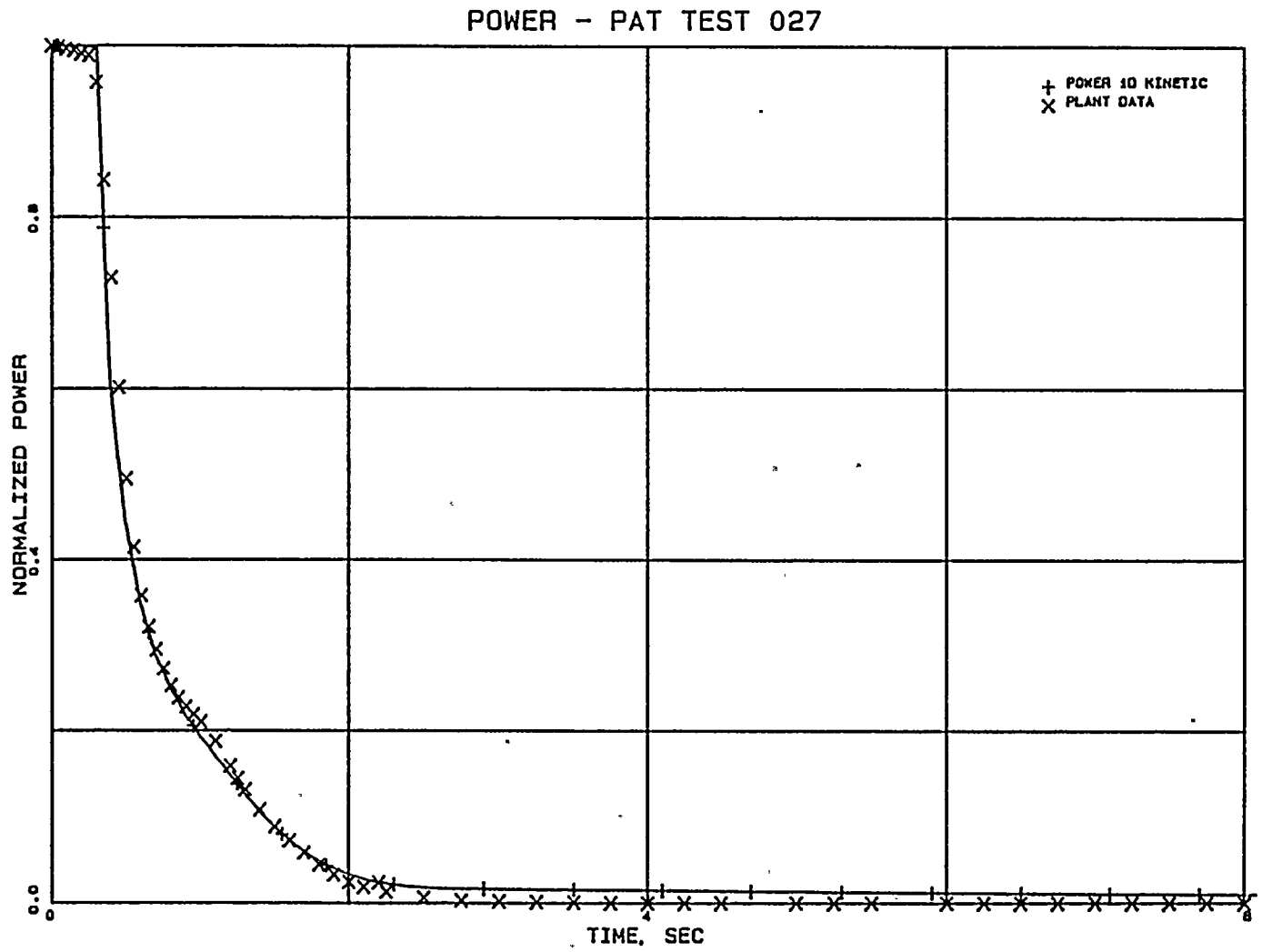
POWER - PAT TEST 027
POWER 1D KINETIC
PLANT DATA
NORMALIZED POWER
0.0
0.4
0.8
0
4
8
TIME, SEC

Figure 3.1.20

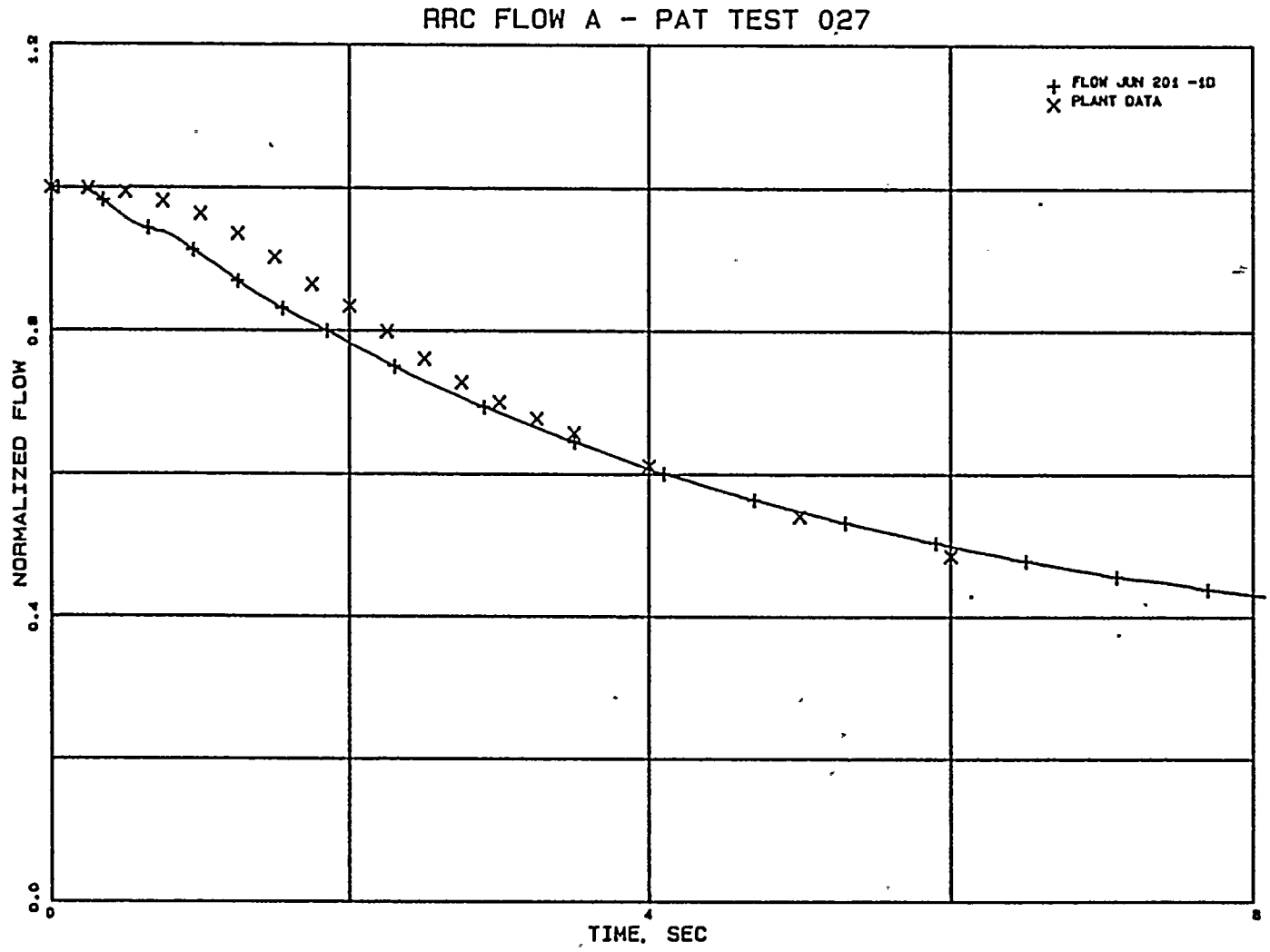
RRC FLOW A - PAT TEST 027
FLOW JUN 201 -10
PLANT DATA
NORMALIZED FLOW
1.2
0.8
0.4
0.0
0
4
8
TIME, SEC

Figure 3.1.21

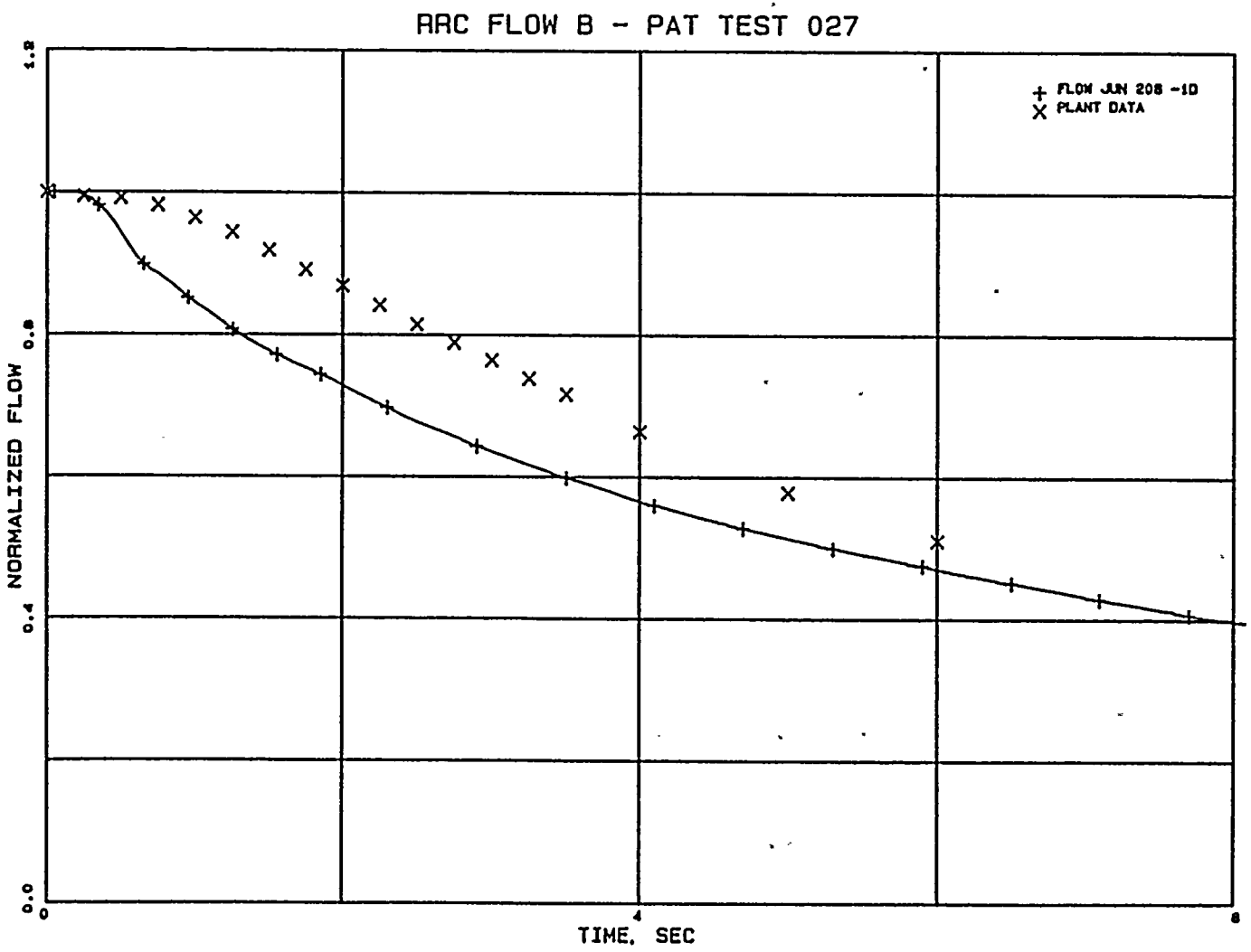
ARC FLOW B - PAT TEST 027
+ FLOW JUN 208 -10
X PLANT DATA
NORMALIZED FLOW
1.2
0.8
0.4
0.0
0
4
8
TIME, SEC

Figure 3.1.22

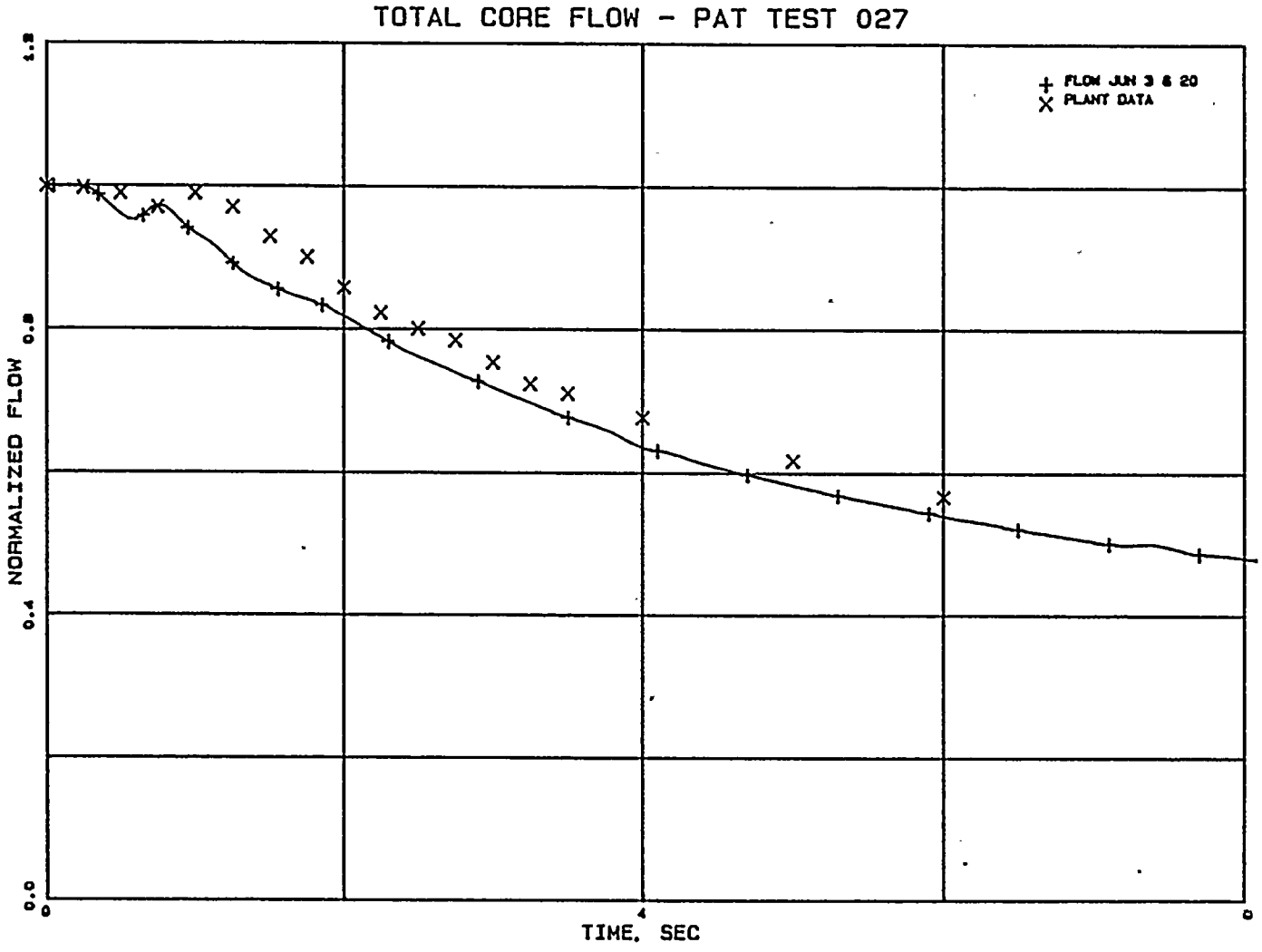
TOTAL CORE FLOW - PAT TEST 027
+ FLOW JUN 3 & 20
X PLANT DATA
NORMALIZED FLOW
1.2
0.8
0.4
0.0
0
4
8
TIME, SEC

Figure 3.1.23

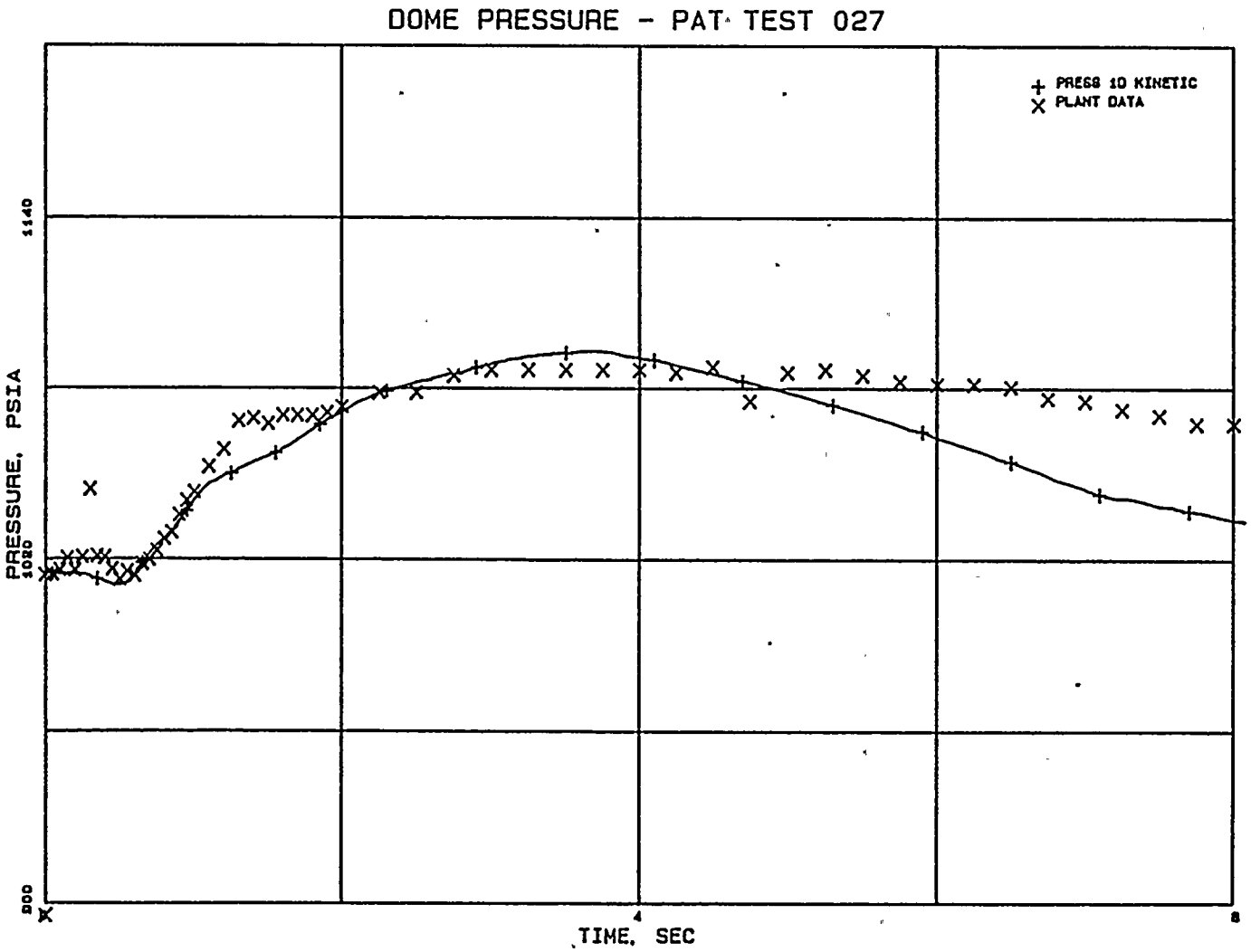
DOME PRESSURE - PAT TEST 027
PRESS 10 KINETIC
PLANT DATA
PRESSURE, PSIA
1140
1020
900
0
4
8
TIME, SEC

Figure 3.1.24

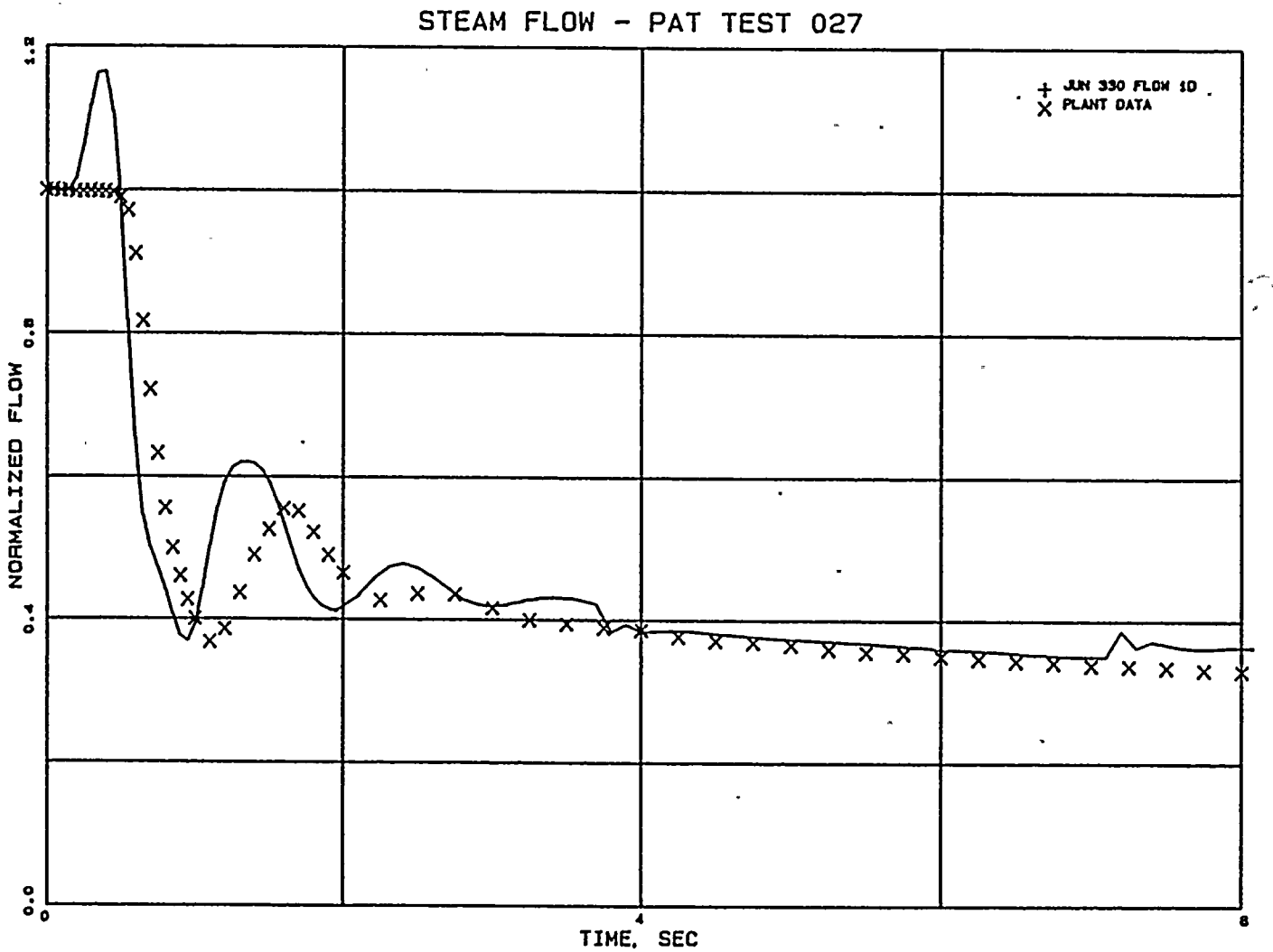
STEAM FLOW - PAT TEST 027
JUN 330 FLOW 1D
PLANT DATA
NORMALIZED FLOW
1.2
0.8
0.4
0.0
0
4
8
TIME, SEC

3.2 Peach Bottom Turbine Trip Tests

Benchmarking of the WNP-2 RETRAN model to the power ascension test measurements verifies the capability and accuracy of most elements in the model. These benchmarks cover expected operation, but normal startup testing does not cover circumstances which challenge the core operating limits. To demonstrate the overall capability of the RETRAN model under design basis conditions, the Supply System performed an analysis of the three pressurization transient tests. (TT1, TT2, TT3) conducted at Peach Bottom Atomic Power Station Unit 2 (PB2).

3.2.1 Test Description

Detailed accounts of the Peach Bottom turbine trip tests can be found in the EPRI report[18]. A brief description is given here.

Turbine trip tests TT1, TT2 and TT3 were performed at PB2 prior to shutdown for refueling at the end of cycle 2 in April 1977. These tests were conducted jointly by Philadelphia Electric Company, GE and EPRI to investigate the effect of the pressure transient generated in the reactor vessel following a turbine trip on the neutron flux in the reactor core. Measurements of major process variables such as core pressure, dome pressure and neutron flux were recorded at a frequency of 166 samples a

second. These measurements provide the best set of data for the qualification of transient analysis methods.

The tests were initiated by manually tripping the turbine (turbine stop valve closure) at three reactor power levels and near rated core flow. The turbine stop valve (TSV) position scram signal was intentionally delayed to allow a significant neutron flux transient to take place in the core, providing adequate qualification data. The power increase was terminated by a trip of the reactor protection system on high neutron flux. To maintain sufficient operating margin, the APRM high neutron flux scram setpoint was set down closer to the initial reactor power level. The initial reactor power, core flow and the APRM scram setpoint for each test are shown in Table 3.2.1.

TABLE 3.2.1

PEACH BOTTOM TURBINE TRIP TESTS

TEST CONDITIONS

	POWER		CORE FLOW		APRM SETPOINT
TEST	(MW)	(% Rated)	(Mlbm/hr)	(% Rated)	(% Rated)
TT1	1562	47.4	101.3	98.8	85
TT2	2030	61.6	82.9	80.9	95
TT3	2275	69.1	101.9	99.4	77

3.2.2 Peach Bottom Unit 2 Model Description

The Peach Bottom model incorporates the modeling techniques of the WNP-2 model. A schematic of the model is shown in Figure 3.2. (The WNP-2 model is shown in Figures 2.1 through 2.4.) The nodalization within the reactor vessel is identical except that the two downcomer volumes are combined into one in the Peach Bottom model. Also the two recirculation loops are combined into one in the Peach Bottom model and the recirculation loop is represented by two nodes whereas the WNP-2 model has five nodes for each recirculation loop. The Peach Bottom model includes the entire main steam bypass system whereas the WNP-2 model uses a negative fill junction. This model is the best estimate bypass system model of Hornyik and Naser[19], and was included to provide a realistic simulation of this component. Because the steam line geometry has a significant effect on pressurization transients, the geometric data for the steam line from Philadelphia Electric Company's topical report[20] was used. The Peach Bottom steam line is modeled with six nodes whereas the WNP-2 steam line is modeled with seven nodes. An additional node was used in the WNP-2 model to provide more accurate pressure for SRVs lifting. SRVs did not open during the Peach Bottom turbine trip tests. The physical dimensions and characteristics of the dominant fuel type were used. The dimensions and characteristics for the dominant 7x7 fuel type were obtained from EPRI documentation[21].

FIGURE 3.2 PB2 RETRAN MODEL

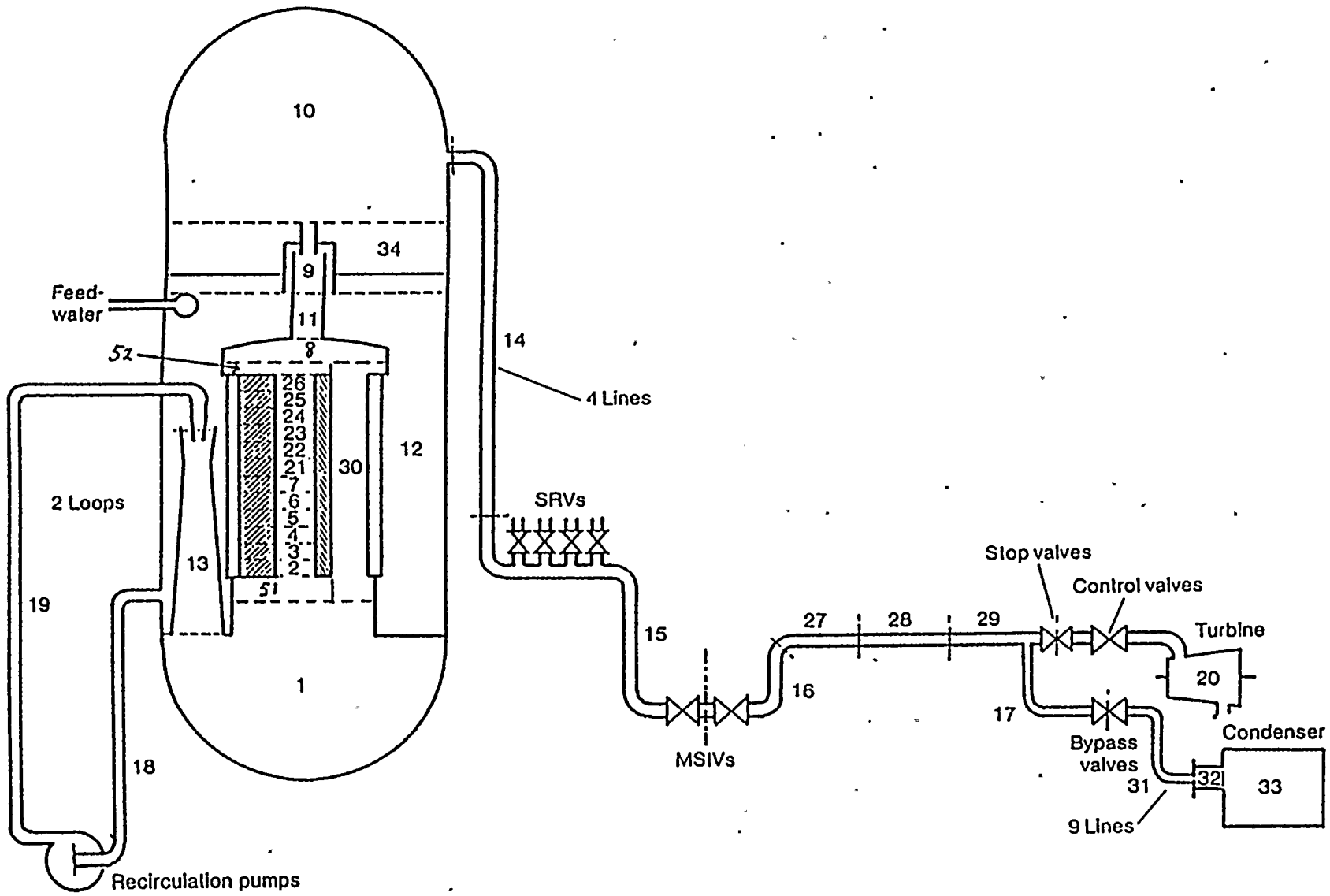

3.2.3 Initial Conditions and Model Inputs

Since comparison with actual measurements was a primary objective, best estimate model inputs developed from original data sources such as drawings and measured plant performance data were used.

The core thermal power, total core flow, core inlet enthalpy and initial steam flow were obtained from the process computer P-1 edits taken before each transient test. The steam dome pressures were obtained from the recorded data. The recirculation system was adjusted to correspond to the initial reactor conditions. The core bypass flow was calculated for each test with the SIMULATE-E MOD03 ("SIMULATE-E") computer code[15]. The loss coefficient at the core bypass region entrance was also adjusted to match the core plate pressure drop calculated by SIMULATE-E. Reactor water levels were initialized to match the test data. Table 3.2.2 lists the initial conditions for each test of the Peach Bottom analyses.

The feedwater flow rate was specified as a constant value for each test. The short duration of the tests minimizes the potential effects of the feedwater control system. The constant flow assumption was validated through an additional analysis using feedwater flow characteristics provided by Philadelphia

Electric Company. Both analyses provided the same results for transient power and pressure responses.

The control rod scram time and speed can be estimated from the measured plant Rod Position Information System drift relay output signals. The average of the measured scram speeds (a sample of 31 of the 185 control rods from TT1) is plotted in Reference 18 and was used with correction for rod acceleration for all three tests. All of the control rods were assumed to insert at the average speed.

The measured time dependent Turbine Stop Valve (TSV) position and the Turbine Bypass Valve (BPV) position were used as RETRAN input. A linear TSV opening was assumed with the stroke time obtained from measured data. The BPV flow area was assumed to be proportional to the measured position. Since the TSV position signal channel malfunctioned during TT1, the average of the signals from TT2 and TT3 was used.

Since the Peach Bottom Turbine trip tests were pressurization transients, they were analyzed using the one-dimensional kinetics model. The SIMULATE-E code was used to generate the RETRAN one dimensional kinetics data at the initial conditions for each test. A stepwise depletion of cycles 1 and 2 based on the EPRI documentation[21] was used to determine the fuel exposure, void history and control history at the time of the tests. The basic

procedures described in Section 2.6 were used to develop each of the three sets of kinetic data.

TABLE 3.2.2

PEACH BOTTOM TURBINE TRIP TESTS

INITIAL CONDITIONS

	TTI	TT2	TT3
Core Thermal Power (MW)	1562.0	2030.0	275.0
Total Core Flow (lbm/sec)	28139.0	23028.0	28306.0
Core Bypass Flow (lbm/sec)	1636.50	1384.87	1762.75
Core Plate Pressure Drop (psid)	16.6	11.61	17.71
Steam Dome Pressure (psia)	991.6	976.1	986.6
Core Inlet Enthalpy (Btu/lbm)	528.0	518.1	521.6
Steam Flow (lbm/sec)	1628.0	2183.0	2461.0
Recirculation Flow (lbm/sec)	9386.0	7686.0	9443.0

3.2.4 Comparison with Measurements

The goal of these Peach Bottom analyses was to demonstrate the Supply System's RETRAN model of PB2 can accurately simulate the power and pressure increase during rapid pressurization transient. Therefore, comparisons of RETRAN calculations to the measured pressures (turbine inlet, steam dome and upper plenum) and LPRM signals are essential. They are presented in the following two sections.

3.2.4.1 Pressure Comparisons

Pressure comparisons are expressed in terms of pressure change from the initial value. This eliminates the need to account for the sensing line elevation head, uncertainties in the pressure loss coefficient and differences between nodal and local pressures.

Pressure transients calculated at three locations are compared with the measured values in Figures 3.2.1 through 3.2.3 (at the turbine inlet), Figures 3.2.4 through 3.2.6 (at steam dome), and Figures 3.2.7 through 3.2.9 (at core upper plenum). The measured pressures are obtained directly from the test data file and have not been filtered. Time shifts (to account for sensing line delay) based on information provided in the EPRI documentation[15] were applied to the calculated pressures. To eliminate the

instrument line effects, the RETRAN model calculated upper plenum pressures are compared to the filtered test data in Figures 3.2.10 through 3.2.12.

The good agreements in turbine inlet pressures and steam dome pressures indicate that the dynamic of the steam lines is well simulated. The first pressure oscillation in the steam dome is slightly overpredicted for TT1 and slightly underpredicted for TT2 and TT3. The upper plenum pressure calculated by RETRAN for TT1 is slightly higher than the measured data. For TT2 and TT3, the calculated and measured upper plenum pressures agree reasonably well. Adequate prediction of the core upper plenum pressure response is essential to transient power predictions. Table 3.2.3 summarizes the calculated and measured steam dome and upper plenum pressures at the peak of first oscillation.

Overall, the RETRAN calculated pressures are in good agreement with the measured data. The discrepancies are within the tolerances due to uncertainties in RETRAN model inputs such as initial steam flow, bypass valve opening delay and turbine stop valve closing time.

TABLE 3.2.3

PEACH BOTTOM TURBINE TRIP TESTS

PRESSURE CHANGE (PSI) AT PEAK OF FIRST OSCILLATION

	STEAM DOME		UPPER PLENUM	
	CALC.	DATA	CALC.	DATA
TT1	34.7	33.4	37.5	34.9
TT2	40.5	41.9	42.3	44.2
TT3	46.2	47.4	48.3	49.9

FIGURE 3.2.1

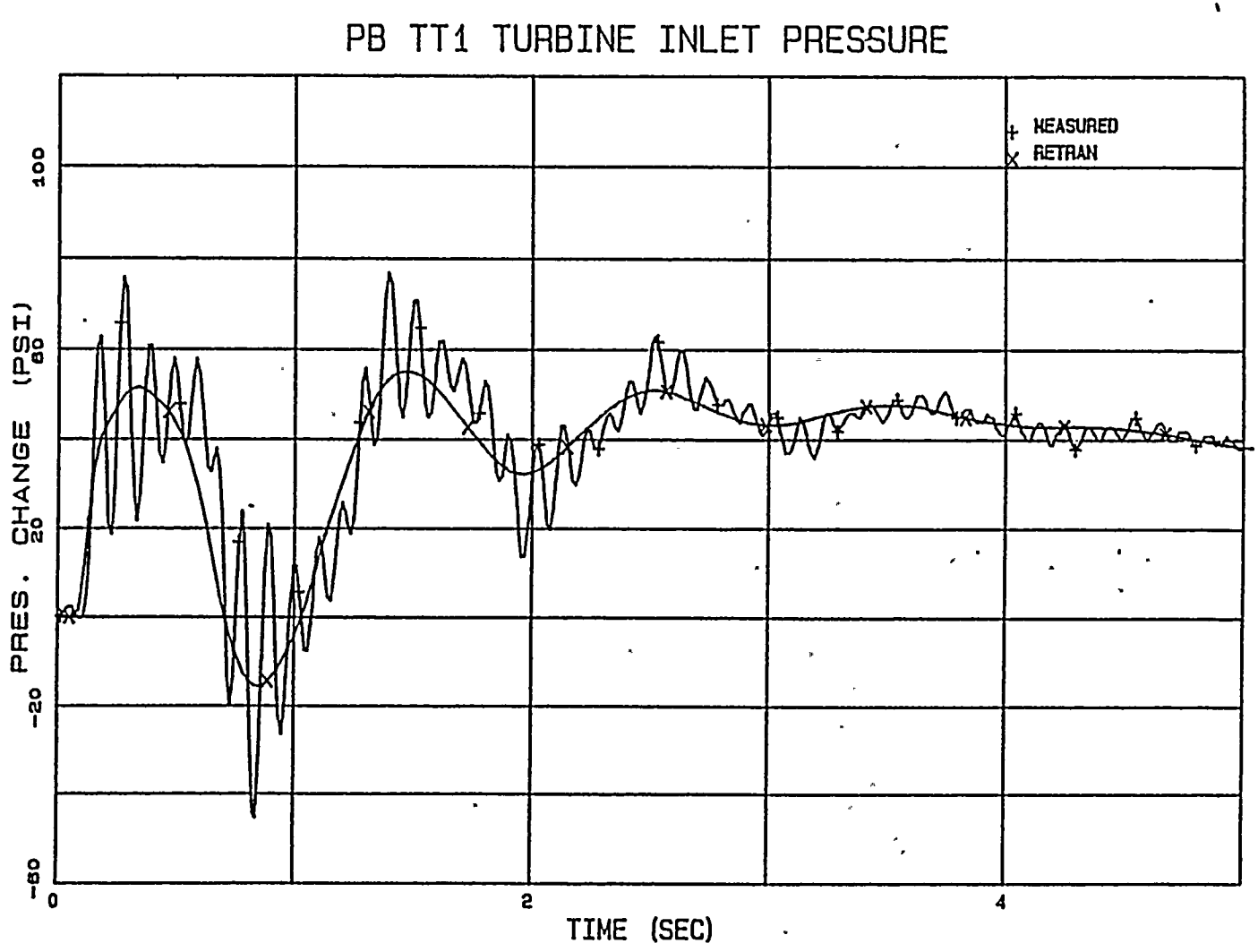
PB TT1 TURBINE INLET PRESSURE
MEASURED
RETRAN
PRES. CHANGE (PSI)
100
80
20
-20
-50
0
2
4
TIME (SEC)

FIGURE 3.2.2

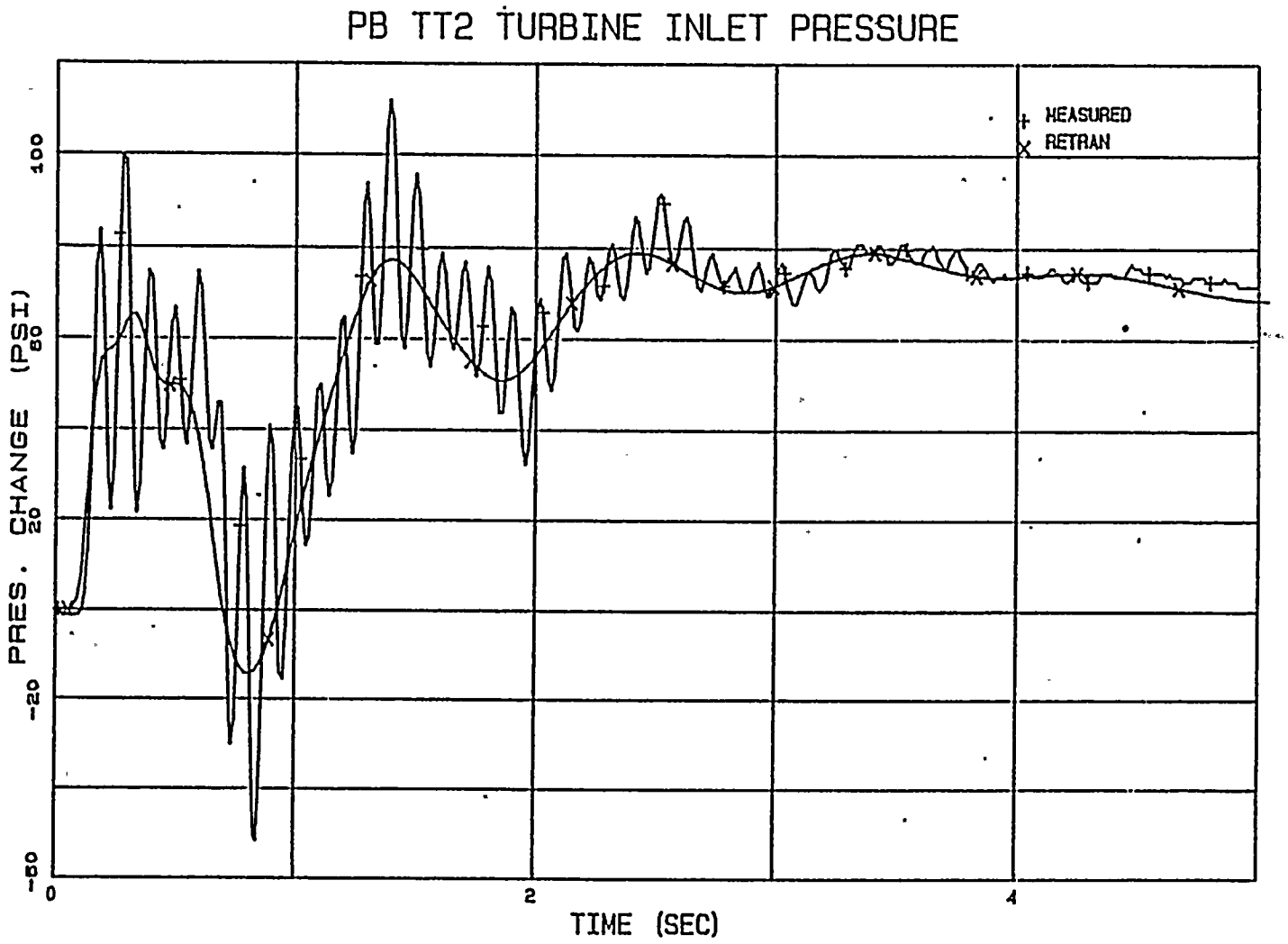
PB TT2 TURBINE INLET PRESSURE
MEASURED
RETRAN
PRES. CHANGE (PSI)
100
80
20
-20
-50
0
2
4
TIME (SEC)

FIGURE 3.2.3

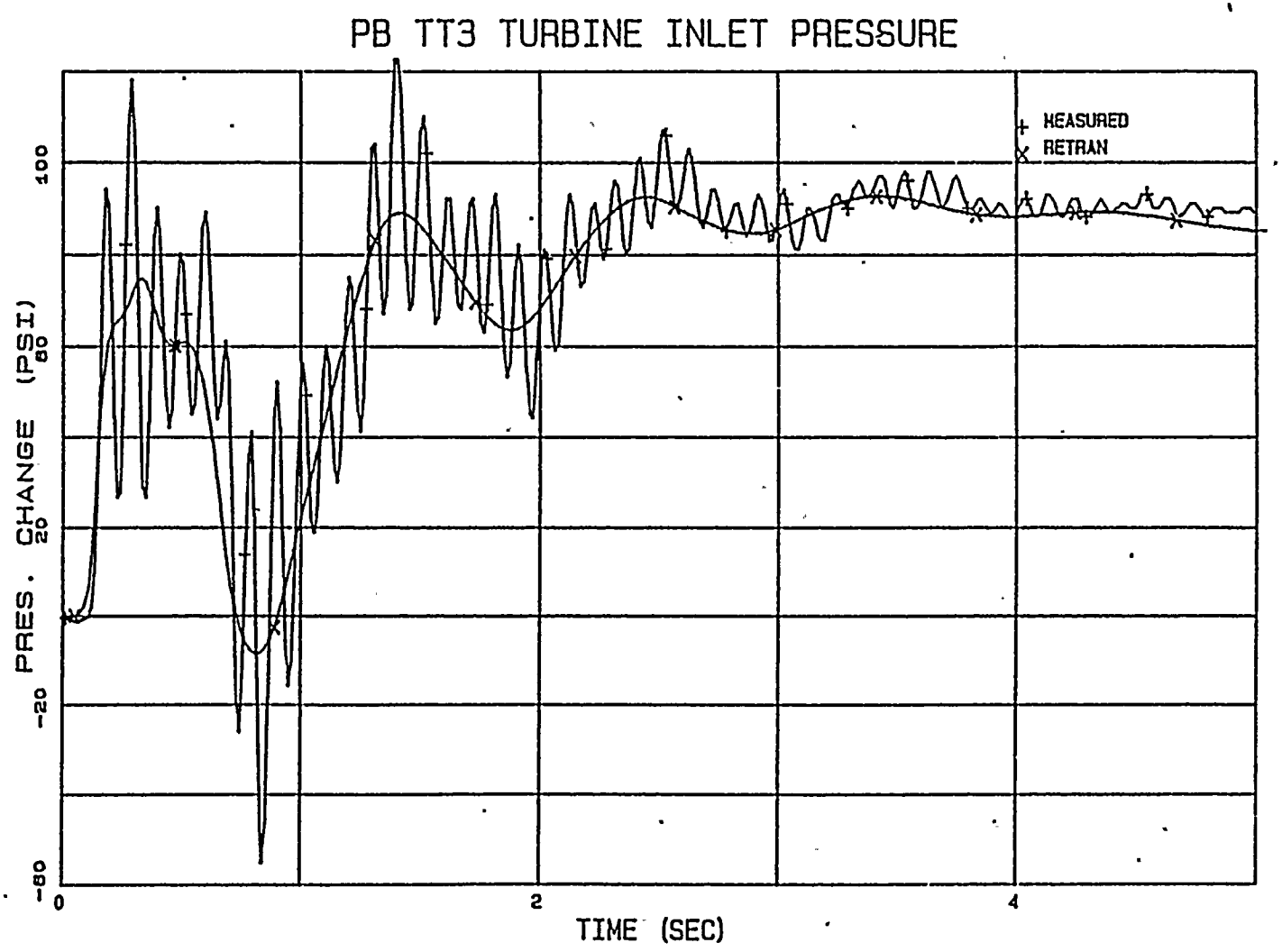
PB TT3 TURBINE INLET PRESSURE
MEASURED
RETRAN
PRES. CHANGE (PSI)
100
80
-20
-80
0
2
4
TIME (SEC)

FIGURE 3.2.4

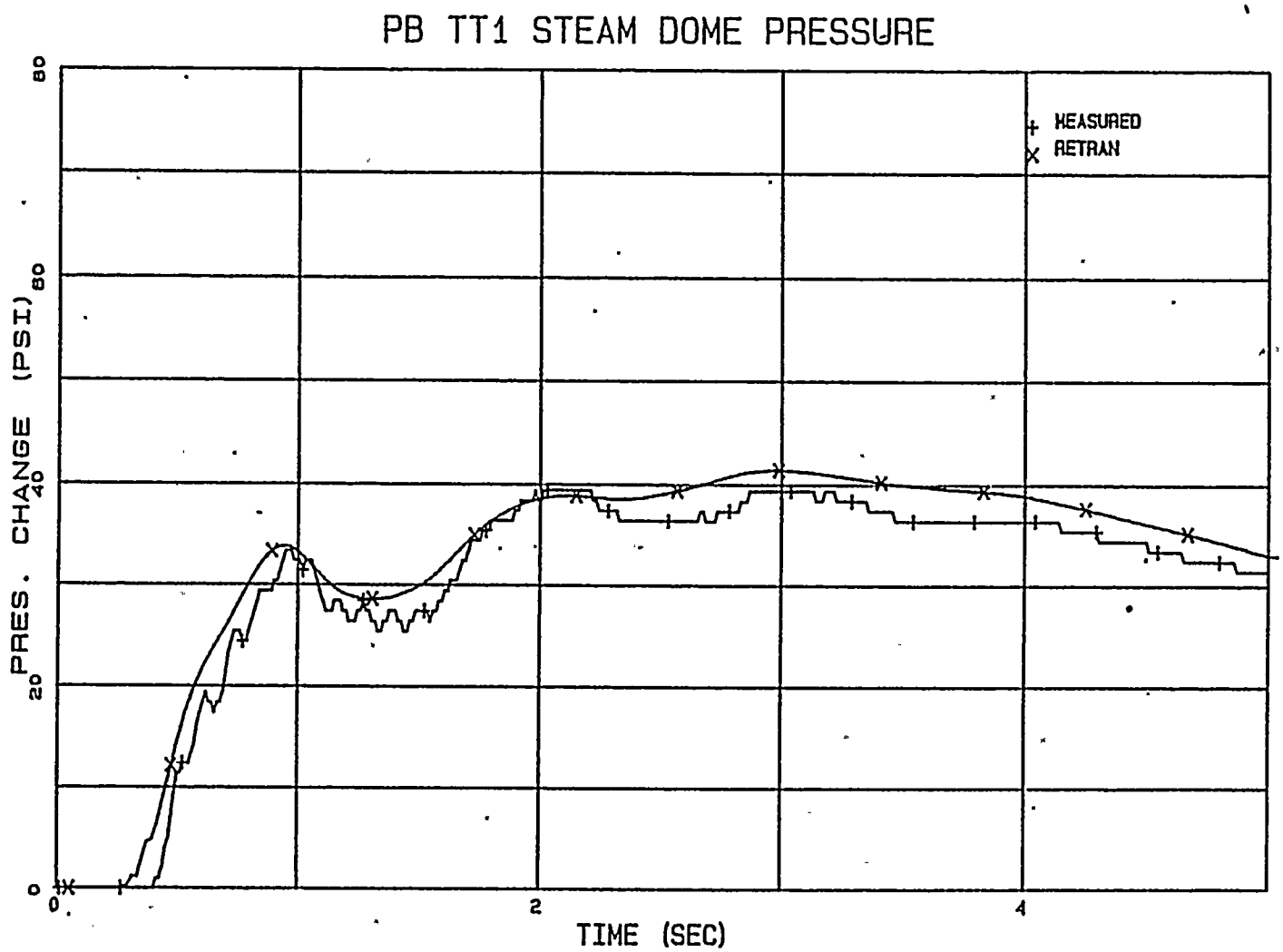
PB TT1 STEAM DOME PRESSURE
MEASURED
RETRAN
PRES. CHANGE (PSI)
0
20
40
60
80
0
2
4
TIME (SEC)

FIGURE 3.2.5

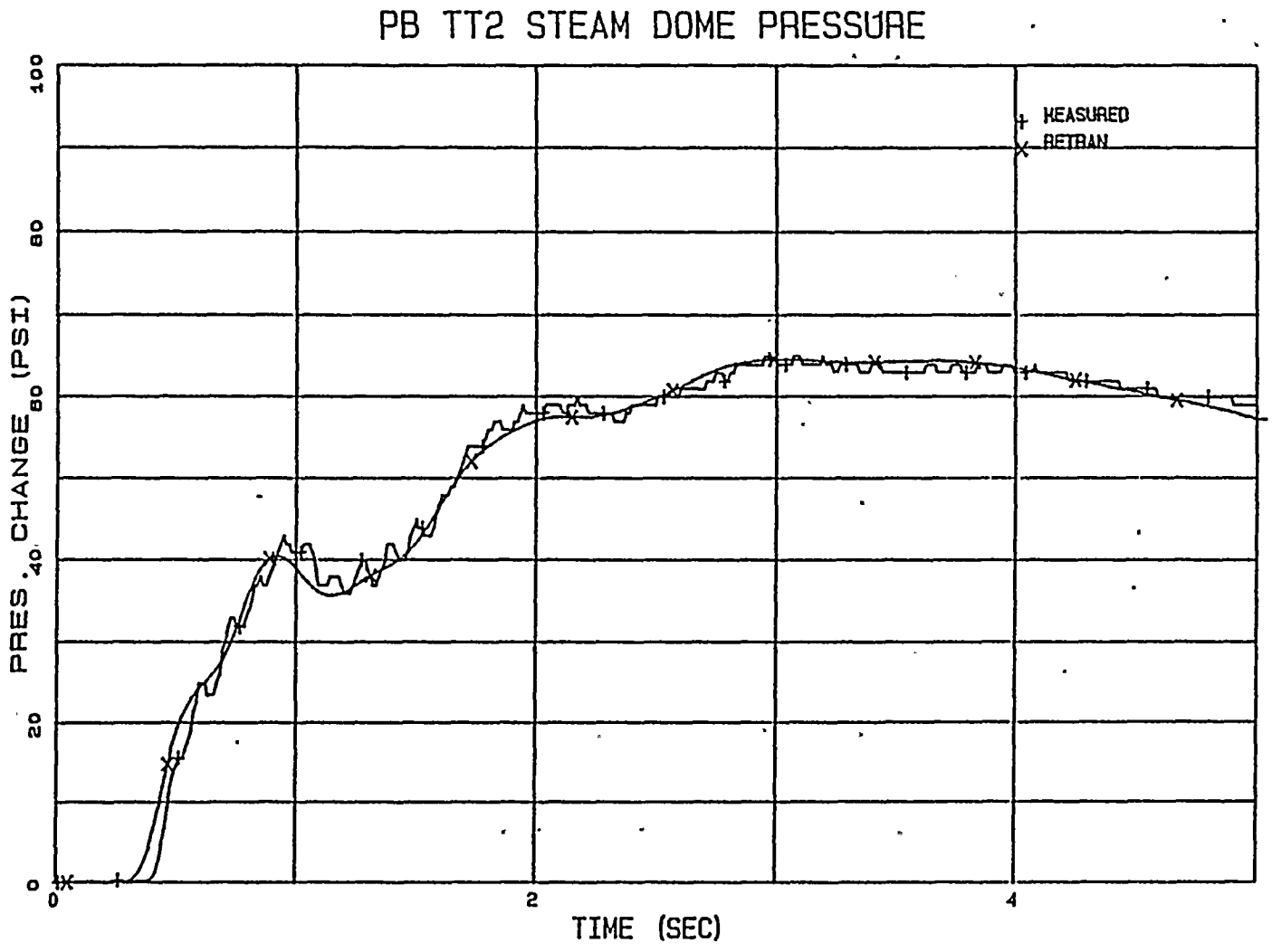
PB TT2 STEAM DOME PRESSURE
MEASURED
RETRAN
PRES. CHANGE (PSI)
0
20
40
60
80
100
0
2
4
TIME (SEC)

FIGURE 3.2.6

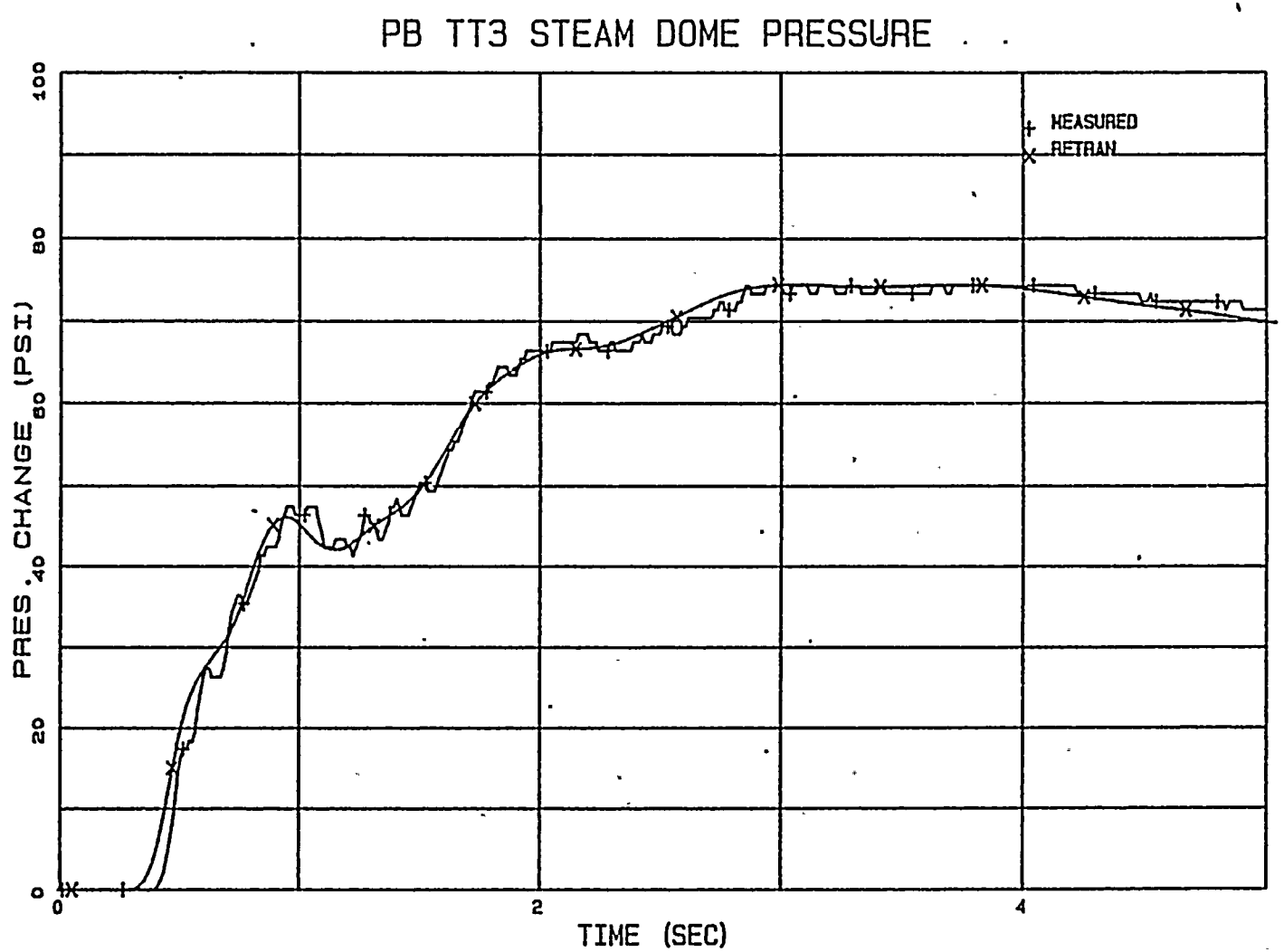
PB TT3 STEAM DOME PRESSURE
MEASURED
RETRAN
PRES. CHANGE (PSI)
0
20
40
60
80
100
0
2
4
TIME (SEC)

FIGURE 3.2.7

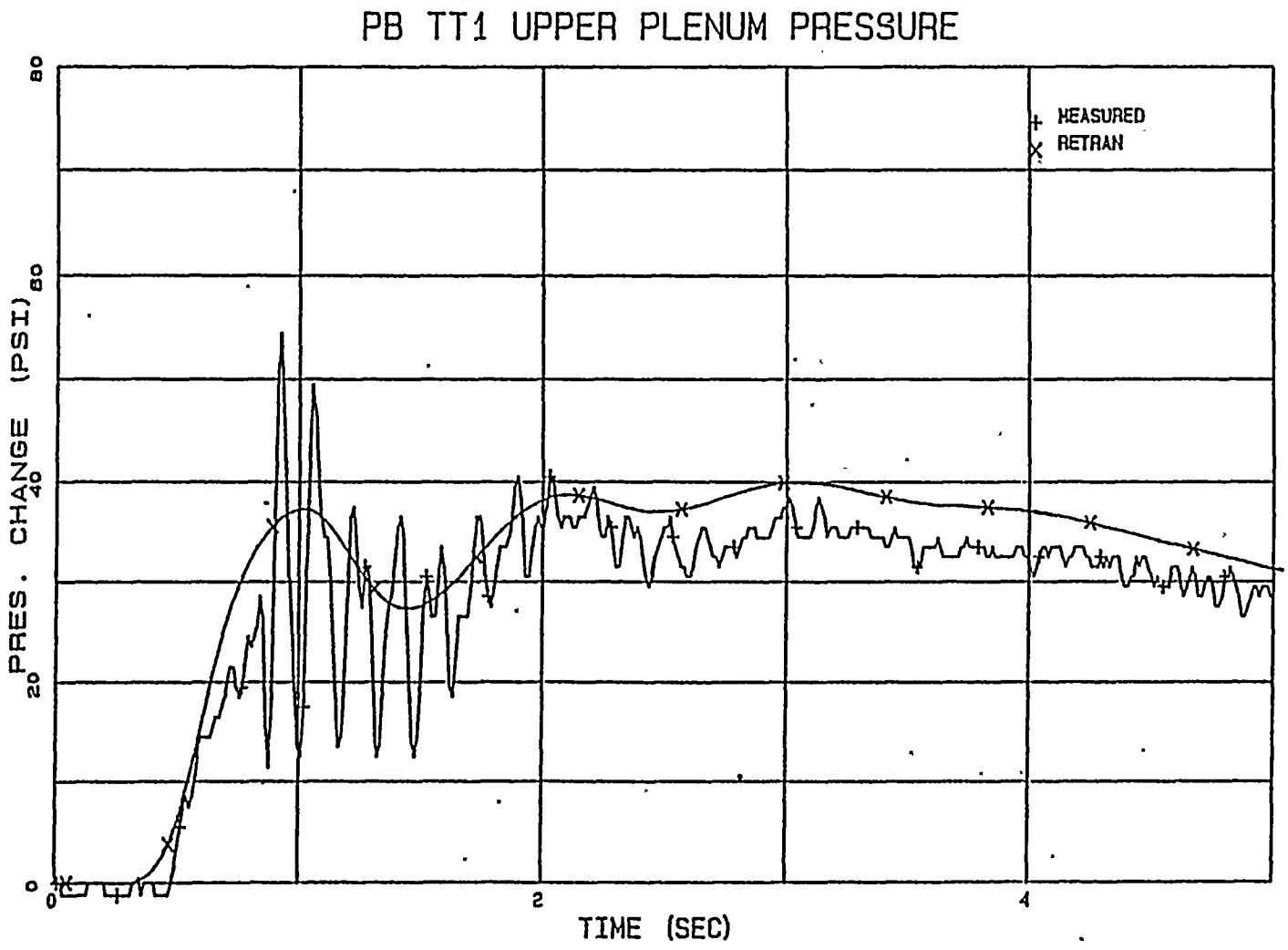
PB TT1 UPPER PLENUM PRESSURE
MEASURED
RETRAN
PRES. CHANGE (PSI)
80
60
40
20
0
0
2
4
TIME (SEC)

FIGURE 3.2.8

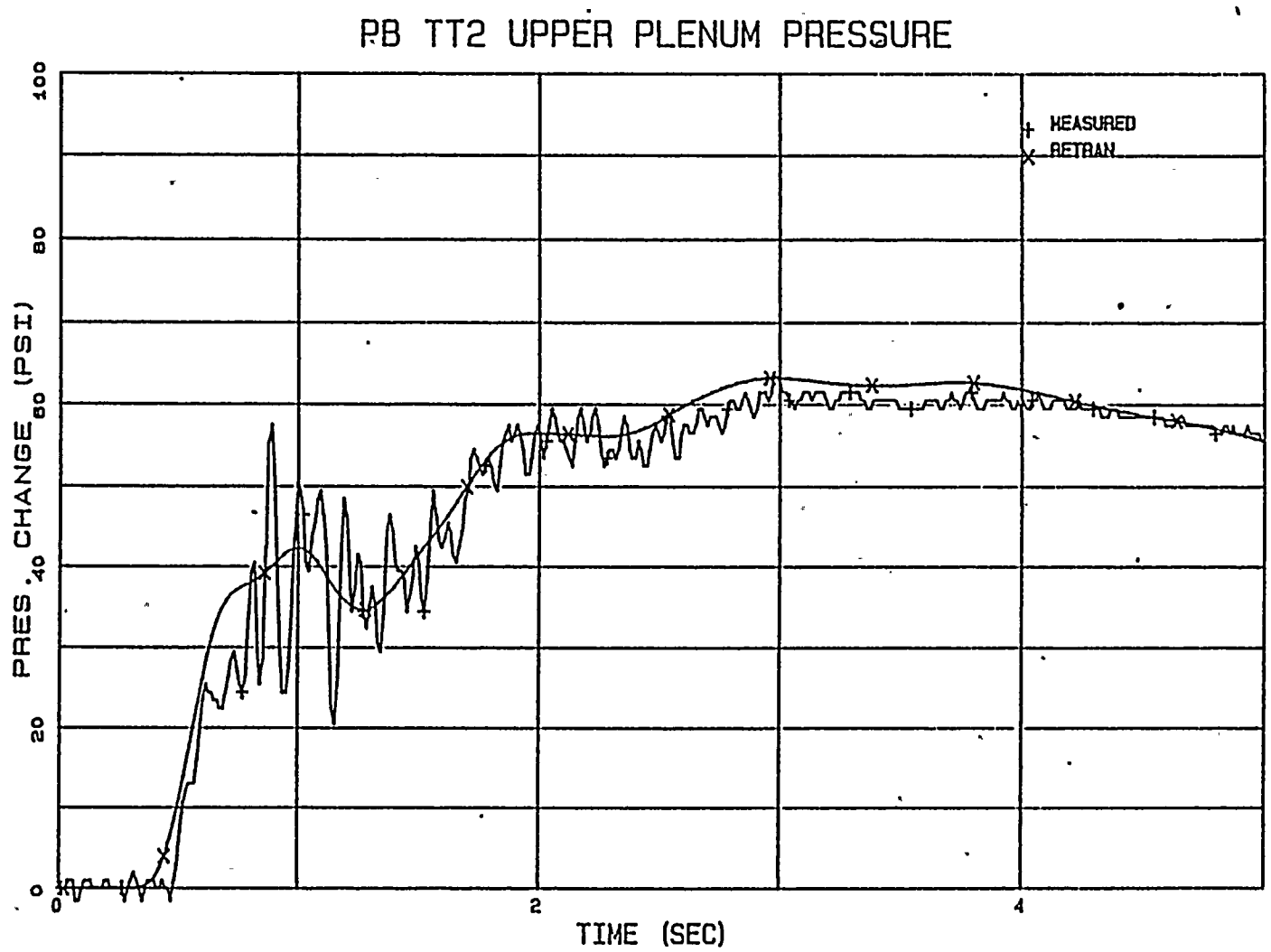
PB TT2 UPPER PLENUM PRESSURE
MEASURED
RETRAN
PRES. CHANGE (PSI)
0
20
40
60
80
100
0
2
4
TIME (SEC)

FIGURE 3.2.9

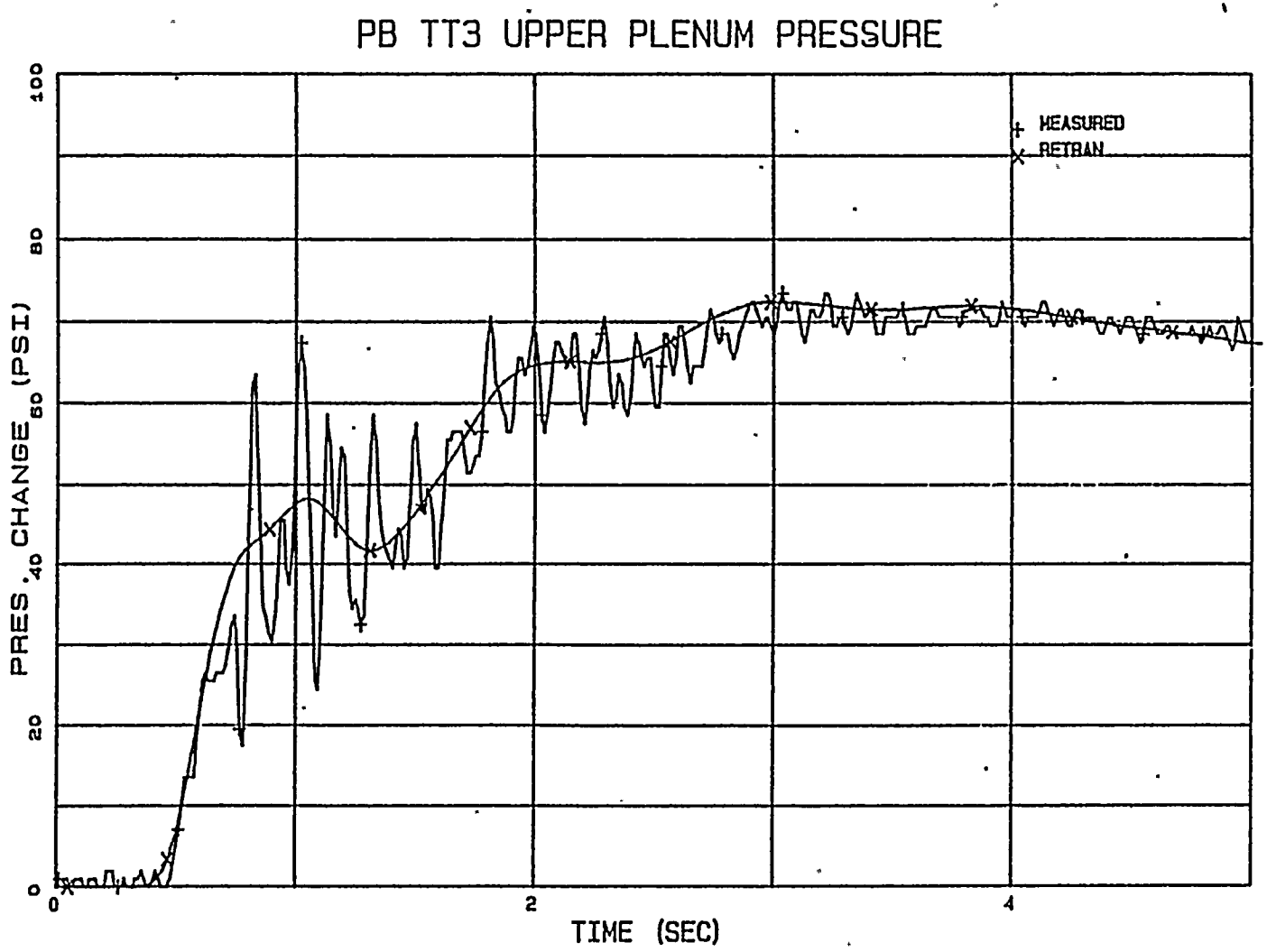
PB TT3 UPPER PLENUM PRESSURE
MEASURED
RETRAN
PRES. CHANGE (PSI)
0
20
40
60
80
100
0
2
4
TIME (SEC)

FIGURE 3.2.10

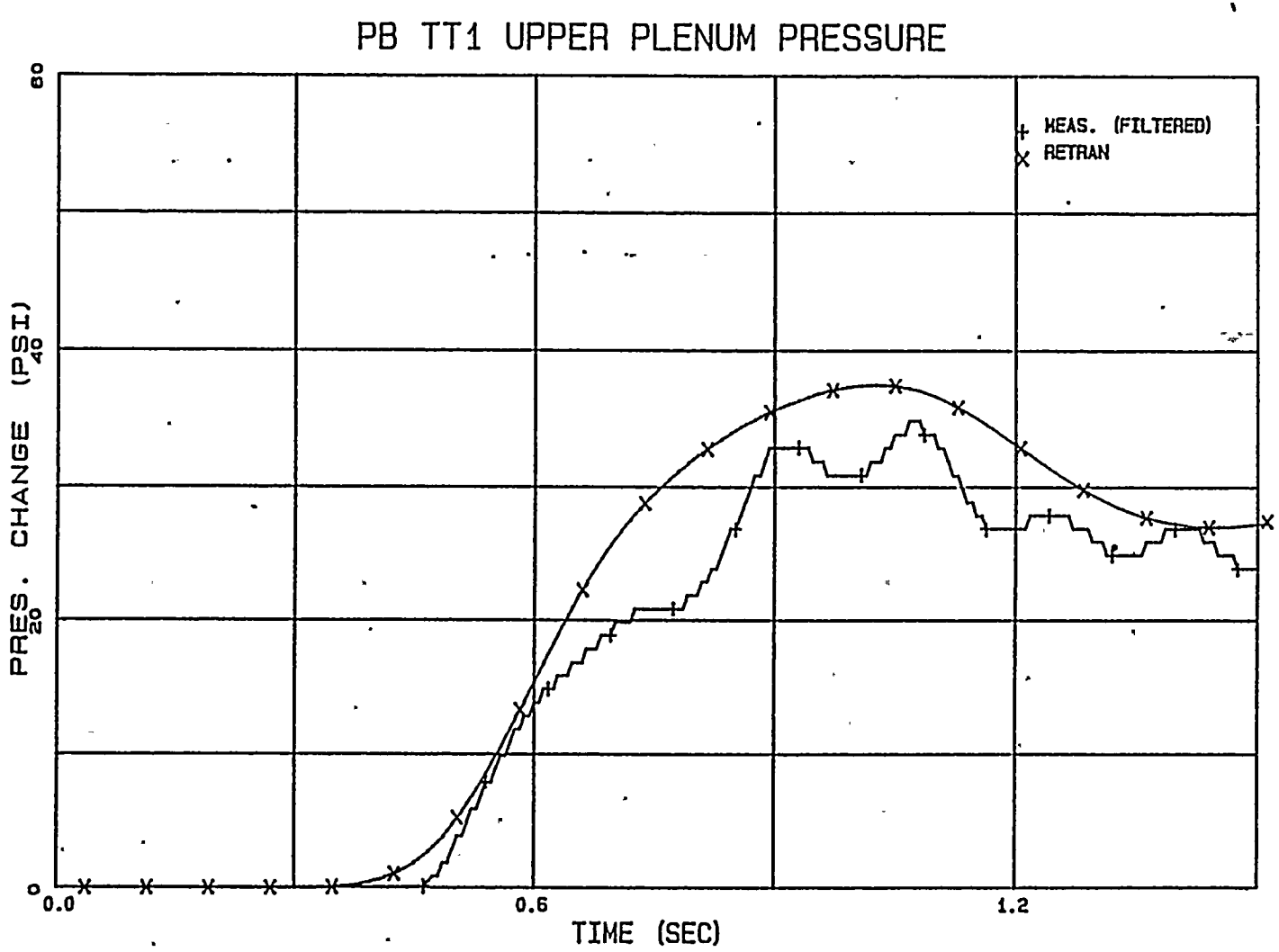
PB TT1 UPPER PLENUM PRESSURE
MEAS. (FILTERED)
RETRAN
PRES. CHANGE (PSI)
0
20
40
60
0.0
0.6
1.2
TIME (SEC)

FIGURE 3.2.11

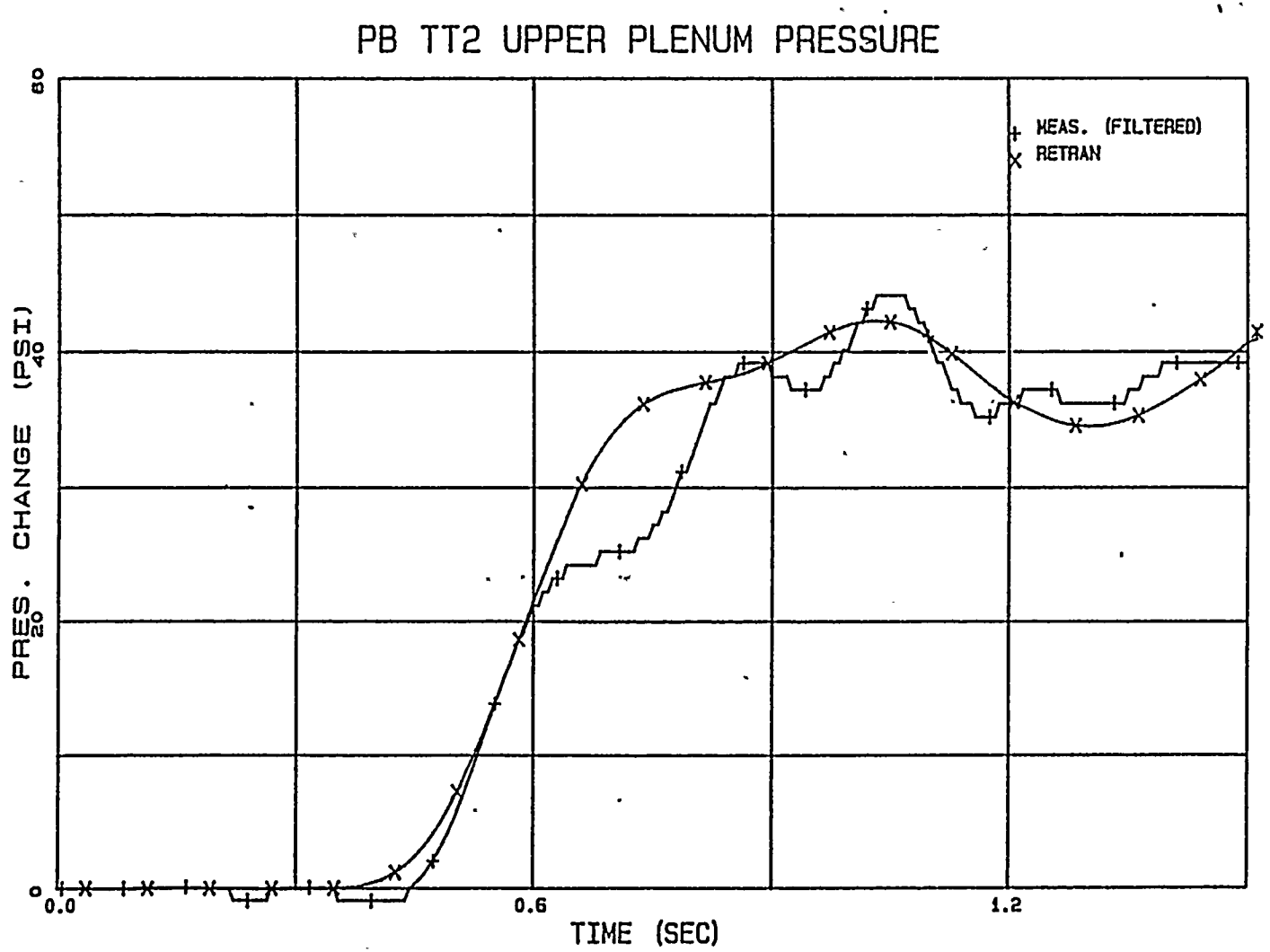
PB TT2 UPPER PLENUM PRESSURE
MEAS. (FILTERED)
RETRAN
PRES. CHANGE (PSI)
60
40
20
0
0.0
0.6
1.2
TIME (SEC)

FIGURE 3.2.12

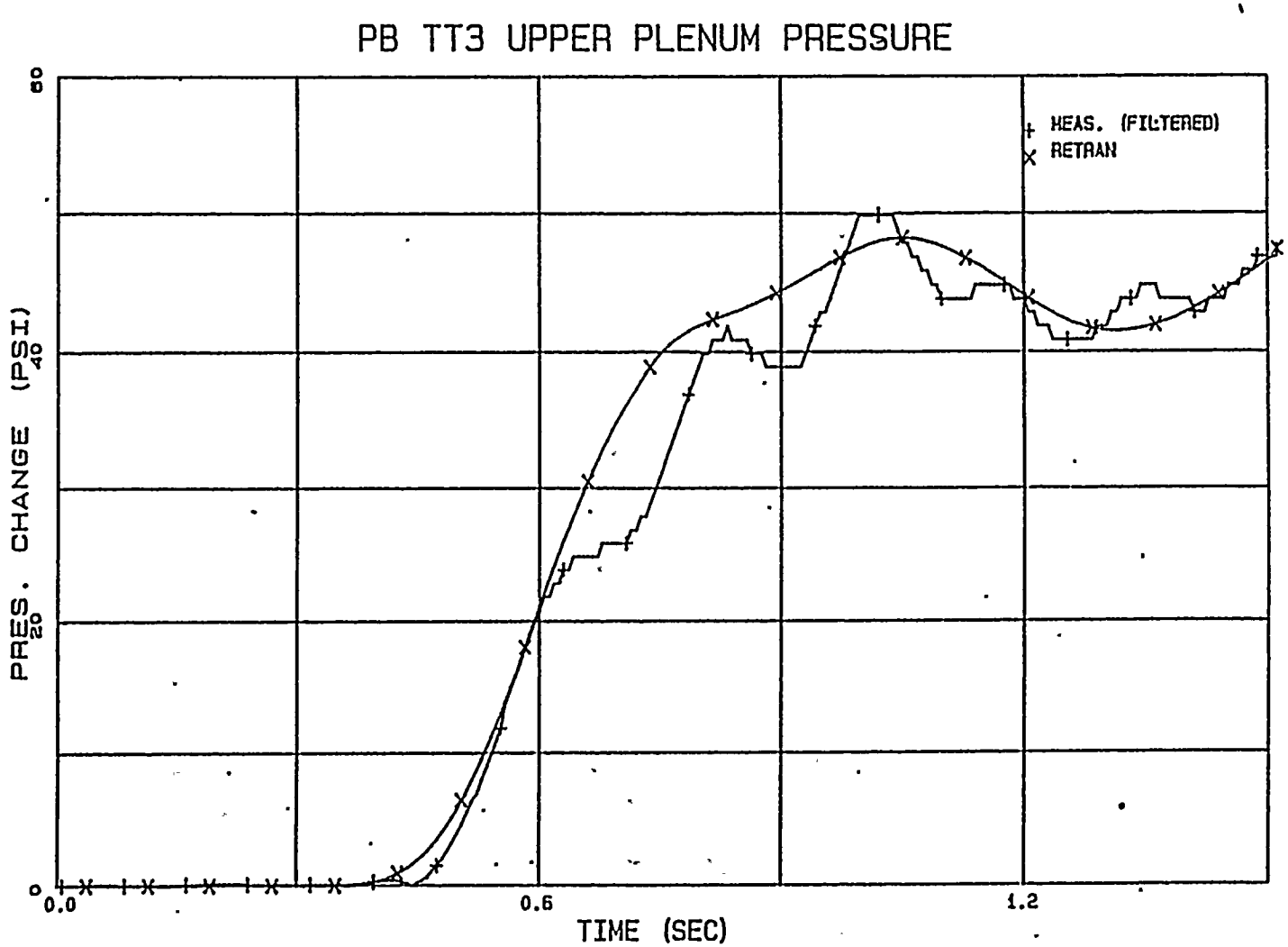
PB TT3 UPPER PLENUM PRESSURE
MEAS. (FILTERED)
RETRAN
PRES. CHANGE (PSI)
0
20
40
60
0.0
0.6
1.2
TIME (SEC)

3.2.4.2 Power and Reactivity Comparisons

The calculated core average neutron powers are compared to the normalized core average LPRM signals for each of the three tests in Figures 3.2.13 through 3.2.15. In all three cases, the rates of power change, timing trends and power peak magnitudes are in good agreement with the measured data. The capability to predict the power transients was further evaluated by comparing the area under the power peak during the pressurization transients to that predicted by RETRAN. In the thermal margin calculation, the critical power ratio is a function of the area under the power peak, not the magnitude of the peak. Tables 3.2.4 presents a summary of the calculated and measured power peaks and the area under the peaks for each test. A comparison of the time of the calculated and measured power peaks is given in Table 3.2.5.

The LPRM detectors are located at four elevations (from bottom to top, levels A, B, C, D). Comparisons of calculated flux to measured flux (average of all LPRMs at a level) at each axial level are presented in Figures 3.2.16 through 3.2.27. The calculated and measured peak values at each level is summarized in Table 3.2.6. Timing trend and relative peak magnitude are predicted well in the individual LPRM levels. This demonstrates that RETRAN is capable of predicting accurately the power shape change during rapid pressurization transient.

The calculated net reactivity, scram reactivity, and net reactivity implied by the data are presented in Figures 3.2.28 through 3.2.30. The implied net reactivity was calculated using an inverse point kinetic algorithm and the average of the measured LPRM signals. Table 3.2.7 summarizes the calculated and implied peak reactivities. The agreement between the calculated and the implied net reactivities is good. The slight overprediction of the peak reactivity for all three tests is caused by the overprediction of the upper plenum pressure at the time of peak reactivity. It is noted that the magnitudes of the overpredictions in reactivity are small relative to those of the neutron power. This is due to the extreme sensitivity of the neutron power to changes in reactivity close to the prompt critical condition. The reactivity figures also show that the calculated TT1 and TT2 net reactivity turns before scram occurs while TT3 net reactivity is turned by scram. The same trends are observed for the implied net reactivities.

TABLE 3.2.4

PEACH BOTTOM TURBINE TRIP TESTS

SUMMARY OF CORE AVERAGE PEAK NEUTRON POWER

	PEAK NEUTRON POWER (NORM)			AREA UNDER PEAK		
	CALC.	DATA	% DIFF.	CALC.	DATA	% DIFF.
TT1	5.41	4.83	12.0	0.960	0.888	8.1
TT2	4.68	4.54	3.1	0.769	0.743	3.5
TT3	5.39	4.90	10.0	0.717	0.669	7.2

TABLE 3.2.5

PEACH BOTTOM TURBINE TRIP TESTS

TIME (SEC) OF PEAK NEUTRON POWER

	CALC.	DATA
TT1	.774	.774
TT2	.720	.726
TT3	.702	.702

TABLE 3.2.6

PEACH BOTTOM TURBINE TRIP TESTS

SUMMARY OF LPRM LEVEL NEUTRON POWER PEAKS

		A	B	C	D	CORE AVG.
TT1	Calculation	3.72	4.98	5.99	6.15	5.41
	Data	3.48	4.46	5.23	5.59	4.83
	% Diff.	6.90	11.7	14.5	10.0	12.0
TT2	Calculation	3.49	4.68	5.09	4.82	4.68
	Data	3.52	4.50	4.91	5.02	4.54
	% Diff.	-0.9	4.0	3.7	-4.0	3.1
TT3	Calculation	3.84	5.42	6.06	5.74	5.39
	Data	3.68	4.83	5.45	5.47	4.90
	% Diff.	4.3	12.2	11.2	4.9	10.0

TABLE 3.2.7

PEACH BOTTOM TURBINE TRIP TESTS

REACTIVITY SUMMARY

	PEAK REACTIVITY ($)			TIME OF PEAK (SEC)	
	CALC.	DATA	% DIFF.	CALC.	DATA
TT1	0.804	0.776	3.6%	0.738	0.744
TT2	0.780	0.767	1.7%	0.690	0.696
TT3	0.836	0.812	2.5%	0.678	0.660

FIGURE 3.2.13

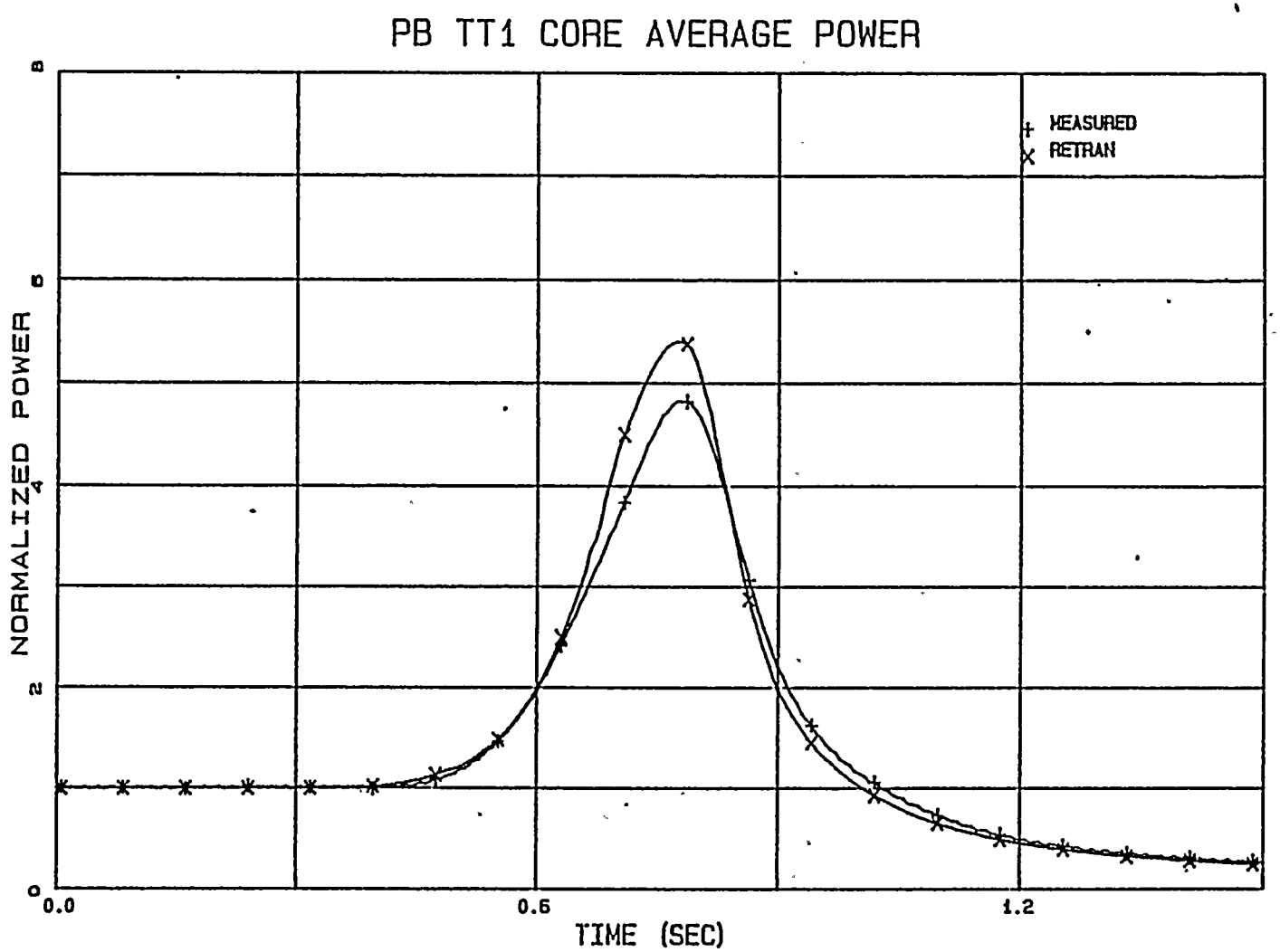
PB TT1 CORE AVERAGE POWER
MEASURED
RETRAN
NORMALIZED POWER
0
2
4
6
8
0.0
0.6
1.2
TIME (SEC)

FIGURE 3.2.14

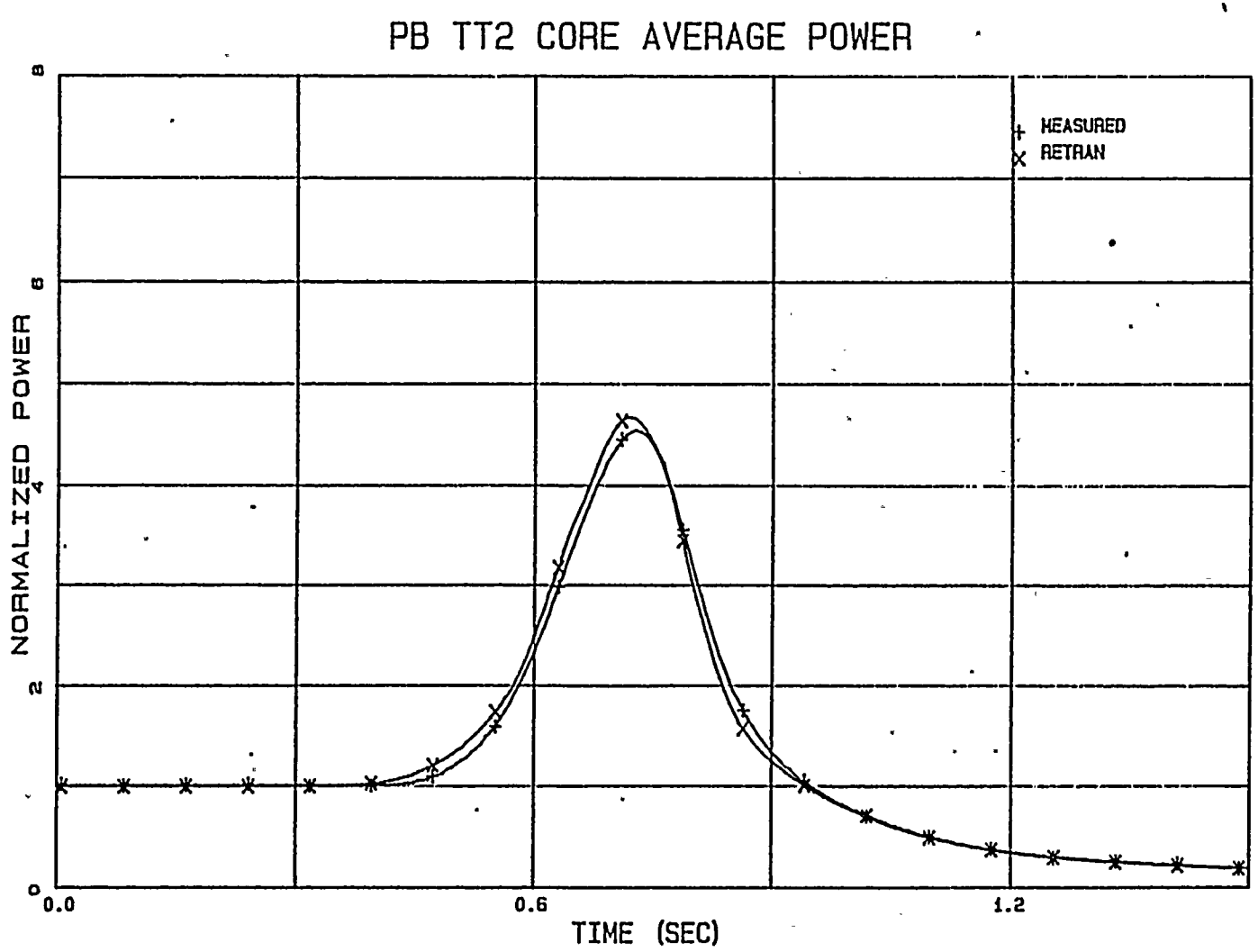
PB TT2 CORE AVERAGE POWER
MEASURED
RETRAN
NORMALIZED POWER
0
2
4
6
8
0.0
0.6
1.2
TIME (SEC)

FIGURE 3.2.15

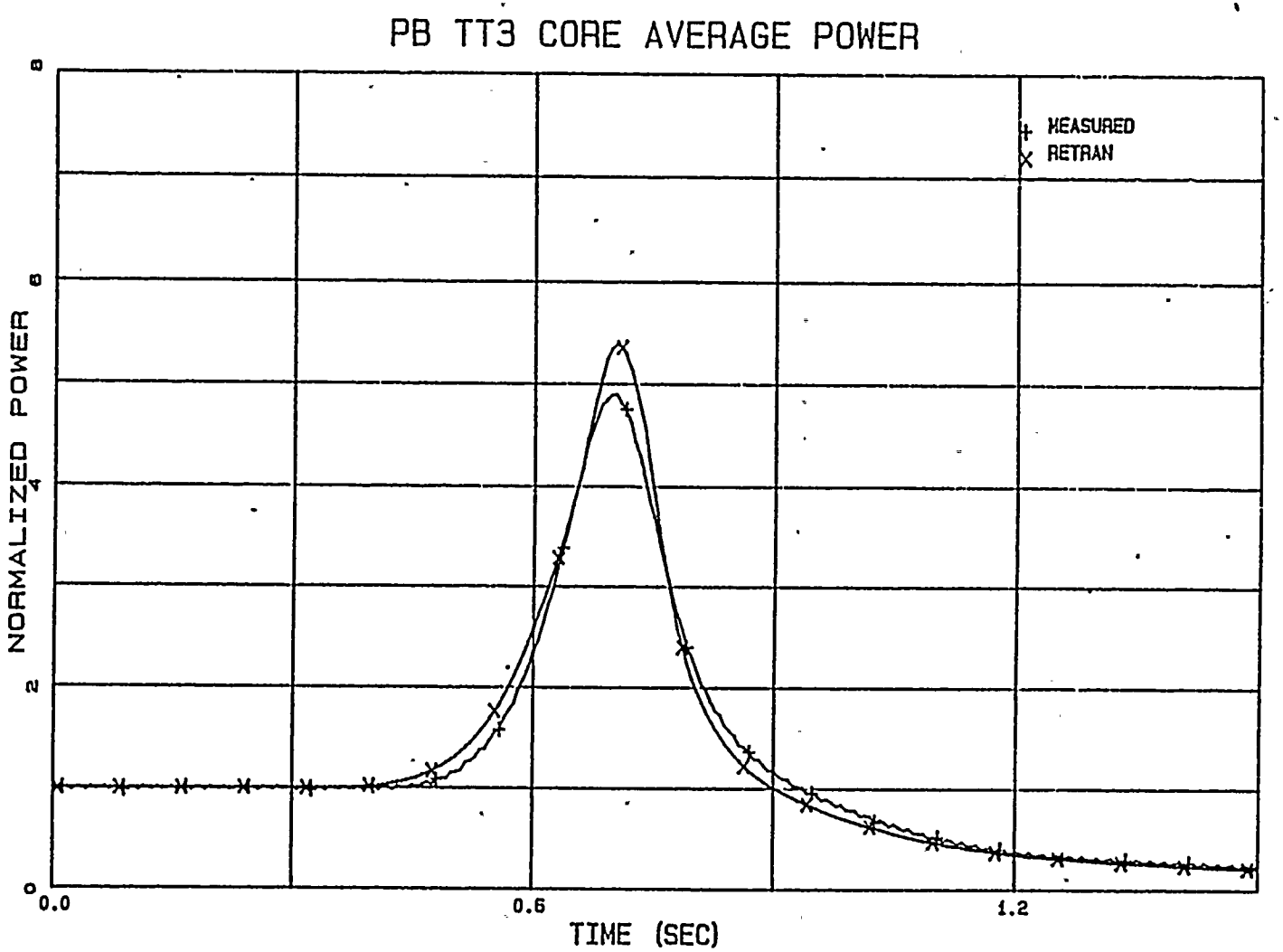
PB TT3 CORE AVERAGE POWER
MEASURED
RETRAN
NORMALIZED POWER
0
2
4
6
8
0.0
0.6
1.2
TIME (SEC)

FIGURE 3.2.16

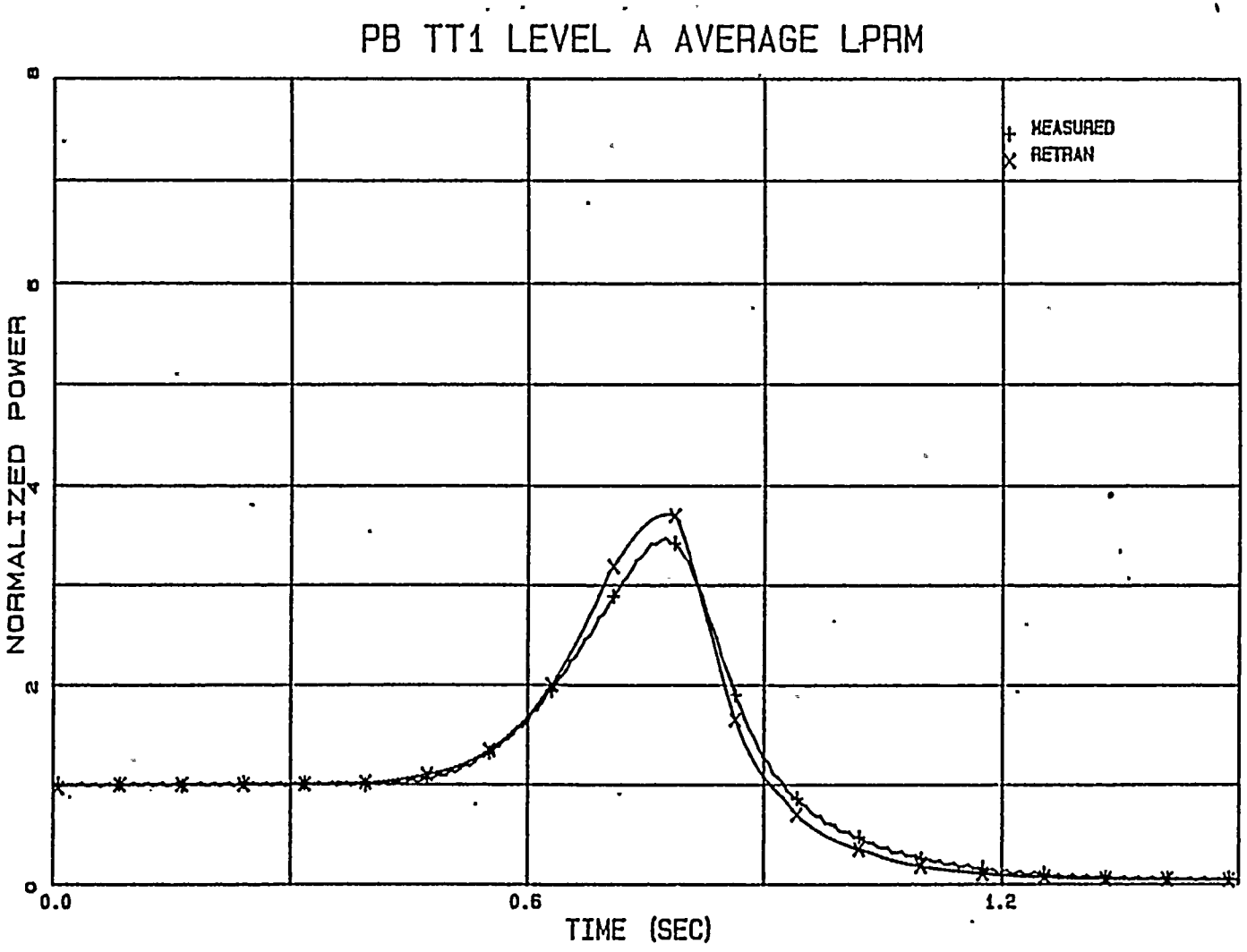
PB TT1 LEVEL A AVERAGE LPRM
MEASURED
RETRAN
NORMALIZED POWER
0
2
4
6
8
0.0
0.6
1.2
TIME (SEC)

FIGURE 3.2.17

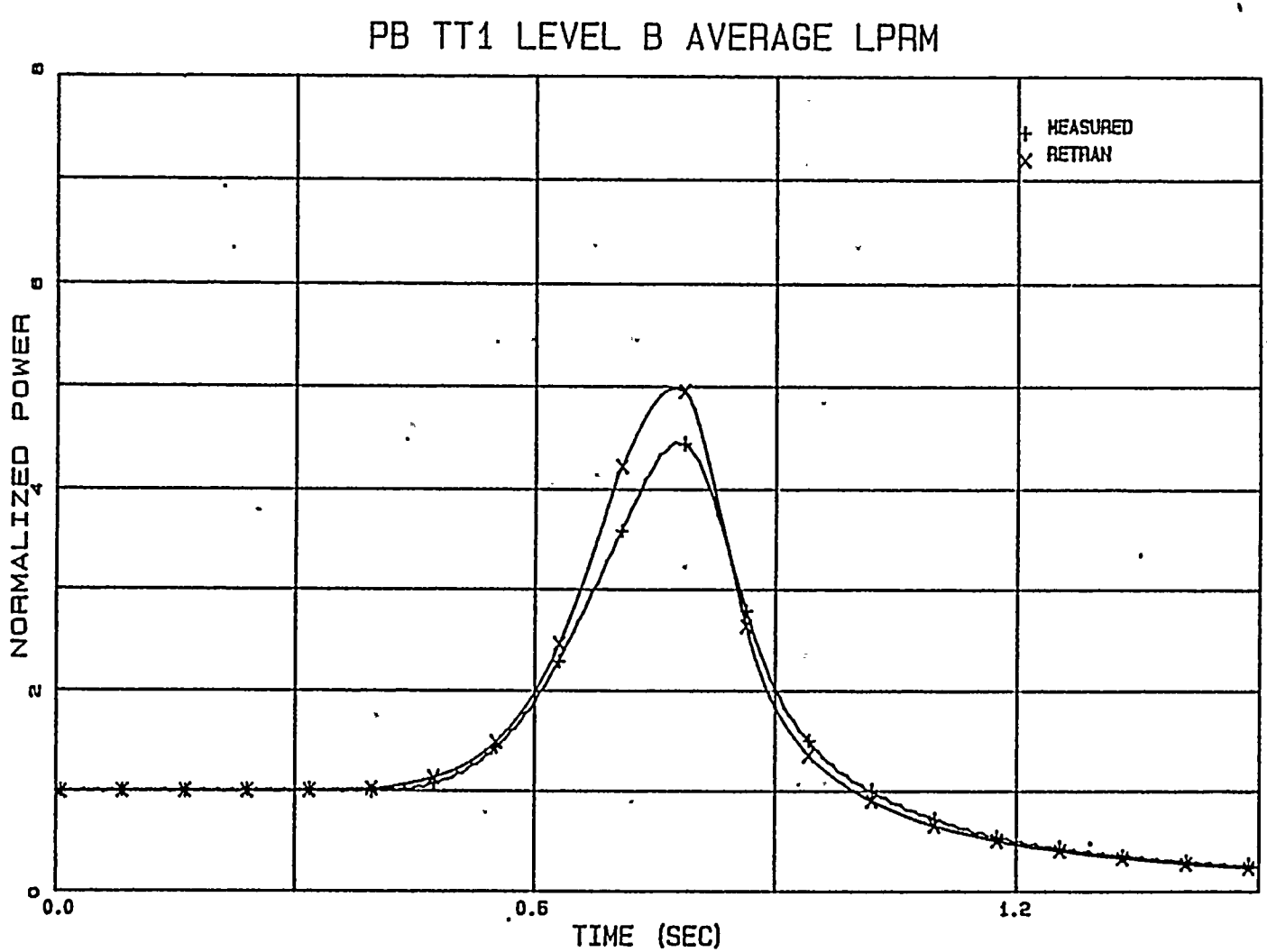
PB TT1 LEVEL B AVERAGE LPRM
MEASURED
RETRAN
NORMALIZED POWER
0
2
4
6
8
0.0
0.6
1.2
TIME (SEC)

FIGURE 3.2.18

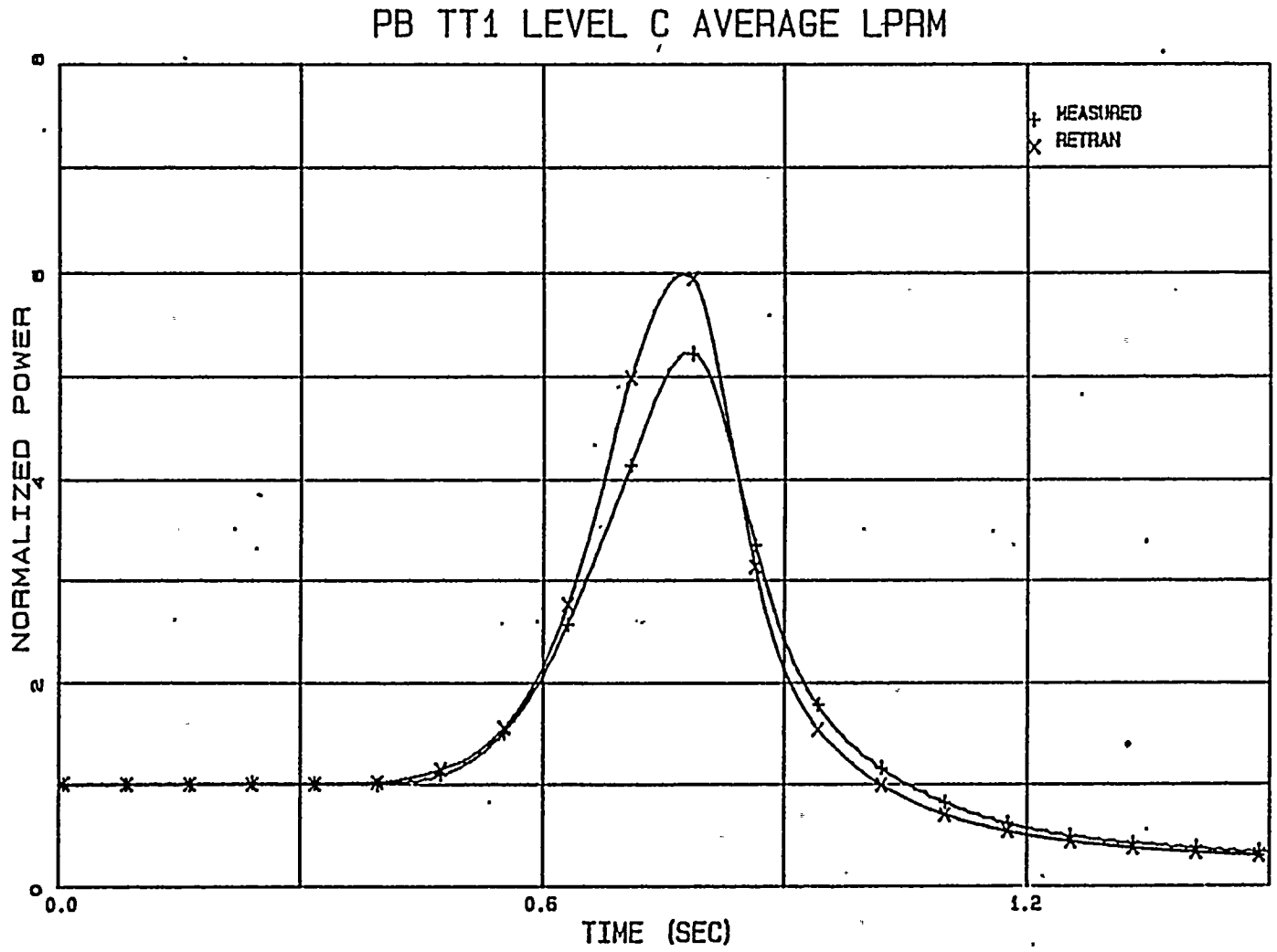
PB TT1 LEVEL C AVERAGE LPRM
MEASURED
RETRAN
NORMALIZED POWER
0
2
4
6
8
0.0
0.6
1.2
TIME (SEC)

FIGURE 3.2.19

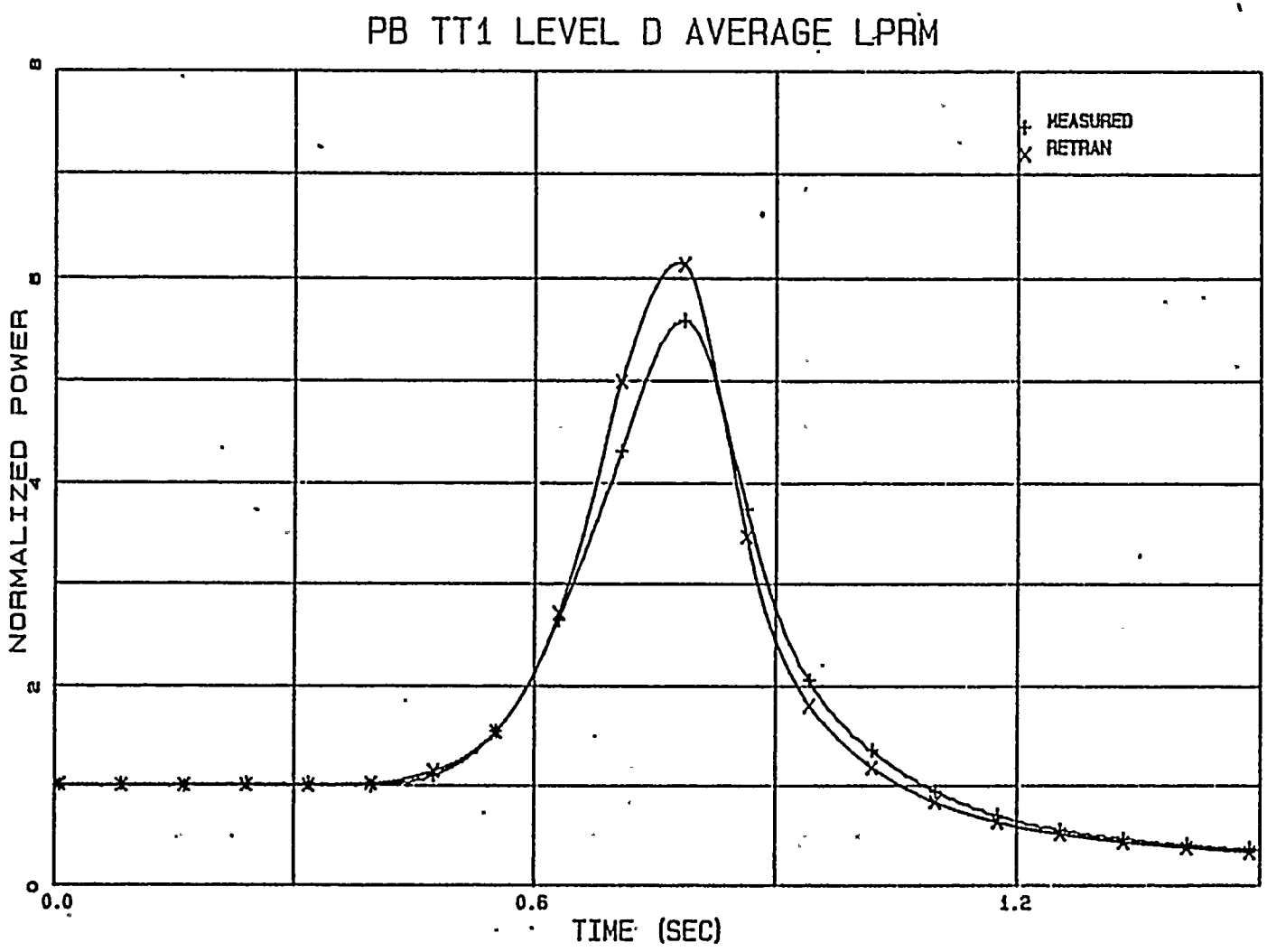
PB TT1 LEVEL D AVERAGE LPRM
MEASURED
RETRAN
NORMALIZED POWER
0
2
4
6
8
0.0
0.6
1.2
TIME (SEC)

FIGURE 3.2.20

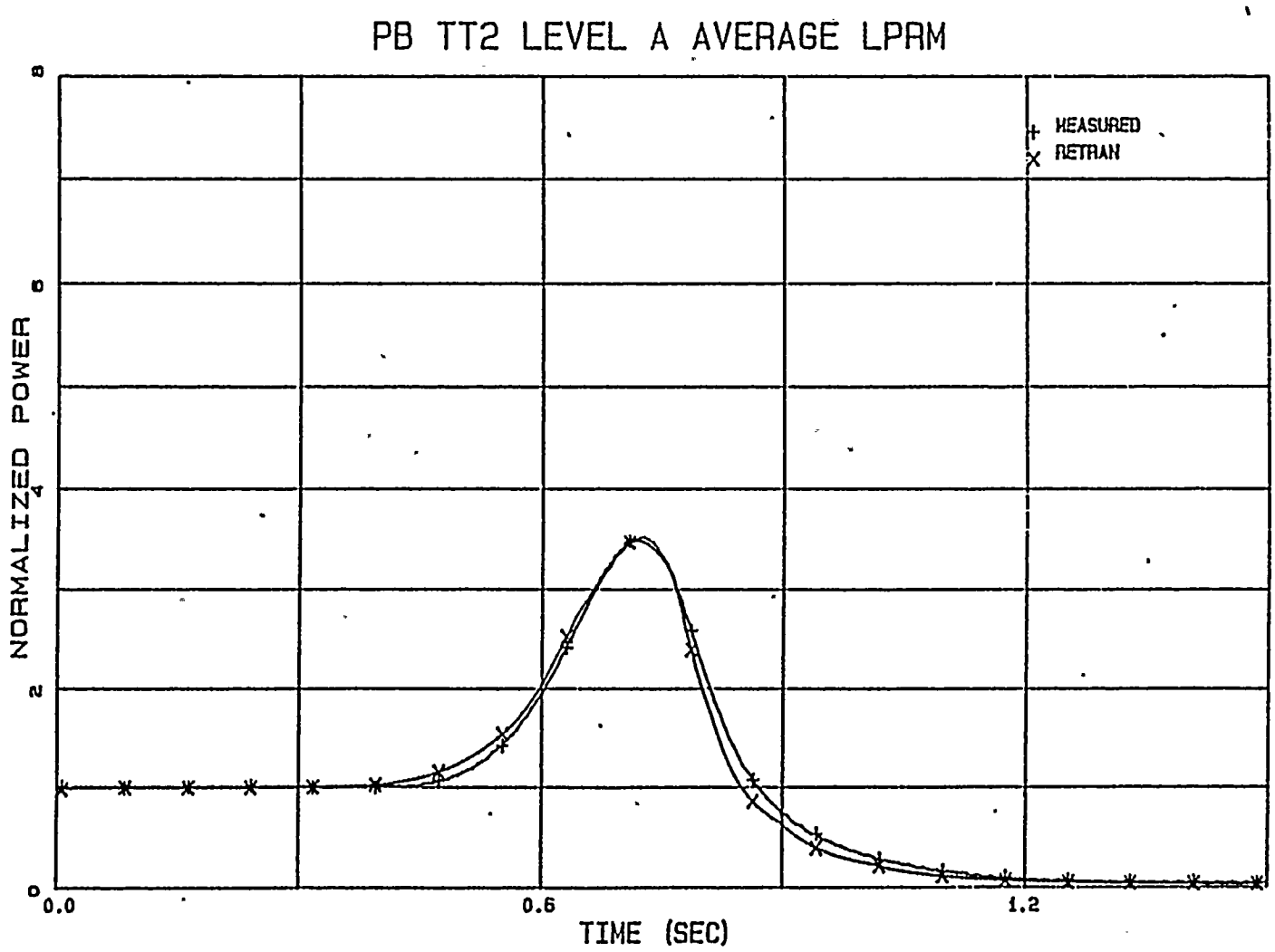
PB TT2 LEVEL A AVERAGE LPRM
MEASURED
RETRAN
NORMALIZED POWER
0
2
4
6
8
0.0
0.6
1.2
TIME (SEC)

FIGURE 3.2.21

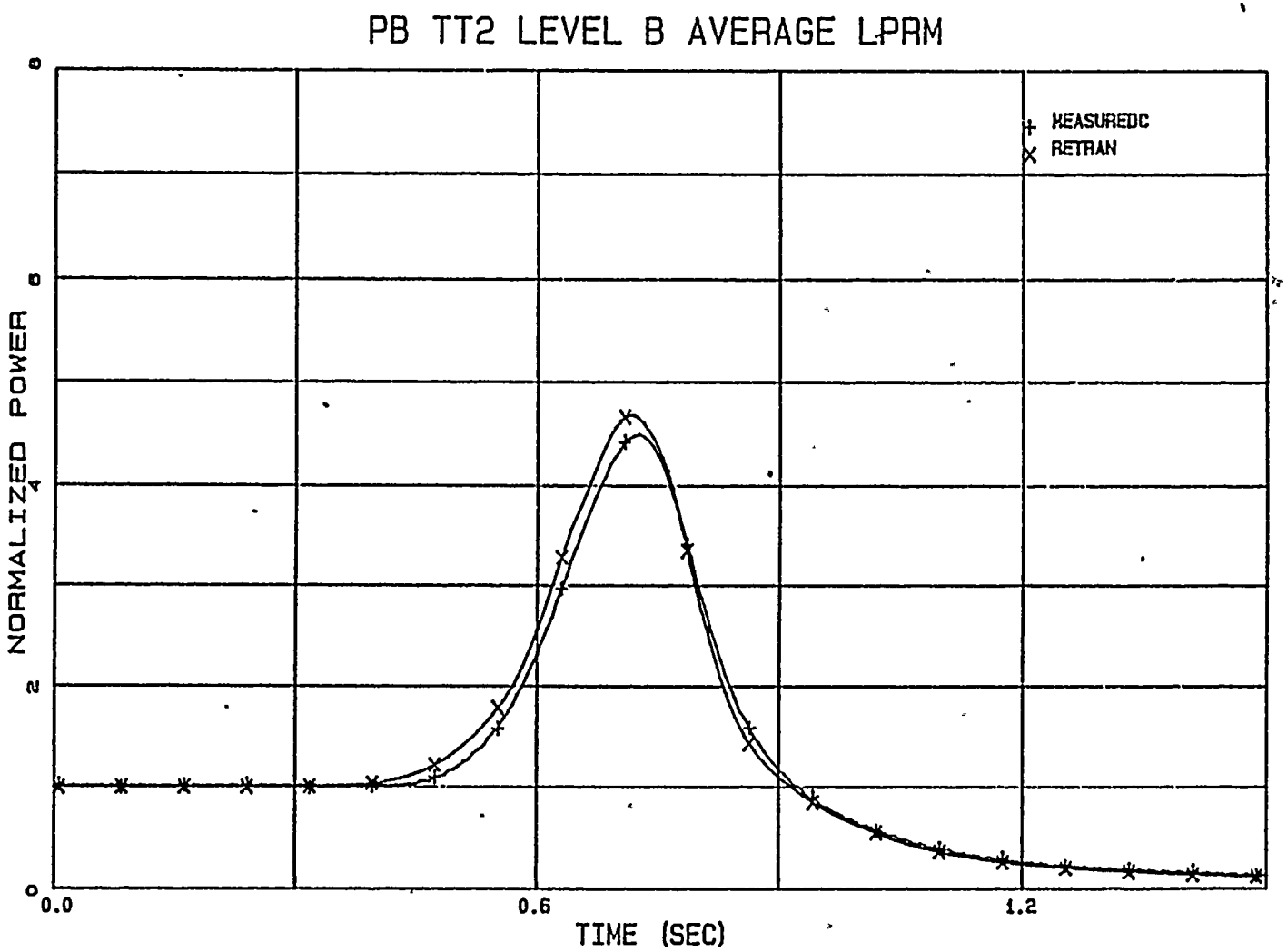
PB TT2 LEVEL B AVERAGE LPRM
MEASUREDC
RETRAN
NORMALIZED POWER
0
2
4
6
8
0.0
0.6
1.2
TIME (SEC)

FIGURE 3.2.22

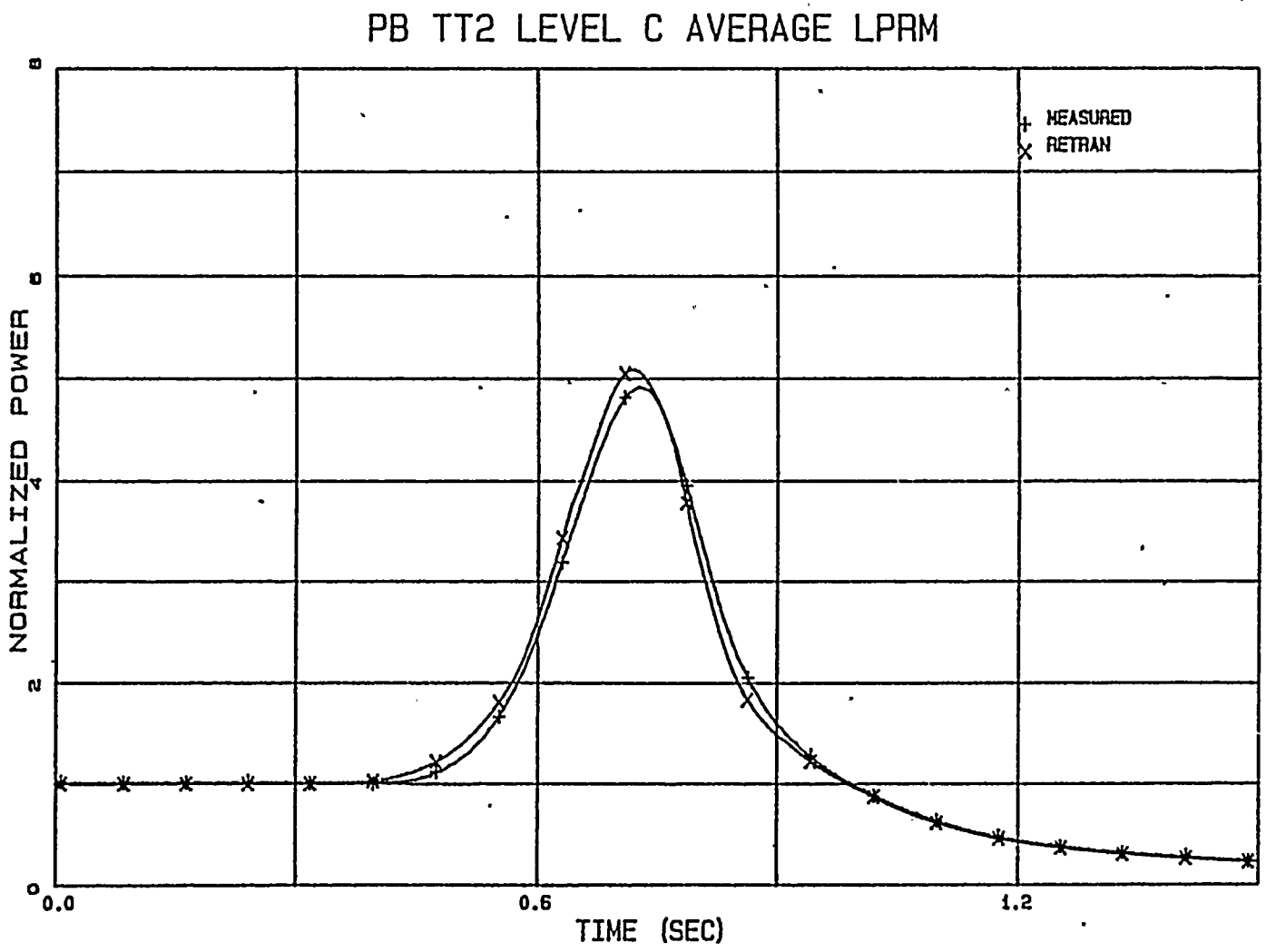
PB TT2 LEVEL C AVERAGE LPRM
MEASURED
RETRAN
NORMALIZED POWER
0
2
4
6
8
0.0
0.6
1.2
TIME (SEC)

FIGURE 3.2.23

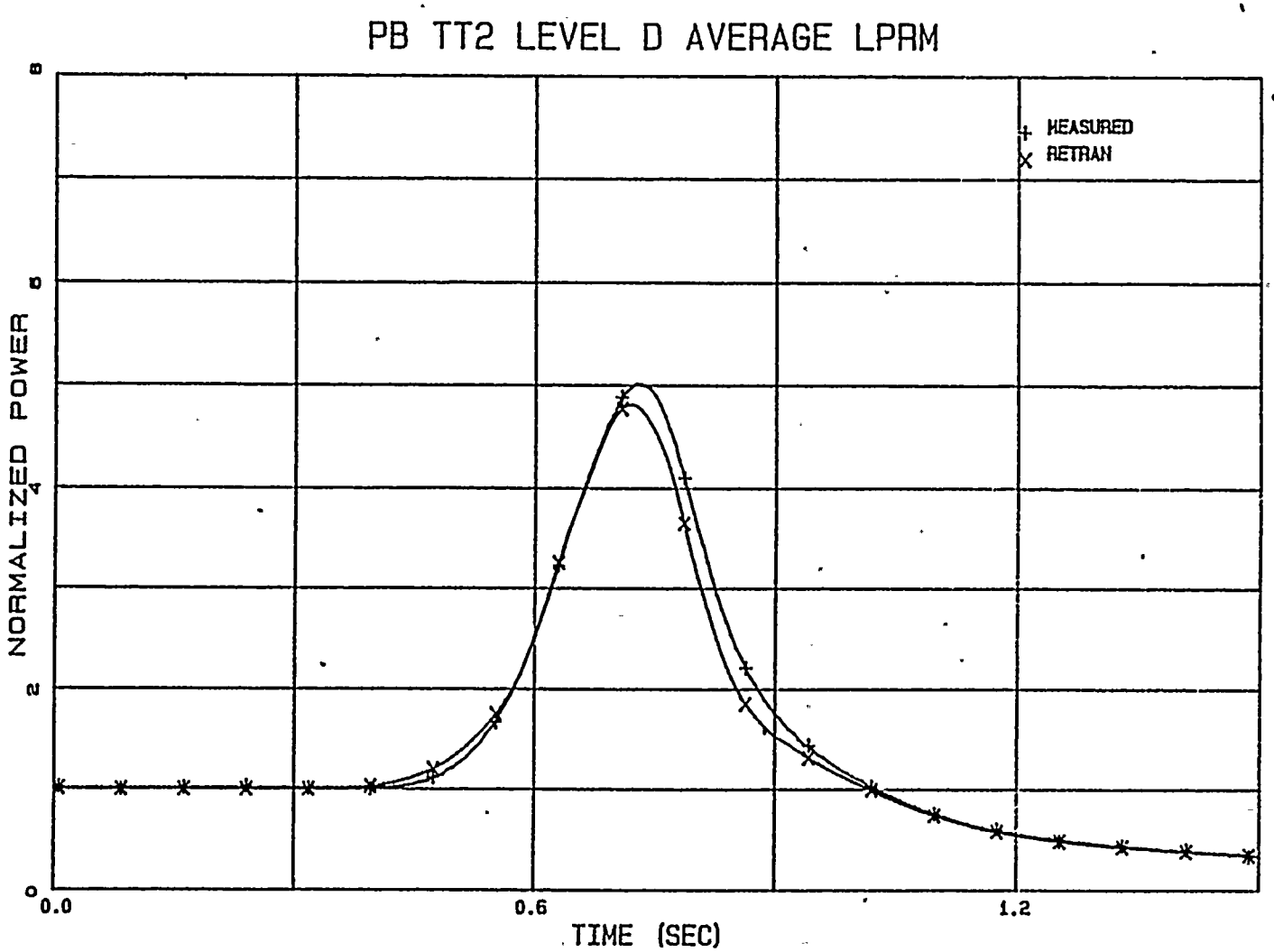
PB TT2 LEVEL D AVERAGE LPRM
MEASURED
RETRAN
NORMALIZED POWER
0
2
4
6
8
0.0
0.6
1.2
TIME (SEC)

FIGURE 3.2.24

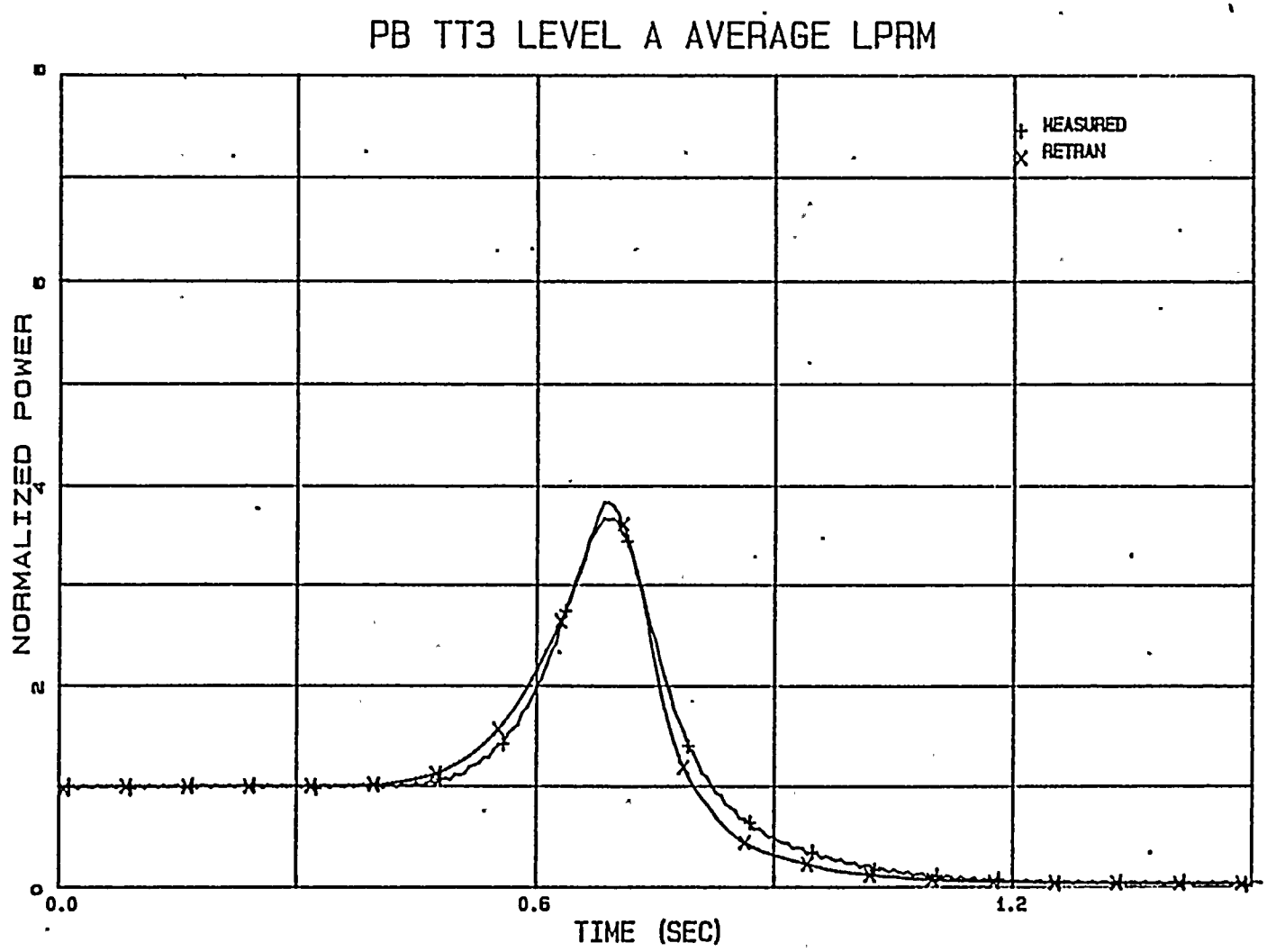
PB TT3 LEVEL A AVERAGE LPRM
MEASURED
RETRAN
NORMALIZED POWER
0
2
4
6
8
0.0
0.6
1.2
TIME (SEC)

FIGURE 3.2.25

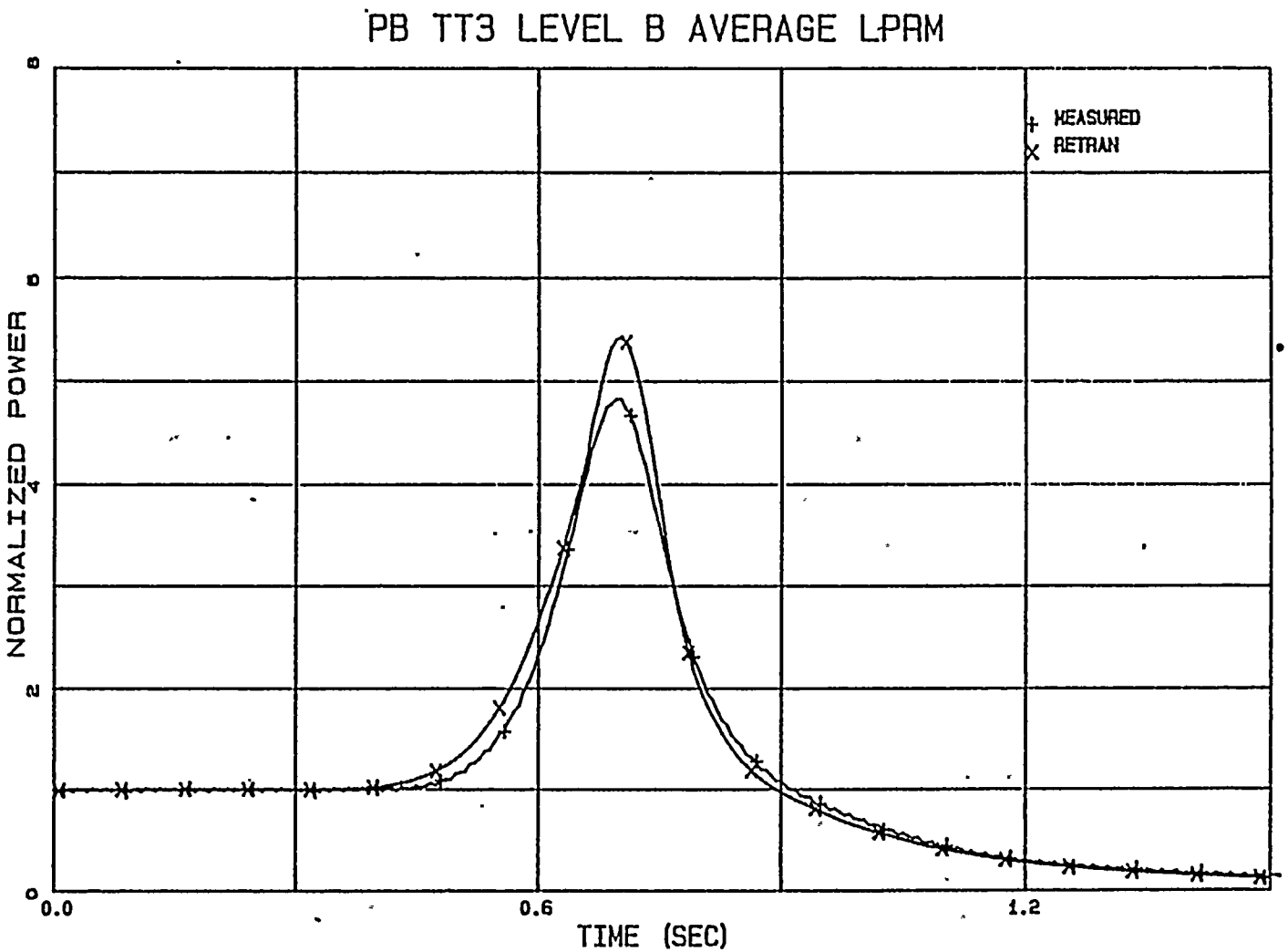
PB TT3 LEVEL B AVERAGE LPRM
MEASURED
RETRAN
NORMALIZED POWER
0
2
4
6
8
0.0
0.6
1.2
TIME (SEC)

FIGURE 3.2.26

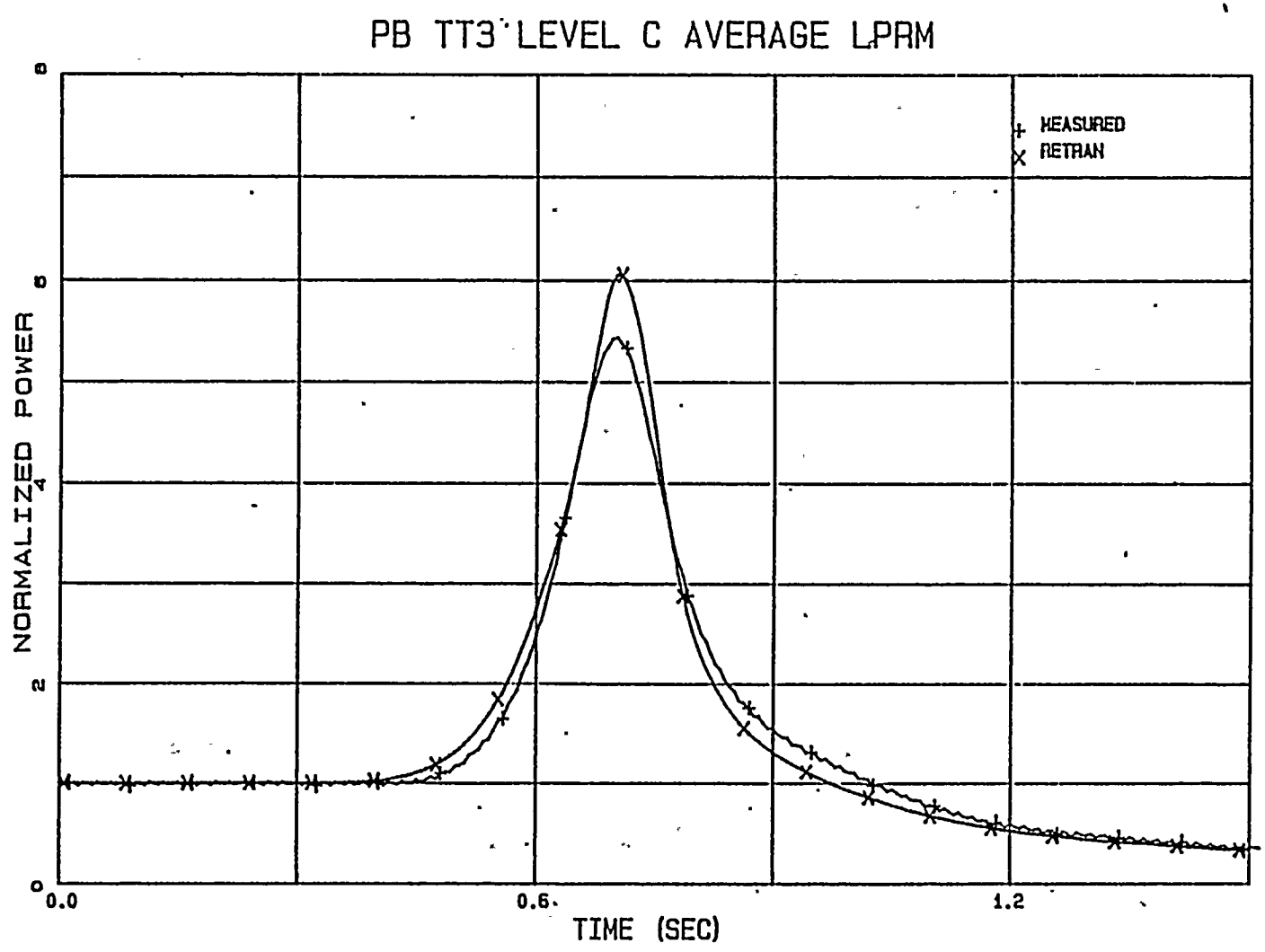
PB TT3 LEVEL C AVERAGE LPRM
MEASURED
RETRAN
NORMALIZED POWER
0
2
4
6
8
0.0
0.6
1.2
TIME (SEC)

FIGURE 3.2.27

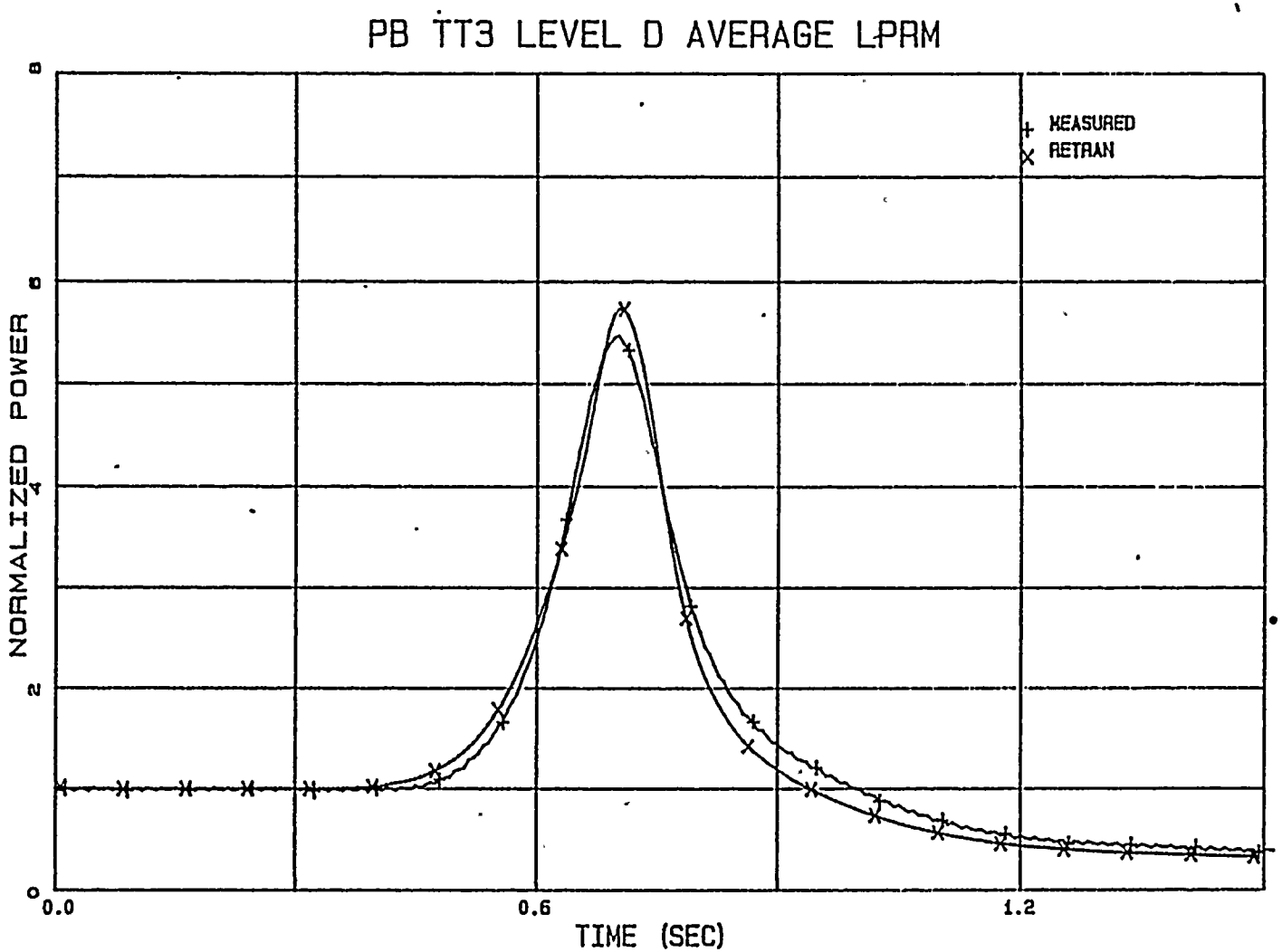
PB TT3 LEVEL D AVERAGE LPRM
MEASURED
RETRAN
NORMALIZED POWER
0
2
4
6
8
0.0
0.6
1.2
TIME (SEC)

FIGURE 3.2.28

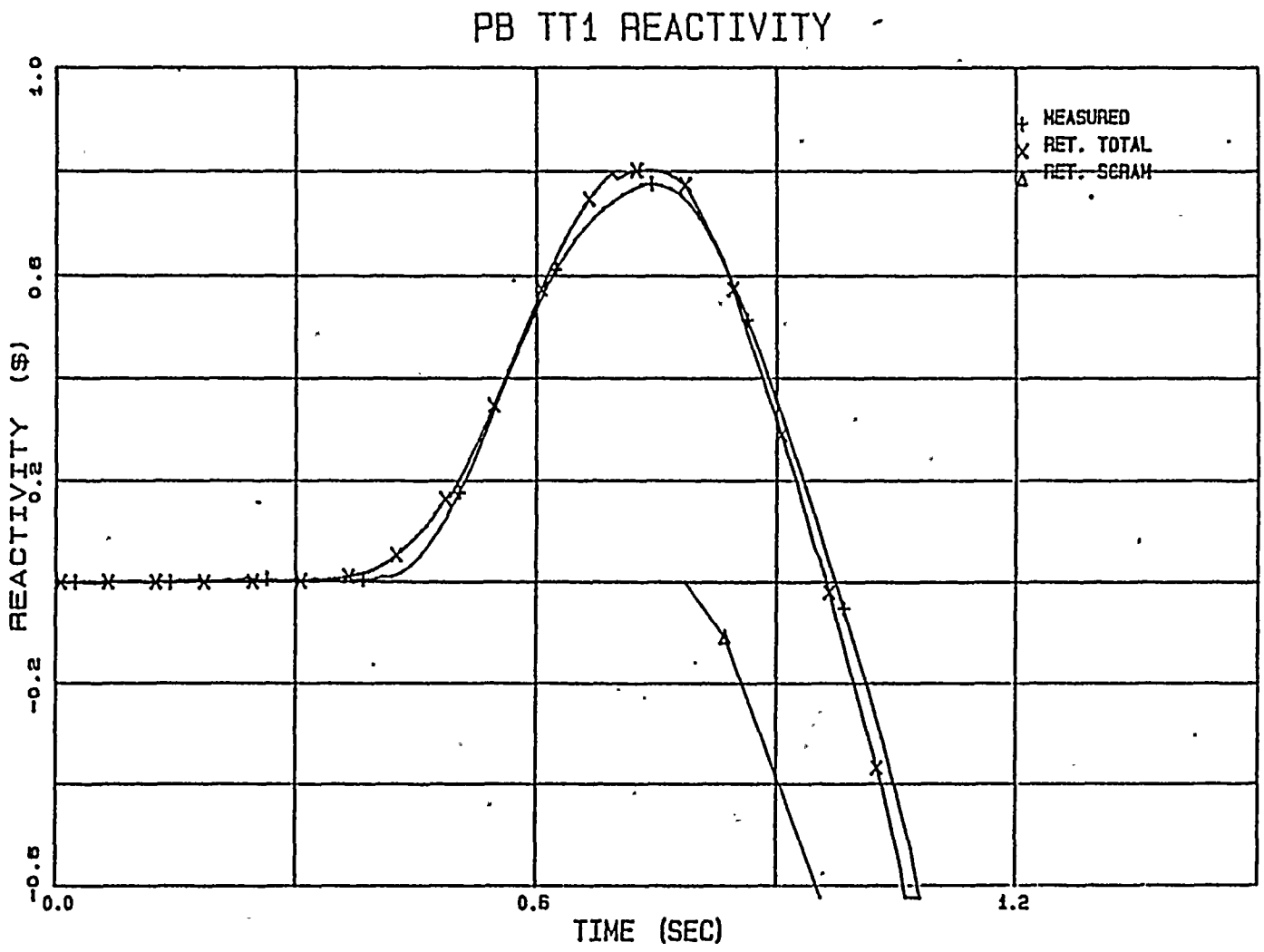
PB TT1 REACTIVITY
MEASURED
RET. TOTAL
RET. SCRAM
REACTIVITY ($)
1.0
0.6
0.2
-0.2
-0.6
0.0
0.6
1.2
TIME (SEC)

FIGURE 3.2.29

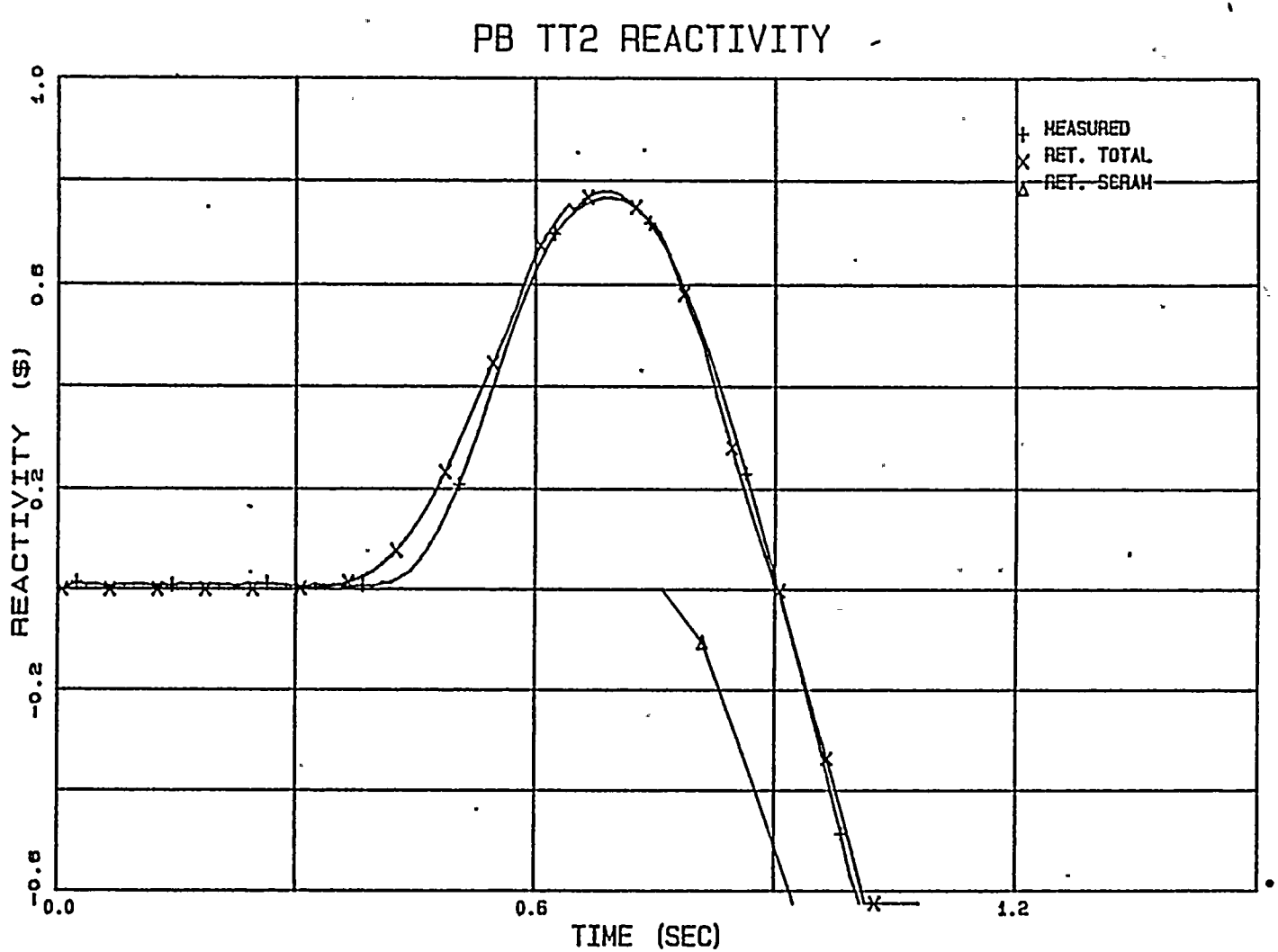
PB TT2 REACTIVITY
MEASURED
RET. TOTAL
RET. SCRAM
REACTIVITY ($)
1.0
0.6
0.2
-0.2
-0.6
0.0
0.6
1.2
TIME (SEC)

FIGURE 3.2.30

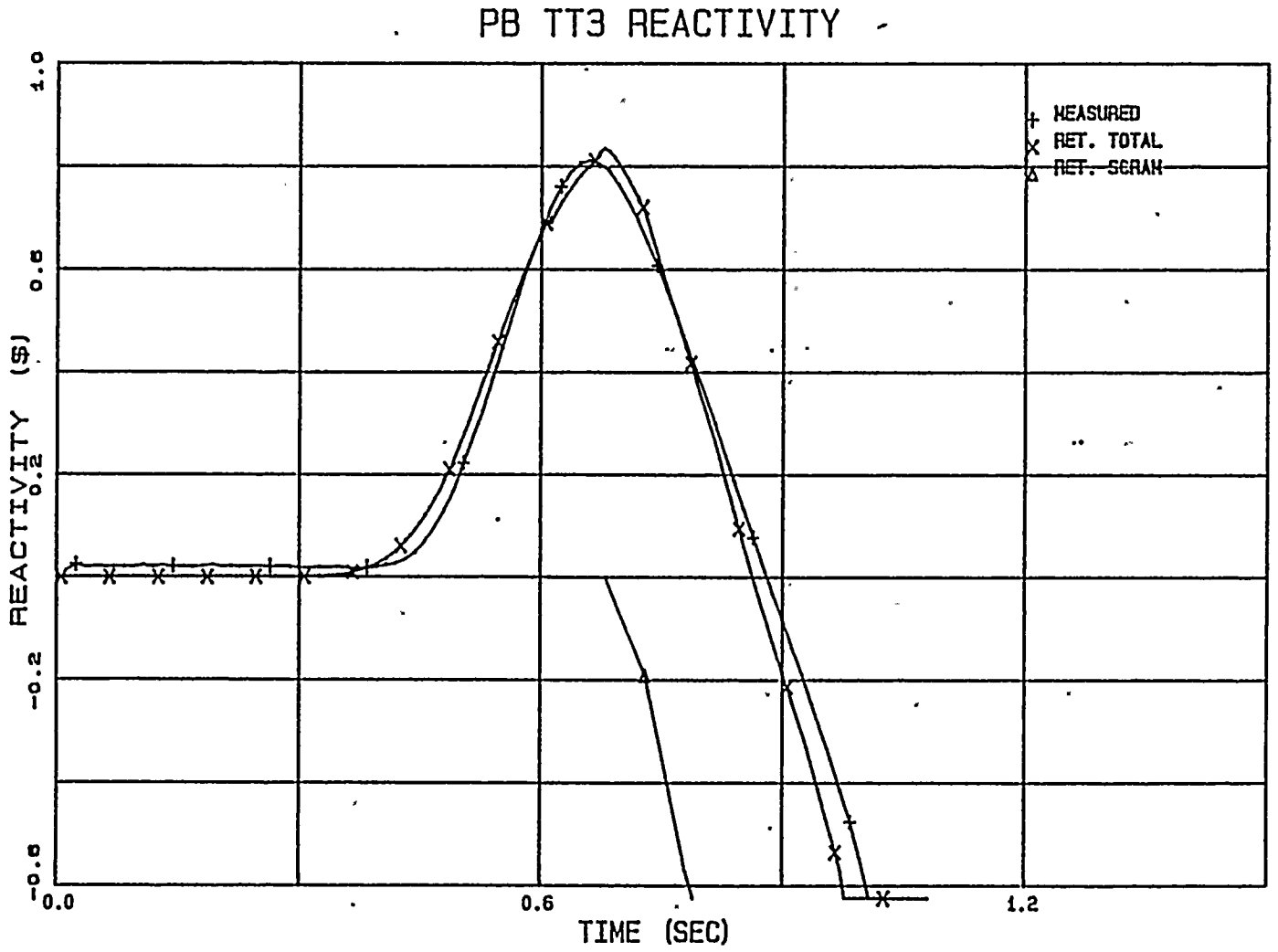
PB TT3 REACTIVITY
MEASURED
RET. TOTAL
RET. SCRAM
REACTIVITY ($)
1.0
0.6
0.2
-0.2
-0.6
0.0
0.6
1.2
TIME (SEC)

4.0 LICENSING BASIS ANALYSIS

A broad spectrum of transient events have been analyzed for WNP-2; the results are presented in the Final Safety Analysis Report. These events cover a wide range of scenarios and conditions contributing to Technical Specification Limits. Most of these transient events are not sensitive to changes in reload core configuration, or are within the conservative limits established by the original FSAR analysis. Changes in fuel design and core configuration are usually bounded by the analysis of selected limiting events. Based on previous analyses performed by vendors for WNP-2[22,23,26] and utilities on similar plants[24], the two most limiting events requiring a reanalysis with each reload core are:

1. Load Rejection Without Bypass (LRNB)
2. Feedwater Controller Failure to Maximum Demand (FWCF)

The results of these transients generally determine Technical Specification limits for minimum critical power ratio (MCPR). This chapter describes the system analysis for these transients. The full licensing FSAR analysis, the sensitivity analysis and the hot channel analysis from which the operating limits are obtained will be described in a separate applications topical report (to be submitted later). The purpose of including this section is merely to indicate the parameters that typically change in modelling conservative FSAR transients and to show the WNP-2 model, with the parameters modified, indeed calculates conservative results.

4.1 Licensing Basis Model

The licensing basis model described in this chapter is a generic model using the Cycle 4 core configuration. For future applications, specific reload configurations and plant parameters will be used. These calculations are typical of planned WNP-2 reload analyses.

The licensing basis RETRAN model is a modification of the WNP-2 best-estimate model. The modifications assure the conservatism of the calculated results by using the values of the key parameters which bound the expected operating range.

Table 4.1 compares licensing basis model inputs with the nominal values. The nominal values and conditions show conservatism in the licensing basis modeling.

The licensing analysis performed in this report uses the end-of-cycle exposure for the calculation of the nuclear design data. At EOC, control rods are withdrawn from the core to counteract the consumption of excess reactivity. The average control rod scram distance is greater with more rods withdrawn, so scram performance degrades near the end of cycle. Scram reactivity insertion rate is the dominant power reversal phenomenon for pressurization transients; the most severe results occur at the maximum cycle exposure, when scram performance is least effective.

TABLE 4.1

INPUT PARAMETERS AND INITIAL TRANSIENT CONDITIONS
COMPARISON OF LICENSING BASIS AND NOMINAL PLANT CONDITIONS

Parameter	Nominal	Licensing Basis
Core Exposure	BOC - EOC	EOC
Thermal Power (MWt)	3323	3468
Steam Flow (lbs/sec)	3970.97	4161.11
Feedwater Flow Rate (lbs/sec)	3970.97	4161.11
Feedwater Temperature (°F)	420[a]	424[a]
Vessel Dome Pressure (psia)	1020	1035
Rod Insertion Speed	Measured	Tech. Spec.
Core Inlet Enthalpy (Btu/lb)	527.6	529.3
Fuel Rod Gap Conductance	Axially Non-uniform	Uniform
Fuel Radial Heat Generation	Non-uniform	Uniform
Jet Pump Ratio	2.33	2.41
Safety/Relief Valves Relief Function (psig)		
Group 1 Opening Setpoint	1076	1106
Group 1 Closing Setpoint	1026	1056
Group 2 Opening Setpoint	1086	1116
Group 2 Closing Setpoint	1036	1066
Group 3 Opening Setpoint	1096	1126
Group 3 Closing Setpoint	1046	1076
Group 4 Opening Setpoint	1106	1136
Group 4 Closing Setpoint	1056	1086
Group 5 Opening Setpoint	1116	1146
Group 5 Closing Setpoint	1066	1096
Opening Stroke Time (sec)	0.07	0.1
Closing Stroke Time (sec)	0.0	0.0
Opening Delay Time (sec)	0.3	0.4

a. RETRAN will adjust this value at initialization to complete the heat balance.

TABLE 4.1

INPUT PARAMETERS AND INITIAL TRANSIENT CONDITIONS
COMPARISON OF LICENSING BASIS AND NOMINAL PLANT CONDITIONS
(Continued)

Parameter	Nominal	Licensing Basis
Safety/Relief Valves Safety Function (psig)		
Group 1 Opening Setpoint	1150	1177
Group 1 Closing Setpoint	1126	1153
Group 2 Opening Setpoint	1175	1187
Group 2 Closing Setpoint	1151	1163
Group 3 Opening Setpoint	1185	1197
Group 3 Closing Setpoint	1161	1173
Group 4 Opening Setpoint	1195	1207
Group 4 Closing Setpoint	1171	1183
Group 5 Opening Setpoint	1205	1217
Group 5 Closing Setpoint	1181	1193
Opening Stroke Time (sec)	0.07	0.1
Closing Stroke Time (sec)	0.0	0.0
Opening Delay Time (sec)	0.3	0.4
Reactor Protection System		
High Flux Scram, % NBR	118	126.2
High Vessel Dome Pressure Scram (psig)	1037	1071
APRM Thermal Trip (% NBR at 100% Core Flow)	113.5	122.03
Low Water Level (L3), in above instrument zero	13	7.5
Turbine Stop Valve Closure Position Scram (% Closed)	5	10
MSIV Closure Position Scram (% Closed)	10	15

TABLE 4.1

INPUT PARAMETERS AND INITIAL TRANSIENT CONDITIONS
COMPARISON OF LICENSING BASIS AND NOMINAL PLANT CONDITIONS
(Continued)

Parameter	Nominal	Licensing Basis
Containment Isolation and Pump Trip		
Low Water Level (L2), in below instrument zero	50	70
Low Pressure in Steamline (psig)	831	795
RPT High Vessel Pressure (psig)	1135	1170
RPT Delay Time (msec)	97	190
High Water Level - Turbine and Feedwaters Pump Trip (inches above instrument zero)	54.5	59.5
Recirculation Pump Moment of Inertia (10^4 lbm - ft^2)	2.27	2.47

The analyses in this report used the technical specification limits on control rod movement versus time. Table 4.2 shows the assumed rod motion following scram[25]. Actual plant performance data shows more rapid insertion.

TABLE 4.2
Technical Specification Limits
Maximum Control Rod Insertion Time to Position
After Deenergization of Pilot Valve Solenoids

Position Inserted from Fully Withdrawn (Notch Number)	Time (Sec)
6.25% (45)	0.430
18.75% (39)	0.868
47.92% (25)	1.936
89.58% (05)	3.497

The initial steam flow in the licensing basis model is conservatively set at 105% NBR. For pressurization transients, higher initial steam flow results in a more rapid pressurization and higher maximum pressures. The initial power is set to 104.4% NBR which is consistent with the maximum steam flow of 105% NBR. The initial reactor dome pressure is conservatively set to a higher value of 1035 psia, allowing less analytical margin to the safety limit.

Unless the problem statepoint requires otherwise, the core flow is initialized at the rated capacity of 108.5 mlb/hr.

The RETRAN model uses a fuel rod gap conductance that remains constant during the transient. The actual gap conductance increases during power increase transients due to fuel pellet expansion. Higher gap conductance will lead to faster heat transfer from the fuel to the coolant, which generates more steam voids. The faster conversion of fuel stored energy to steam voids in the core helps to mitigate the transient due to negative void reactivity feedback. Therefore, the use of a constant gap conductance is conservative for system analyses involving power increases such as pressurization transients.

Conservative equipment design specifications and plant technical specification limits are used in the RETRAN model input. These include relief valve opening response, closure rates for main steam isolation valves, turbine stop and control valves, reactor protection system setpoints and delays.

A conservative moment of inertia for the recirculation pump is used in the licensing basis model. A larger value results in longer coastdown time after pump trip, delaying the effect of void formation in the core and increasing the process of void collapsing. Positive reactivity effects are magnified by this conservatism.

4.2 Load Rejection Without Bypass (LRNB)

Whenever external disturbances result in loss of electrical load on the generator, fast closure of the turbine control valves (TCV) is initiated. The turbine control valves are required to close as rapidly as possible to minimize overspeed of the turbine generator rotor. Closure of the main turbine control valves will cause a sudden reduction in steam flow which results in an increase in system pressure and reactor shutdown.

4.2.1 Sequence of Events

A loss of generator electrical load at high power with bypass failure produces the sequence of events listed in Table 4.3.

The closure characteristics of the turbine control valves are assumed such that the turbine control valves operate in the full arc (FA) mode and have a full stroke closure time, from fully open to fully closed, of 0.15 seconds. Sensitivity study[7] has shown that the most severe initial condition for this transient is the assumption of full arc operation at 105% NBR steam flow. The plant value of 0.07 seconds given in Table 4.3 represents actual expected closure time, since the turbine control valves are partially open during normal operation.

TABLE 4.3

Sequence of Events for LRNB Transient

Time-Sec	Event
0.0	Turbine generator power load unbalance (PLU) devices trip to initiate turbine control valve fast closure when loss of electrical load is detected.
0.0	Turbine bypass valves fail to operate
0.0	Fast turbine control valve closure initiates scram trip
0.0	Fast turbine control valve closure initiates a recirculation pump trip (RPT)
0.07	Turbine control valves closed
0.19	Recirculation pump motor/circuit breakers open, causing decrease in core flow
0.28	Control rod insertion starts (scram trip signal at 0 sec, RPS delay : 0.08 sec, solenoid deenergizing delay : 0.2 sec)
1.35	Group 1 relief valves actuated
1.40	Group 2 relief valves actuated
1.44	Group 3 relief valves actuated
1.50	Group 4 relief valves actuated
1.63	Group 5 relief valves actuated
4.43	Group 5 relief valves close
5.0	End of simulation

4.2.2 Results of LRNB RETRAN Analysis

The WNP-2 LRNB analysis at the end of cycle 4 conditions was performed with the licensing basis model. Since most of the fuel in the core at EOC4 was the Advanced Nuclear Fuels (ANF) design, the average fuel parameters in the best-estimate model were changed from the GE design to the ANF design. The fast closure of the turbine control valves (TCV) is simulated by linearly decreasing the flow at fill Junction 380 (representing steam flow to the turbine) to zero at 0.07 seconds. Rapid closure of the TCV initiates a scram.

Several key results of this analysis were compared with analyses of record[26] performed by Advanced Nuclear Fuels (ANF). It should be noted that both sets of analyses were performed conservatively. This comparison is intended to show the similarity of results rather than to demonstrate analytical accuracy. The accuracy of the WNP-2 RETRAN model is demonstrated by the benchmarks of power ascension tests reported in Section 3.1.

The pressure in the steam line increases rapidly as shown in Figure 4.2.1. The acronym "LRNB LBM" in the figure stands for Load Rejection without Bypass Licensing Basis Model. Figure 4.2.2 shows the vessel steam flow. The flow oscillations are caused by the pressure wave propagated upstream to the reactor vessel. The decreased steam flow at about 0.4 seconds causes the rapid

pressurization of the steam dome and inside the core as shown in Figures 4.2.3, 4.2.4 and 4.2.5. After 0.42 seconds, the net reactivity becomes positive because the positive void reactivity exceeds the negative scram reactivity. It peaks with a value of approximately 0.76$ at 0.78 seconds then begins to decrease as the scram reactivity increases, as shown in Figure 4.2.6.

The ANF prediction[26] of dome pressure during the transient is also shown in Figure 4.2.3. The WNP-2 RETRAN model predicts a pressure which is higher than that predicted by ANF throughout the transient.

The reactor power, shown in Figure 4.2.7, increases rapidly and reaches a peak value of 398% NBR at 0.89 seconds then rapidly decreases as Doppler feedback and scram reactivity terminate the power excursion. ANF's prediction of core power is also shown in Figure 4.2.7. The power history predicted by RETRAN peaks earlier in the transient than the ANF prediction at a lower maximum power level. The earlier power peak can be attributed in part to the higher pressure throughout the transient. The lower magnitude of the peak is likely to be caused by differences in neutronics calculations leading to differences in kinetics data and cross sections.

Figure 4.2.8 shows the core average clad surface heat flux. The initial reduction in clad-to-coolant heat transfer is caused by the

rise in saturation temperature of the liquid phase due to initial pressure rise in the core. As the power rises, the heat flux quickly reverses and begins to rise, reaching a peak of 133.4% of the rated power value at 1.1 seconds. Following the peak, the heat flux decreases as the core power decreases with a delay determined by the fuel rod time constant. ANF's calculation of core average heat flux is also shown in Figure 4.2.8. The two models predict consistent trends in heat flux and agree closely in the later part of the transient.

The water level and feedwater flow during LRNB are shown in Figures 4.2.9 and 4.2.10. When the TCV fast closure calls for scram, the feedwater controller reduces the water level setpoint by 18 inches. It then responds to this setpoint change by reducing feedwater flow. Pressure variations, steam flow oscillations, and void collapse contribute to the changing water level throughout the remainder of the transient.

Figures 4.2.11 and 4.2.12 give the void fractions at mid-core and core exit. Core voids collapse as the steamline pressure wave reaches the core. For the remainder of the transient, variations in steam flow and pressure drive oscillations in the void fraction. Figure 4.2.13 shows the recirculation flow. The recirculation pumps start to coast down after RPT initiation at 0.19 seconds, causing flow reduction in the core as shown in Figure 4.2.14.

FIGURE 4.2.1

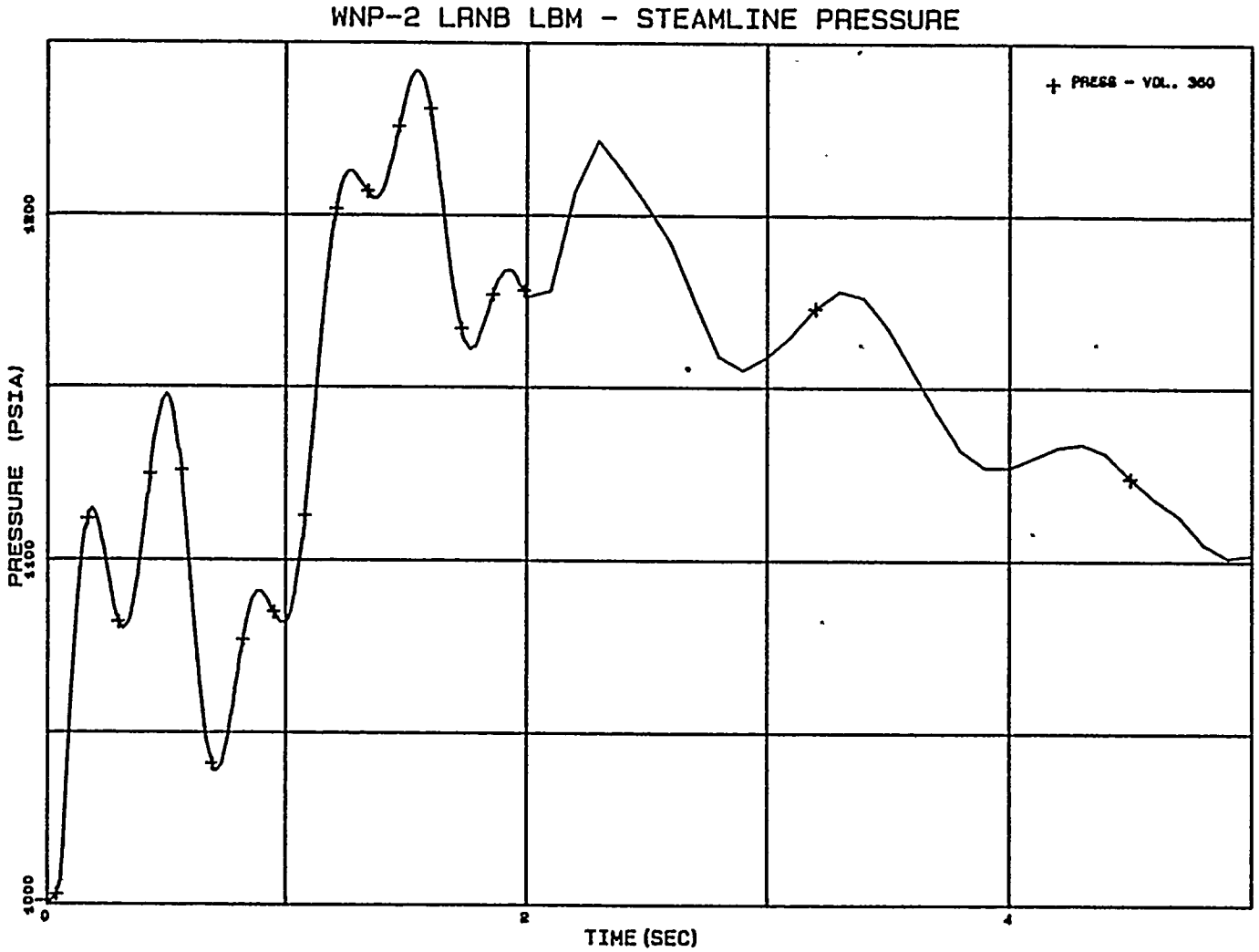
WNP-2 LANB LBM - STEAMLINE PRESSURE
+ PRESS - VOL. 360
PRESSURE (PSIA)
1200
1100
1000
0
2
4
TIME (SEC)

FIGURE 4.2.2

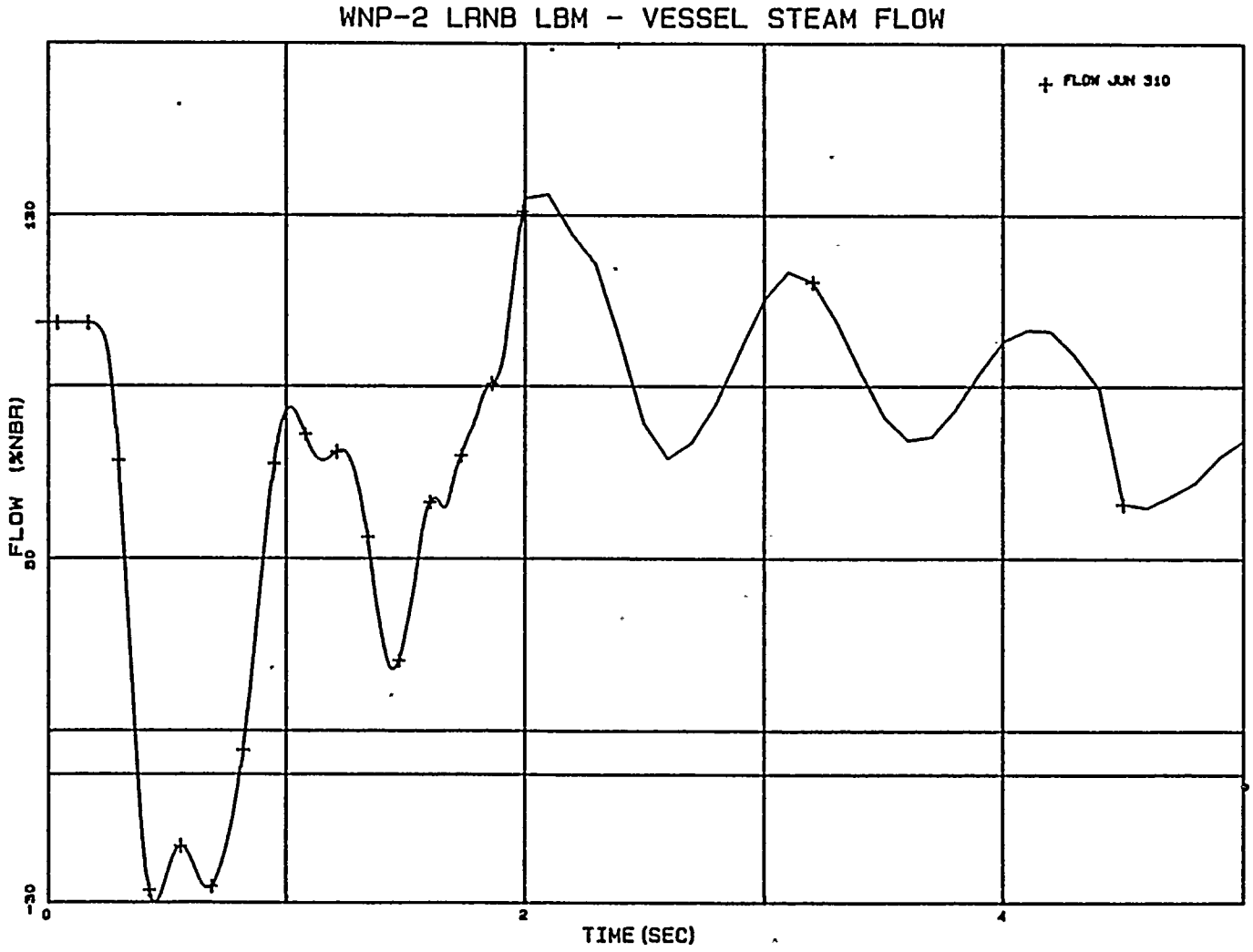
WNP-2 LRNB LBM - VESSEL STEAM FLOW
+ FLOW JAN 310
130
50
-30
FLOW (%NBR)
0
2
4
TIME (SEC)

FIGURE 4.2.3

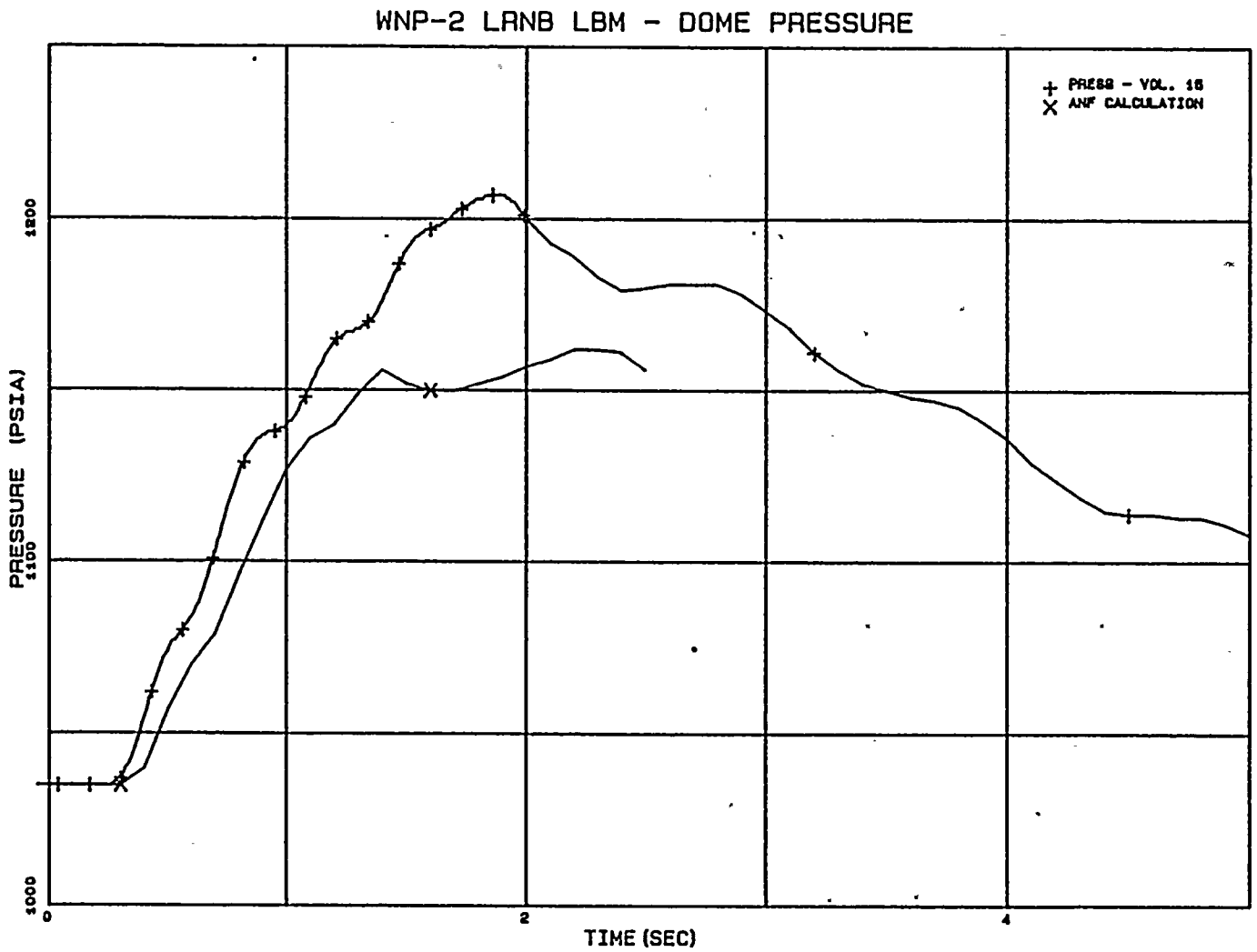
WNP-2 LANB LBM - DOME PRESSURE
PRESS - VOL. 16
ANF CALCULATION
PRESSURE (PSIA)
1200
1100
1000
0
2
4
TIME (SEC)

FIGURE 4.2.4

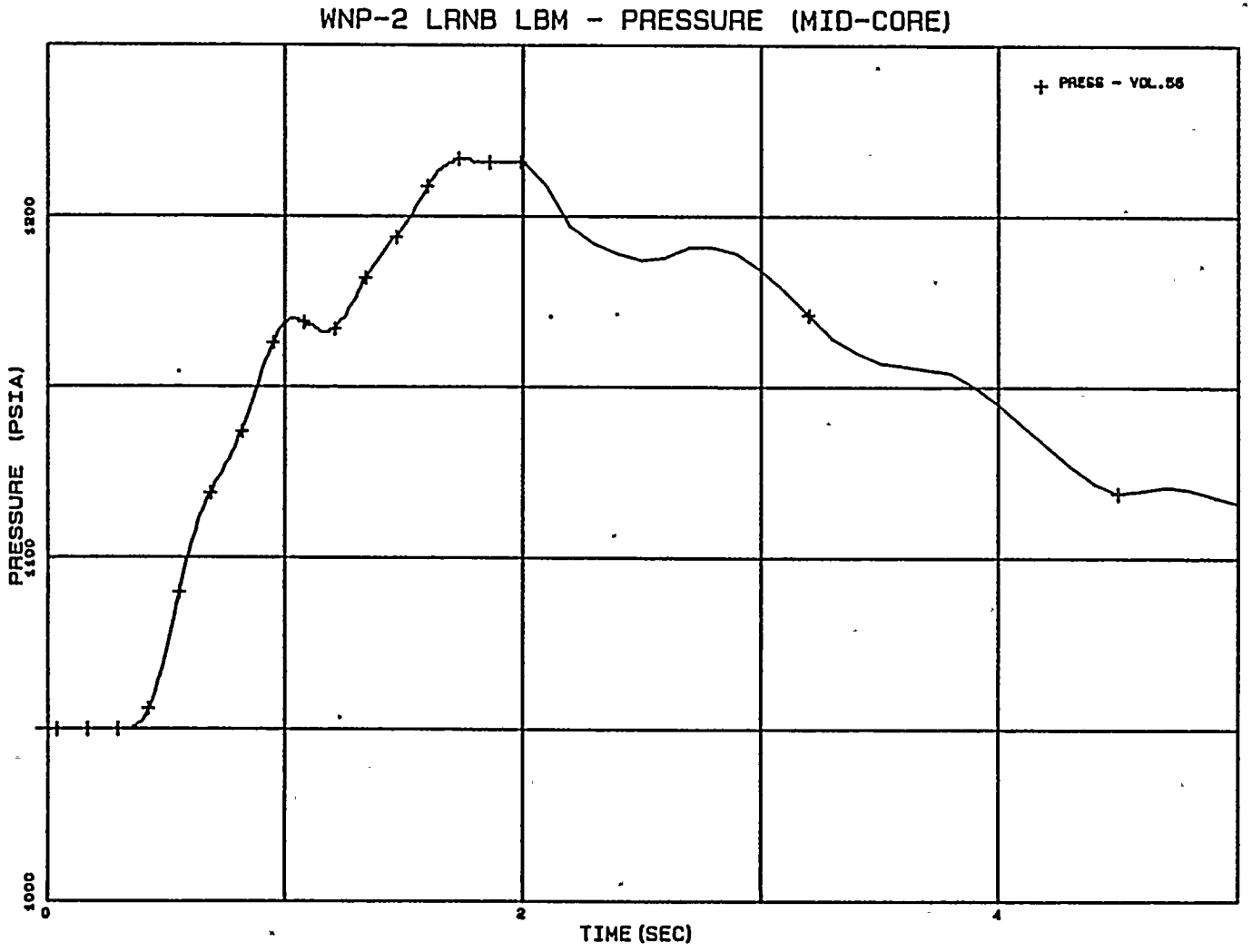
WNP-2 LRNB LBM - PRESSURE (MID-CORE)
+ PRESS - VOL.56
PRESSURE (PSIA)
1200
1100
1000
0
2
4
TIME (SEC)

FIGURE 4.2.5

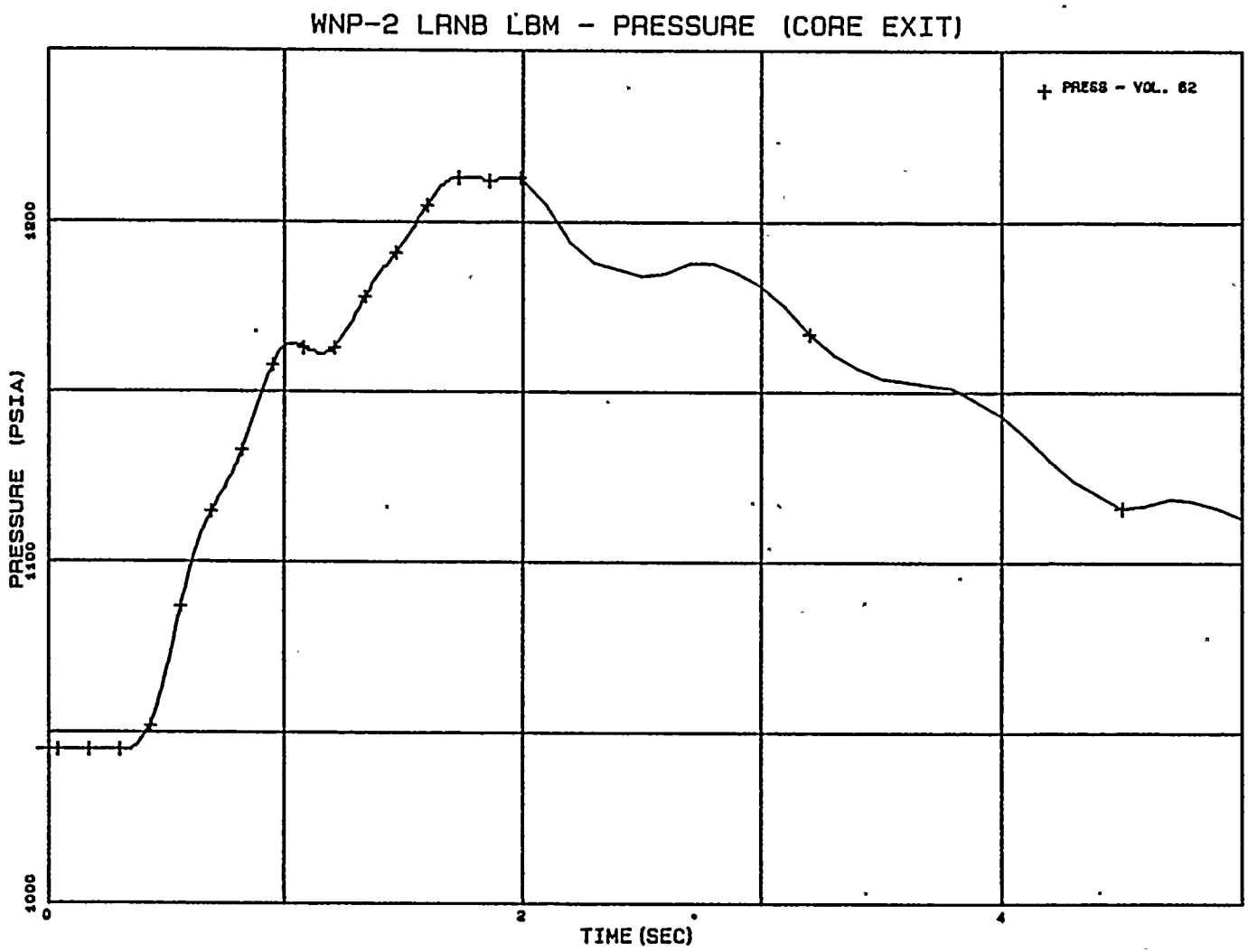
WNP-2 LANB LBM - PRESSURE (CORE EXIT)
+ PRESS - VOL. 62
PRESSURE (PSIA)
1200
1100
1000
0
2
4
TIME (SEC)

FIGURE 4.2.6

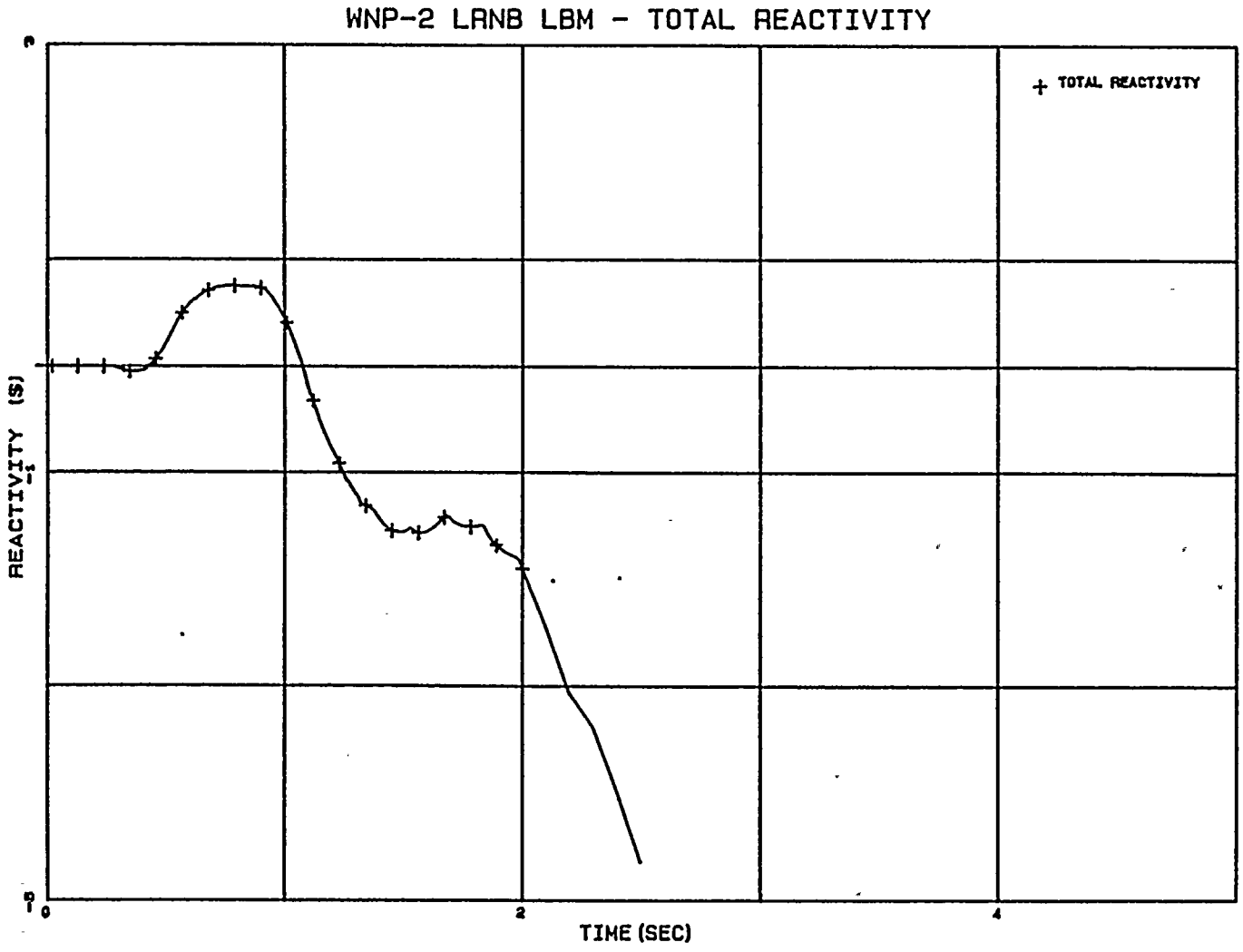
WNP-2 LANB LBM - TOTAL REACTIVITY
+ TOTAL REACTIVITY
REACTIVITY ($)
1
0
-1
0
2
4
TIME (SEC)

FIGURE 4.2.7

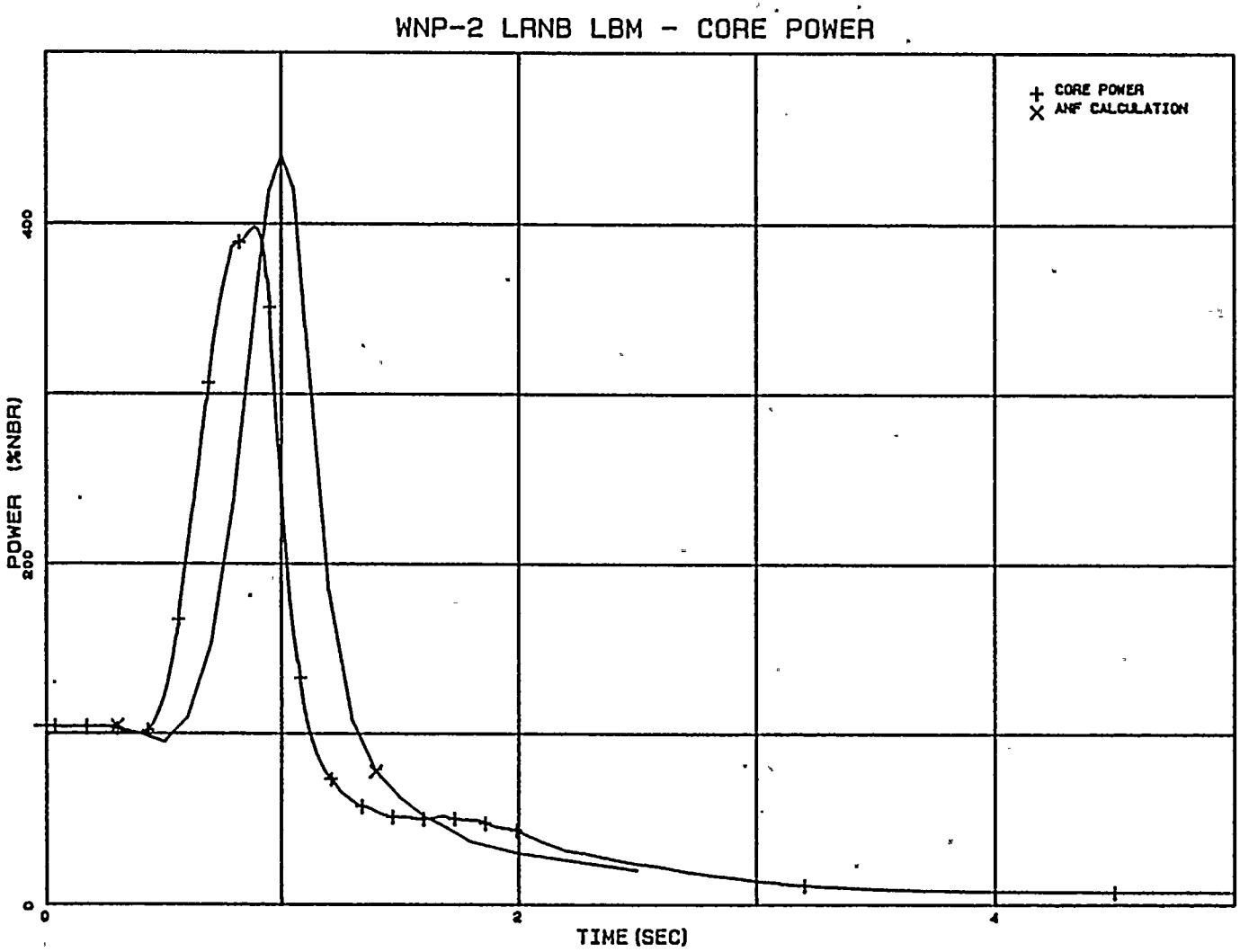
WNP-2 LANB LBM - CORE POWER
+ CORE POWER
X ANF CALCULATION
POWER (%NBR)
400
200
0
0
2
4
TIME (SEC)

FIGURE 4.2.8

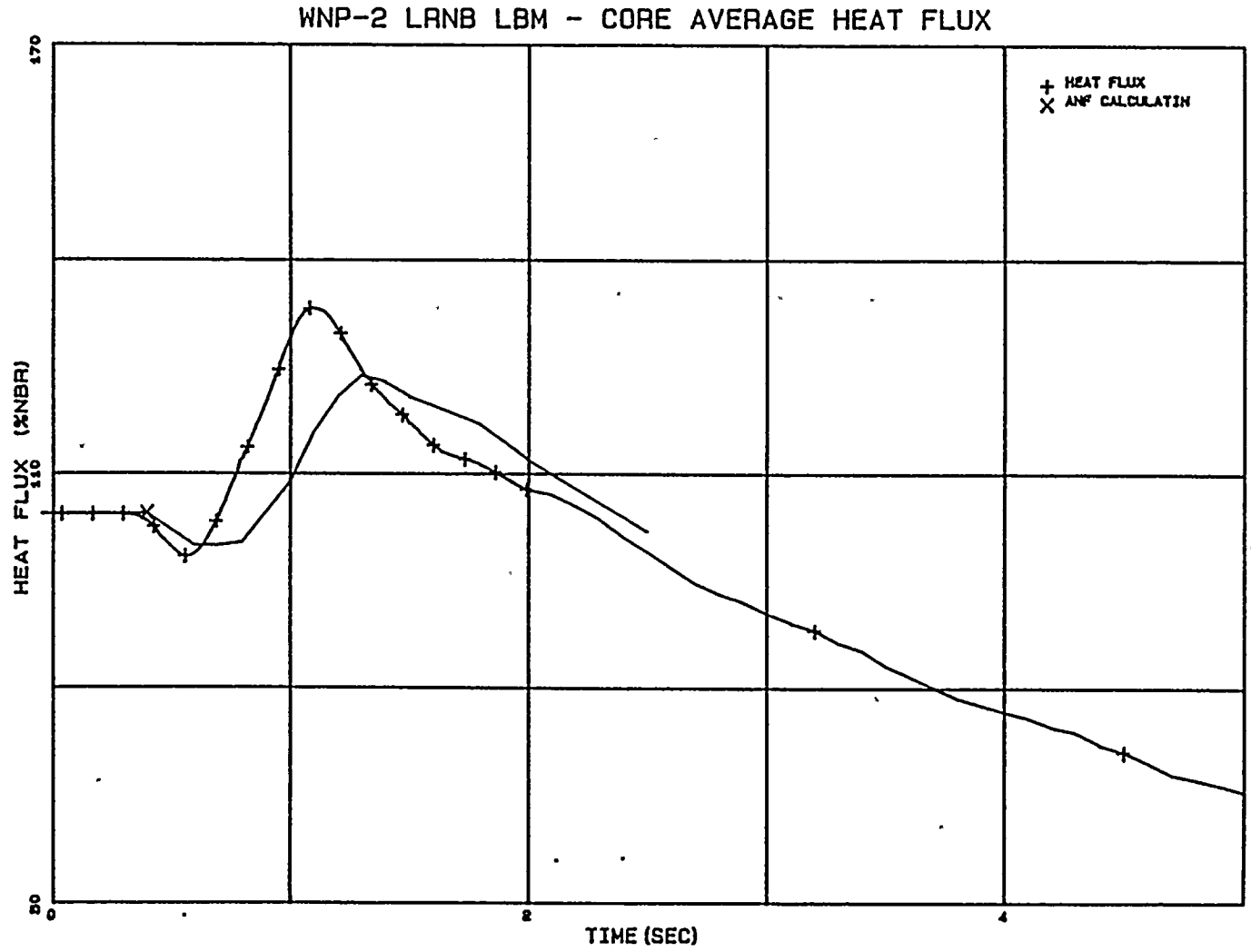
WNP-2 LRNB LBM - CORE AVERAGE HEAT FLUX
+ HEAT FLUX
X ANF CALCULATIN
HEAT FLUX (%NBR)
170
110
50
0
2
4
TIME (SEC)

FIGURE 4.2.9

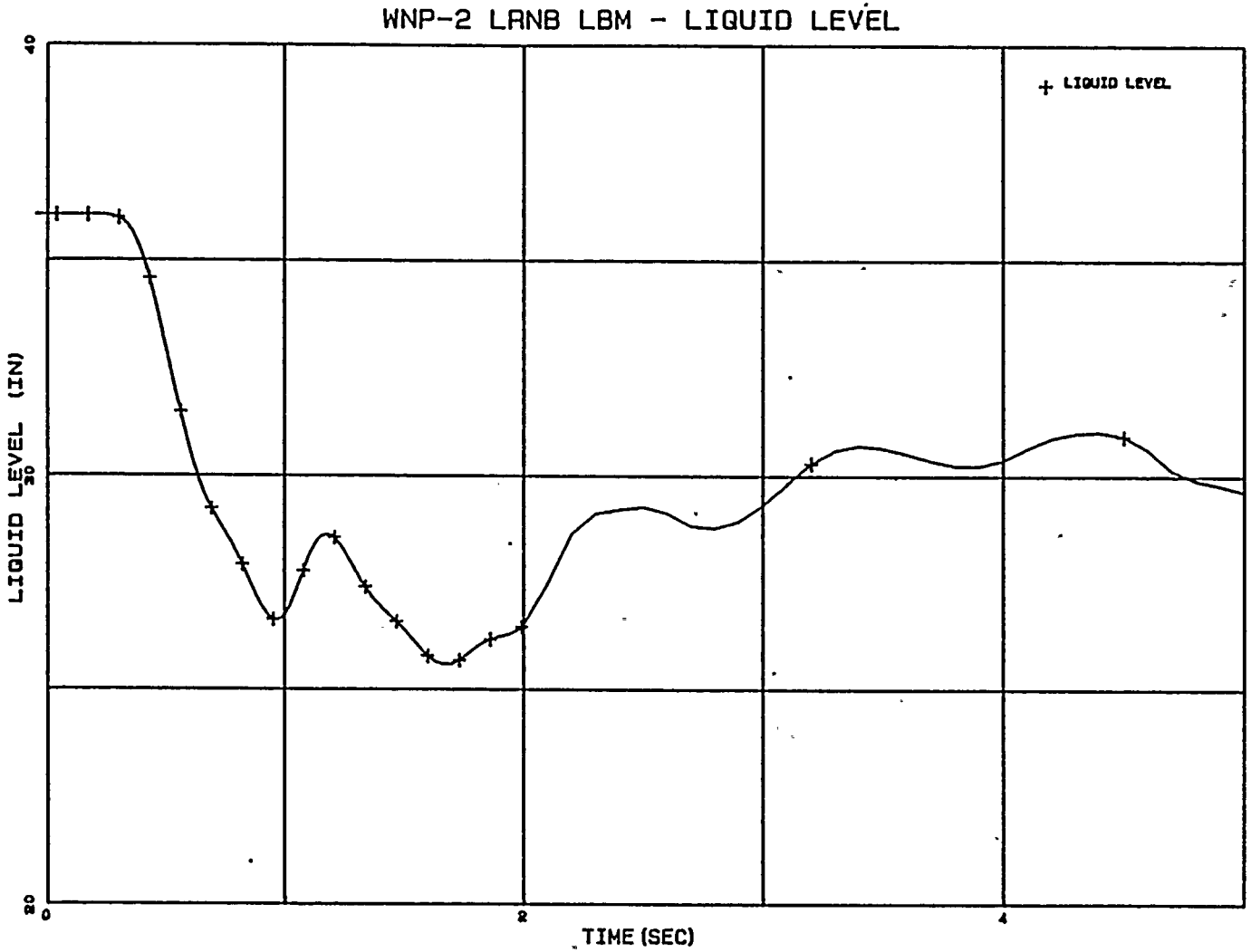
WNP-2 LANB LBM - LIQUID LEVEL
+ LIQUID LEVEL
LIQUID LEVEL (IN)
40
30
20
0
2
4
TIME (SEC)

FIGURE 4.2.10

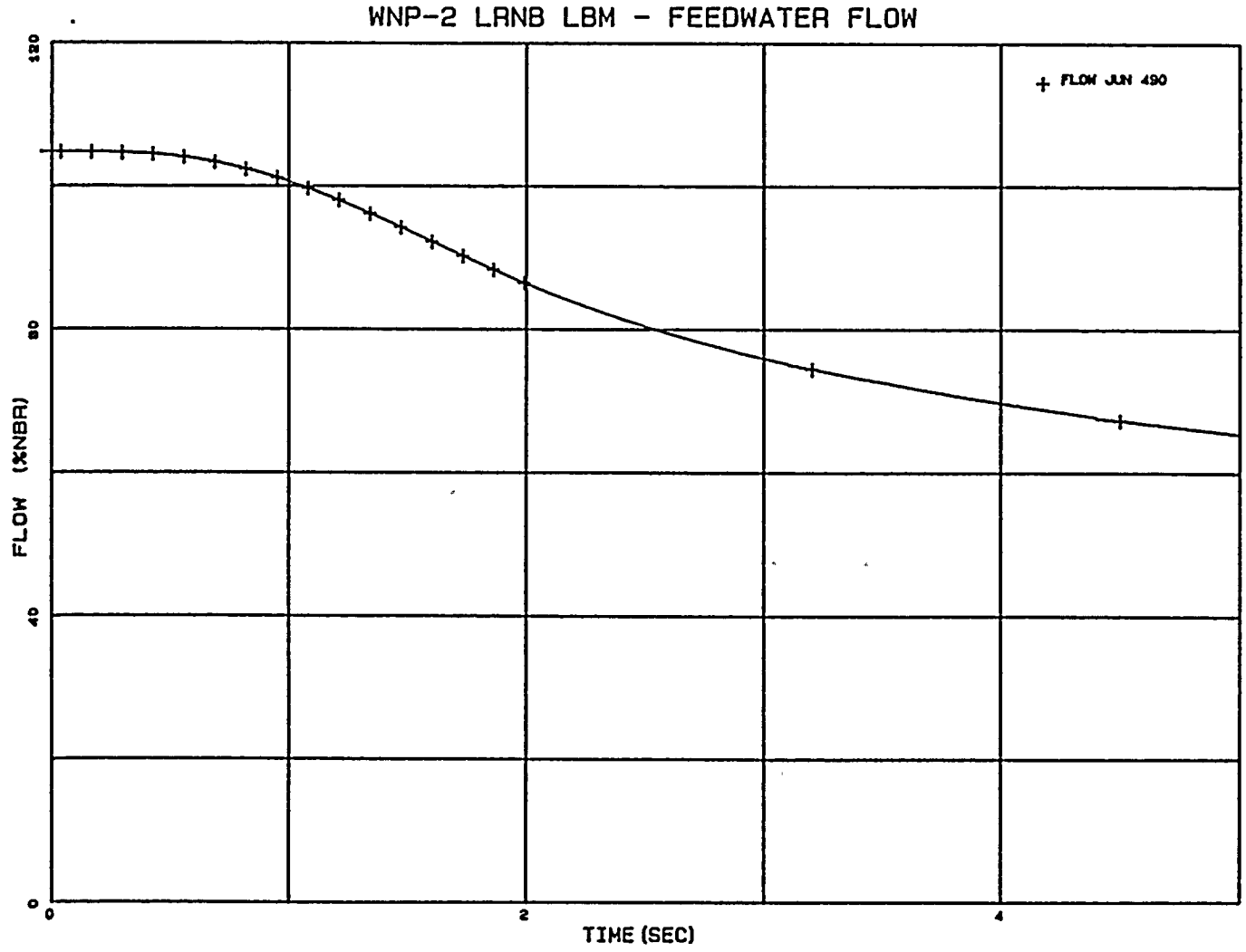
WNP-2 LRNB LBM - FEEDWATER FLOW
+ FLOW JUN 490
120
80
40
0
FLOW (%NBR)
0
2
4
TIME (SEC)

FIGURE 4.2.11

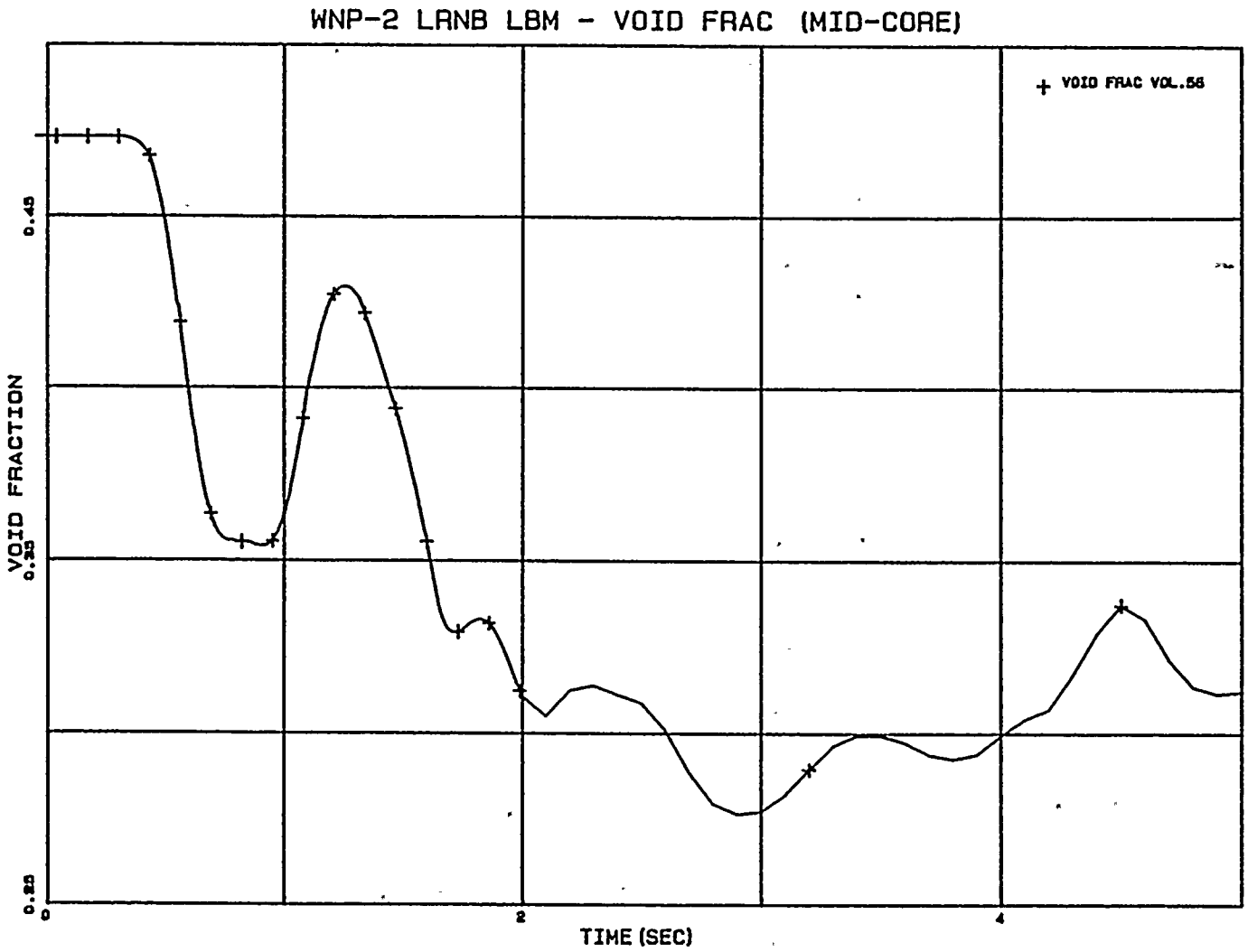
WNP-2 LANB LBM - VOID FRAC (MID-CORE)
+ VOID FRAC VOL.56
VOID FRACTION
0.45
0.25
0.05
0
2
4
TIME (SEC)

FIGURE 4.2.12

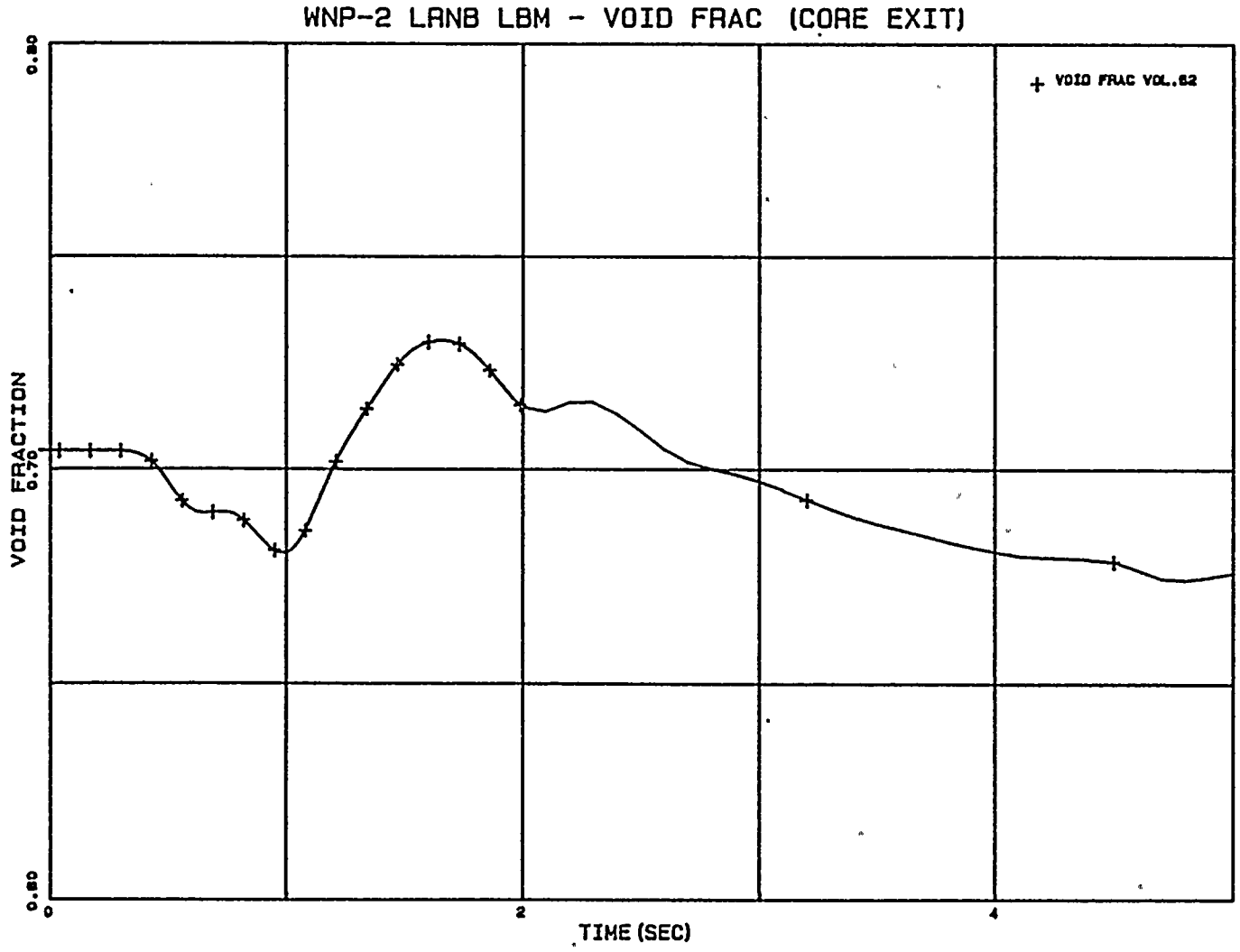
WNP-2 LANB LBM - VOID FRAC (CORE EXIT)
+ VOID FRAC VOL.62
VOID FRACTION
0.80
0.70
0.60
0
2
4
TIME (SEC)

FIGURE 4.2.13

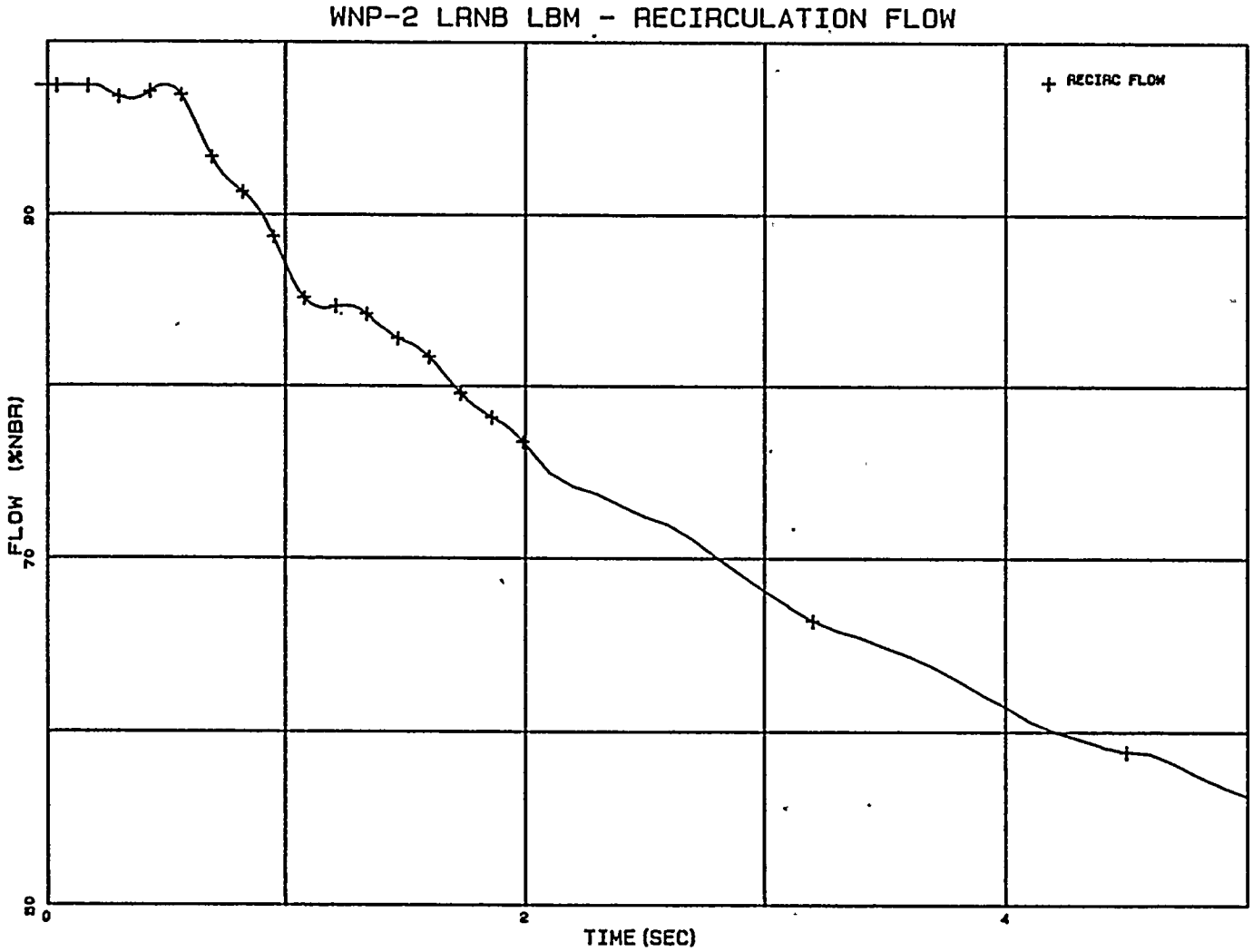
WNP-2 LRNB LBM - RECIRCULATION FLOW
+ RECIRC FLOW
FLOW (%NBR)
90
70
50
0
2
4
TIME (SEC)

FIGURE 4.2.14

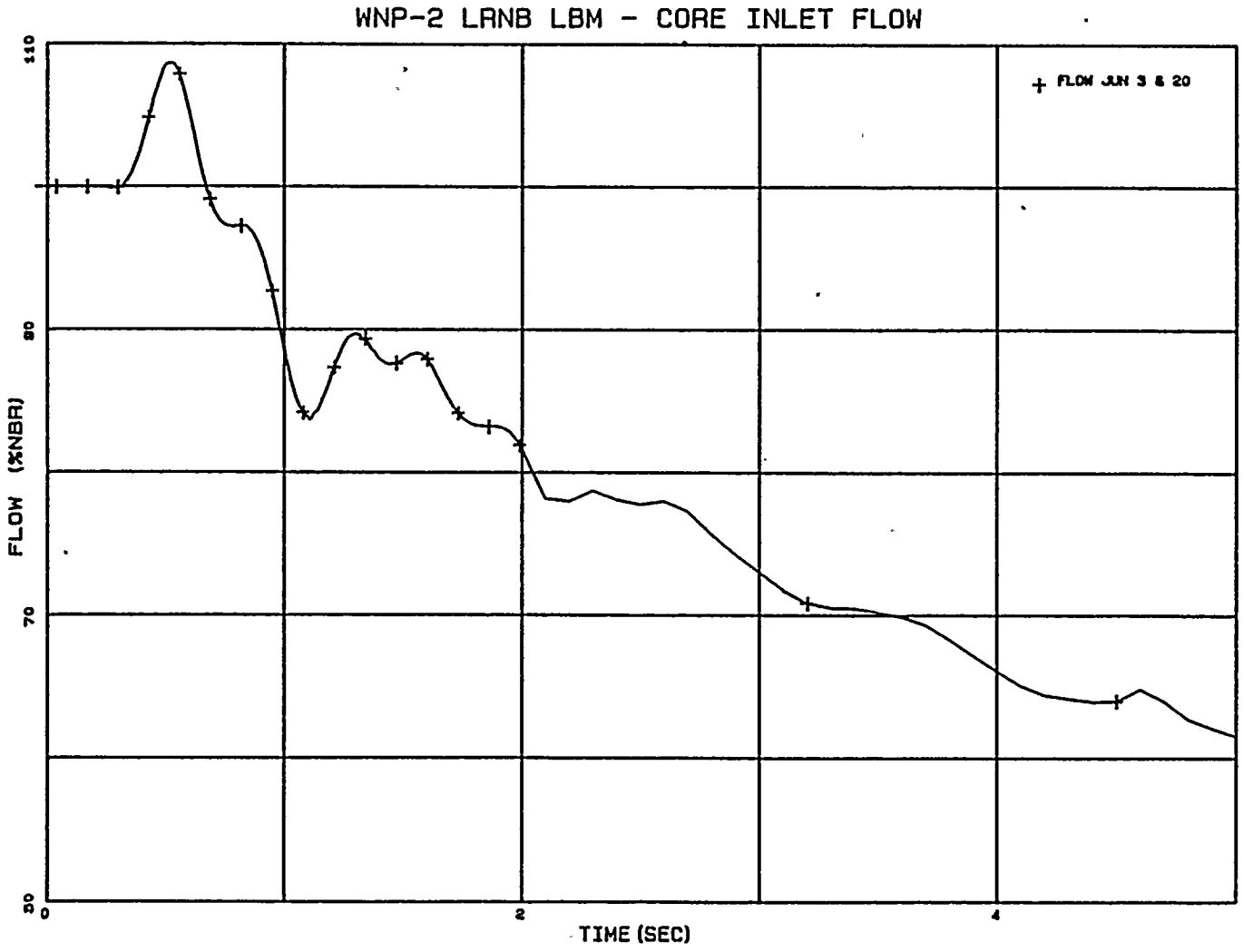
WNP-2 LANB LBM - CORE INLET FLOW
+ FLOW JUN 3 & 20
FLOW (%NBR)
110
90
70
50
0
2
4
TIME (SEC)

4.3 Feedwater Controller Failure to Maximum Demand (FWCF)

This analysis postulates the feedwater controller failure causing an increase in feedwater flow. The most severe event of this type is a failure at maximum flow demand. The feedwater controller is forced to its upper limit at the beginning of the event.

4.3.1 Sequence of Events

When feedwater flow exceeds steam flow, the water level rises. With the feedwater controller disabled, the water level eventually rises to the high-level reference point, at which time the feedwater pumps and the main turbine are tripped and a scram is initiated. Table 4.4 lists the sequence of events for this transient.

The transient is simulated by programming an upper limit failure in the feedwater system such that 146 percent feedwater flow occurs at the design pressure of 1020 psig.

An increase in feedwater flow will cause a corresponding drop in feedwater temperature. However, the relatively large time constant of the feedwater heaters (order of minutes) plus the flow transport time (about 10 seconds from heaters to vessel and about 3 seconds from sparger to core) delay the cold water effects until the event has run its course and no further consequences are expected.

Feedwater temperature is therefore assumed to remain constant.

4.3.2 Results of FWCF RETRAN Analysis

The FWCF event was analyzed at EOC4 conditions using the licensing basis model. As in the LRNB case, the fuel parameters were changed to reflect the ANF design.

The feedwater flow is shown in Figure 4.3.1. The increased feedwater, after a transport delay through the lower downcomer and recirculation loops, causes an increase in the core inlet subcooling as shown in Figure 4.3.2. The reactor water level also increases as the feedwater flow increases as shown in Figure 4.3.3. The water level reaches the high level setpoint at approximately 17.7 seconds, causing a turbine trip (Figure 4.3.4). The vessel pressure begins to increase after the closure of the turbine stop valves. The turbine bypass valves open (Figure 4.3.5). For high initial power levels the bypass, which has a design capacity of 25% of rated steam flow, will not divert all of the steam flow and the pressure increases as shown in Figure 4.3.6. As the pressure increases, the core void collapses. The positive void reactivity from core pressurization is initially high enough to overcome the negative scram reactivity (Figure 4.3.7). A rapid increase in power begins at 18.1 seconds (Figure 4.3.8), reaching a peak of 245% NBR at 18.6 seconds. Trailing the reactor power, the core average heat flux peaks at 124% NBR at 18.8 seconds (Figure 4.3.9).

The relief valves open after the vessel pressure reaches the opening setpoints (Figures 4.3.10 through 4.3.14) and additional steam is relieved to the suppression pool. The vessel pressure begins to decrease rapidly. Figure 4.3.15 shows the vessel steam flow. The fast closure of the turbine stop valves generate pressure waves which lead to the oscillations in steam flow. The core inlet flow and exit flow are shown in Figures 4.3.16 and 4.3.17. Due to the coastdown of the recirculation pumps, the core flow reduces near the end of the transient (Figure 4.3.18). Figures 4.3.19 and 4.3.20 show the mid-core and core exit pressures. Figures 4.4.21 and 4.4.22 show the mid-core and core exit void fractions. The transient is terminated by the Doppler feedback and the control rod scram.

The RETRAN results were not compared with ANF analyses of record for the FWCF transient because different initial conditions were assumed in the two analyses. The ANF analysis assumed an initial power level of 47% of rated, while the example calculation reported here was performed at an initial power level of 104.4% of rated.

TABLE 4.4

Sequence of Events for Feedwater Controller Failure

Time-Sec	Event
0	Initiate simulated failure of 146% upper limit on feedwater flow
17.60	L8 vessel Level setpoint trips feedwater pumps
17.66	L8 vessel level setpoint trips main turbine. Turbine bypass operation initiated
17.67	Reactor scram trip actuated from main turbine stop valve position switches (10% closure)
17.86	Recirculation pump trip (RPT) actuated by stop valve position switches (10% closure)
19.12	Group 1 relief valves actuated
19.33	Group 2 relief valves actuated
19.39	Group 3 relief valves actuated
19.47	Group 4 relief valves actuated
19.70	Group 5 relief valves actuated
20.56	Group 5 relief valves start to close
20.90	Group 4 relief valves start to close
21.74	Group 3 relief valves start to close
23.49	Group 2 relief valves start to close
24.0	End of simulation

FIGURE 4.3.1

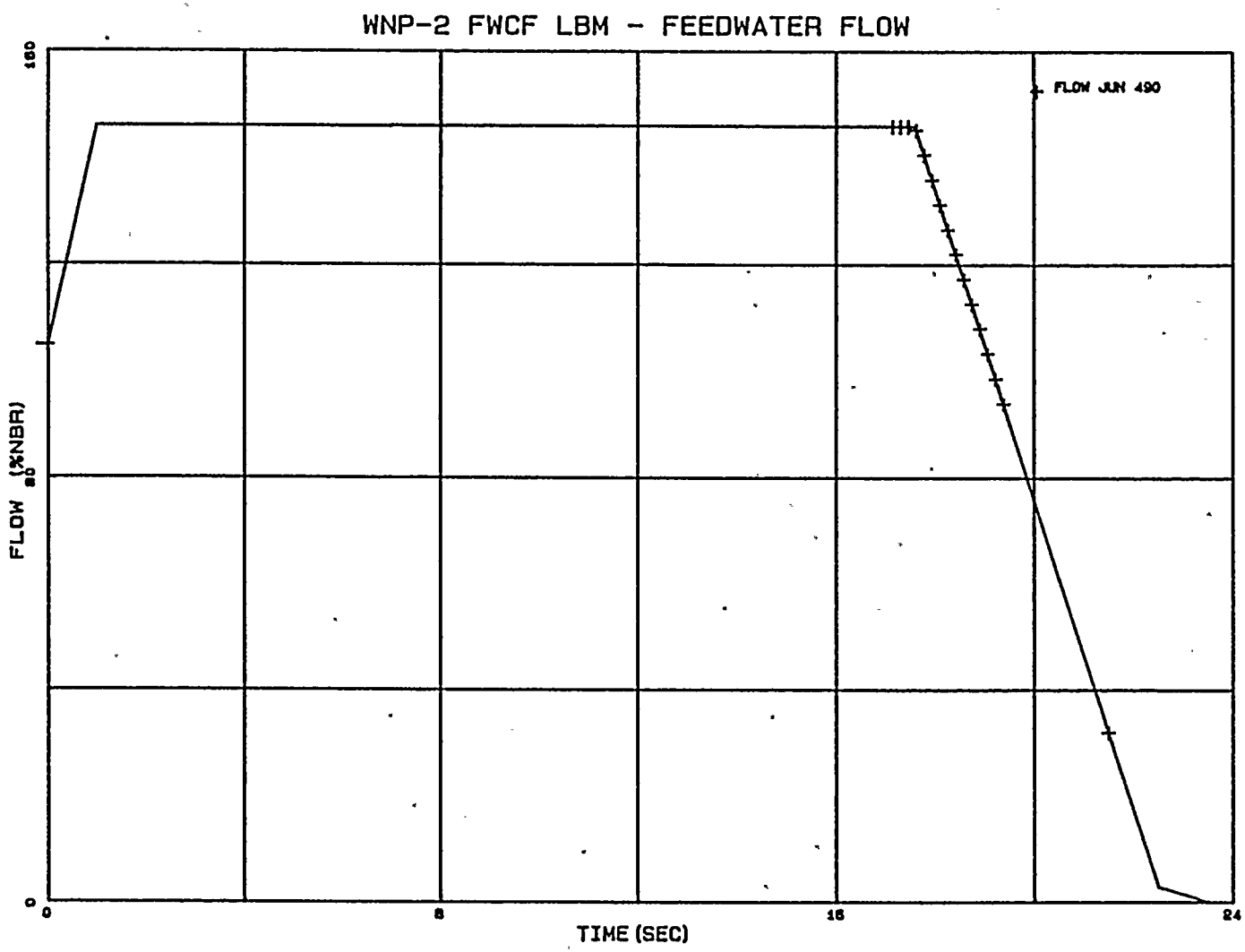
WNP-2 FWCF LBM - FEEDWATER FLOW
FLOW JUN 490
FLOW (%NBR)
160
80
0
0
8
16
24
TIME (SEC)

FIGURE 4.3.2

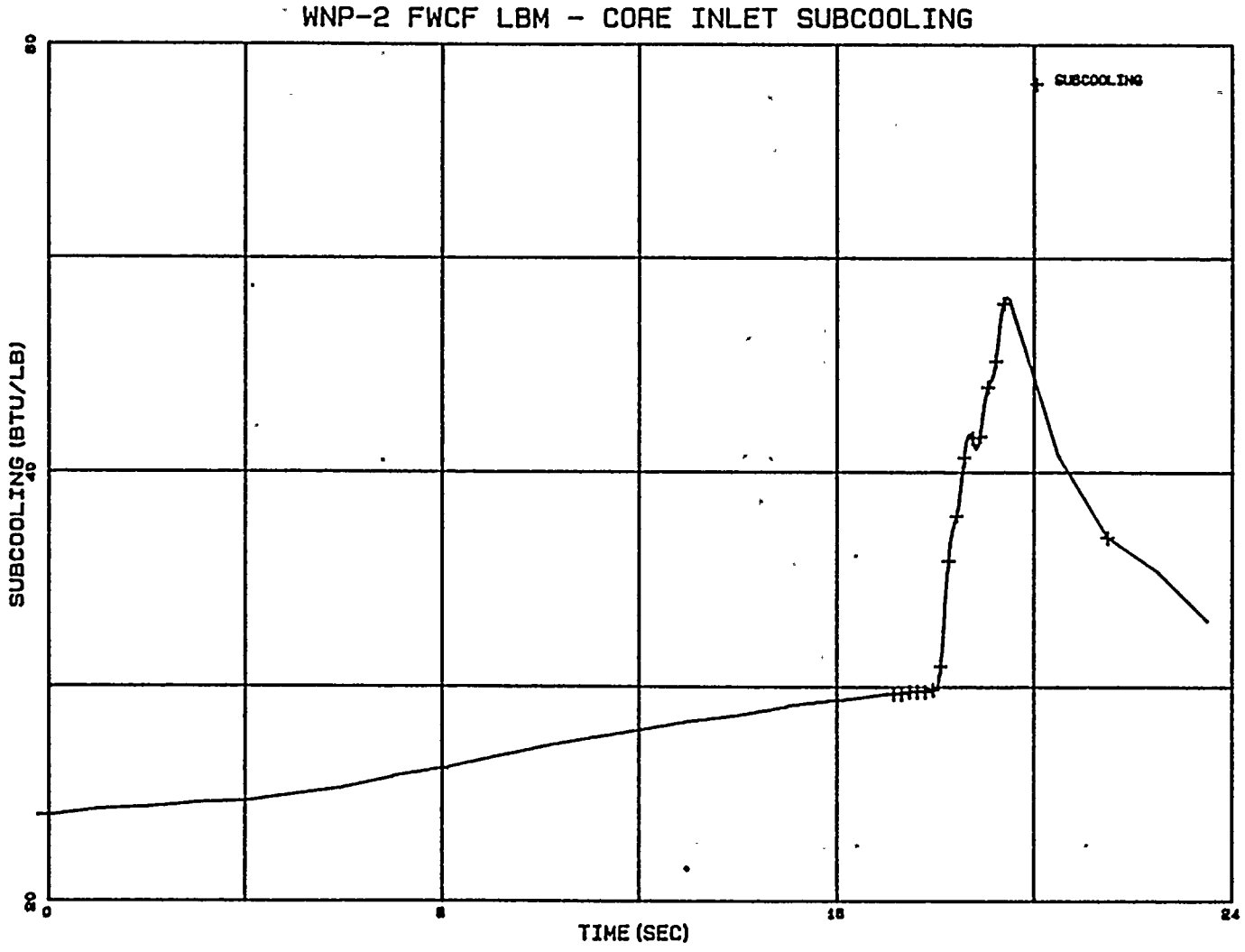
WNP-2 FWCF LBM - CORE INLET SUBCOOLING
SUBCOOLING
SUBCOOLING (BTU/LB)
80
40
20
0
8
16
24
TIME (SEC)

FIGURE 4.3.3

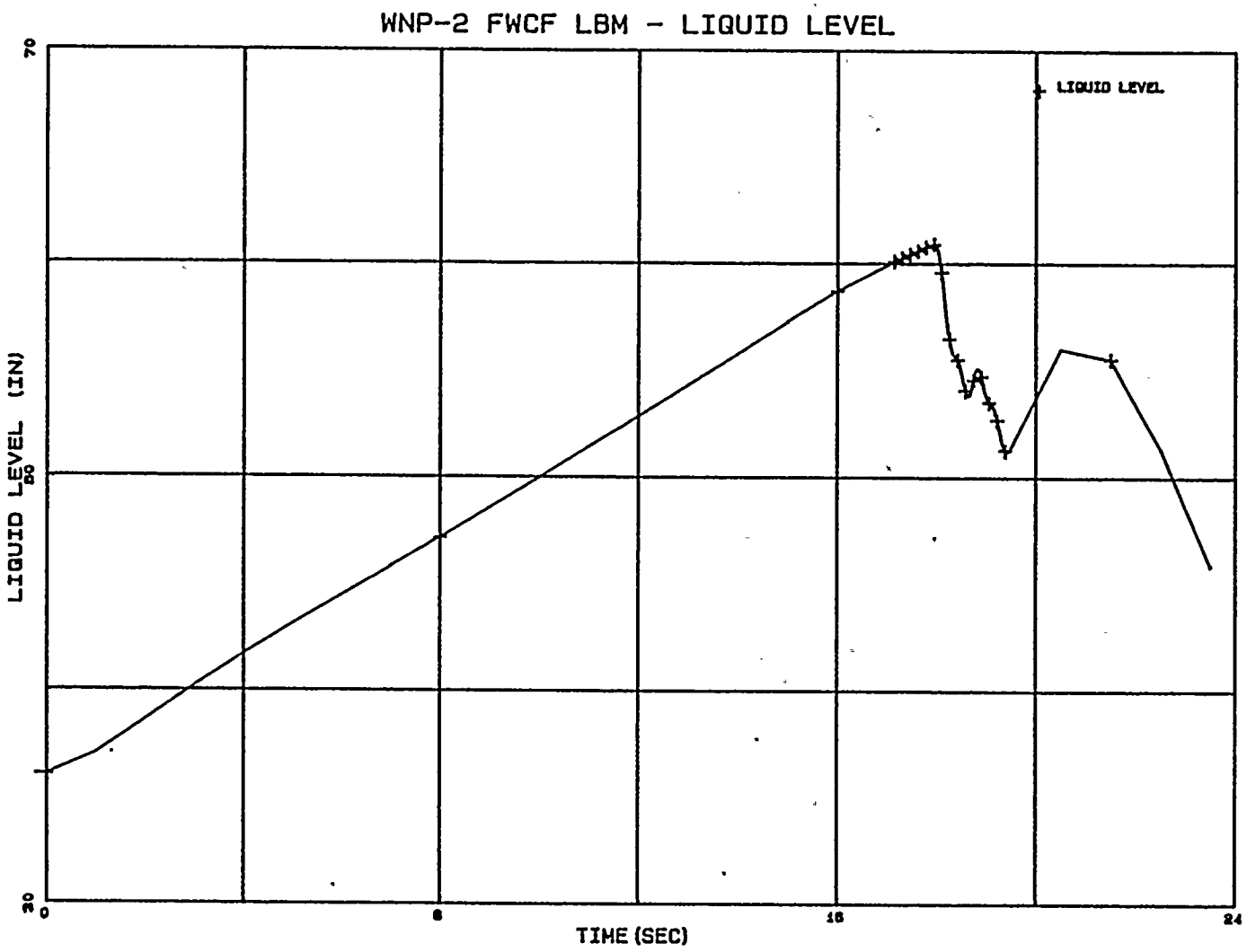
WNP-2 FWCF LBM - LIQUID LEVEL
LIQUID LEVEL
LIQUID LEVEL (IN)
70
60
30
0
8
16
24
TIME (SEC)

FIGURE 4.3.4

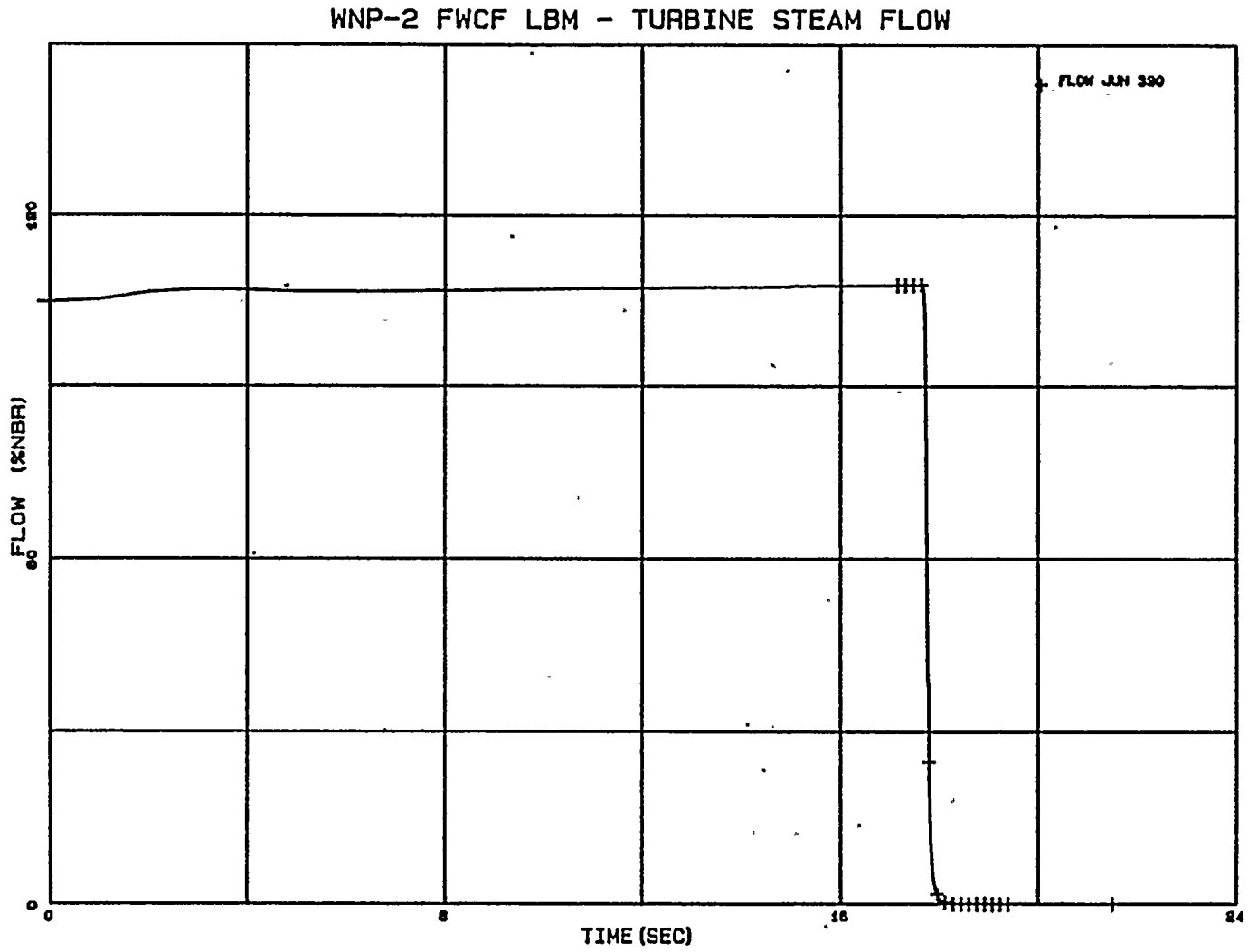
WNP-2 FWCF LBM - TURBINE STEAM FLOW
FLOW JUN 330
120
60
0
FLOW (%NBR)
0
8
16
24
TIME (SEC)

FIGURE 4.3.5

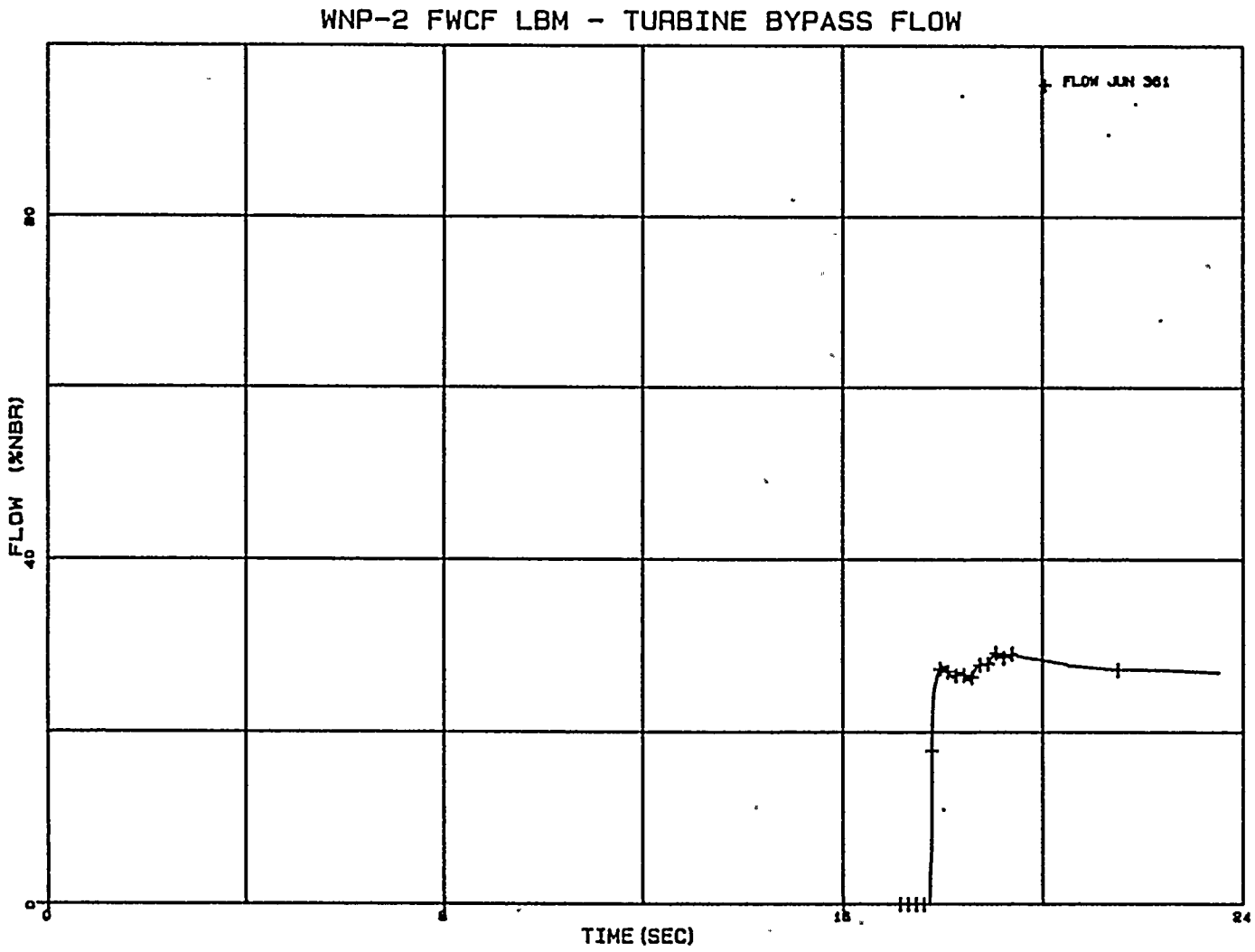
WNP-2 FWCF LBM - TURBINE BYPASS FLOW
FLOW JUN 361
80
40
0
FLOW (%NBR)
0
8
16
24
TIME (SEC)

FIGURE 4.3.6

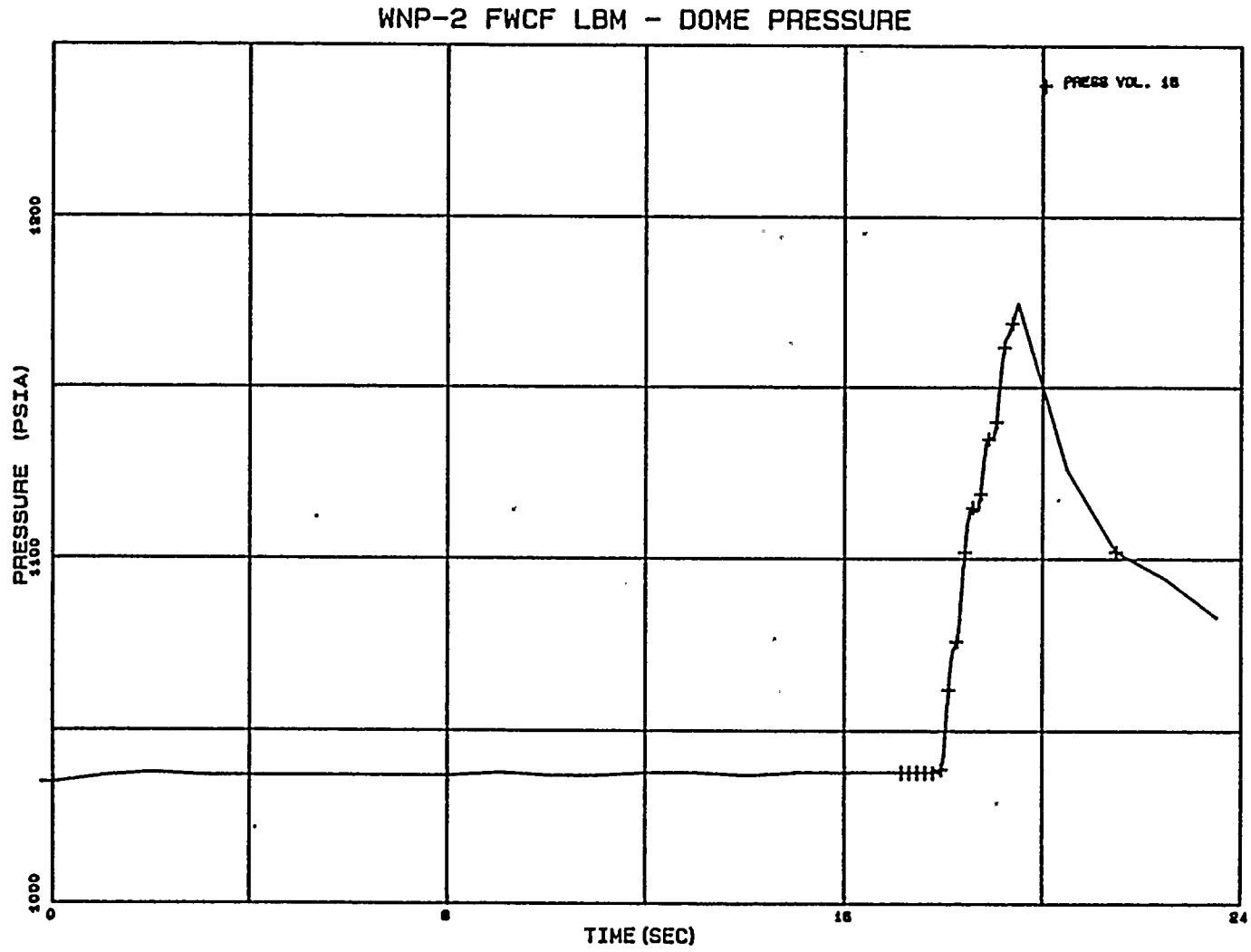
WNP-2 FWCF LBM - DOME PRESSURE
PRESS VOL. 16
PRESSURE (PSIA)
1200
1100
1000
0
8
16
24
TIME (SEC)

FIGURE 4.3.7

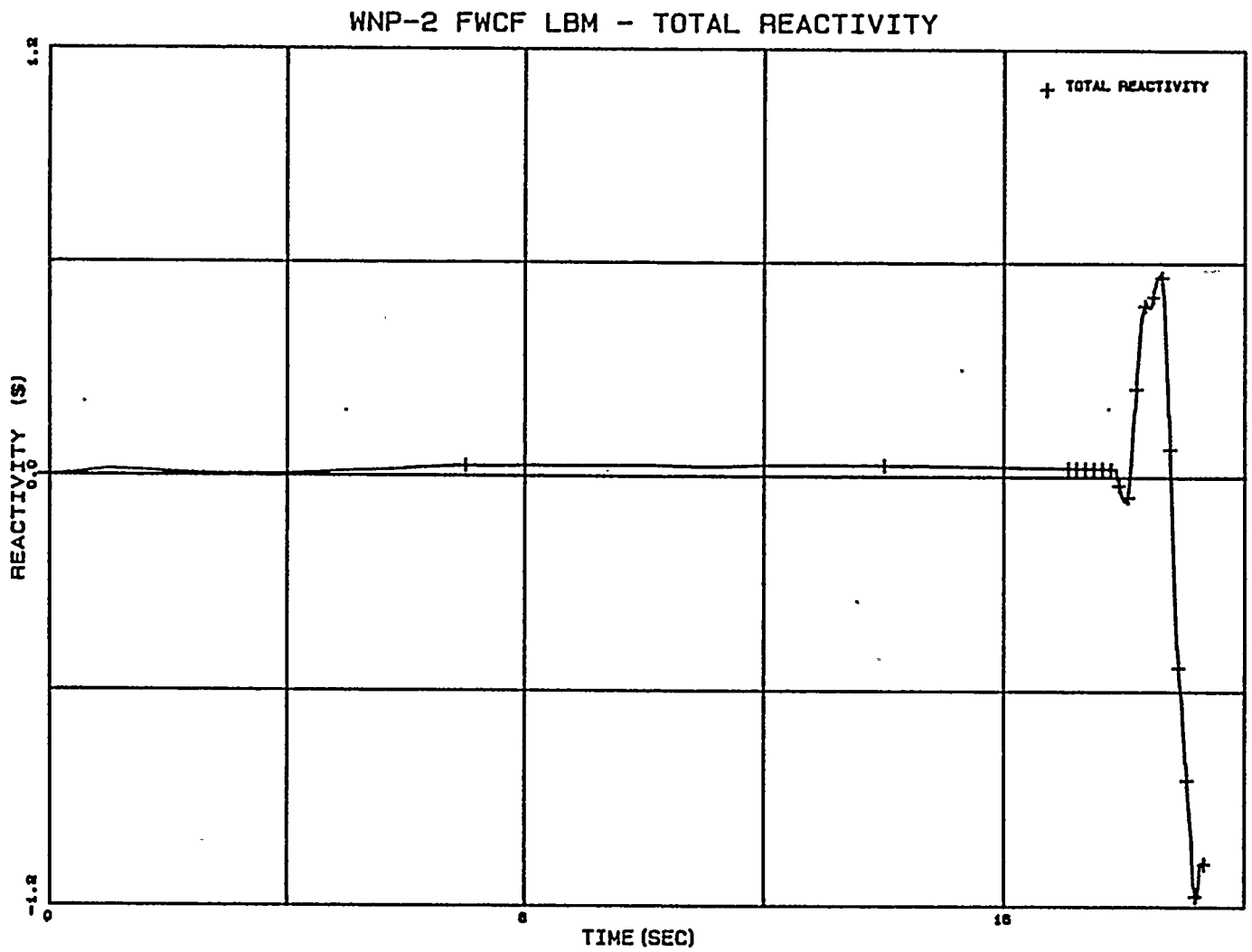
WNP-2 FWCF LBM - TOTAL REACTIVITY
+ TOTAL REACTIVITY
REACTIVITY ($)
1.0
0.0
-1.0
0
8
16
TIME (SEC)

FIGURE 4.3.8

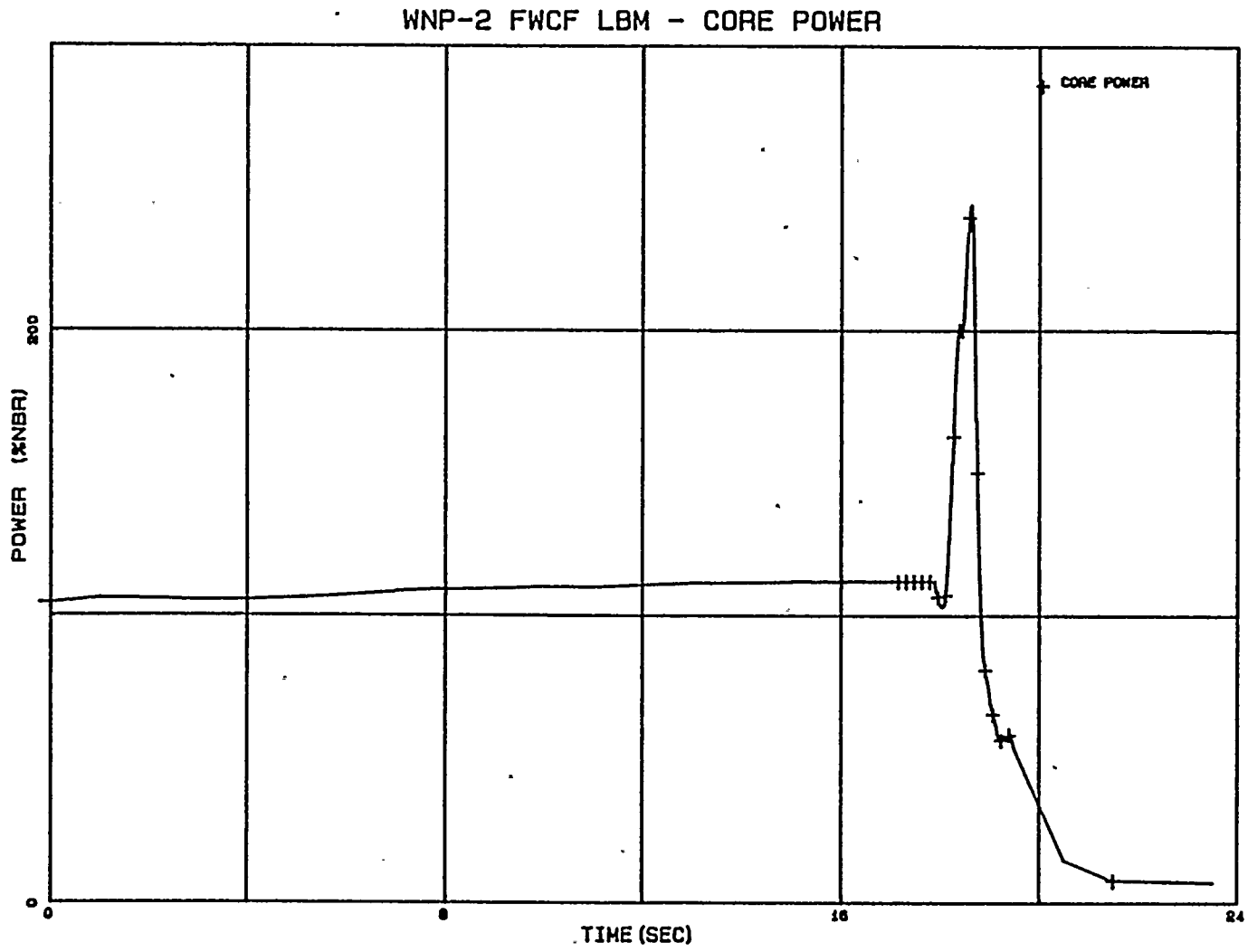
WNP-2 FWCF LBM - CORE POWER
CORE POWER
POWER (%NBR)
200
0
0
8
16
24
TIME (SEC)

FIGURE 4.3.9

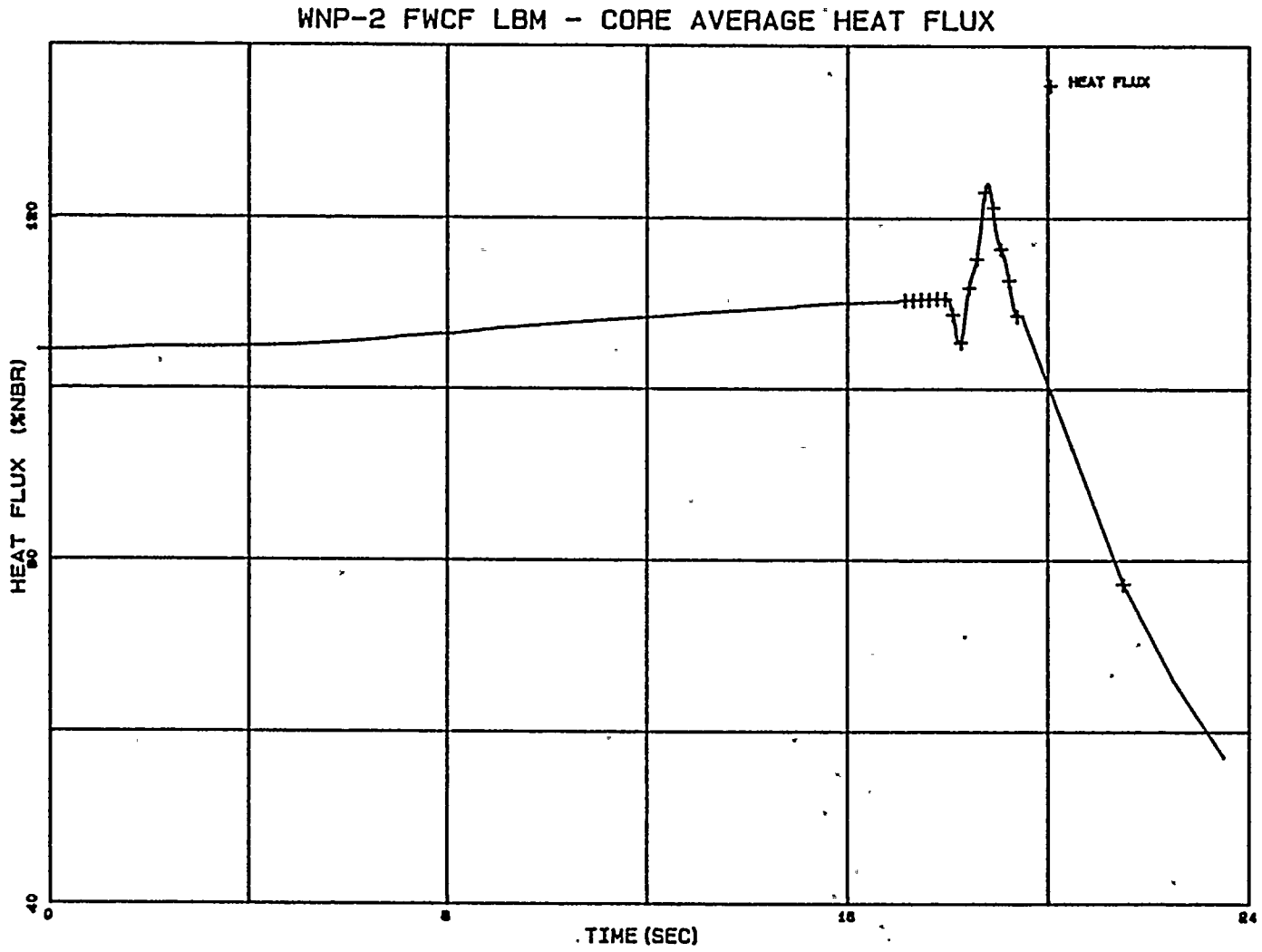
WNP-2 FWCF LBM - CORE AVERAGE HEAT FLUX
HEAT FLUX
HEAT FLUX (%NBR)
100
80
40
0
8
16
24
TIME (SEC)

FIGURE 4.3.10

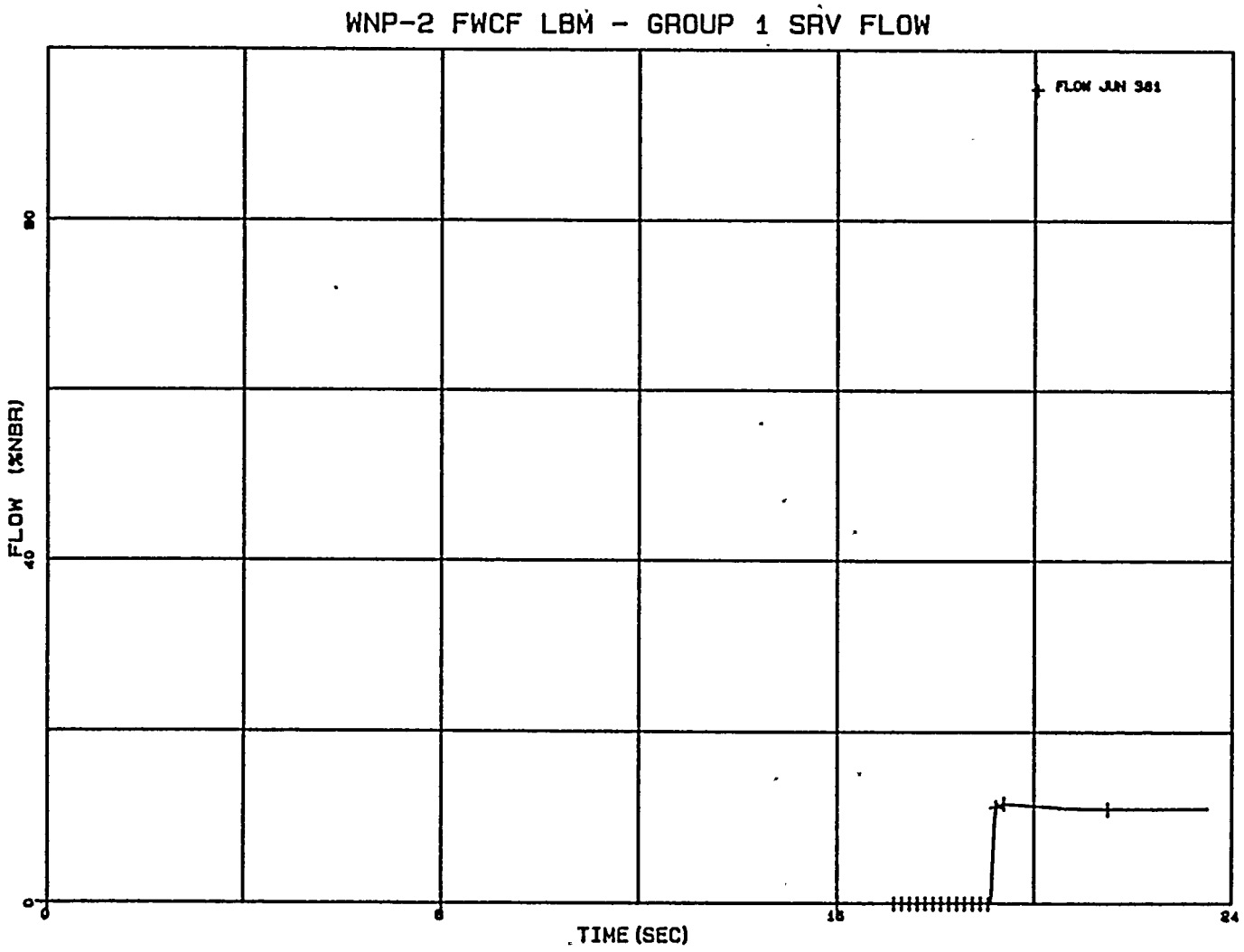
WNP-2 FWCF LBM - GROUP 1 SRV FLOW
FLOW JUN 381
80
40
0
FLOW (%NBR)
0
8
16
24
TIME (SEC)

FIGURE 4.3.11

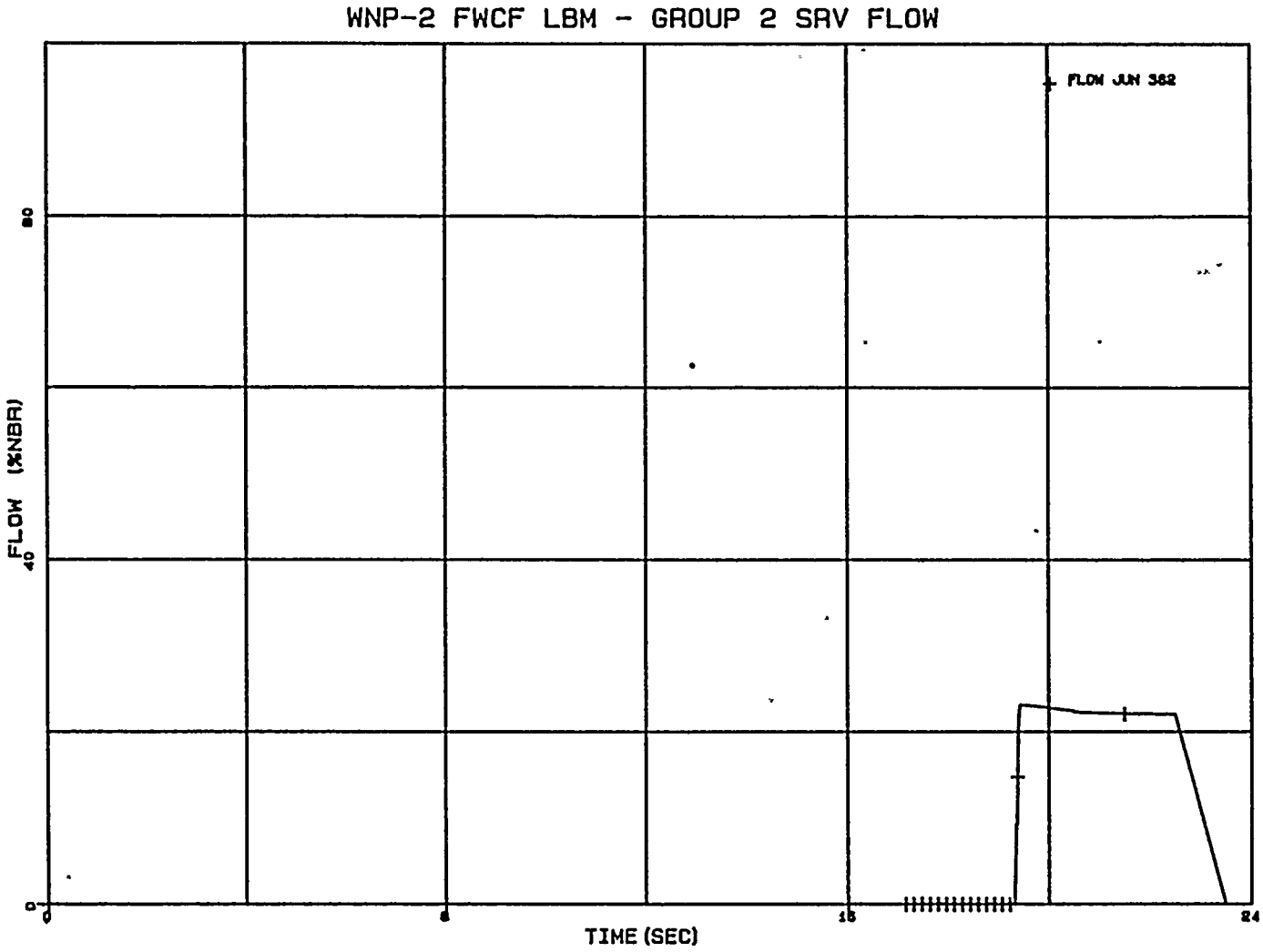
WNP-2 FWCF LBM - GROUP 2 SRV FLOW
FLOW JUN 382
80
40
0
FLOW (%NBR)
0
8
16
24
TIME (SEC)

FIGURE 4.3.12

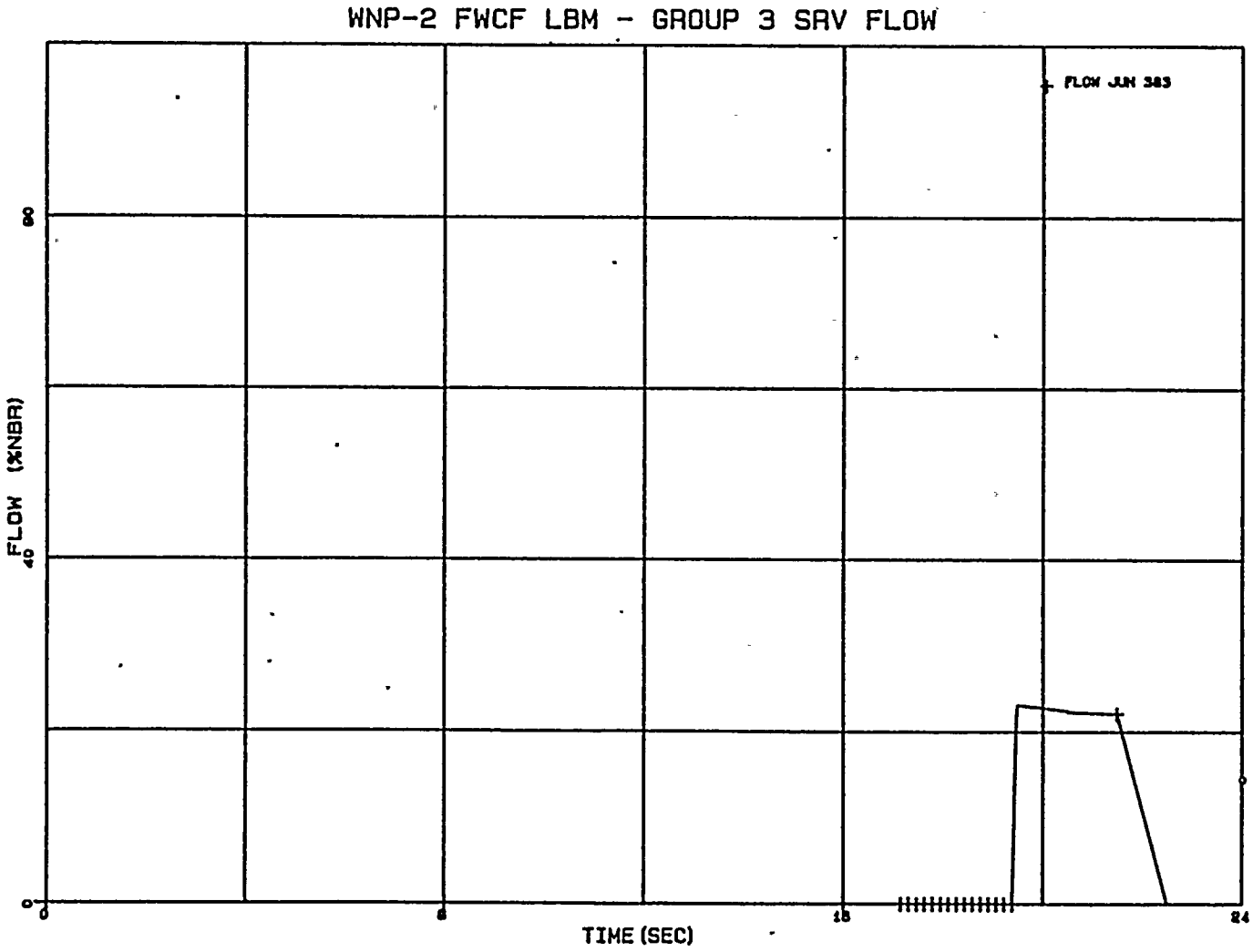
WNP-2 FWCF LBM - GROUP 3 SRV FLOW
FLOW JUN 383
60
40
0
FLOW (%NBR)
0
8
16
24
TIME (SEC)

FIGURE 4.3.13

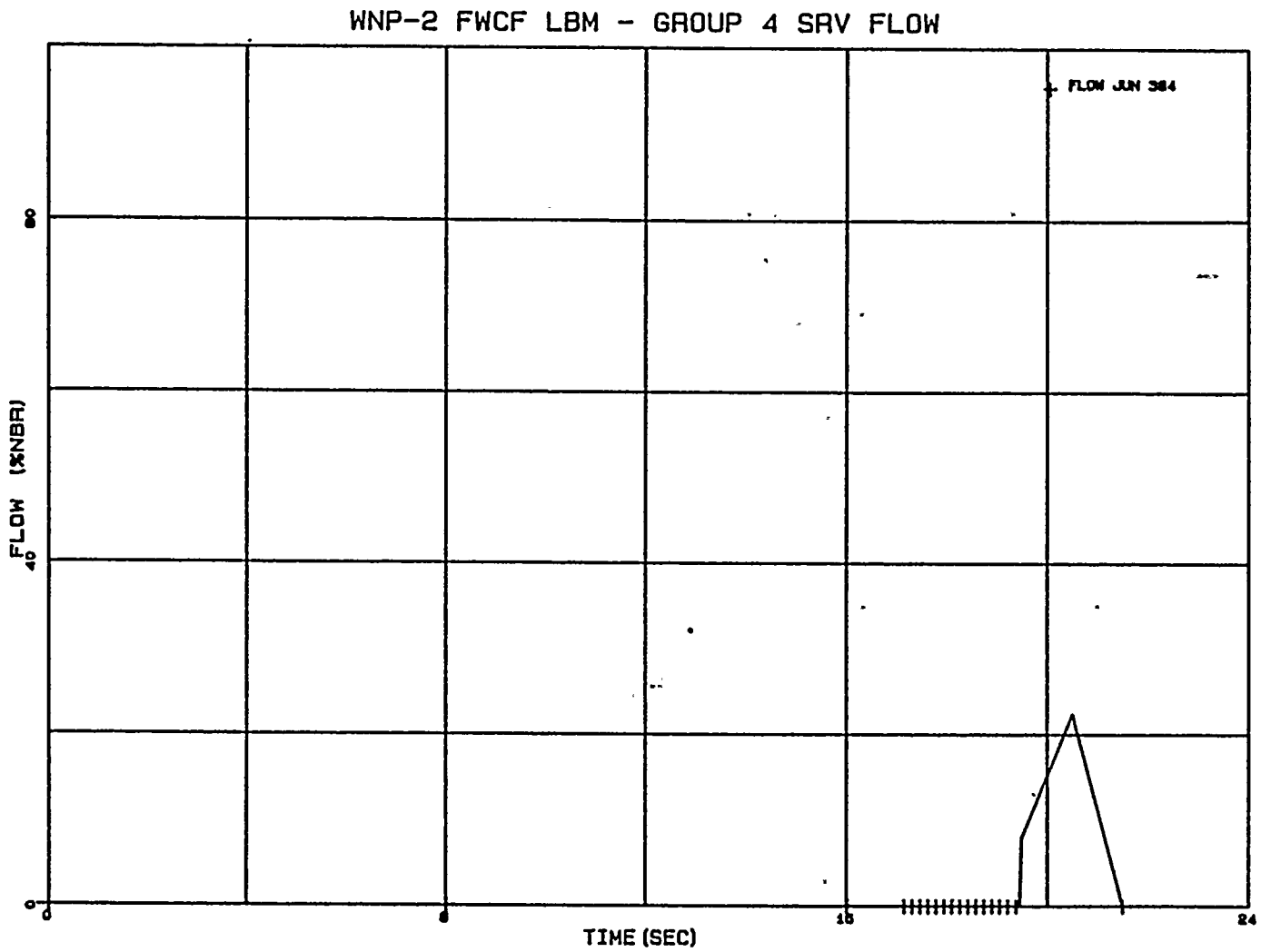
WNP-2 FWCF LBM - GROUP 4 SRV FLOW
FLOW JUN 384
FLOW (%NBR)
80
40
0
0
8
16
24
TIME (SEC)

FIGURE 4.3.14

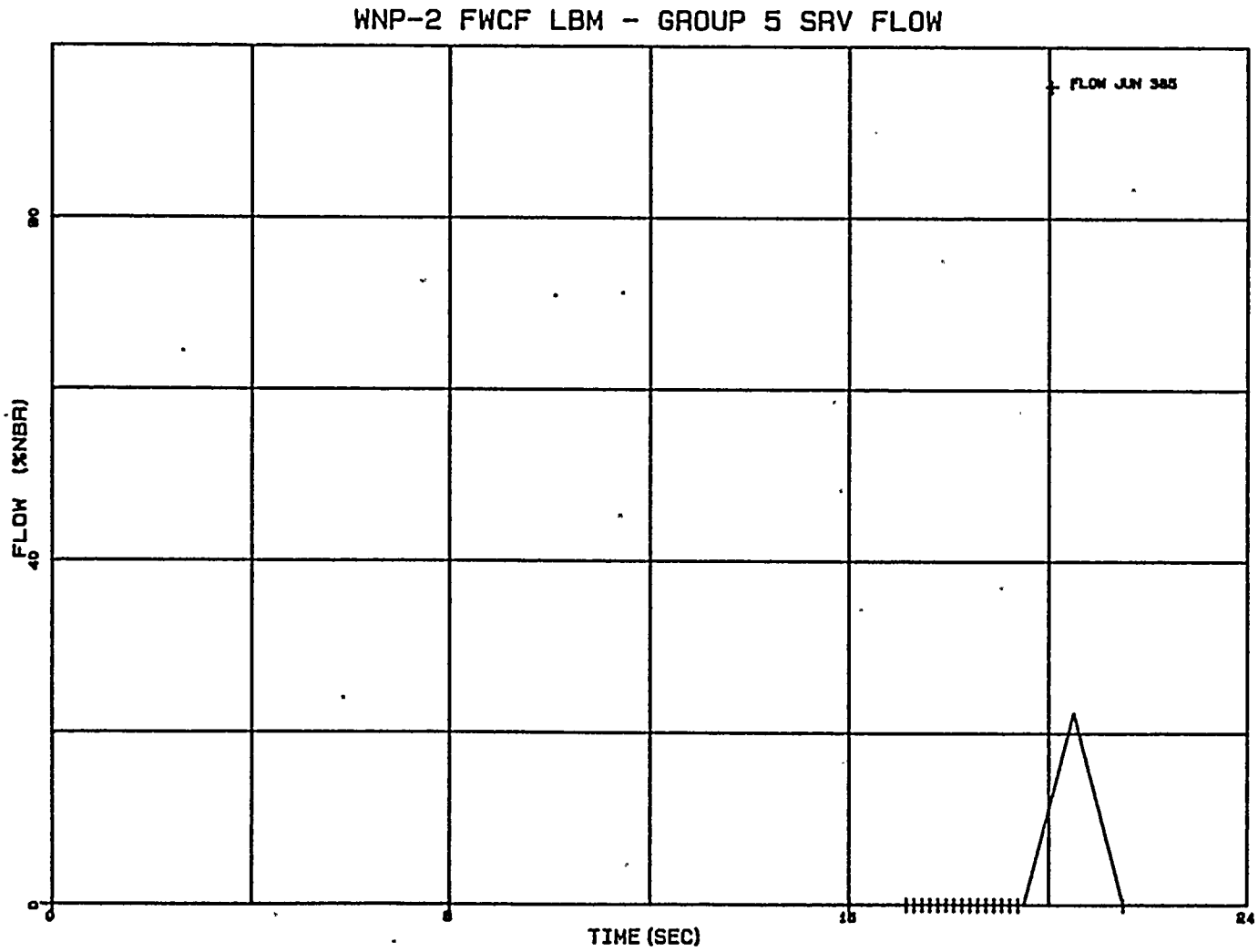
WNP-2 FWCF LBM - GROUP 5 SRV FLOW
FLOW JUN 385
80
40
0
FLOW (%NBR)
0
8
16
24
TIME (SEC)

FIGURE 4.3.15

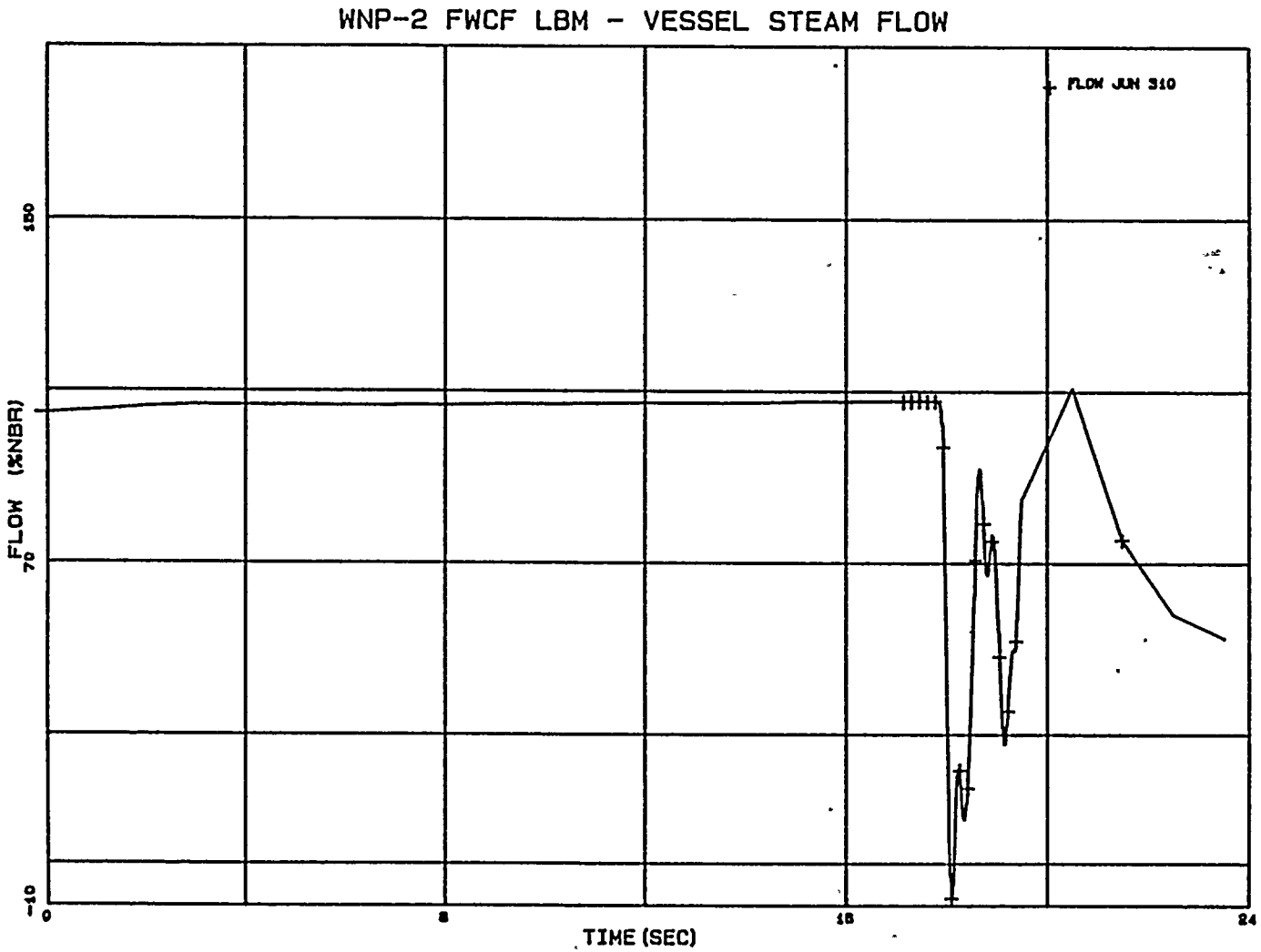
WNP-2 FWCF LBM - VESSEL STEAM FLOW
FLOW JUN 310
150
70
-10
FLOW (%NBR)
0
8
16
24
TIME (SEC)

FIGURE 4.3.16

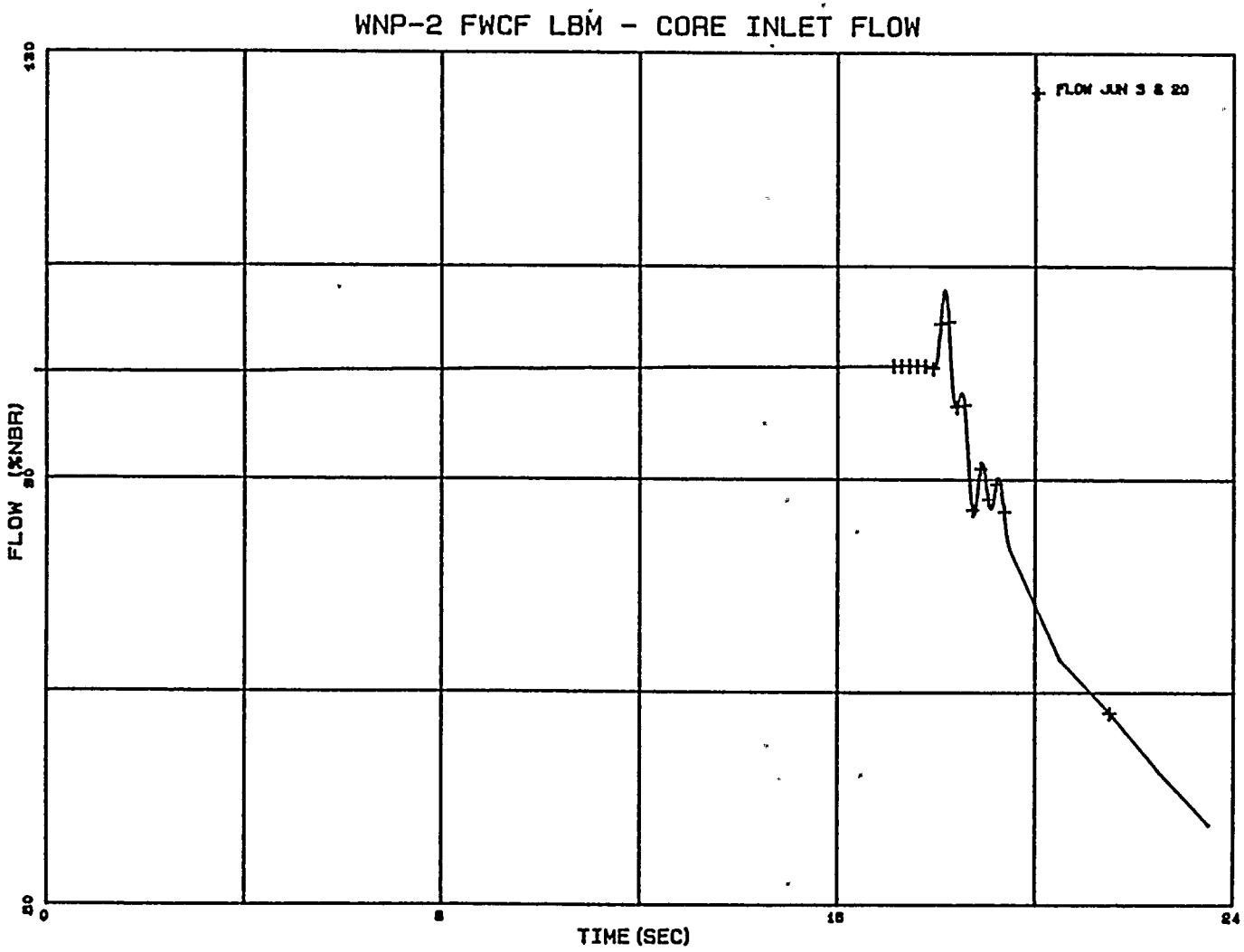
WNP-2 FWCF LBM - CORE INLET FLOW
FLOW JUN 3 & 20
FLOW (%NBR)
120
80
40
0
8
16
24
TIME (SEC)

FIGURE 4.3.17

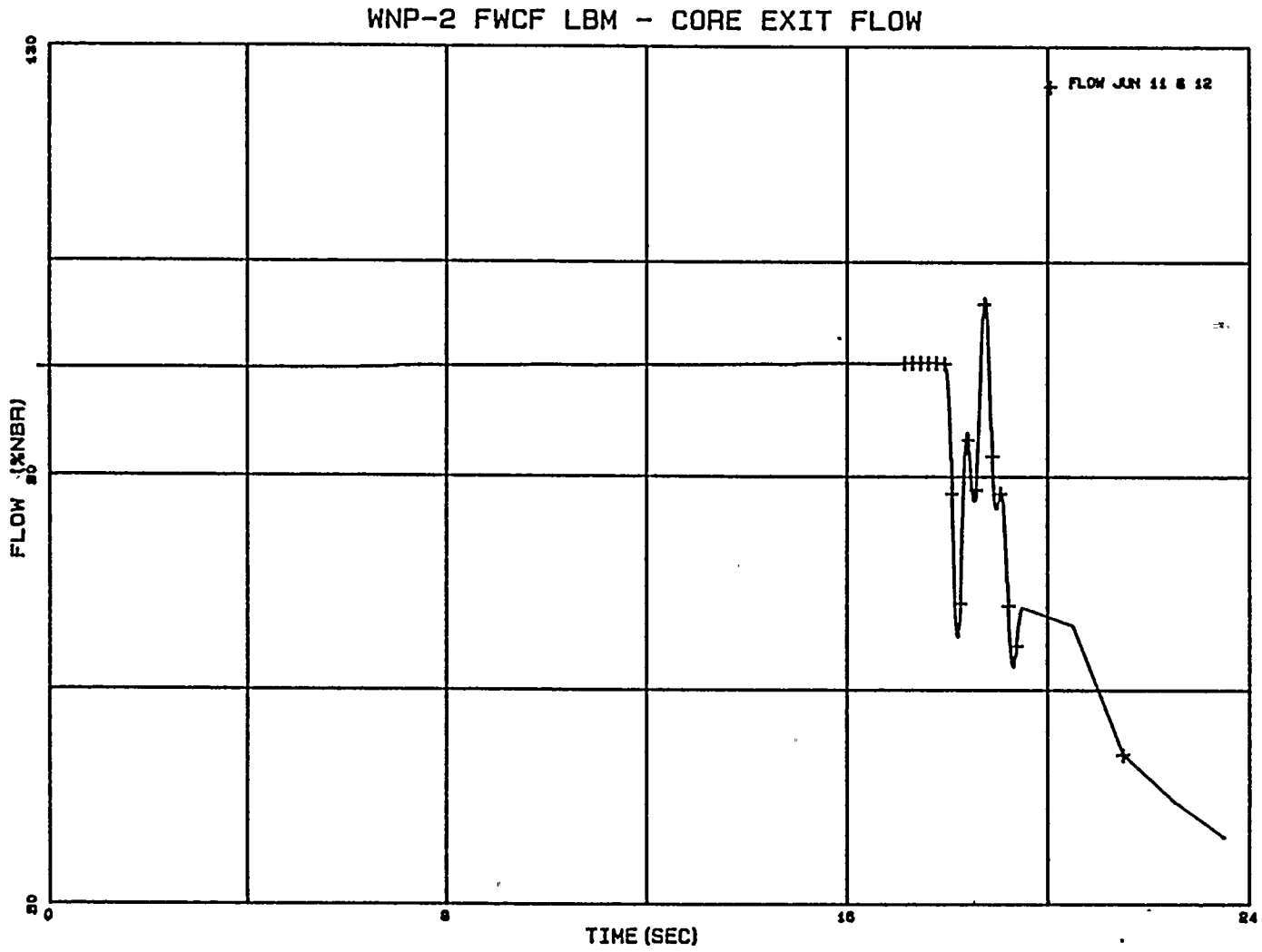
WNP-2 FWCF LBM - CORE EXIT FLOW
FLOW JUN 11 & 12
130
80
30
FLOW (%NBR)
0
8
16
24
TIME (SEC)

FIGURE 4.3.18

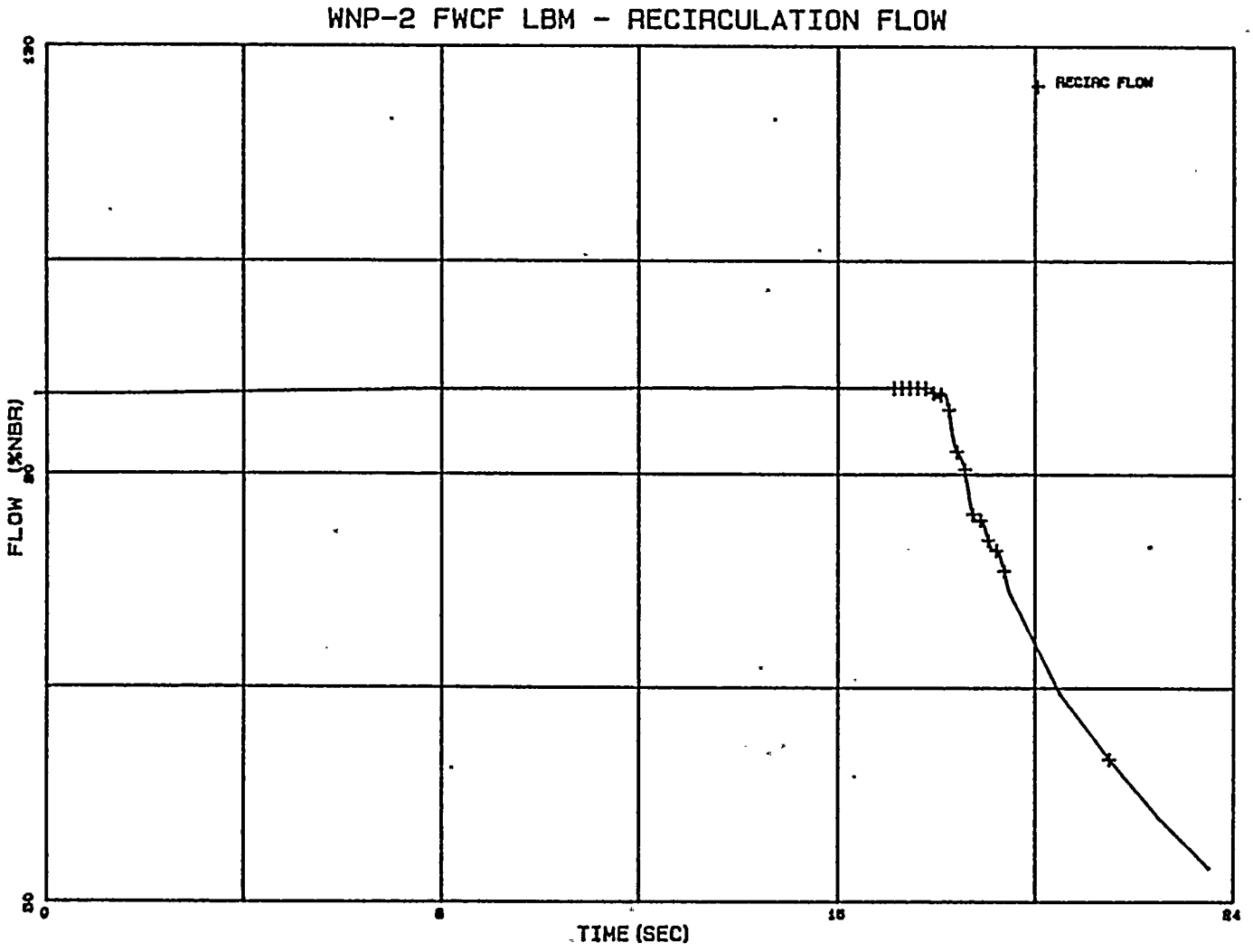
WNP-2 FWCF LBM - RECIRCULATION FLOW
RECIRC FLOW
FLOW (%NBR)
100
80
50
0
8
16
24
TIME (SEC)

FIGURE 4.3.19

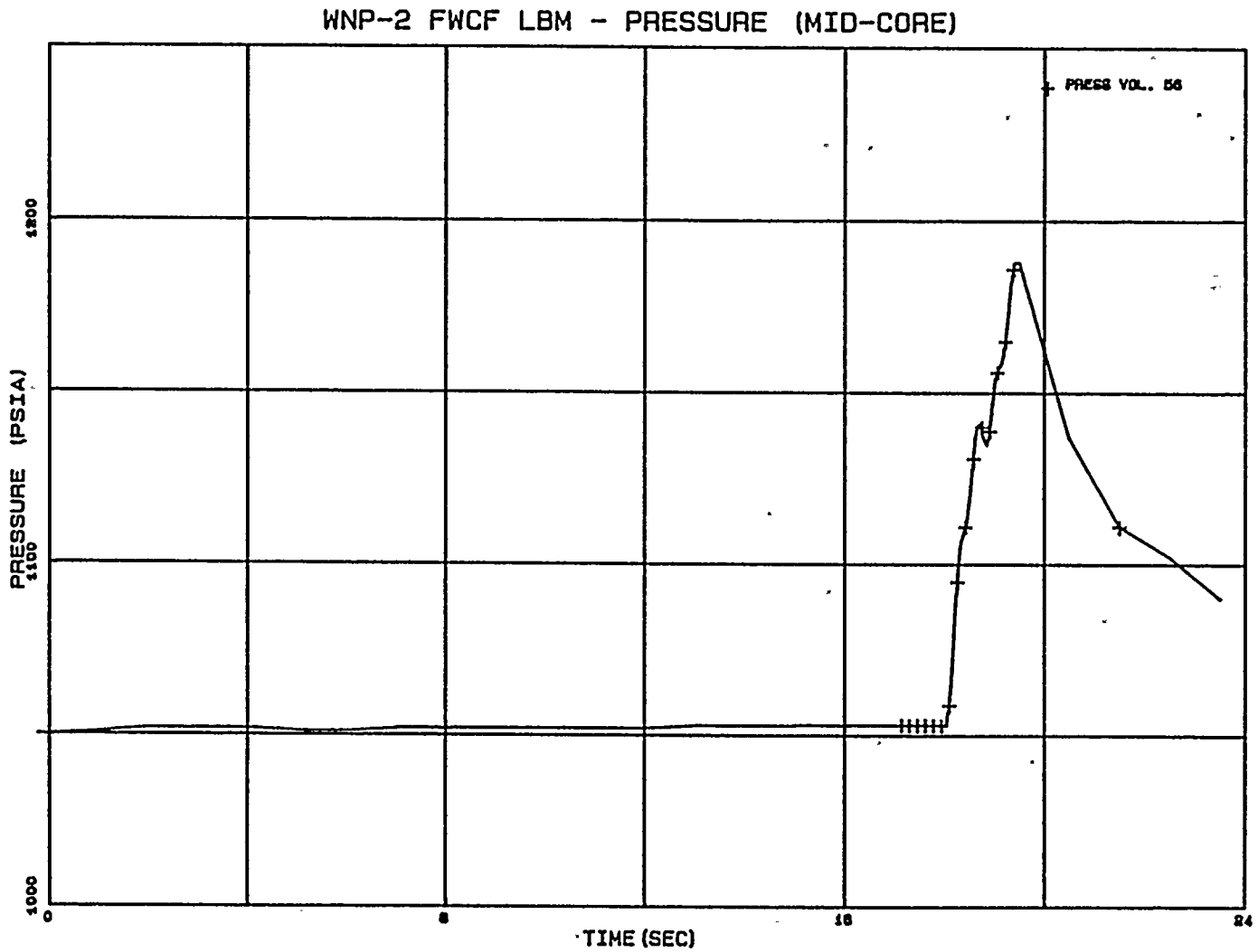
WNP-2 FWCF LBM - PRESSURE (MID-CORE)
PRESS VOL. 56
PRESSURE (PSIA)
1200
1100
1000
0
8
16
24
TIME (SEC)

FIGURE 4.3.20

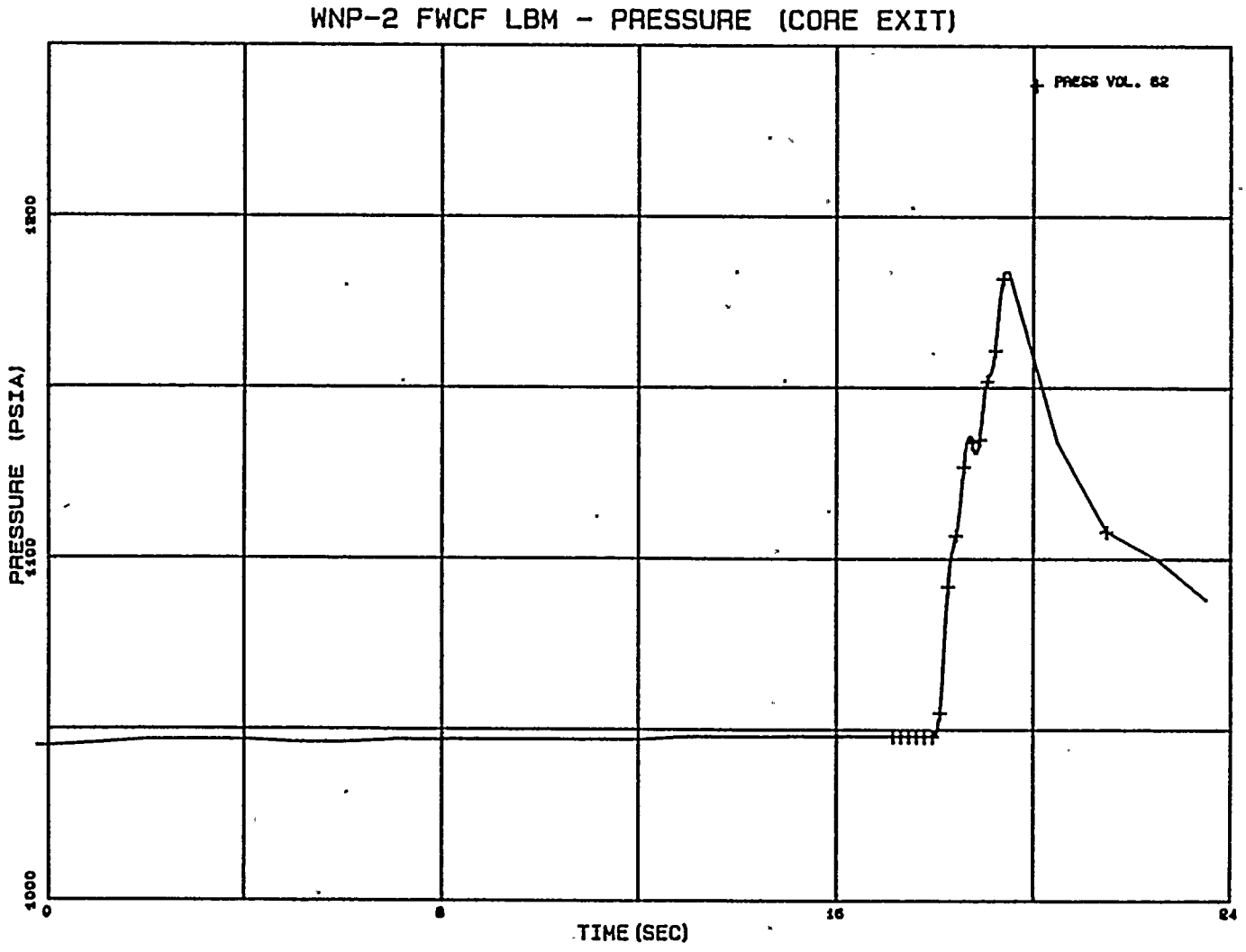
WNP-2 FWCF LBM - PRESSURE (CORE EXIT)
1 PRESS VOL. 82
PRESSURE (PSIA)
1200
1100
1000
0
8
16
24
TIME (SEC)

FIGURE 4.3.21

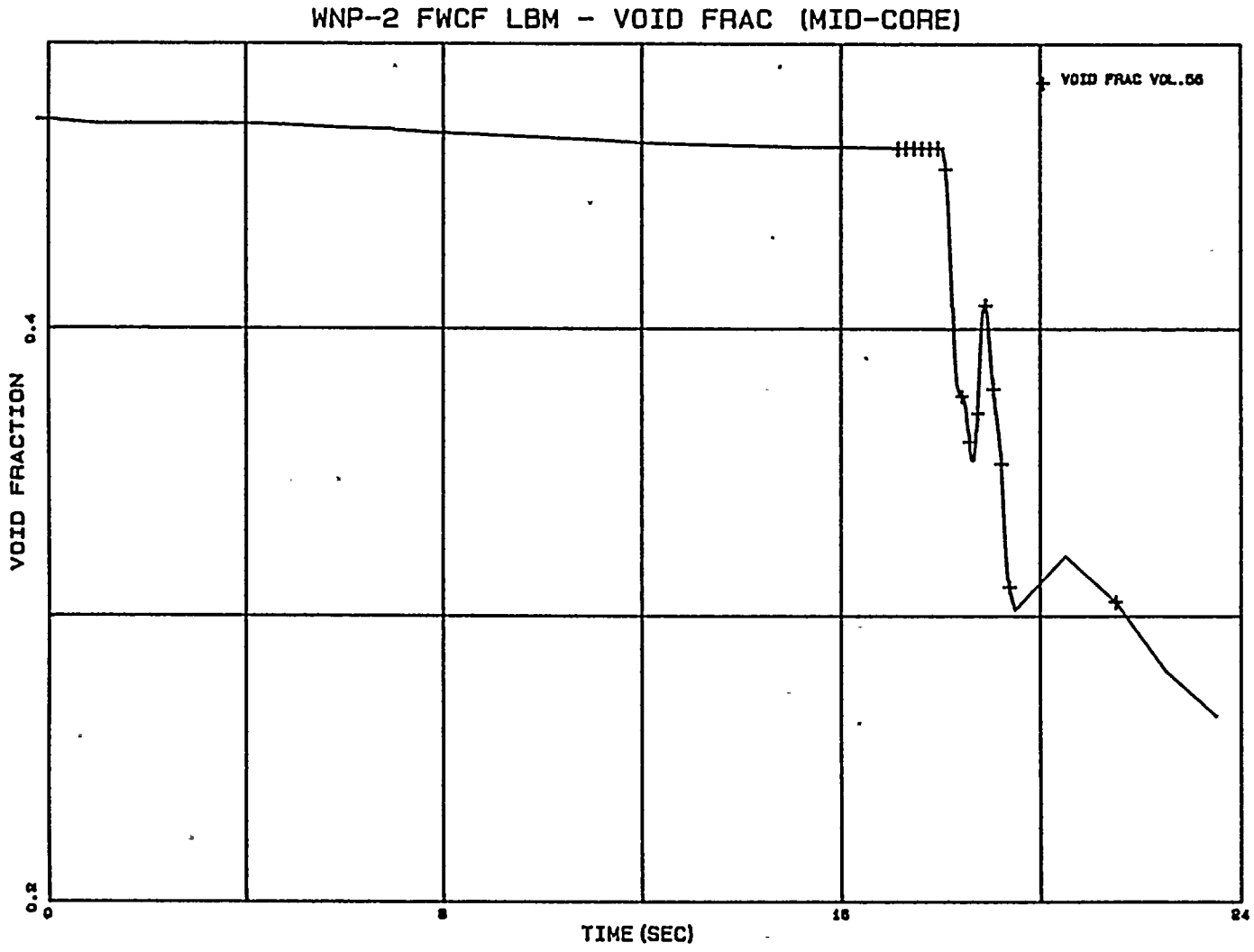
WNP-2 FWCF LBM - VOID FRAC (MID-CORE)
VOID FRAC VOL.56
VOID FRACTION
0.4
0.8
0
8
16
24
TIME (SEC)

FIGURE 4.3.22

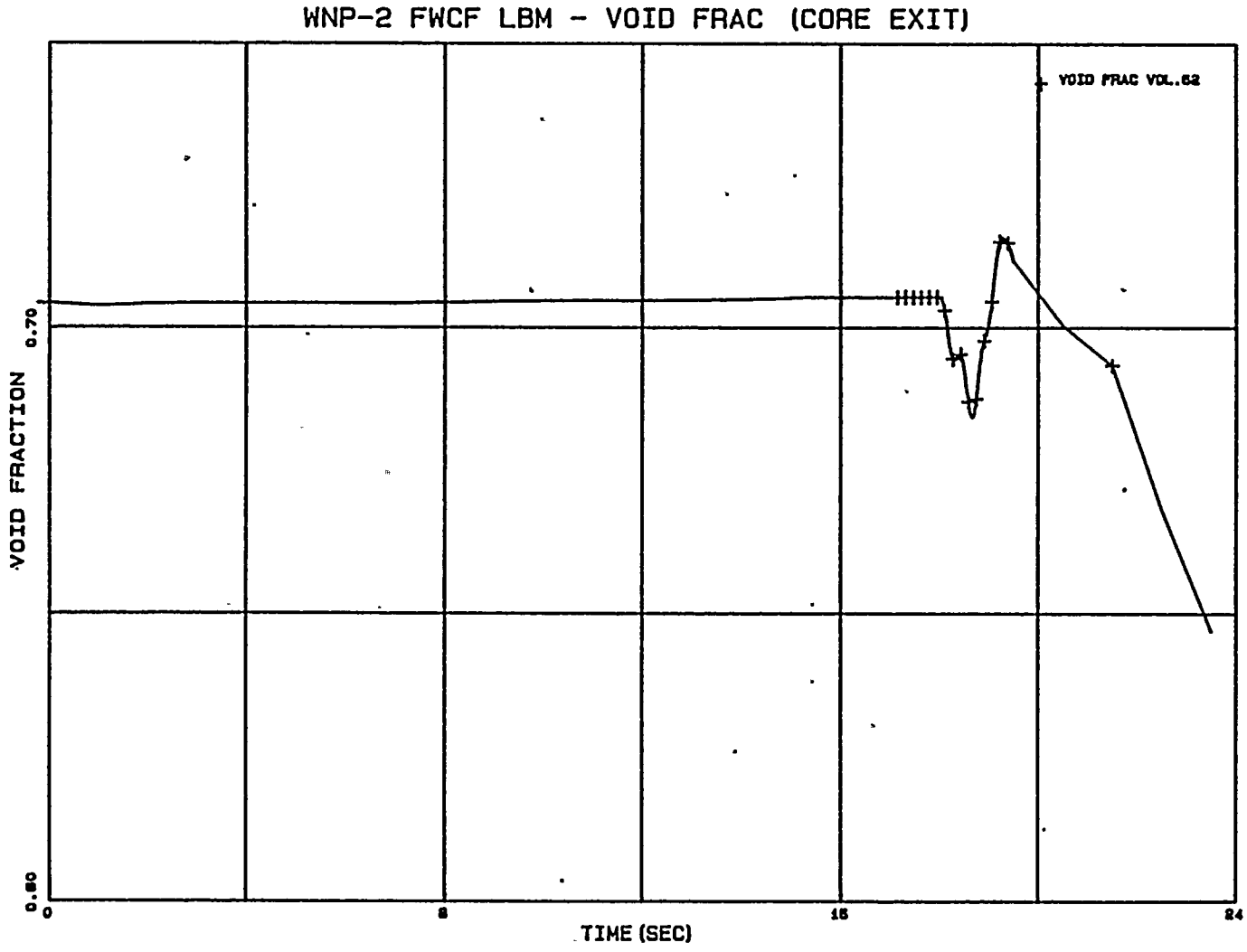
WNP-2 FWCF LBM - VOID FRAC (CORE EXIT)
VOID FRAC VOL.62
VOID FRACTION
0.70
0.60
0
8
16
24
TIME (SEC)

4.4 Summary of Transient Analysis

The key transient simulation results for the two MCPR limiting transients as calculated by RETRAN are summarized in Table 4.5.

TABLE 4.5

Summary of Thermal-Limiting Transient Results

	LRNB	FWCF
Max Power (%NBR)	398	245
Time at max power (seconds)	0.89	18.6
Max core avg heat flux (%NBR)	133	124
Time at max heat flux (seconds)	1.1	18.8
Max dome pressure (psia)	1207	1175
Time at max dome pressure (sec)	1.9	19.5

5.0 SUMMARY AND CONCLUSIONS

Benchmark analyses covering specific Power Ascension Tests as described in Section 3.1 demonstrate the capability of the WNP-2 RETRAN model to predict core and system behavior during normal operation and mild transients. These analyses validate the modeling of the feedwater and pressure regulator control systems and the performance of the recirculation pumps, jet pumps, and steam lines as modeled for WNP-2.

Benchmark analyses covering the turbine trip tests performed at Peach Bottom 2 at the end of Cycle 2 as described in Section 3.2 demonstrate RETRAN's ability to model conditions more challenging than the WNP-2 startup tests and the Supply System technical staff's competence to perform these analyses. These analyses validate the capabilities of the modeling beyond the normal operating envelope of the reactor.

Example calculations covering typical limiting transients as reported in Chapter 4 demonstrate the WNP-2 RETRAN model's ability to predict system performance under conditions which challenge operating limits. These analyses show consistency with existing analyses of record and validate the Supply System technical staff's ability to formulate and analyze limiting transient events.

The analyses performed in this report demonstrate the ability of the WNP-2 RETRAN model and the qualifications of the Supply System technical staff to predict the course of a wide variety of transient events. The model is applicable to the evaluation of normal and anticipated operation for plant operational support and core reload analysis.

6.0 REFERENCES

1. J.H. McFadden et al., "RETRAN-02 - A Program for Transient Thermal-Hydraulic Analysis of Complex Fluid Flow Systems," EPRI NP-1850-CCM-A, Revision 4, Volumes I-III, Electric Power Research Institute, November 1988.

2. B.M. Moore, A.G. Gibbs, J.D. Imel, J.D. Teachman, D.H. Thomsen, and W.C. Wolkenhauer, "Qualification of Core Physics Methods for BWR Design and Analysis," WPPSS-FTS-127, Washington Public Power Supply System, March 1990.

3. J.A. McClure et al., "SIMTRAN-E - A SIMULATE-E to RETRAN-02 Data Link," EPRI NP-5509-CCM, Electric Power Research Institute, December 1987.

4. C.W. Stewart et al.,"VIPRE-01 - A Thermal-Hydraulic Code for Reactor Cores," EPRI NP-254-CCM-A, Revision 3, Volumes I-III, Electric Power Research Institute, August 1989.

5. D.L. Hagerman, G.A. Reymann, and R.E. Manson, "MATPRO - Version 11 (Revision 2): A Handbook of Materials Properties for Use in the Analysis of Light Water Reactor Fuel Rod Behavior," NUREG/CR-0479, TREE-1280, Revision 2, Idaho National Engineering Laboratory, August 1981.

6. "WREM, Water Reactor Evaluation Model, Revision 1," NUREG-75/065, U.S. Nuclear Regulatory Commission, May 1975.

7. WPPSS Nuclear Plant 2 Updated Final Safety Analysis Report, Washington Public Power Supply System, 1989.

8. "Qualification of the One-Dimensional Core Transient Model for Boiling Water Reactors," NEDO-24154, Volume 1, General Electric Company, October 1978.

9. Letter, J. Armenta (GE) to W.C. Wolkenhauer (WPPSS), "Instruction for Use of 4-Quadrant Curve," dated March 26, 1985.

10. "Recirculation System Performance," Publication 457HA802, General Electric Company, September 1976.

11. B.J. Gitnick et al., "FIBWR - A Steady-State Core Flow Distribution Code for Boiling Water Reactors," EPRI NP-1924-CCM, Electric Power Research Institute, July 1981.

12. R.E. Polomik and S.T. Chow, "Hanford-2 Nuclear Power Station Control System Design Report," GEZ-6894, General Electric Company, February 1980.

13. "Turbine Dynamic Response Parameters," Publication CT-24659, Westinghouse Electric Corporation, August 1979.

14. M. Edenius, A. Ahlin, and H. Haggblom, "CASMO-2, A Fuel Assembly Burnup Program, User's Manual," STUDSVIK/NR-81/3, Studsvik Energiteknik AB, March 1981.

15. D.M. Ver Planck, W.R. Cobb, R.S. Borland, B.L. Darnell, and P.L. Versteegen, "SIMULATE-E (Mod. 3) Computer Code Manual," EPRI NP-4574-CCM, Part II, Electric Power Research Institute, September 1987.

16. J.D. Atchison, "Final Report on Anticipated Transients Without Scram Analyses for the WNP-2 Nuclear Power Plant," EI International Inc., December 1989.

17. "Power Ascension Test Program," WNP-2 Plant Procedure Manual, Section 8.2, Washington Public Power Supply System, 1984.

18. L.A. Carmichael and R.O. Niemi, "Transient and Stability Tests at Peach Bottom Atomic Power Station Unit 2 at End of Fuel Cycle 2," EPRI NP-564, Electric Power Research Institute, June 1978.

19. K. Hornyik and J.A. Naser, "RETRAN Analysis of the Turbine Trip Tests at Peach Bottom Atomic Power Station Unit 2 at End of Cycle 2," EPRI NP-1076-SR, Electric Power Research Institute, April 1979.

20. A.M. Olson, "Methods for Performing BWR System Transient Analysis," PECO-FMS-0004-A, Philadelphia Electric Company, November 1988.

21. N.H. Larsen, "Core Design and Operating Data for Cycles 1 and 2 of Peach Bottom Unit 2," EPRI NP-563, Electric Power Research Institute, June 1978.

22. J. E. Krajicek, "WNP-2 Cycle 2 Plant Transient Analysis", XN-NF-85-143, Exxon Nuclear Co., Inc., Richland, WA, December 1985.

23. J. E. Krajicek, "WNP-2 Cycle 5 Plant Transient Analysis", ANF-89-01, Rev. 1, Advanced Nuclear Fuels Corp., Richland, WA, March 1989.

24. S. L. Forkner, et al., "BWR Transient Analysis Model Utilizing the RETRAN Program", TVA-TR81-01, Tennessee Valley Authority, December 1981.

25. WPPSS Nuclear Plant 2 Technical Specifications, Docket No. 50-397.

26. J. E. Krajicek and M. J. Hibbard, "WNP-2 Cycle 4 Plant Transient Analysis", ANF-88-01, Advanced Nuclear Fuels Corp., Richland, WA, January 1988.